Pentaarylcyclopentadienylsystems
Anions, Radicals and Cations

Dissertation

zur Erlangung des akademischen Titels
Doktor der Naturwissenschaften (Dr. rer. nat.)

vorgelegt von
Yannick Schulte
geboren in Essen

Fakultät für Chemie der Universität Duisburg-Essen
Essen 2023

DOI: 10.17185/duepublico/81777
URN: urn:nbn:de:hbz:465-20240320-114134-8

Die hier vorliegende Arbeit wurde im Zeitraum von 2019 bis 2023 im Arbeitskreis von Herrn Prof. Dr. Stephan Schulz des Institutes für Anorganische Chemie an der Universität Duisburg-Essen, Campus Essen angefertigt.

Einreichung der Dissertation:	18.09.2023
Tag der Disputation:	08.12.2023

Vorsitzender:	Prof. Dr. Sebastian Schlücker
Gutachter:	Prof. Dr. Stephan Schulz
	Prof. Dr. Gebhard Haberhauer
	Prof. Dr. Wolfram Sander

„Das Rätsel gibt es nicht.“

Ludwig Wittgenstein

Abstract

The aim of this work is to study the chemistry of pentaarylcyclopentadienyl systems. Pentaarylcyclopentadienes with different substituents are synthesized in order to influence their electronic and steric properties. Deprotonation of these pentaarylcyclopentadienes allows the preparation of the corresponding anions in the form of alkali metal salts. These anions can be used in salt metathesis reactions to generate cyclopentadienylpnictogen dichlorides, which serve as synthetic building blocks for "$PnCl_2$" synthons as well as for the synthesis of tetrel(II) metallocenes. In addition, these anions can be oxidized to cyclopentadienyl radicals, which exhibit intriguing Jahn-Teller distortions and exist as two distinct valence tautomers that have been observed for the first time via single-crystal X-ray diffraction (sc-XRD).

The cyclopentadienyl radicals can be used directly for the synthesis of metallocenes or half-metallocenes using activated elemental metals. In addition, attempts were made to synthesize potentially antiaromatic cyclopentadienyl cations; however, isolation of the products was not achieved due to decomposition reactions. To overcome this problem, perfluorination and the use of oxidation-resistant solvents were employed, leading to the successful synthesis and characterization of the first crystalline salt of a cyclopentadienyl cation stable at room temperature. The antiaromatic singlet state of this cyclopentadienyl cation is stabilized by the environment in the crystal. In addition, the corresponding perfluorinated pentaphenylcyclopentadienyl radical was prepared and used as a one-electron oxidizing agent, forming a stable, weakly coordinating anion.

Zusammenfassung

Das Ziel dieser Arbeit ist die Untersuchung der Chemie von Pentaarylcyclopentadienylsystemen. Es werden Pentaarylcyclopentadiene mit verschiedenen Substituenten und unterschiedlichen elektronischen und sterischen Eigenschaften synthetisiert. Die Deprotonierung dieser Pentaarylcyclopentadiene ermöglicht die Herstellung der entsprechenden Anionen in Form von Alkalimetallsalzen. Diese Anionen können in Salzmetathesereaktionen zur Erzeugung von Cyclopentadienylpnictogendichloriden verwendet werden, die als Synthesebausteine für "$PnCl_2$"-Synthone sowie für die Synthese von Tetrel(II)-Metallocenen dienen.

Darüber hinaus können diese Anionen oxidiert werden, um Cyclopentadienyl-Radikale zu bilden, die Jahn-Teller-Verzerrungen aufweisen und als zwei verschiedene Valenztautomere existieren, die zum ersten Mal über Kristallstrukturen nachgewiesen wurden. Die Cyclopentadienylradikale können direkt für die Synthese von Metallocenen oder Halbmetallocenen unter Verwendung aktivierter elementarer Metalle verwendet werden. Darüber hinaus wurden Versuche unternommen die entsprechenden potenziell antiaromatischen Cyclopentadienylkationen zu synthetisieren. Ihre Isolierung wurde jedoch aufgrund von Zersetzungsreaktionen nicht erreicht.

Dieses Problem konnte durch die Verwendung perfluorierter Pentaarylcyclopentadienylsysteme und oxidationsbeständiger Lösungsmittel überwunden werden, was zur erfolgreichen Synthese und Charakterisierung des ersten kristallinen, bei Raumtemperatur stabilen Salzes eines Cyclopentadienyl-Kations führte. Der antiaromatische Singulett-Zustand dieses Cyclopentadienylkations wird durch die Umgebung im Kristall stabilisiert.

Darüber hinaus wurde das entsprechende perfluorierte Pentaphenylcyclopentadienylradikal hergestellt und als Ein-Elektronen-Oxidationsmittel verwendet.

Acknowledgements

I would like to begin by expressing my gratitude to Prof. Dr. Stephan Schulz, my doctoral supervisor, for providing me with the opportunity to conduct my research within his group. I am truly thankful for the guidance throughout my doctoral journey. I am also appreciative of the exceptional working conditions that were provided in his research group.

I would like to extend my thanks to Prof. Dr. Gebhard Haberhauer for graciously accepting the role of second reviewer for my thesis and to Prof. Dr. Sebastian Schlücker as the chairperson of the examination committee. My appreciation goes to Dr. Christoph Wölper for his extensive practical and theoretical lessons in the field of crystallography and for his tireless efforts and help in collecting and refining the crystal structure data.

I am grateful to Beate Römer, Dr. Thorsten Schaller, and Dr. Felix Niemeyer for their countless NMR measurements. I would like to extend my special thanks to Robin Meya and Beate Römer for their support with elemental analyses.

Furthermore, I would like to acknowledge the contributions of Dr. George E. Cutsail III and Dr. Blaise L. Geoghegan, who conducted measurements and simulations of the EPR spectra in the context of our collaborative work. I would also like to thank Daniel SantaLucia for his measurement and analysis of susceptibility data.

I am grateful to Anja Scheidereiter for her assistance with administrative matters at the university, for which I am truly thankful.

I would like to express my heartfelt appreciation to all members of the research group for fostering a remarkable working atmosphere and for the wonderful time we have shared together over the years. A special thanks to my office colleagues Alexander Gehlhaar, Micha Weinert, Christoph Helling, Kevin Huse, Charlotte van Halteren, and Pratima Dhawan and to my laboratory colleagues Swarup Ghosh, Eduard Glöckler, Dominik Wäsche, Anna Bücker, Joost Möbius, Oussama Tihouna, and Jill-Mara Reher for creating a supportive environment and engaging in stimulating discussions on both research-related and unrelated topics.

Finally, I would like to convey my deepest appreciation to all the individuals who have accompanied and supported me throughout my studies, with special thanks to my family, my girlfriend, and my friends for their unwavering encouragement.

Table of Contents

1 Introduction

The cyclopentadienyl anion is among the most frequently used ligands in organometallic chemistry. Its use in transition metal chemistry dates back to the serendipitous observations of Kealy, Pauson, Miller, Tebboth and Tremaine who prepared a volatile iron(II) cyclopentadienide (*i.e.* ferrocene) either during the attempted synthesis of fulvalene by one-electron oxidation of the cyclopentadienyl anion with $FeCl_3$[1] or by the reaction of cylopentadiene vapor at 300 °C with finely divided elemental iron.[2]

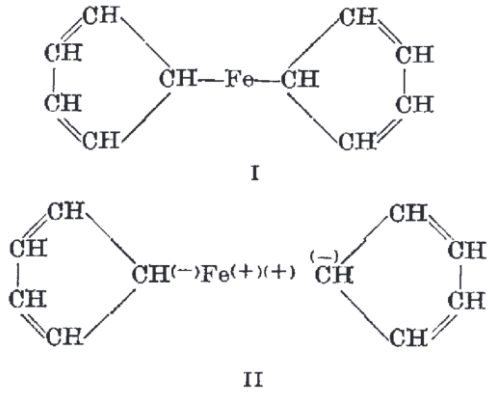

Figure 1: Lewis formula of ferrocene, postulated by Kealy and Pauson.[1] Miller, Tebboth and Tremaine formulated an analogous structure.[2]

The Lewis structure proposed by these researchers may seem clumsy from a modern point of view. Nonetheless, they rightly pronounce the aromaticity of the formed cyclopentadienyl compound:

> "The remarkable stability of this substance is, of course, in sharp contrast to the failures of earlier workers to prepare similar compounds and must be attributed to the tendency of the cyclopentadienyl group to become 'aromatic' by acquisition of a negative charge, resulting in important contributions from the resonance form (II) and intermediate forms."[1]

The aromaticity of the cyclopentadienyl anion was already widely accepted at this time, as it was part of the seminal works of Hückel.[3]

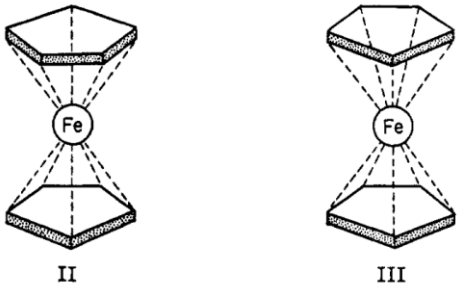

Figure 2: Structure of ferrocene, postulated by Wilkinson *et al.*[4]

Only four months later, Wilkinson *et al.* had reproduced the results and came to the right conclusions concerning the structure of ferrocene (Figure 2), based on the methods available in 1952, *i.e.* IR and UV/Vis spectroscopy, and determination of its molar magnetic susceptibility and dipole moment.[4] Its amenability to Friedel-Crafts Acylation and otherwise low reactivity made them also recognize its aromaticity.[5]

During the following years, the cyclopentadienyl complexes of nearly all transition metals were prepared. This was later recalled as "the event that led to the development of the modern field of organometallic chemistry".[6] Cyclopentadienyl compounds of the p-block elements followed, *e.g.* by the Jutzi group.[7]

As is often the case in science,[8] this fundamental research was at first driven by curiosity.[9] Nonetheless, commercially relevant applications followed, especially the zirconocene or hafnocene derived Kaminsky catalysts.[10] Many other cyclopentadienyl complexes did not find application in the chemical industry (possibly due to their high cost), but are of scientific interest. Among these are for example useful reductants like decamethylsamarocene[11] or cobaltocene[12], oxidants like ferrocenium salts,[4] or low valent compounds like (pentamethylcyclopentadienyl)aluminium(I) or decaisopropyluranocene.

2 Theoretical Background

2.1 Aromaticity and Antiaromaticity

Faraday's discovery of benzene in 1825 was recognized as a groundbreaking chemical achievement.[13] Benzene and its derivatives, often a component of essential oils, were soon called aromatics, initially because of their often pleasant and strong odor.[14] The name soon became more generally applied and was defined by the reactivity of aromatics, which is distinct from that of alkenes, i.e. aversion to addition reactions and preference for substitution reactions. However, it took several decades for scientists to gain a deeper understanding of the structure of benzene. In 1858, Kekulé's daydream by the fireplace was the beginning of a chain of events that shed light on benzene's unique bonding situation.[15] To understand the significance of this hypothesis, it is important to remember that it was the first proposal for a cyclic molecular structure.[16] This was at a time when even the existence of electrons was unknown.[17] Despite this progress, 19th-century chemists struggled to explain the low reactivity and relative inertness of benzene towards hydrogenation.

In 1911, Willstätter's synthesis of 1,3,5,7-cyclooctatetraene further complicated the situation by challenging the prevailing notion that all cyclic conjugated polyenes would behave like aromatics.[18] It became clear that the number of π electrons played a crucial role in the chemical behavior of these cyclic compounds,[19] but it was not until Hückel's seminal work in the application of quantum mechanics to fully conjugated monocyclic alkenes (also termed *annulenes*) that an explanation for this phenomenon emerged.[3] Hückel used the approximations that only the π electrons needed to be taken into account and that only the orbitals of neighbouring atoms interacted. This led to what is now known as Hückel's rule, which states that cyclic molecules with (4n+2) π electrons (where n is a natural number) have exceptional stability.

Initially, only benzene and the cyclopentadienyl anion were known as monocyclic representatives. Both obey Hückel's rule with n = 1. However, in 1958 and 1960, Breslow's cyclopropenyl cation (n = 0) and Katz's cyclooctatetraene dianion (n = 2)

were discovered, further confirming the predictions of Hückel's rule and extending it to other natural numbers.[20] Like other aromatic molecules, these compounds also exhibited aromaticity and displayed enhanced thermodynamic stability, equalized bond lengths, and maintained cyclic delocalization of electrons during chemical reactions.

On the other hand, the concept of antiaromaticity, introduced by Breslow in the 1960s, describes the destabilizing effect of cyclic π conjugation in systems with 4n π electrons.[21] Antiaromatic molecules often avoid this destabilization through distortion, representing transition states rather than stable compounds. Isolating antiaromatic systems poses a significant challenge due to their inherent instability and high reactivity. Furthermore, the fact that the triplet states of these systems are aromatic renders the isolation of the antiaromatic state nearly impossible in some cases.

Historically, the cyclopropenyl anion, the cyclobutadiene molecule, and the cyclopentadienyl cation were considered examples of 4n π-electron systems with antiaromatic character. Without the need to actually isolate them, Breslow was able to experimentally demonstrate the destabilization of cyclopropenyl anions by harmonic AC voltammetry and deuterium exchange experiments.[22] He also showed that the stability of the corresponding radicals was in between aromatic and antiaromatic molecules. In the following years, cyclobutadienes were investigated as other potential antiaromatic systems. Due to the high reactivity of these systems, this has often required the use of spectroscopic techniques that circumvent their isolation; for example, unsubstituted cyclobutadiene has been studied in the gas phase[23] and in matrices at low temperature,[24] but it is too reactive to be isolated.

After decades of unsuccessful attempts,[24] the progress to “bottleable” compounds and the elucidation of their crystal structure was made possible by the use of sterically shielded cyclobutadiene derivatives with *t*-butyl or trimethylsilyl substituents.[25]

However, the cyclopropenyl anion is now considered to be non-aromatic rather than antiaromatic,[26] and the cyclobutadiene molecule is regarded as an exception, that is difficult to classify,[27] leaving the cyclopentadienyl cation as a simple prototype of an antiaromatic system.

Unfortunately, the cyclopentadienyl cation ($C_5H_5^+$) is unstable[28] and has a triplet ground state, as demonstrated by low-temperature electron spin resonance (ESR) experiments.[29] This also applies to substituted cyclopentadienyl cations like $C_5Cl_5^+$.[30] According to Baird's rule, 4n π ring systems have aromatic triplet states, as the bonding energy is significantly higher than that of the diradical reference structure.[31,32] Therefore, the ground states of $C_5H_5^+$ and $C_5Cl_5^+$ are considered aromatic rather than antiaromatic. In contrast, pentaaryl-substituted cyclopentadienyl cations favor the singlet ground state, with a small energy gap between singlet and triplet states.[33–36] These species persist as relatively stable entities in solution due to the substantial delocalization of positive charge and steric shielding effects.

When the work presented here was begun, there had been no reports of structurally characterized cyclopentadienyl cations using single-crystal X-ray diffraction (sc-XRD) due to their high lability[21] and only cyclopentadienyl cations with strongly electron-donating substituents have proven to be stable species.[37] Attempts have been made to isolate crystalline salts of cyclopentadienyl cations. These have not been successful, leading to decomposition via various side reactions. For instance, heating a solution of the $C_5Me_5^+$ cation results in the formation of tetramethylpentafulvene and $C_5Me_5H_2^+$,[38] while the $C_5Ph_5^+$ cation decomposes through C–H cleavage and additional C–C bond formation.[39] Dimerization was observed for the $C_5Cl_5^+$ and $C_5Br_5^+$ cations.[40] In 2002, a stable $B(C_6F_5)_4$ salt of the pentamethylcyclopentadienyl cation ($C_5Me_5^+$) was reported,[38] but subsequent studies revealed it to be the pentamethylcyclopentenyl cation.[41] More recently, the reaction of triplet tetrachlorocyclopentadienylidene with BF_3 resulted in the formation of a zwitterion consisting of an antiaromatic singlet cyclopentadienyl cation and a negatively charged BF_3 unit.[42]

2.1.1 Measures of Aromaticity and Antiaromaticity

The inherent ambiguity surrounding the concept of aromaticity has led to the search for a precise and measurable definition, resulting in the emergence of various aromaticity criteria and indices.[43]

In the absence of most of the concepts of modern physical chemistry, aromaticity was initially defined purely in terms of chemical reactivity. Those unsaturated molecules that preferred substitution reactions to addition reactions were considered aromatic. This criterion (as well as others) was later criticized because it applied to benzene but not to many compounds usually considered aromatic. For example, it has long been known that many benzenoid hydrocarbons undergo addition reactions rather than substitution. Phenanthrene and anthracene add bromine, and the latter serves as a diene in Diels-Alder reactions. Fullerenes are aromatic, but substitution is not possible.[44]

Nonetheless, aromaticity can also be investigated by more quantitative means.

A frequently used criterion is bond lengths equalization. While aromatic compounds are expected to show equal bond lengths, the bond lengths in non-aromatic or antiaromatic compounds alternate.

In the mid-1960s, the Harmonic Oscillator Measure of Aromaticity (HOMA) index, a quantitative measure for the averaging of bond lengths was established and defined as the normalized function of the variance of the bond lengths around the circumference of the molecule.[45] This approach was limited to purely carbocyclic π electron systems. To overcome this, the average bond length can be replaced with the optimal bond length, R_{opt}, which can be estimated for each type of bond (including those with heteroatoms) for which the lengths of the double and single bonds are available.[46]

$$HOMA = 1 - \frac{\alpha}{n}\sum_{i}^{n}(R_{opt} - R_i)^2$$

n is the number of bonds in the ring and α is a normalizing constant that was chosen in a way that HOMA index equals 1 for a system where all $R_i = R_{opt}$ and HOMA equals 0 for the hypothetical structure of "cyclohexatriene".

R_{opt} was estimated by minimizing the deformation energy due to stretching and bending of the double and single bonds, respectively, under the assumption that both the harmonic potential for the deformation energy, and the force constant for the stretching deformation for the double bond is twice that for the single bond.
Values typically used are R_{opt} = 1.388 Å for a C−C bond and α = 257.7 Å^{-2}.[46]
However, geometric criteria for aromaticity can be problematic, because some bond-length equalized systems are not aromatic. For example, borazine has six π electrons and equalized bond lengths, but it is typically not considered to be aromatic, because its π electrons are largely localized on the nitrogen atoms.[43] Tetracene and phenanthrene, which are typically considered aromatic, have widely varying bond lengths.[43]
Another possible approach to investigate aromaticity is by energetic criteria - aromatic systems typically have enhanced stability.[44] This approach typically relies on the comparison with reference systems. For example, the hydrogenation enthalpy of benzene can be compared to cyclohexene and is found to be 35.2 kcal/mol lower than expected.[44] The stabilization energy obtained in this way obviously depends on the chosen reference system and is also influenced by ring strain and steric effects.[44]
Even more important are magnetic criteria. Aromatic compounds typically show exalted diamagnetic susceptibility, while antiaromatic compounds often show exalted paramagnetic susceptibility.[44] Unfortunately, this effect depends on the ring area.
The development of NMR spectroscopy has enhanced the use of magnetic criteria, because it allows insight in the magnetic field strengths at the location of a defined nucleus. Due to ring current effects, annulenes often exhibit unusual chemical shifts for example in their ^{1}H or ^{13}C NMR spectra. Due to the abundance of NMR spectroscopy, this is perhaps the most often used criterion today. For aromatic systems, the ring currents lead to a deshielding of atoms which are outside or part of the ring and to a shielding of atoms inside the ring. The effect for antiaromatic systems is the opposite.[47]

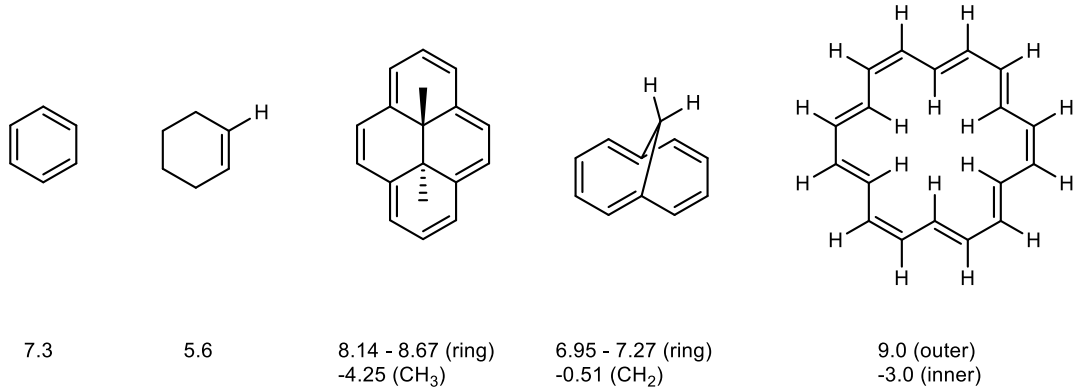

Figure 3: ^{1}H NMR chemical shifts in ppm for different aromatic or non-aromatic systems.[43]

Positions inside the ring or above the ring planes are preferentially used because the induced effects are larger,[43] but are often not accessible in smaller rings. This can be overcome by using the chemical shift of a lithium ion as a magnetical probe. Lithium cations are well suited because they typically form complexes at the optimal sites, *i.e.*, the π faces of aromatic systems. Due to the predominantly electrostatic nature of lithium bonding, the experimental ^{7}Li chemical shifts tend to be very similar for most compounds, but can be strongly influenced by the proximity of π systems.[43]

Obviously, it is not possible to prepare the corresponding Li complex for each system under investigation. Moreover, the system is influenced - albeit only slightly - by the proximity of a lithium ion.[43] The use of calculated chemical shifts (Nucleus Independent Chemical Shifts; NICS) therefore expands the possibilities enormously.[43,48]

NICS offers several advantages over other aromaticity criteria. Firstly, it does not necessitate the use of reference standards, increment schemes, or calibration equations for evaluation. Secondly, unlike the susceptibility which relies on the ring area, NICS demonstrates only a modest dependence on the size of the ring. However, it does exhibit a reliance on the number of π electrons. For instance, systems with 10 π electrons yield significantly higher NICS values compared to those with six π electrons, such as the cyclooctatetraene dication and dianion.[43]

2.2 The Jahn-Teller Effect and Valence Tautomerism

In 1937, Jahn and Teller proved by theoretical considerations that a non-linear molecule in a spatially degenerate electronic state is unstable and will reduce its symmetry to lift the degeneracy.[49] A molecule is spatially degenerate when it has molecular orbitals that have the same energy eigenvalue but are filled to different extents. In this situation (for non-linear molecules) there will always be a distortion of the molecule that lowers the energy of the orbitals which are filled to a higher extent and raises the energy of orbitals which are filled to a lower extent, resulting in an overall gain in stability.

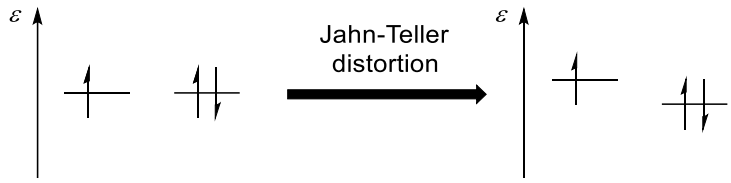

Figure 4: Jahn-Teller distortion of a hypothetical molecule with two degenerate molecular orbitals and 3 electrons.

A Jahn-Teller distortion also occurs in the case of the cyclopentadienyl radical. While the Cp anion with fully filled orbitals assumes a fully symmetric (D_{5h}) shape, the symmetry of the Cp radical, which has one electron less in its orbitals, is lowered to C_{2v}. There are two different ways in which this distortion can occur, depending on which orbital is filled to what extent (cf. Figure 4).

The two differently distorted forms can be called "valence tautomers" if the transitions between these differently distorted forms are interpreted as breaking and forming double and single bonds.

IUPAC defines valence tautomerism as follows:[50]

> The term describes simple reversible and generally rapid isomerizations or degenerate rearrangements involving the formation and rupture of single and/or double bonds, without migration of atoms or groups; e.g.

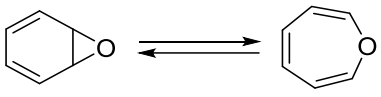

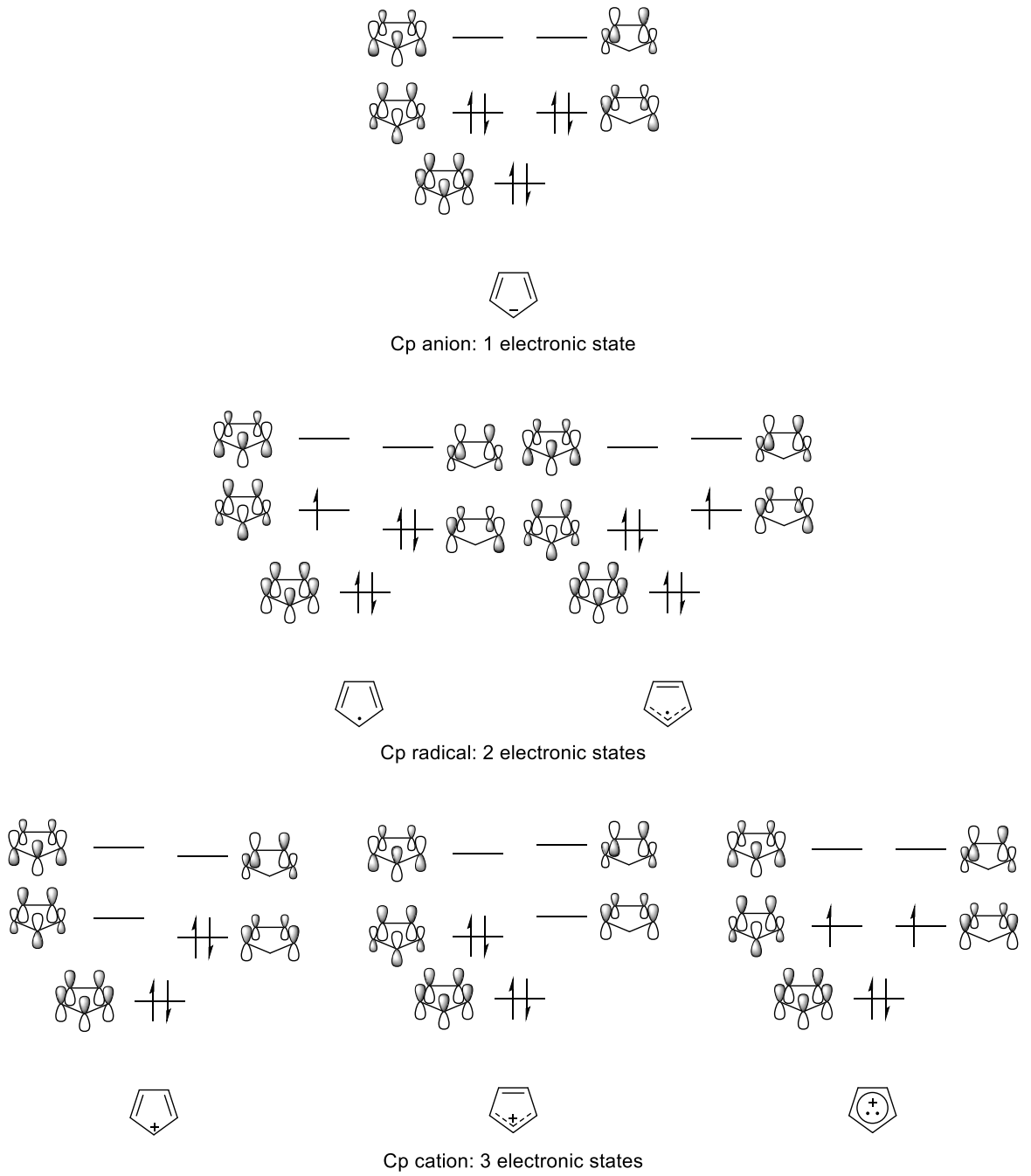

Figure 5: MO diagrams for the different electronic states of Cp anions, radicals, and cations, accompanied by the Lewis structures visualizing the bond length alternations. (Additional excited electronic states exist, but are omitted for clarity).

Sc-XRD analysis has revealed Jahn-Teller distortion in numerous annulenes that do not conform to Hückel's rule. However, at the beginning of the research described here, no sc-XRD data were available for cyclopentadienyl cations, and all known structures of Cp radicals exhibited severe disorder or were substituted in a way that itself strongly influenced their structure.

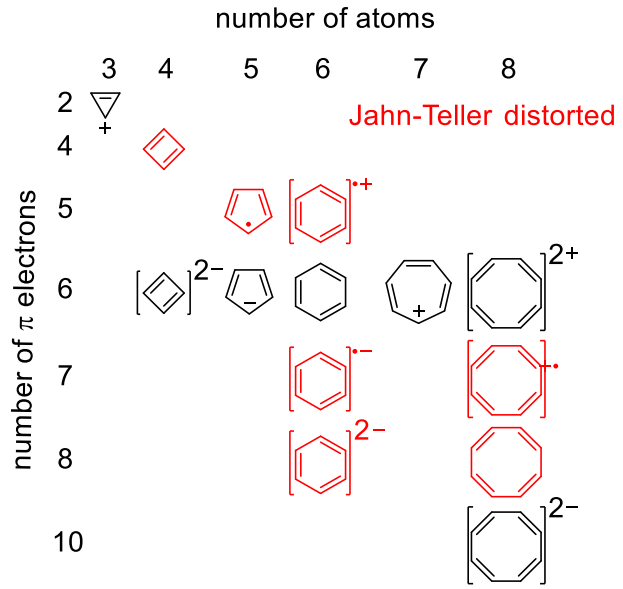

Figure 6: Annulenes with known crystal structures. For exact substitution patterns see the references.[51,52–54]

2.3 Super Acids and Weakly Coordinating Anions

As established by Lewis, acids are compounds which are able to accept electron pairs and bases are compounds which can donate electron pairs.[55] In honor of him, these reagents are also called *Lewis acids* and *bases*.

Because of the abundance of water as a solvent, protons play an especially important role as Lewis acids. Compounds which can release protons therefore have their own name and are called *Brønsted acids* or *Brønsted-Lowry acids*.[56] (Historically, Brønsteds concept is older and was preceded by concepts which relied on the taste of substances or the color change of plant dyes.)[57]

The proton – possessing no electrons – is not susceptible to electronic repulsion, but is itself able to strongly polarize the electron shell of other molecules. Due to their high electron affinity, "naked" protons cannot be observed in the condensed state. Protons are always interacting with molecules of the acid or the solvent.

For Brønsted acids in aqueous solution or in other solvents that can accept protons, the strength of an acid can be measured by its acid dissociation constant, *i.e.* the extent to which the acid protonates the solvent.[58] There are many strong acids which are able to protonate water nearly quantitatively, rendering this measure for their strength insignificant and limiting their utility. The choice of solvent generally has a levelling effect on the maximum acidity that can be reached in this medium,

because only bases that have a higher basicity than the solvent will react quantitatively with the acid.[59]

This problem can be overcome by the use of less basic solvents. $AlCl_3$ in organic solvents and neat sulfuric acid are common examples for acidic media that can exceed the acidity that is amenable in dilute aqueous solutions. Acids which are stronger than these "conventional" acids are considered *super acids*.[59]

In contrast to Brønsted acids in water, there is no single scale of acidity for Lewis or Brønsted acids in other solvents, because the equilibrium constant for their reaction with bases depends on the environment and the order of acidity can be reversed depending on the circumstances. Nonetheless, acids can be compared when a specific reference system is chosen. A well-established reference system is for example the protonation of electron-deficient anilines or other very weak bases as indicators, which can be followed by UV/Vis or NMR spectroscopy.[59,60] By using several pairs of conjugated acids and bases with overlapping ranges this method can be used to define an extension of the pH scale in aqueous solutions to other solvents, known as *Hammett acidity function* (H_0). The H_0 values in different solutions are only comparable if the ratio between the equivalence points of the different indicators is independent of the medium.[60] This assumption is fulfilled well enough to enable at least qualitative comparisons.[59]

Another elegant approach is to measure the electrochemical potential at a reversible hydrogen electrode (H_2/Pt) and compare it with the potential of a redox couple whose potential is assumed to be independent of the solvent like ferrocene/ferrocenium.[61] This method yields another extension of the pH scale and is known as the *Strehlow redox function* ($R_0(H)$).[62] It has been used to compare the acidity of solutions of various Lewis acids in anhydrous HF solution, although it is somewhat limited, because solutions which react with H_2/Pt do not yield meaningful results.

The acidity of Lewis acids can also be evaluated by quantum mechanical computations. In this case, the enthalpy of reaction between the Lewis acid and a model base, often a fluoride or a hydride ion, are calculated, leading to the fluoride (FIA) or hydride ion affinities (HIA).[63] The order of FIA values roughly agrees with

the experimentally determined other acidity measures from Table 1 and has been recently newly determined for an extensive set of compounds with modern methods.[63]

Table 1: pH, pF, R_0(H), and H values of solutions of different buffers in anhydrous HF, determined electrochemically.[61] *Cave*: The pH_{HF} and pF_{HF} values correspond to much higher acidities than the corresponding values in H_2O.[61]

buffer	pH_{HF}	pF_{HF}	R_0(H)	H_0	FIA
SbF_5 (1 mol/L)	0	13.7	−27.9	−22.1	362
$AsF_5/(AsF_6)^-$	2.1	11.6	−25.8	−20.0	323
$TaF_5/(TaF_6)^-$	4.6	9.1	−23.3	−17.5	
$BF_3/(BF_4)^-$	6.6	7.1	−21.3	−15.5	258
$NbF_5/(NbF_6)^-$	7.0	6.7	−20.9	−15.1	
$PF_5/(PF_6)^-$	9.5	4.2	−18.4	−12.6	276
KF (1 mol/L)	13.7	0	−14.2	−8.4	

The conjugate base of a strong acid is necessarily a weak base and does show a low tendency to coordination. Anions which possess this property are called weakly coordinating anions. Their salts show a high solubility in organic solvents, can stabilize unusual electrophilic species and the low electric field at their surface can establish "pseudo gas-phase conditions" in condensed phases.[64] Beside the anions mentioned above, there are newer examples which have been designed to have a low charge density. This is achieved by a low charge – typically singly negative – and by a large size that is often realized by large organic substituents. Fluorination of these substituents distributes the charge and leads to higher stability towards nucleophilic attack. These requirements are for example met by tetrakis(pentafluorophenyl)borate[65] tetrakis(nonafluoro-*tert*-butoxy)aluminate,[66] a variety of carborate anions[67], or many others.[64,68]

The stability of Weakly Coordinating Anions (WCAs) has been compared by computationally studying their stability towards ligand abstraction by the trimethylsilyl cation (Table 2).[69]

Table 2: Reaction energies ΔU in kJ/mol for ligand abstraction by the trimethylsilyl cation for different WCAs in the gas phase, in chlorobenzene solution, and in 1,2-difluorobenzene.[69]

Anion	ΔU (gas)	ΔU (PhCl)	ΔU ($F_2C_6H_4$)
BF_4	−622	−272	−210
PF_6	−566	−228	−168
AsF_6	−534	−203	−145
SbF_6	−471	−164	−109
Sb_2F_{11}	−437	−149	−98
Sb_3F_{16}	−404	−140	−93
Sb_4F_{21}	−402	−145	−100
$[B(OTeF_5)_4]$	−404	−157	−114
$[As(OTeF_5)_6]$	−388	−144	−102
$[Sb(OTeF_5)_6]$	−337	−94	−52
$[Al(OC(CF_3)_3)_4]$	−400	−142	−96
$[(RO)_3AlFAl(OR)_3]$	−301	−65	−23
$R = OC(CF_3)_3$			
$[B(C_6F_5)_4]$	−488	−232	−187
$[B(CF_3)_4]$	−348	−49	+5

The stability of the complex aluminate bases is probably overestimated in this study because they typically decompose by fluoride abstraction and release of perfluoroisobutylene oxide instead of simple ligand abstraction.[70] Moreover, it is noteworthy that among the fluoroantimonates, the Sb_3F_{16} anion is the most stable in polar media. Both higher and lower degrees of condensation (Sb_2F_{11} and Sb_4F_{21}) result in a destabilization.

2.4 Carbocations

A carbocation is a cation that has a substantial portion of its positive charge on a carbon atom.[50] Carbocations can be further divided into carbenium ions, that have at least one important contributing structure containing a tervalent carbon atom with a vacant p-orbital, and carbonium ions which have a higher number of

substituents and often involve three-center-two-electron bonds.[71] Unfortunately both terms are also often used with other meanings.[50]

The actual existence of carbocations has long been unproven. This changed, when compounds containing the tritylium cation were discovered[72] and were soon recognized to behave „salt-like“.[73] The similar nature of many dyes was soon understood.[74]

These triarylmethyl cations were regarded as a peculiar, isolated phenomenon, much like Gomberg's triarylmethyl radicals. In general, hydrocarbon cations were thought to be inherently unstable, and their existence was even questioned due to their transient nature.[71] The realization that carbocations might be intermediates in reactions between neutral molecules came from the observation that the rate of some reactions increased with the dielectric constant of the solvent and in the presence of Lewis acids.[75]

The development of mass spectrometry confirmed the presence of gaseous cations, but it provided no insight into their structure or their behavior in solution chemistry. The direct observation and comprehensive study of stable, long-lasting carbocations, apart from strongly stabilized ones, remained a challenging objective that had yet to be achieved.[71]

The transient nature of carbocations in reactions is a result of their reactivity towards nucleophiles in a system. To isolate them, it is crucial to eliminate the presence of nucleophiles, including nucleophilic solvents or counterions.

In order of increasing rigor, this principle was successfully used by Meerwein to isolate trialkyloxonium salts, by Seel to isolate acetyl tetrafluoroborate, and finally by Olah to isolate a variety of carbocations.[76] The latter was particularly successful because he used very strong Lewis acids such as SbF_5 and weakly basic solvents such as SO_2, SO_2ClF, HSO_3F or HF, often at low temperatures. The carbocations were typically characterized using NMR spectroscopy.[71]

2.4.1 Selected Results

In Friedel-Crafts chemistry, it was observed that the acylation of aromatics with pivaloyl chloride not only yielded the expected ketones but also *t*-butylated

products. It was hypothesized that the formation of these products involved the decarbonylation of the intermediate pivaloyl complex or cation.[77] Consequently, it was not surprising that the $(CH_3)_3CCOF\text{-}SbF_5$ complex exhibited a significant propensity for decarbonylation. Tracking of this process using NMR spectroscopy led to the observation of the formation of the first stable, long-lived alkyl cation salt, specifically *t*-butyl hexafluoroantimonate.

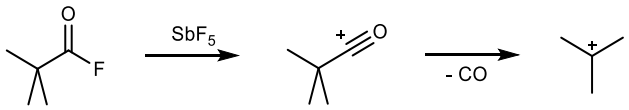

Figure 7: Synthesis of the pivaloyl cation and its decarboxylation to the *t*-butyl cation.

This groundbreaking discovery resulted in other general methods to obtain long-lived alkyl cations in solution.

A noteworthy dispute in carbocation chemistry occurred when non-classical cations were discovered, which questioned the prevailing comprehension of organic structural chemistry during that era. The 2-norbornyl cation played an important role in this debate.[78] In 1949, it was reported that the acetolysis of *exo*-2-norbornyl-*p*-bromobenzenesulfonate was 350 times faster than that of its endo isomer and that the same *exo* acetate was obtained from both reactants under racemization. [79]

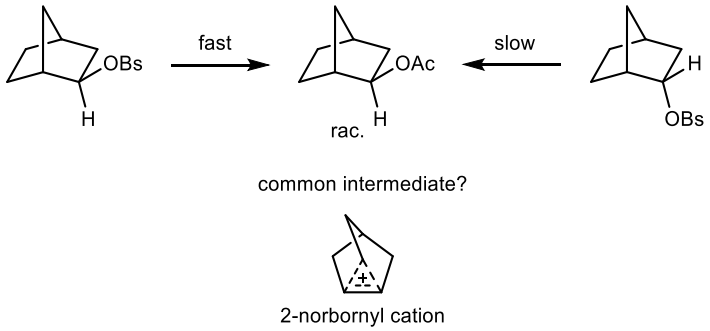

Figure 8: Acetolysis of Norbornylbrosylates and the 2-norbornyl cation.

The explanation of the observations based on bridged or non-classical cations was questioned and an alternative rationalization based on classical cations was proposed. This led to a prolonged debate spanning several decades and involving extensive analysis of spectroscopic and kinetic data.[78] Over time, evidence for a non-classical structure gradually emerged. However, an important missing piece of evidence was finally provided in 2013 through the use of low temperature sc-XRD.

This breakthrough conclusively demonstrated that, at least under these specific conditions,[78] the 2-norbornyl cation is non-classical.[80]

A carbon centered cation which is interesting to discuss in the light of antiaromaticity is the hexamethylbenzene dication. It is prepared by slow dissolution of hexamethyl Dewar benzene epoxide in magic acid (HSO3F/excess SbF5) followed by crystallization *via* addition of an excess of anhydrous HF at low temperatures. When an excess of SbF_5 is used, the dication remains fairly stable in solution at low temperatures.[81] Formally, it should have 4 π electrons and could potentially be planar, making it a candidate for an antiaromatic system. But it evades antiaromaticity through a remarkably strong distortion, as first demonstrated by NMR spectroscopy and reactivity studies beginning in 1973,[82] and later confirmed by sc-XRD.[81]

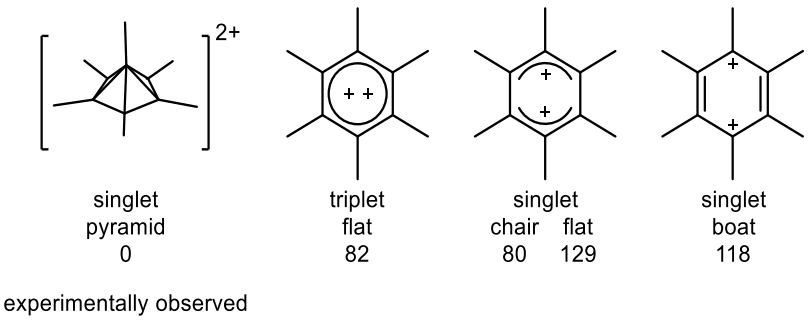

Figure 9: Calculated relative energies of $C_6(CH_3)_6^{2+}$ isomers in kcal/mol.[81]

Some carbon centered radical cations are also worth mentioning, even though they are often not considered "carbocations".[83] Benzene radical cations have for example been investigated in detail. They also show a Jahn-Teller distortion with two possible valence tautomers which have both been observed in the crystalline state (cf. Figure 10).[52–54]

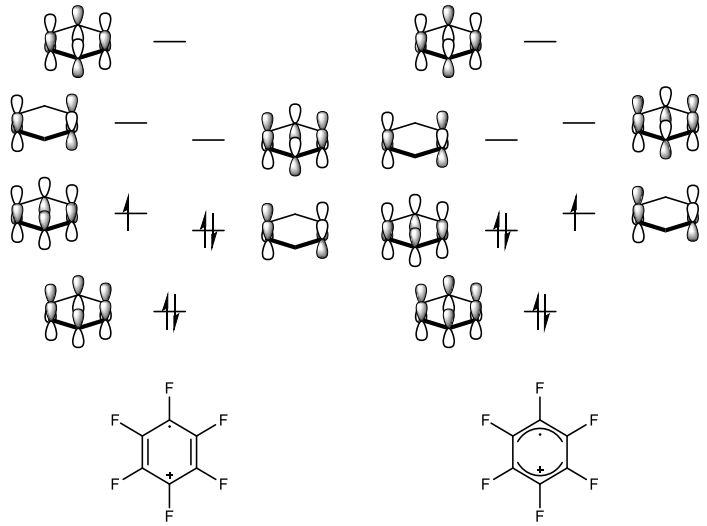

Figure 10: Molecular orbitals of the hexafluorobenzene cation radical.[54]

Another radical cation of interest in this context is the hexamethylbenzene radical cation. This can be prepared in *o*-difluorobenzene, dichloromethane or sulfur dioxide as solvent from hexamethylbenzene by oxidation with iodine and silver tetrakis(perfluoro-*t*-butoxy)aluminate.[84] The reaction of this radical cation with elemental gallium or indium leads to the formation of the hexamethylbenzene complexes of the monovalent gallium or indium ions. The hexamethylbenzene radical cation is thus to be regarded as a ligand-forming oxidizing agent and in this respect is very similar to the cyclopentadienyl radicals.[84]

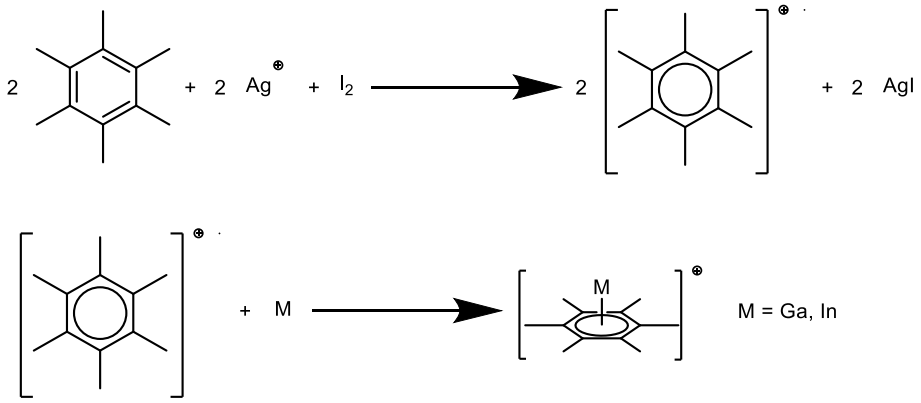

Scheme 1: Reaction of elemental gallium or indium with the hexamethylbenzene radical cation as a ligand-forming oxidant.

2.5 Pentaarylcyclopentadienyl Systems

2.5.1 Ligand Synthesis

The steric protection of reactive systems has emerged as a prominent strategy in organic and organometallic chemistry. It serves as a key approach to successfully isolate challenging targets that would otherwise be difficult to obtain. This strategy has also been applied to cyclopentadienyl systems.

Unfortunately, despite the ease of availability and affordability of the dimer of unsubstituted cyclopentadiene, the synthesis of numerous cyclopentadiene derivatives often involves intricate multi-step procedures. [85]

However, a notable exception is the synthesis of pentaarylsubstituted cyclopentadienes, which provides a contrasting simplicity.

Pentaarylcyclopentadienes are traditionally prepared through laborious multi-step Aldol C–C coupling reactions, which offer the advantage of adaptability for the synthesis of unsymmetrical pentaarylcyclopentadienes.[35,36] Nonetheless, it is a laborious multi-step procedure.

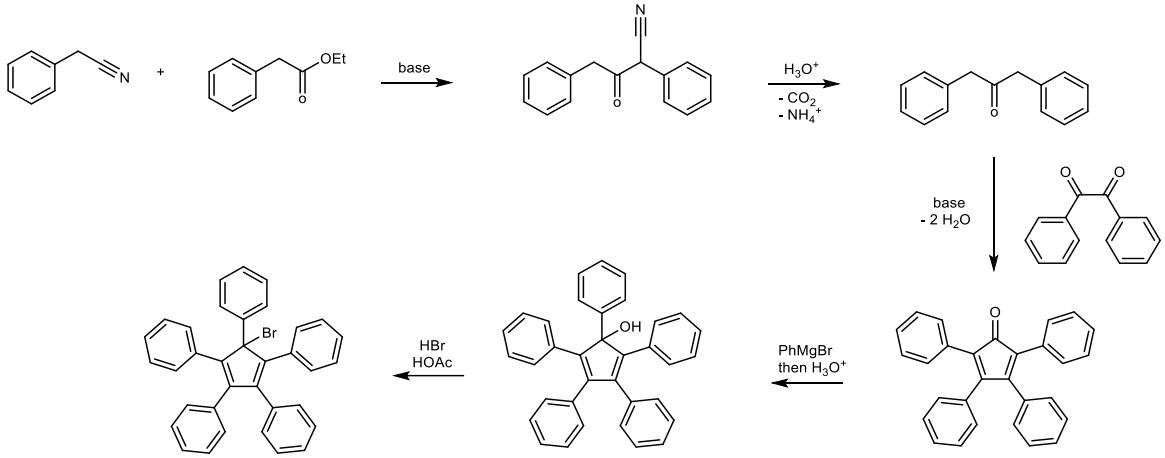

Scheme 2: Example for a synthesis of pentaphenylcyclopentadiene via classical carbonyl reactions.[35,36]

The synthesis of symmetrically substituted Pentaarylcyclopentadienes was significantly improved by Dyker and Miura *et al.*, who designed a one-step synthesis through multiple palladium-catalyzed cross-coupling reactions between zirconocene dichloride and bromoarenes.[86–88]

The synthesis is preferably carried out with aryl bromides. Aryliodides lead by homocoupling to biphenylderivatives as main products. Arylchlorides have not

been investigated, but are generally less reactive than arylbromides in palladium-catalyzed cross-coupling reactions.[88]

When triarylphosphanes are used as ligands in catalytically active palladium complexes, it is observed that the aryl groups used in the phosphane are found in the product. With the exception of the synthesis of pentaphenylcyclopentadiene, where triphenylphosphane can be used, the use of tri-*t*-butylphosphane is recommended, where this problem does not occur.[86]

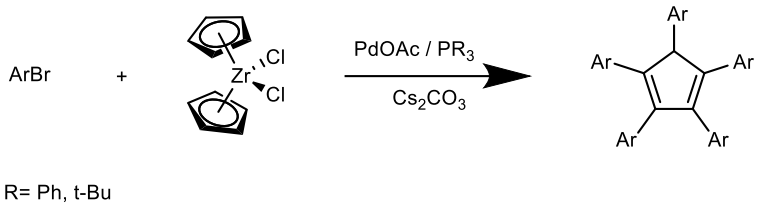

Scheme 3: Synthesis of pentarylsubstituted cyclopentadiene by fivefold Pd-catalyzed cross coupling[88]

2.6 Pentaarylcyclopentadienyl Anions and Pentaarylcyclopentadienyl Metal compounds

2.6.1 Compounds with Monovalent Metals

Sodium, potassium and cesium pentaphenylcyclopentadienide are accessible by the reaction of pentaphenylcyclopentadiene with the alkali metals in boiling toluene.[89] The synthesis of the corresponding lithium compound succeeds using *n*-butyllithium (Scheme 4).[89] In this synthesis, the high reaction temperature of 110 °C is striking, indicating low reactivity of pentaarylcyclopentadienes toward metal alkyls.

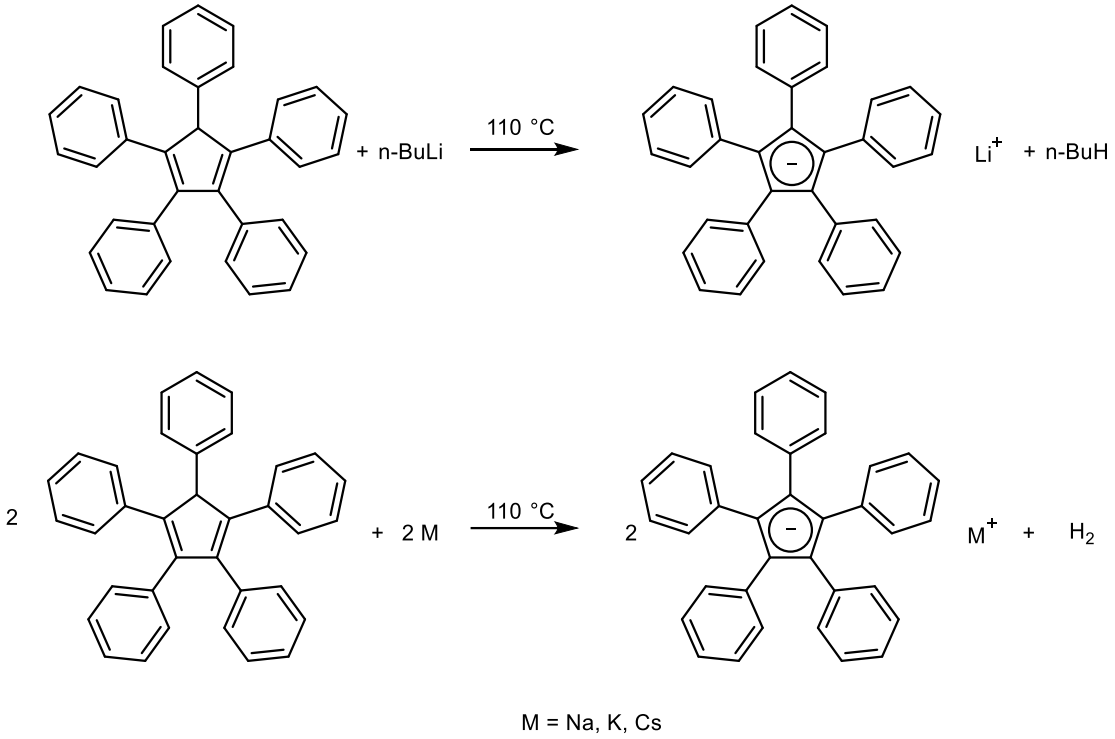

Scheme 4: Synthesis of alkali metal pentaphenylcyclopentadienides.[89]

Giesbrecht *et al*. applied a similar synthetic route to alkyl substituted ligands in the *meta*-position and were able to determine the crystal structures of the substituted lithium cyclopentadienides thus obtained. The crystal structures obtained by them under different crystallization conditions (Figure 11) testifies to the dynamic behavior of the compounds in solution, which could also be verified by ^{7}Li NMR spectroscopy.[90] The ^{7}Li NMR spectrum of the lithium pentakis(3,5-dimethylphenyl)cyclopentadienide shows three signals were be assigned by the authors to different lithium species, which also appear in a similar way in the crystal structures.

As expected from the large steric demand of the ligands, the Li-Cp distance in the aryl-substituted lithium cyclopentadienides is 2.094 Å for the lithium atom coordinated by two ligands (Li1 in Figure 11, top left), significantly higher than the distance of 1.969 Å observed in the unsubstituted compounds.[90] The crystal structure of potassium pentakis-(4-n-butylphenyl)cyclopentadienide is also known (Figure 13) and shows the opposite effect. The aryl-substituted cyclopentadienyl ligands are not further apart here than in unsubstituted potassium cyclopentadienide, as would be expected due to their high steric demand, but come

closer together, as evidenced by a reduced K-Cp distance of 2.664 Å compared to 2.816 Å. This effect is attributed to hydrogen bonds between the *ortho*-carbon atoms of opposing ligands.[91]

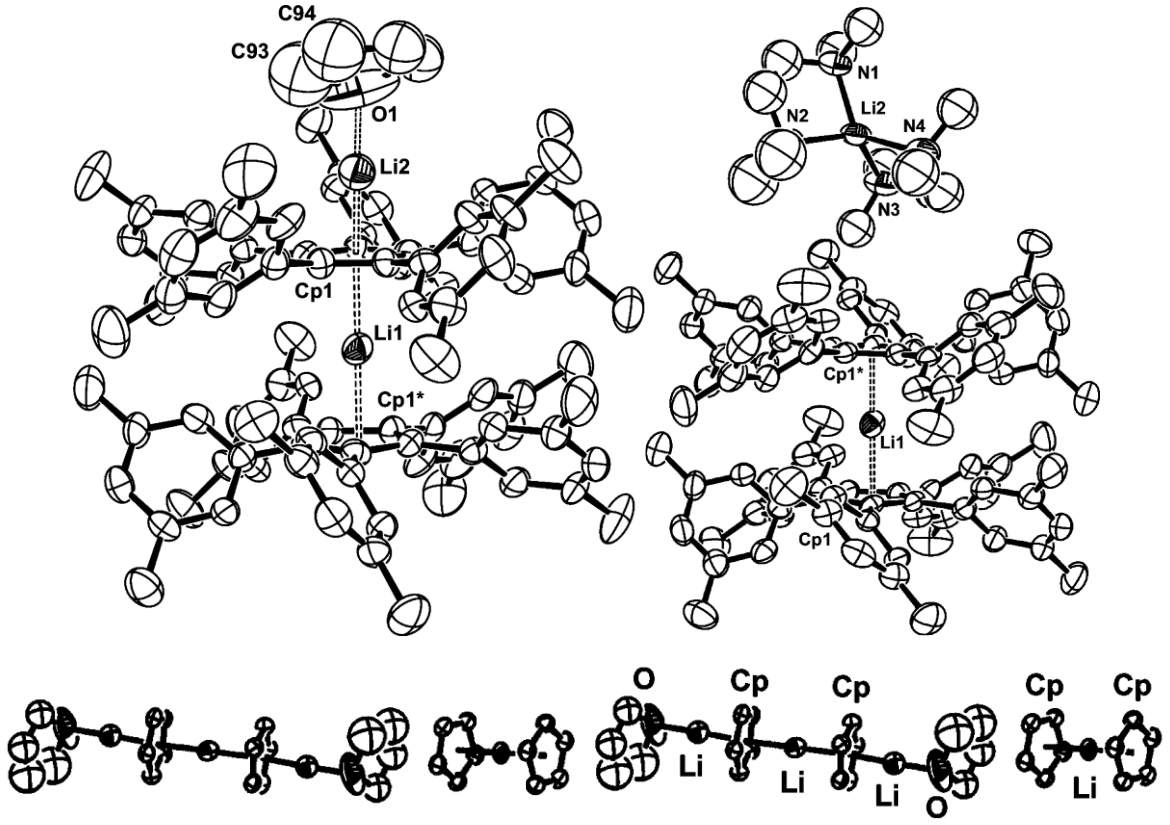

Figure 11: Sections from the crystal structures of lithium pentakis(3,5-dimethylphenyl)cyclopentadienide after crystallization from THF (top left and bottom) or a mixture of THF and tetramethylethylenediamine (top right). Hydrogen atoms and the aryl groups in the lower image are omitted for clarity.[90]

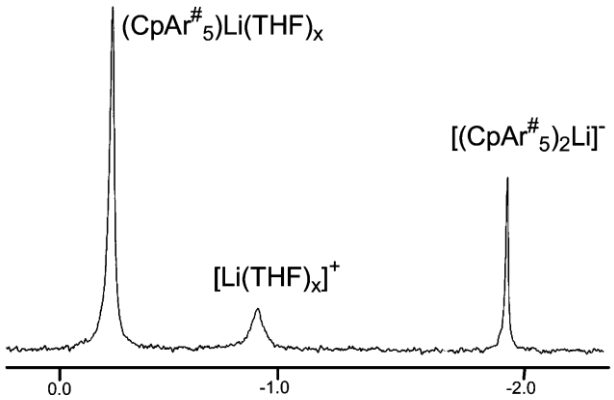

Figure 12: ^{7}Li NMR spectrum of lithium pentakis(3,5-dimethylphenyl)cyclopentadienide in THF-d_8.[90]

These hydrogen bonds are probably also the reason for the linear environment of half of the potassium ions. While the polymeric chains of unsubstituted potassium cyclopentadienide are bent from potassium ion to potassium ion by an angle of 138° in each case, two different types of potassium ions occur in potassium pentakis(4-*n*-butylphenyl)cyclopentadienide, one of which is exactly linearly coordinated because the potassium ions are located on inversion centers of the crystal. The coordination geometry of the other type of potassium ions also deviates only slightly from linearity at 167.7°.[91,92]

Also of note, potassium pentakis(4-*n*-butylphenyl)cyclopentadienide crystallizes from a diethyl ether-containing solvent mixture in solvent-free form.[91] This fact also indicates a particularly high stability of the obtained complex.

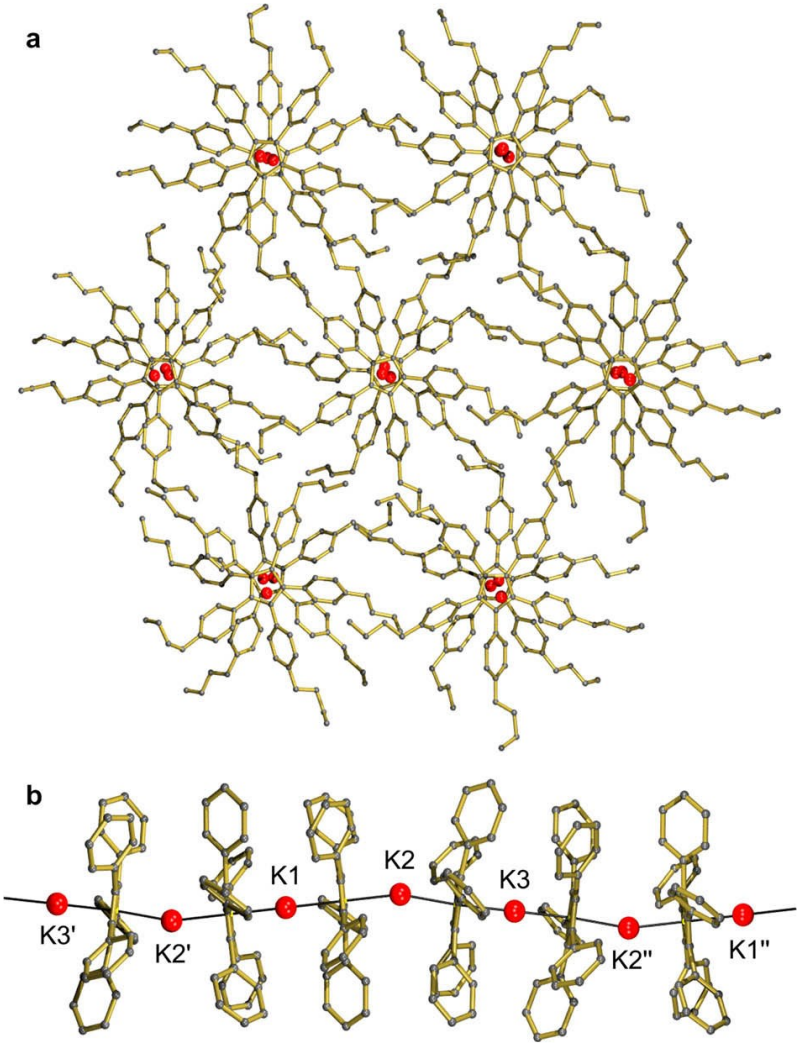

Figure 13: Crystal structure of potassium pentakis(4-*n*-butylphenyl)cyclopentadienide with viewing direction parallel (a) or perpendicular (b) to the polymeric chain structures. The hydrogen atoms as well as the butyl groups in figure b are omitted for clarity.[91]

The sodium, indium(I) and thallium(I) complexes of *para*-alkyl substituted pentaphenylcyclopentadienes were investigated for their suitability to form liquid crystalline mesophases.[93] While this desired goal was not achieved by the authors, they were nevertheless able to develop methods for the synthesis of the desired target compounds. Thus, the deprotonation of the cyclopentadienes studied succeeds with both sodium amide and thallium(I) ethanolate in THF. The indium(I) complexes are accessible by salt metathesis between the sodium cyclopentadienides and indium(I) chloride (Scheme 5).[93]

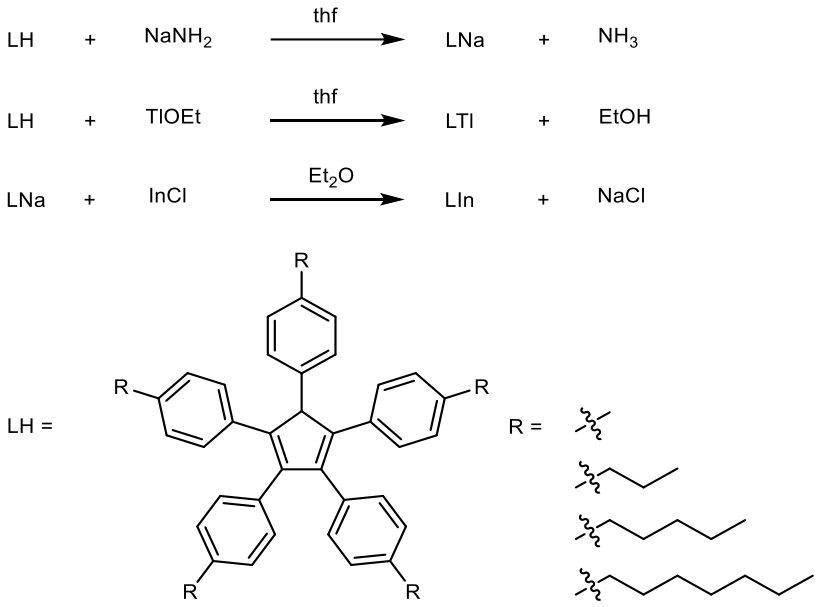

Scheme 5: Possibilities for the synthesis of the sodium, indium(I) and thallium(I) derivatives of *para*-alkylated pentaphenylcyclopentadienes.[93]

In DMSO, all the complexes obtained are completely dissociated, as evidenced by the absence of metal-^{13}C coupling in the NMR spectra of the products.

2.6.2 Compounds with Divalent Metals

So far, the decaarylmetallocenes of the divalent metals calcium, barium, germanium, tin, lead, ytterbium, europium, samarium, iron and nickel are known.[94–96] All unsubstituted decaphenylmetallocenes exhibit low solubilities in common organic solvents at room temperature. For example, boiling 1-methylnaphthalene is reported as a suitable solvent for the crystallization of decaphenylstannocene.[94]

One way around this problem is to isolate the solvent-separated ion pairs $[M(THF)_6][C_5Ph_5]_2$, which can then be converted to the desired decaphenylmetallocenes by precipitation with toluene (Scheme 6).[95]

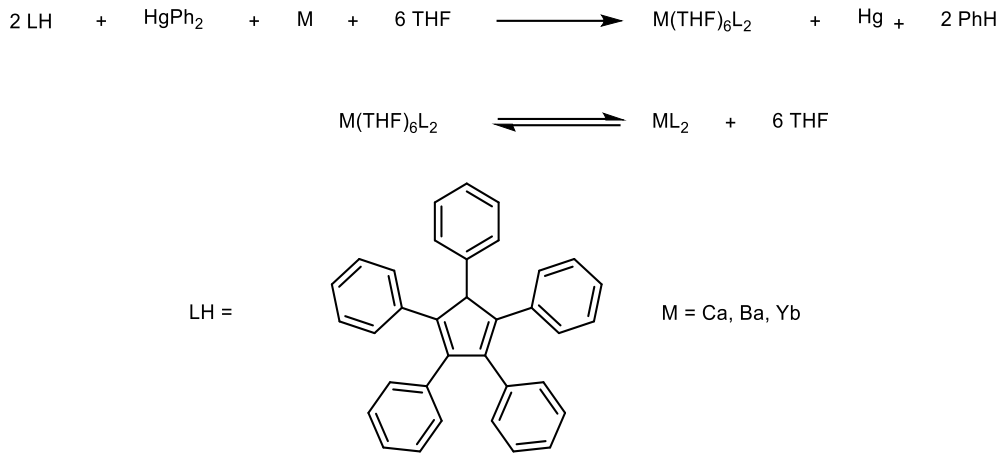

Scheme 6: Synthesis of decaphenylcalcocene, -barocene, and -ytterbocene via the solvent-separated ion pairs.[95]

Harder *et al.* have taken a different route to increase the solubility of decaarylmetallocenes and thus use the pentakis(4-*n*-butylphenyl)cyclopentadienyl ligand ($Cp^{Big\ n\text{-}Bu}$), whose derivatives are very soluble in organic solvents. For this ligand the compounds with divalent calcium, strontium, barium, tin, europium, yttrium, ytterbium and samarium are known.[91,97,98]

The syntheses of the alkaline earth metal complexes again show the low tendency of the pentaarylcyclopentadienes to react with metal alkyls. Despite the high basicity of the alkaline earth metal benzyls used, reaction times in these cases were up to 72 h at 60 °C.[91]

An analysis of the crystal structures of the above compounds leads to the conclusion that hydrogen bonds between the *ortho*-carbon atoms of the ligands also play a major structure-determining role in these systems.[99]

These are also the reason why all known representatives of the decaphenylmetallocenes crystallize in the arrangement with S_{10} symmetry (Figure 14), since only in this arrangement suitably oriented CH–C contacts are possible.[99]

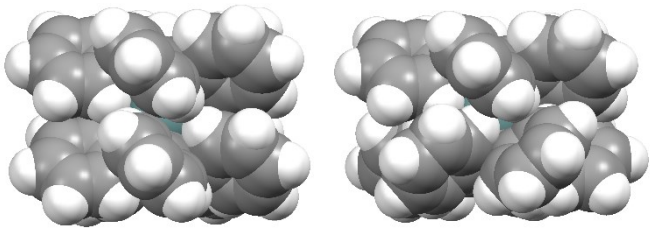

Figure 14: Conformational isomers of decaarylmetallocenes with D_5 symmetry (left) and S_{10} symmetry (right).

The attraction of the ligands mediated by the hydrogen bonds can also be seen from the fact that the aryl groups of the ligands are bent toward the metal when the distance is sufficiently large. The diffraction angle is an approximately linear function of the distance between the metal ion and the cyclopentadienyl ring.[99]

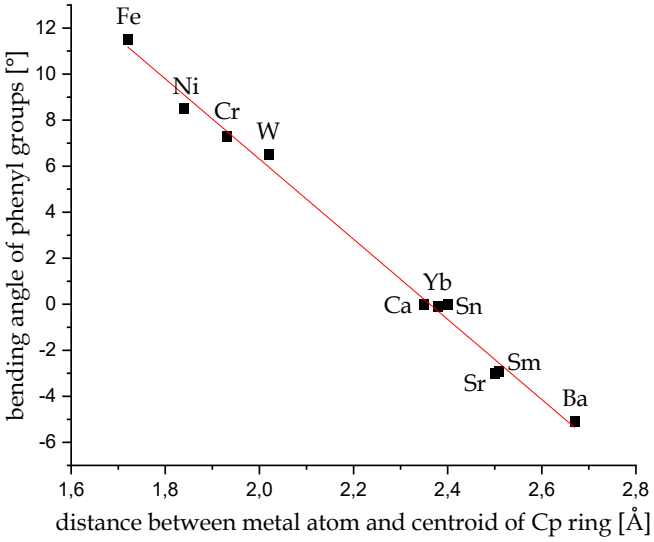

Figure 15: Dependence of the bending angle on the distance between the metal ion and the geometric center of the cyclopentadienyl ring.[99]

For small cations, the opposite effect is observed and the aryl groups bend away from the metal. Steric reasons are probably responsible for this effect.

While the influence of a single one of these hydrogen bonds is only relatively small with 2 - 5 kcal/mol, the total influence of all ten hydrogen bonds is probably significant for the structure formation.[97]

Due to the great steric demand and the high rigidity of this ligand class, their complexes have further unusual properties. For example, all known decaarylmetallocenes have a linear structure, in contrast to differently substituted

metallocene derivatives of tin and lead.[94,97] This is seen as an indication that the angled arrangement of many unsubstituted metallocenes is not due to electronic reasons, but results from van der Waals attraction of the ligands.[97] This argument does not hold for the calcium, strontium, barium and lanthanoid(II) metallocenes. They, too, show a parallel position of the ligands and a linear ligand-metal-ligand arrangement on time average. However, a high anisotropy of the electron density at the metal center indicates a highly fluctuating structure in which the metal center is bent out of the line connecting the ligand centers.[97,98]

An unusual application for organometallics of some decaarylmetallocenes is in cancer therapy. Decaphenylgermanocene and -stannocene, for example, show promising properties as cancerostatic agents with significantly higher activity than the free ligands.[100,101] Among the organometallic compounds, cancerostatic properties are otherwise known almost only from the compounds of the platinum metals.[100,101]

Decaphenyleuropocene further exhibits strong luminescence in the solid and in solution at an emission wavelength of 606 nm and with a quantum yield of 45%.[96] Due to the small ionic radius of the iron(II) ion (75 pm)[102] the synthesis of a decaphenyl ferrocene is fraught with difficulties, in contrast to the synthesis of the unsubstituted ferrocene. However, the synthesis succeeds by reacting pentaphenylcyclopentadienyl bromide with iron pentacarbonyl followed by disproportionation.[93]

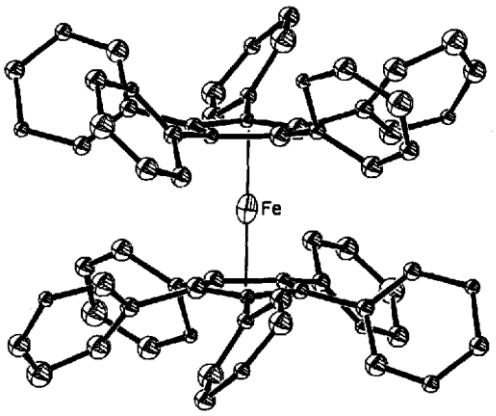

Figure 16: Solid-state structure of decaphenylferrocene.[93]

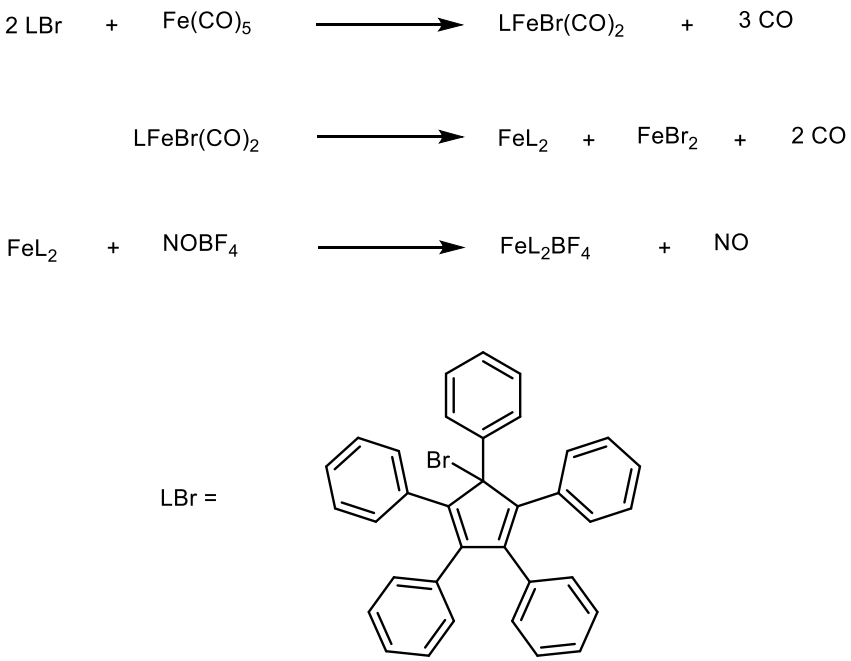

Scheme 7: Synthesis of decaphenylferrocene and oxidation with nitrosyltetrafluoroborate to give decaphenylferrocenium tetrafluoroborate.[93]

The decaphenylferrocene thus obtained can be oxidized in a further synthesis step with nitrosyltetrafluoroborate to give decaphenylferrocenium tetrafluoroborate (Scheme 7).

Decaphenylferrocene is stable to humid air and dilute hydrochloric acid and is sparingly soluble at room temperature in all solvents studied. Decaphenylferrocenium tetrafluoroborate, on the other hand, dissolves well in polar organic solvents.[93]

The large steric demand of the pentaphenylcyclopentadienyl ligand is demonstrated by the example of ferrocene by the existence of another coordination isomer in which one of the ligands η^6 is bonded via a phenyl group, thus partially evading the steric pressure of the other ligand (Figure 17).[103]

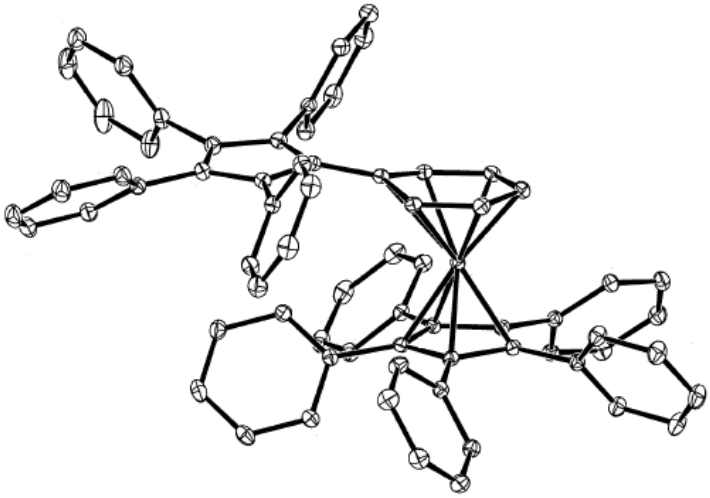

Figure 17: Solid-state structure of the coordination isomer of decaphenylferrocene.[103]

The isomeric decaphenylferrocene converts to the symmetric form upon heating in solution or under acid catalysis.[103]

Since the pentaarylcyclopentadienyl ligands in the decaaryl metallocenes show strong attractive interactions with each other and the coordination of a third of these ligands is simultaneously impossible for steric reasons, the oxidation number +II is strongly preferred in the corresponding metal complexes.. The strong attractive interactions of the ligands are reflected in the relatively simple synthesis of the lanthanoid(II) metallocenes and in the fact that the Schlenk equilibrium for the half-sandwich complexes of the alkaline earth metals is completely on the side of the homoleptic complexes.[96–98]

When it is attempted to synthesize trivalent ytterbium complexes of the $Cp^{Big\ n\text{-}Bu}$ ligands, spontaneous reduction of the metal center occurs and the homoleptic complex $(Cp^{Big\ n\text{-}Bu})_2Yb$ is formed (Scheme 8).

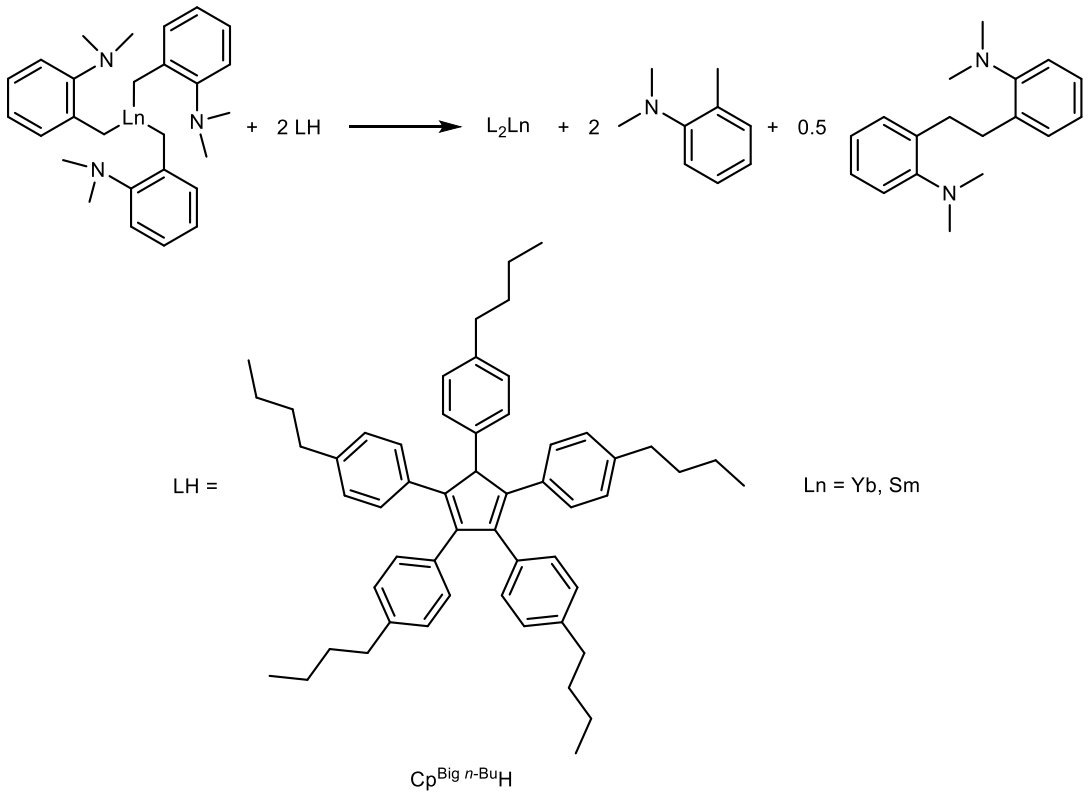

Scheme 8: Formation of ytterbium(II) and samarium(II) decaaryl metallocenes by spontaneous reduction,[98] and definition of $Cp^{Big\ n\text{-}Bu}H$.

While the spontaneous reduction of europium ($E°(Eu^{3+}/Eu^{2+}) = -0.35$ V)[104] is a frequently observed process, there are few other examples of such a process for ytterbium ($E°(Yb^{3+}/Yb^{2+}) = -1.15$ V).[104] For example, the reduction of $(MeC_5H_4)_2YbMe$ with elimination of ethane to $(MeC_5H_4)_2Yb$ succeeds only with the addition of diethyl ether and after heating to 80 °C for several hours.[98]

The spontaneous reduction to the lanthanoid(II) decaryl metallocenes succeeds even in the case of the even more reducing samarium ($E°(Sm^{3+}/Sm^{2+}) = -1.55$ V).[98,104] Samarium(II) compounds are so reducing that samarium(II) iodide has found many applications in organic chemistry as a one-electron reducing agent, for example, for reductive initiation of radical reactions.[105] Decamethylsamarocene is even reactive enough to react with elemental nitrogen.[106] In this context, the spontaneous reduction of a samarium(III) compound to a samarium(II) compound is noteworthy. $(Cp^{Big\ n\text{-}Bu})_2Sm$ on the other hand, is so stable that it behaves inertly toward most of the potential reactants studied.[106,107] The only exceptions where a reaction was observed were cuminil and the combination of phenazine and dioxygen (Scheme 9). No reaction was observed

with ketones, white phosphorus, dinitrogen, carbon dioxide, carbon monoxide, pyridines or alkenes.

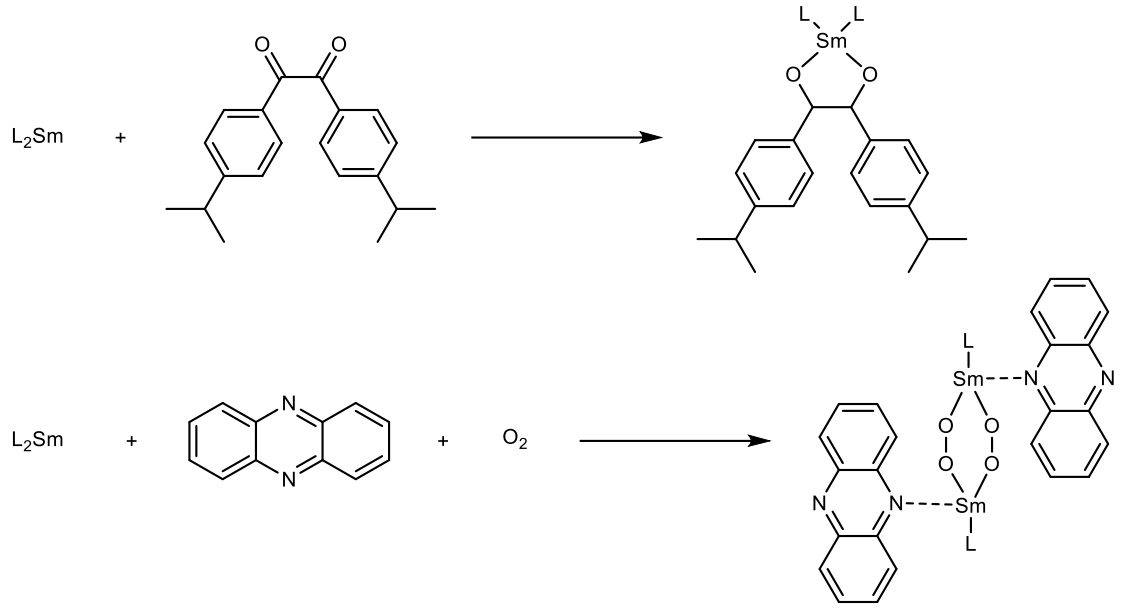

Scheme 9: Reaction of ($Cp^{Big\ n\text{-}Bu}$)$_2$Sm with cuminil and with oxygen in the presence of phenazine (L = $Cp^{Big\ n\text{-}Bu}$).

It is assumed that in the case of both ytterbium and samarium a lanthanoid(III) complex forms first, which in addition to the two $Cp^{Big\ n\text{-}Bu}$ ligands also contains a dimethylaminobenzyl ligand bonded to the metal, which is then cleaved off in the sense of a sterically induced reduction. The 1,2-bis-(2-(dimethylamino)phenyl)ethane expected as a by-product in this case could be detected in the reaction mixture. Nevertheless, the postulated reaction mechanism cannot be definitively proven beyond doubt. The intermediate formation of $Cp^{Big\ n\text{-}Bu}$ radicals seems likely due to their stability. The reactivity of the related, sterically also strongly overloaded samarium complex Sm(Cp*)$_3$ is much better studied. Although it is a samarium(III) complex, it has a strong reducing effect. This is explained by the fact that Sm(Cp*)$_3$ is in equilibrium on the one hand with decamethylsamarocene Sm(Cp*)$_2$ and the dimer of the pentamethylcyclopentadienyl radical (Cp*)$_2$ and on the other hand with the separated ion pair [Sm(Cp*)$_2$]$^+$[Cp*]$^-$. Both Sm(Cp*)$_2$ and the free pentamethylcyclopentadienyl anions can then act as reducing agents.[108]

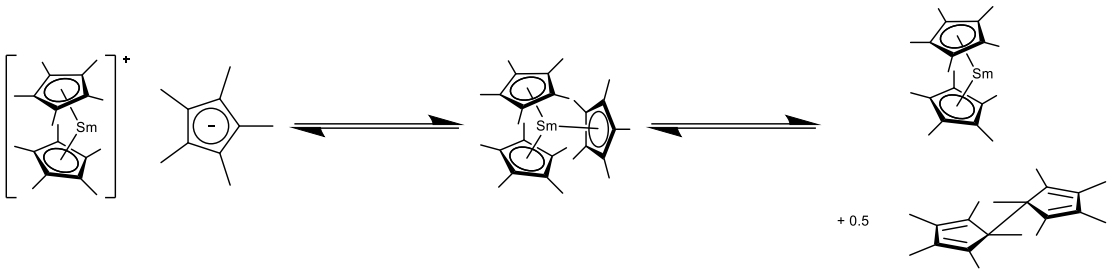

Scheme 10: Equilibrium of $Sm(Cp^*)_3$ with $Sm(Cp^*)_2$ and $[Sm(Cp^*)_2]^+$ $[Cp^*]^-$.[108]

The equilibrium between $Sm(Cp^*)_3$ on one side, and $Sm(Cp^*)_2$ and $(Cp^*)_2$ on the other side is strongly reminiscent of the mechanism of sterically induced reduction of pentaarylcyclopentadienyl-substituted ytterbium and samarium compounds postulated above.[108,109] In the first case, however, the equilibrium is far on the side of the trivalent compound, in the second case on the side of the divalent compounds. This particular stability of the divalent decaarylmetallocenes is again attributed to the formation of a hydrogen bonding network between the ligands, as already mentioned.[98]

2.6.3 Other Compounds of Pentaaryl Cyclopentadienyl Anions

In contrast to the reactions of the corresponding europium, ytterbium and samarium compounds, the reaction of $Cp^{Big\ n\text{-}Bu}H$ with tris-(2-dimethylaminobenzyl) yttrium does not lead to the spontaneous reduction of the metal to form a sandwich complex due to the significantly lower stability of the divalent oxidation state. Instead, the reaction stops at the stage of the isolatable half-sandwich complex.[98]

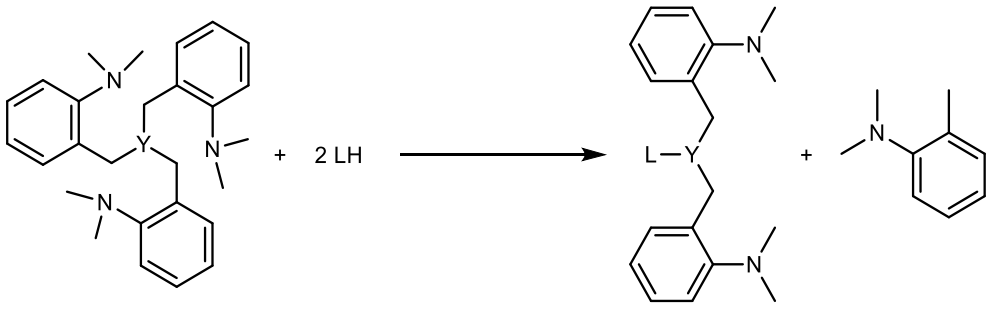

Scheme 11: Synthesis of the complex $Cp^{Big\ n\text{-}Bu}Y(2\text{-}Me_2N\text{-}benzyl)_2$ (L = $Cp^{Big\ n\text{-}Bu}$).[98]

Despite the great stability of the homoleptic complexes of pentaarylcyclopentadienyl ligands, some half-sandwich complexes of this ligand type with transition metals are also known. For example, salt metathesis of

$Cp^{Big\ n\text{-}Bu}K$ with iron(II), nickel(II), and cobalt(II) bromide in THF yields the respective half-sandwich complexes $Cp^{Big\ n\text{-}Bu}FeBr$, $Cp^{Big\ n\text{-}Bu}NiBr$, and $Cp^{Big\ n\text{-}Bu}CoBr$ (Scheme 12). The syntheses were also performed with the similar $Cp^{Big\ Et}$ ligand.[110]

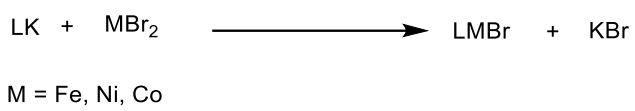

Scheme 12: Synthesis of transition metal half-sandwich complexes (L = $Cp^{Big\ n\text{-}Bu}$).[110]

Such half-sandwich complexes are useful intermediates for introducing $Cp^{Big\ Et}$-metal fragments into other compounds.[110,111] That this stabilization of the half-sandwich complex also succeeds when pentaarylcyclopentadienyl ligands are used seems at first surprising, since in the case of the alkaline earth metal and lanthanide complexes of this ligand it has been shown that the Schlenk equilibrium is on the side of the homoleptic complexes.[112] A possible explanation for this different behavior lies in the smaller ionic radii of iron, nickel and cobalt compared to the alkaline earth metals and lanthanides. While for the latter there is an attraction of the ligands by hydrogen bonds, which is also noticeable by a convergence of the aryl groups of the ligands, a repulsive interaction is more likely to occur at smaller distances between the ligands due to a smaller size of the metal ion.

In this case, the boundary between attractive or repulsive interaction of the ligands would be assumed to be approximately at a metal-ligand distance of 2.3 Å (Figure 15).

The large steric demand of pentaarylcyclopentadienyl ligands promises applications in the synthesis of particularly selective catalysts. In some cases, this concept has been realized.

While mixtures of chromium(III)-2-ethyl hexanoate, triethylaluminum and hexachloroethane as chloride source normally catalyze the polymerization of ethene, the addition of pentaphenylcyclopentadiene to this system leads to the selective formation of 1-hexene (selectivity of 70%), a valuable starting material for the preparation of copolymers.[113]

The enantioselectivity of chiral catalysts can also be greatly enhanced by the introduction of a pentaphenylcyclopentadienyl group. Scheme 13 shows the use of

a chiral substituted ferrocene as a nucleophilic catalyst for the enantioselective acetylation of alcohols.

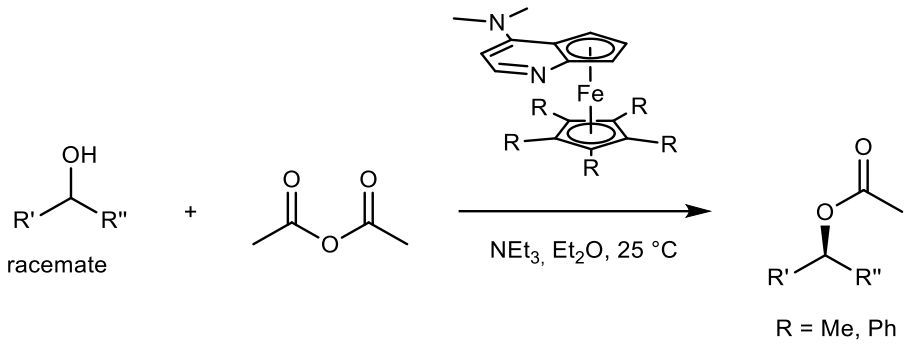

Scheme 13: Enantioselective acetylation of alcohols using a substituted pentaphenylferrocene as a chiral catalyst.[114]

The sterically less demanding pentamethylcyclopentadienyl complex (R = Me) shows almost no enantioselectivity, while the use of the corresponding pentaphenylcyclopentadienyl complex (R = Ph) leads to high enantiomeric excesses between 95.2% and 99.7%.[114]

The promising results in the use of the pentaphenylcyclopentadienyl ligand to increase the selectivity of catalysts suggest a reasonable use of this ligand in Kaminsky catalysts. Pentaphenylcyclopentadienylzirconium trichloride and some related compounds are known but have not been evaluated for their ability to polymerize alkenes.[115] However, they exhibit Lewis acidic properties and can catalyze Diels-Alder reactions.[115]

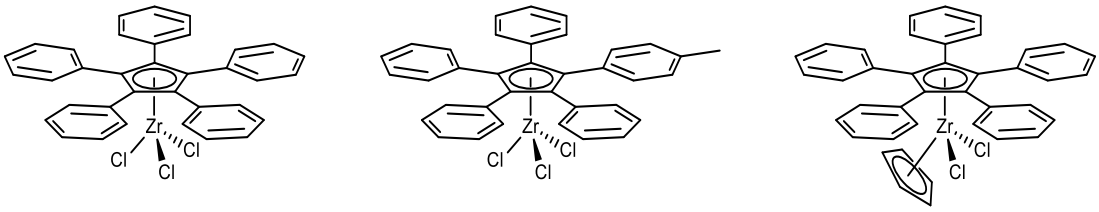

Scheme 14: Known zirconium compounds with pentaarylcyclopentadienyl ligands.[115]

2.7 Cyclopentadienyl Radicals

2.7.1 Reactivity

Due to their large conjugated π electron system, pentaarylcyclopentadienyl systems form stable radicals that do not dimerize. The longest-known representative of this group of substances, the pentaphenylcyclopentadienyl radical, was first prepared

in 1925 and can be stored indefinitely in the absence of oxygen.[116] Pentakis-(4-alkylphenyl)cyclopentadienyl radicals, on the other hand, are known to decompose in solution at room temperature within hours to days, with the substituted cyclopentadiene, among others, being reformed.[117]

The ESR spectrum of the pentaphenylcyclopentadienyl radical shows a multiplet with 33 lines resulting from the hyperfine structure splitting with the phenyl protons. The measured g-value of 2 is identical to that of the free electron within the limits of measurement accuracy.[118]

The pentaarylcyclopentadienyl radicals are strongly colored in solution and as solids, which simplifies their optical detection in solution and makes it easy to tailor reaction times to individual reactants.[116,117]

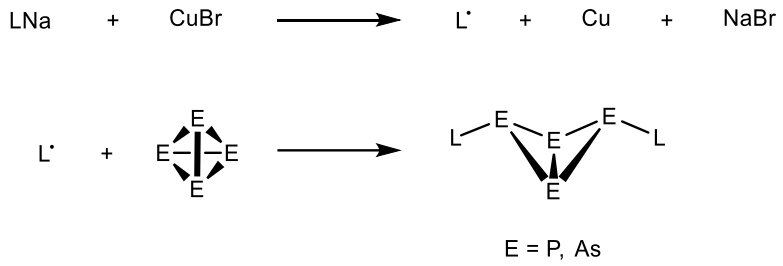

Scheme 15: Reaction of different alkyl substituted pentaarylcyclopentadienyl radicals with white phosphorus and yellow arsenic under homolytic bond breaking of a P–P and As–As bond, respectively.[117,119]

However, despite these promising properties as reactants for the synthesis of organometallic derivatives, very few examples of the application of the pentaarylcyclopentadienyl radicals have been published. These are mainly limited to the activation of white phosphorus and yellow arsenic (Scheme 15), and to the synthesis of decaphenylnickelocene from nickel(0)-alkene complexes.

In addition, it is known that pentaarylcyclopentadienyl radicals can act as single-electron oxidizing agents toward transition metal halides. This reaction has been studied with cobalt(II) iodide and nickel(II) iodide (Scheme 16).[110]

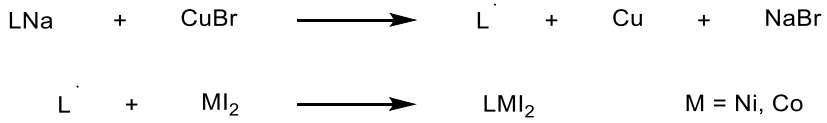

Scheme 16: Reaction of nickel(II) and cobalt(II) iodide with pentaarylcyclopentadienyl radicals (L = Cp$^{Big\ n\text{-}Bu}$).[110]

Another known stable substituted cyclopentadienyl radical is the pentaisopropylcyclopentadienyl radical. This can be obtained from sodium pentaisopropylcyclopentadienide with both iron(II) bromide and bromine as oxidizing agent at low temperatures (Scheme 17).[120,121]

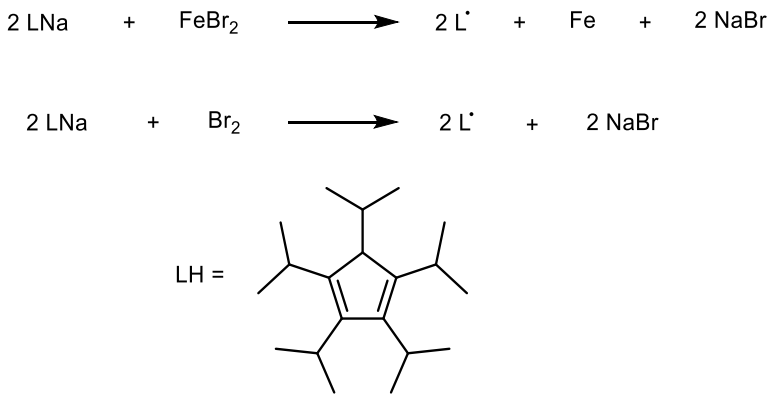

Scheme 17: Syntheses of the pentaisopropylcyclopentadienyl radical.[120,121]

The ESR spectrum of the pentaisopropylcyclopentadienyl radical shows a broad singlet at room temperature that is split by hyperfine coupling at 190 K to form a multiplet with 20 lines. A simulation of the spectrum yields a coupling constant of 0.16 G to the methine protons and 0.32 G to the methyl protons. The small coupling constant to the methine protons is due to the fact that the CH bond is nearly perpendicular to the π-orbitals.[120] The observed g-value of 2.0025 is identical to that of the free electron within the limits of measurement accuracy.

The reaction of the pentaisopropylcyclopentadienyl radical with metallic calcium, strontium, barium, samarium, europium, and ytterbium leads directly to the decaisopropyl metallocenes. In the latter case mercury was used to activate the metal.[122]

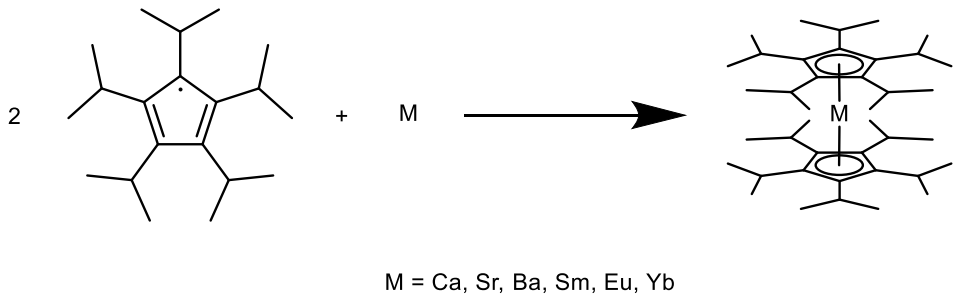

Scheme 18: Synthesis of decaisopropyl metallocenes by reaction of decaisopropylcyclopentadienyl radical with different metals.[122,123]

In the case of the alkaline earth metals, the reaction in liquid ammonia is particularly suitable, since the metals are soluble in this reaction medium with the formation of electride solutions.[123] However, the reaction also succeeds in THF using ultrasound.[123]

2.7.2 Crystal Structures

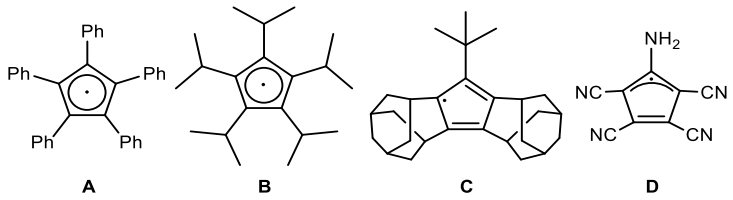

Figure 18: Cp radicals with known crystal structures.

When the work described here was begun, only 4 cyclopentadienyl radicals were characterized by sc-XRD. Unfortunately, the crystal structures of symmetrically substituted cyclopentadienyl (Cp) radicals **A** and **B** (Figure 18) display significant crystallographic disorder, making it impossible to determine their exact symmetry. In contrast, asymmetrically substituted Cp radicals such as **C** and **D**, as well as other cyclopentadienyl and fluorenyl-based radicals, have yielded high-quality crystal structures that reveal deviations from five-fold symmetry. However, it should be noted that the unequal electronic influences of the various substituents in these asymmetrically substituted Cp radicals can interfere with the fundamental electronic factors contributing to the deviation from five-fold symmetry in these compounds.

2.8 Cyclopentadienyl Cations

Cyclopentadienyl cations are typically unstable compounds.[28] As singlet systems they are antiaromatic and therefore destabilized and as triplet systems, they are aromatic,[31,124] but still very reactive. The study of cyclopentadienyl systems often involves their stabilization in a frozen matrix at low temperatures. This has for example been accomplished in frozen SbF_5 for the parent $C_5H_5^+$ and $C_5Cl_5^+$, which exhibit a triplet ground state.[29,30,125] The singlet ground state is more stable for pentaarylcyclopentadienyl cations and due to steric shielding and charge delocalization they are persistent enough to be observed in chloroform or dichloromethane solutions at low temperatures.[21,33–36]

2.9 Fluorinated Cyclopentadienyl Ligands

While electron-rich cyclopentadienyl ligands are widely used in organometallic chemistry, cyclopentadienyl ligands with fluorinated substituents are relatively rare. This rarity can be attributed to the challenges associated with both the synthesis of these ligands and their subsequent coordination to transition metals. However, due to the electron withdrawing properties of fluorinated substituents, complexes containing such ligands often exhibit enhanced oxidative stability or other desirable properties.[126]

Examples of fluorinated Cp ligands include $C_5F_5^-$, $C_5(CF_3)_5^-$ and $C_5(C_6F_5)_4H^-$. The preparation of these ligands often requires the use of sophisticated experimental techniques or reagents like the use of elemental fluorine or flash vacuum pyrolysis.

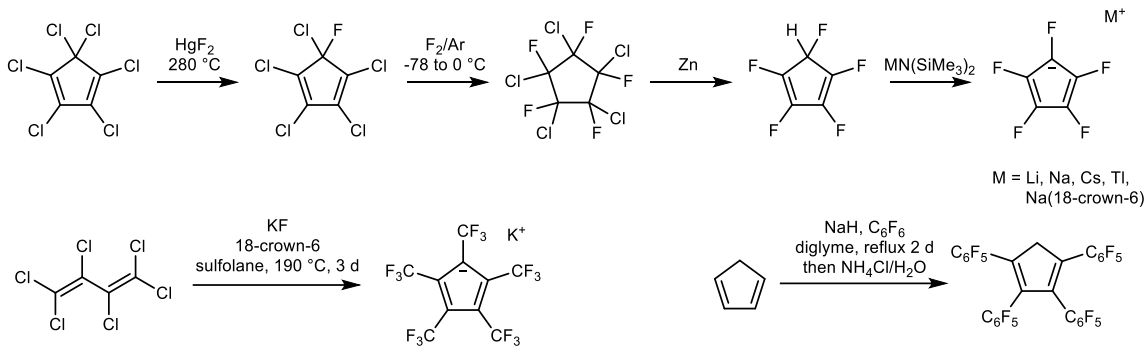

Scheme 19: Synthesis of pentafluorocyclopentadiene,[127–129] pentakis(trifluoromethyl) cyclopentadiene and tetrakis(pentafluorophenyl)cyclopentadiene.

Pentafluorocyclopentadiene can be synthesized through a three-step process involving the exhaustive fluorination of pentachlorofluorocyclopentadiene using elemental fluorine, followed by reduction with zinc (Scheme 19). Regrettably, its salts decompose in solution, resulting in the formation of metal fluorides. However, it has been observed that the salts of cesium and thallium decompose relatively slowly at room temperature.[129]

The authors who prepared the pentafluorocyclopentadienyl anion also tried to generate the corresponding cation, but these attempts were unsuccessful. The precursor hexafluorocyclopentadiene was prepared in a similar way as pentafluorocyclopentadiene (Scheme 20). A reaction was only achieved with the very strong fluoride acceptors AsF_5 and SbF_5, but did not lead to the desired cation. Instead, addition to a double bond was observed.

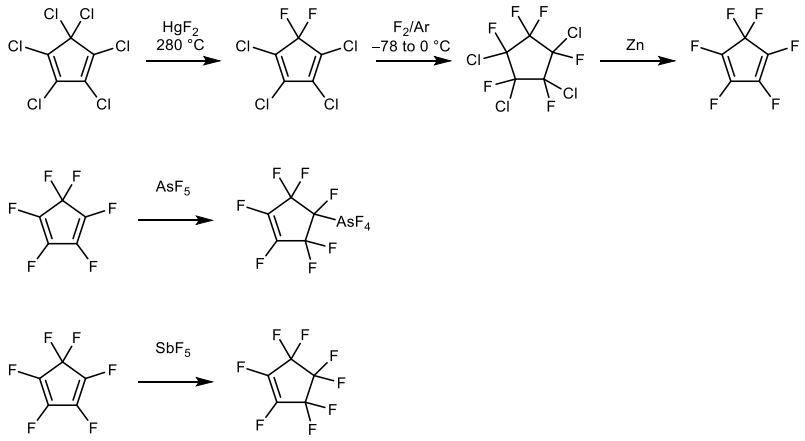

Scheme 20: Adverse side reactions during the attempted synthesis of the pentafluorocyclopentadienyl cation.[127]

3 Motivation and Scope of the Work

The primary objective of this study is to conduct a comprehensive investigation into the chemistry of pentaarylcyclopentadienyl systems. Special attention will be given to the synthesis, isolation, and characterization of their stable neutral radicals, particularly through the utilization of sc-XRD to determine their solid-state structures. Additionally, the study aims to explore their reactivity with activated forms of metals, such as amalgams, as this synthetic route holds promise for the direct preparation of cyclopentadienyl metal complexes from elemental metals. Furthermore, the synthesis and attempted isolation of the corresponding cyclopentadienyl cations will be pursued.

Another focal point of this research is the synthesis of a perfluorinated pentaphenylcyclopentadienyl system, along with an investigation into its chemistry, including the exploration of its anion, radical, and cation.

4 Results

4.1 Pentaarylcyclopentadienes

The palladium-catalyzed arylation of cyclopentadiene or zirconocene dichloride has been mainly used in the preparation of the pentaarylcyclopentadienes described here. Unfortunately, the synthesis described in the literature uses very large amounts of catalyst (5% – 12% Pd compared to cyclopentadiene).[86–88] It was found that the yield of the reaction is not greatly reduced when smaller amounts (1%) of catalyst are used.

In addition, the scope of the reaction is unfortunately limited when carried out in DMF, as suggested in the literature, because DMF can reduce aryl bromides under these conditions.[130] In the case of sterically unhindered aryl bromides, the product of this reaction is the corresponding biphenyl. For more hindered aryl bromides, the corresponding arene is formed.

The limits of this synthesis were tested by using different para-substituted aryl bromides. The most electron-rich aryl bromide that can be used in the classical synthesis is 4-methoxybromobenzene. In contrast, 4-dimethylaminobenzene does not give the desired product, but only 4,4'-bis(dimethylamino)biphenyl. On the electron-poor side, the most electron-poor arene that has been used in a known synthesis in the literature is 4-trifluoromethylbromobenzene, but a significant decrease in yield (19%) is already observed in this case.[131]

To address the issue of unwanted reduction of the bromoarene, diglyme can be employed as a solvent instead of DMF. This solvent change enabled the successful synthesis of a diverse range of differently substituted pentaarylcyclopentadienes with varying solubilities, steric demands, and electronic properties (Figure 19).

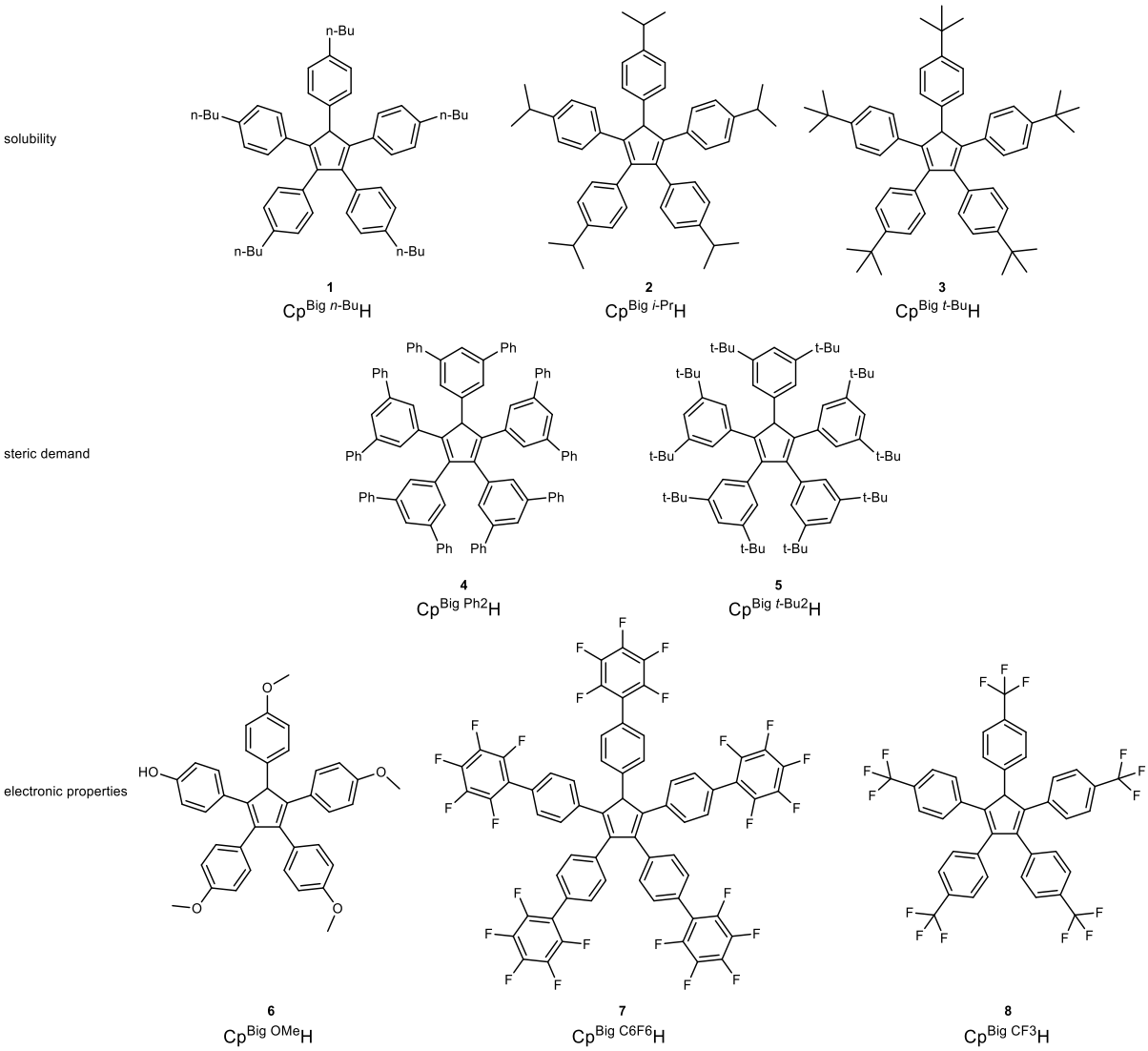

Figure 19: Synthesized pentaarylcyclopentadienes, varied properties, numbering, and naming scheme.

4.2 Pentaarylcyclopentadienyl Anions

The synthesis of a series of salts of all non-radioactive alkali metals has been carried out with $Cp^{Big\ n\text{-}Bu}$, $Cp^{Big\ i\text{-}Pr}$, and $Cp^{Big\ t\text{-}Bu}$. The reaction of cyclopentadienes with equimolar amounts of alkali metal amides $MN(SiMe_3)_2$ (M = Li, Na, K, Rb, Cs) at room temperature has been found to be particularly suitable for the preparation of alkali metal salts of these cyclopentadienes because of the high solubility of these amide bases in most organic solvents and because of their ready availability for all alkali metals. These metal cyclopentadienyl compounds were obtained as colorless, crystalline solids in high yields.

Compounds **9** to **23** (Table 3) are soluble in organic solvents such as acetonitrile, toluene and THF, respectively. ^{13}C NMR resonances of the C_5 ring are almost

identical for **1 - 15**, proving the ionic nature of the metal cyclopentadienyl bonds.[132] In addition, the metal cyclopentadienyls except for the potassium salts (**3**, **8**, **13**) were characterized by heteronuclear (^{7}Li, ^{23}Na, ^{87}Rb, ^{133}Cs) NMR spectroscopy.[132]

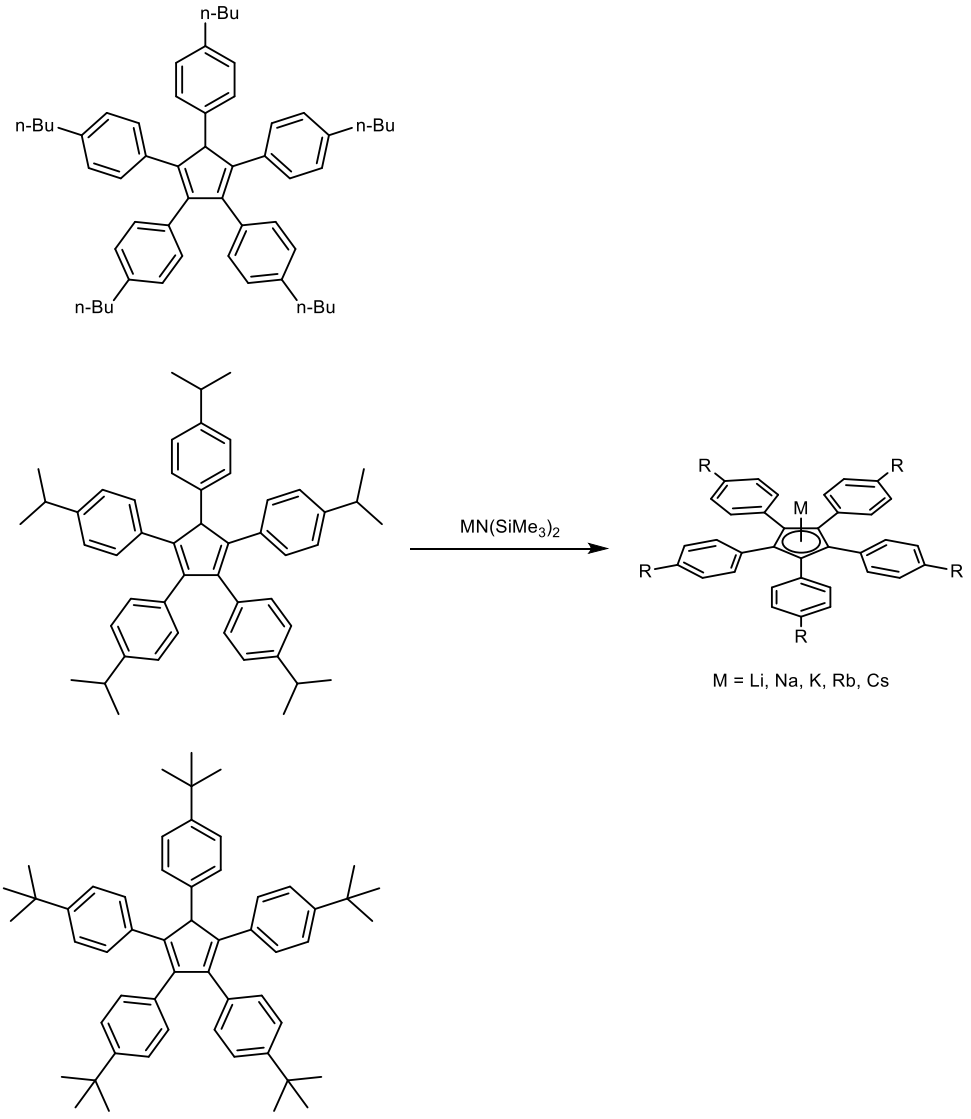

Scheme 21: Synthesis of alkali metal salts.

Table 3: **Numbering scheme of pentaarylcyclopentadienyl alkaline metal compounds.**

metal	R = 4-*i*-Pr-Ph	R = 4-*n*-Bu-Ph	R = 4-*t*-Bu-Ph
Li	**9**	**14**	**19**
Na	**10**	**15**	**20**
K	**11**	**16**	**21**
Rb	**12**	**17**	**22**
Cs	**13**	**18**	**23**

4.2.1 Crystal Structures

Unfortunately, the majority of metal cyclopentadienyl complexes could not be structurally characterized by single-crystal X-ray diffraction. This was primarily due to prohibitive disorder issues caused by the incompatibility of the ligand's fivefold symmetry with a gapless periodic packing. As a result, voids were created, allowing for the presence of disordered solvent molecules or permitting alkyl substituents to occupy more than one position, especially in the case of *n*-butyl substituted complexes.

In contrast, complexes with *i*-Pr and *t*-Bu groups exhibited lower degrees of conformational freedom, resulting in higher-quality data sets for the $Cp^{Big\ i\text{-}Pr}M$ and $Cp^{Big\ t\text{-}Bu}M$ complexes and the succesful refinement of six crystal structures (Figure 20 – Figure 25) which have been extensively discussed in a separate publication.[132] The structures show either infinite chains with alternating Cp anions and solvent coordinated metal ions (Figure 20 – Figure 22) or solvent separated ion pairs which often feature $Cp^{Big_2}M^-$ anions (Figure 23 – Figure 25).

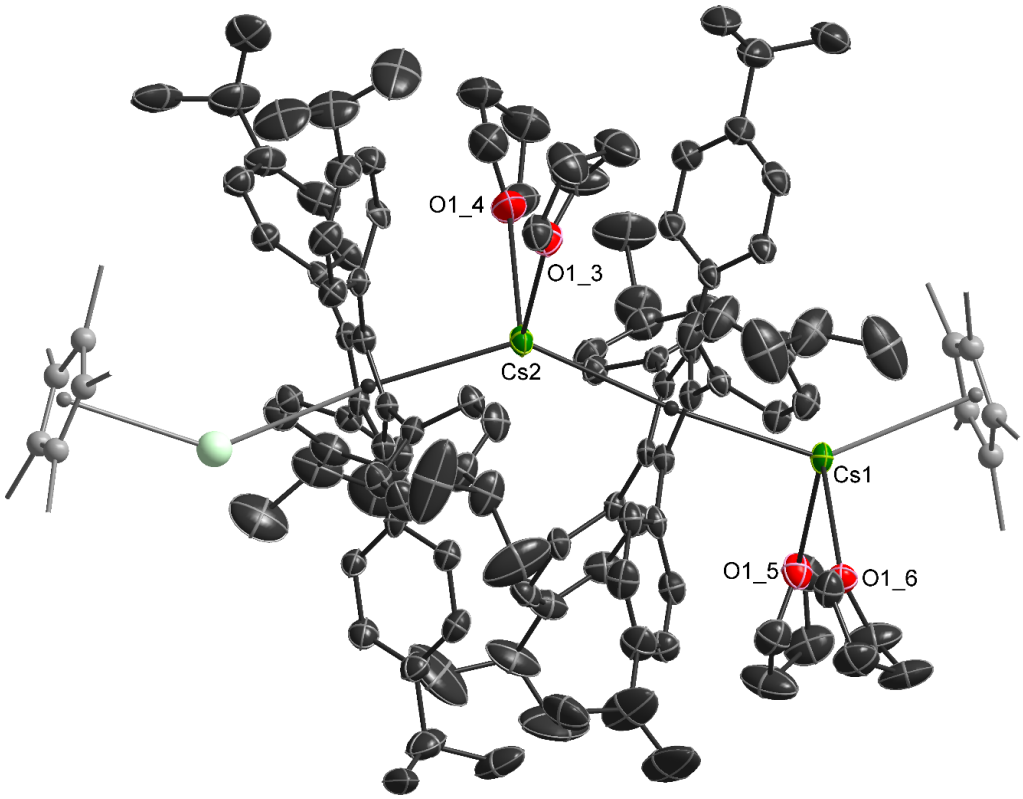

Figure 20: Solid-state structure of 13a; H atoms are omitted for clarity; thermal ellipsoids are shown at 50% probability levels. Pale colored atoms are generated by symmetry. Alternate positions of disordered solvent molecules and lattice solvent molecules are omitted for clarity.

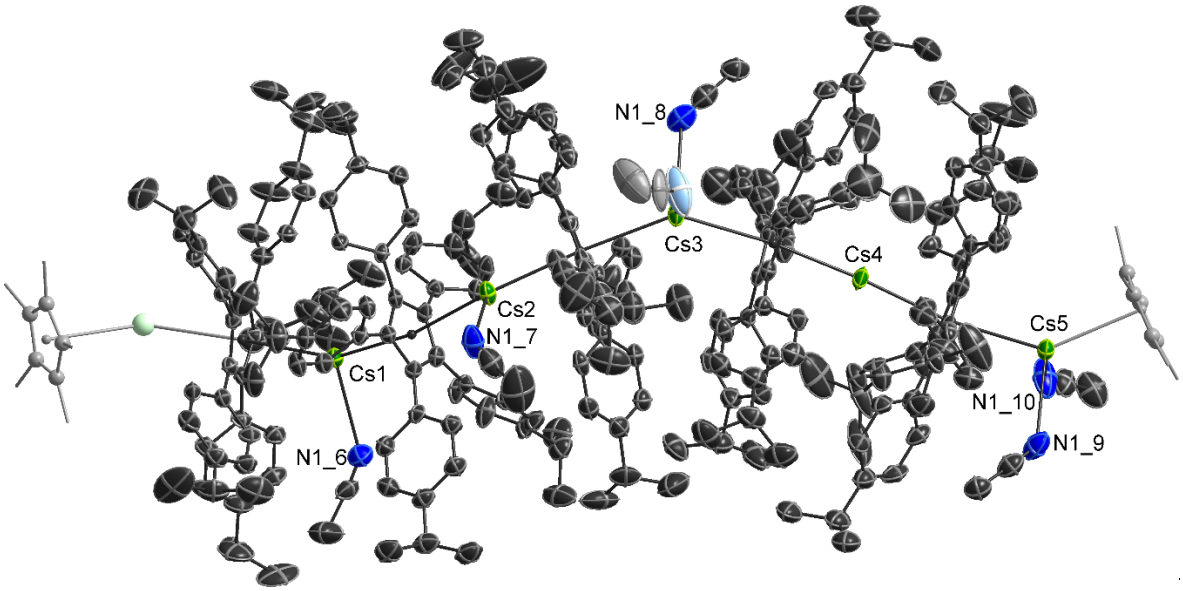

Figure 21: Solid-state structure of 13b; H atoms are omitted for clarity; thermal ellipsoids are shown at 50% probability levels. Pale colored atoms are generated by symmetry. Alternate positions of disordered solvent molecules and lattice solvent molecules are omitted for clarity.

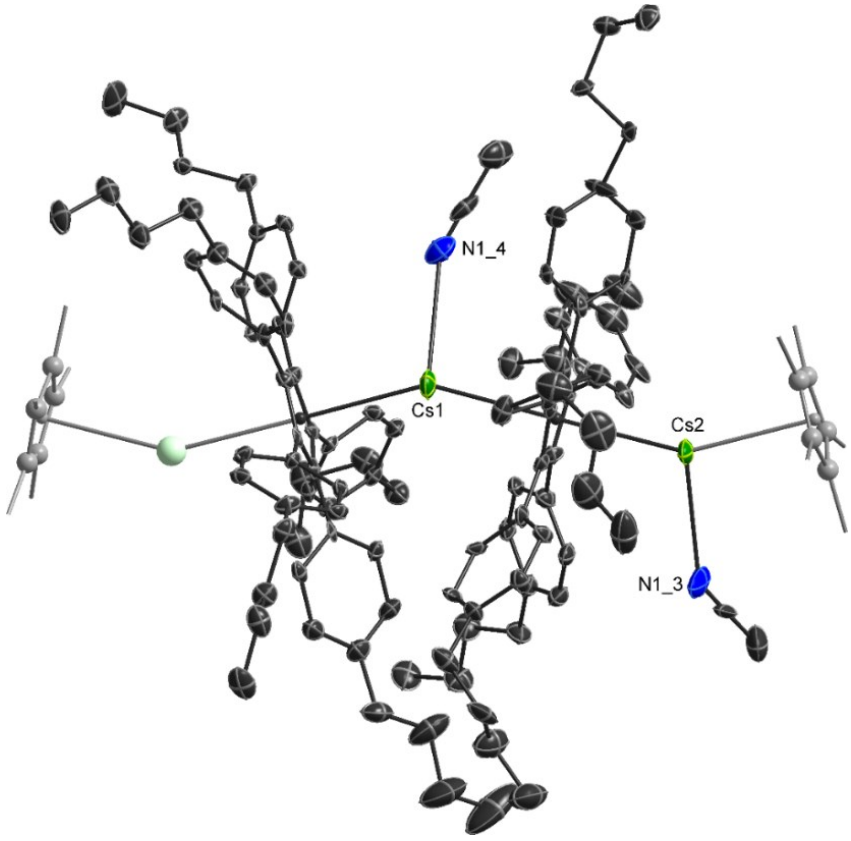

Figure 22: Solid-state structure of 18; H atoms are omitted for clarity; thermal ellipsoids are shown at 50% probability levels. Pale colored atoms are generated by symmetry. Alternate positions of disordered solvent molecules and lattice solvent molecules are omitted for clarity.

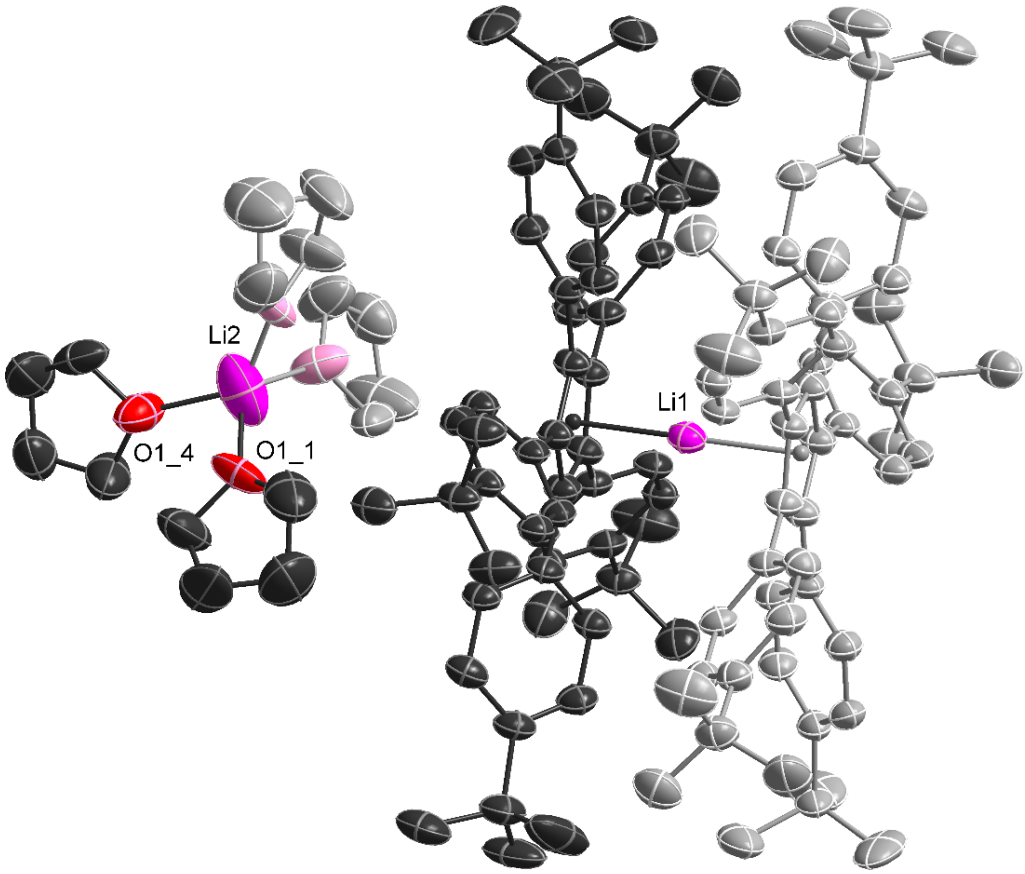

Figure 23: Solid-state structure of 19; H atoms are omitted for clarity; thermal ellipsoids are shown at 50% probability levels. Pale colored atoms are generated by symmetry. Alternate positions of disordered solvent molecules and lattice solvent molecules are omitted for clarity.

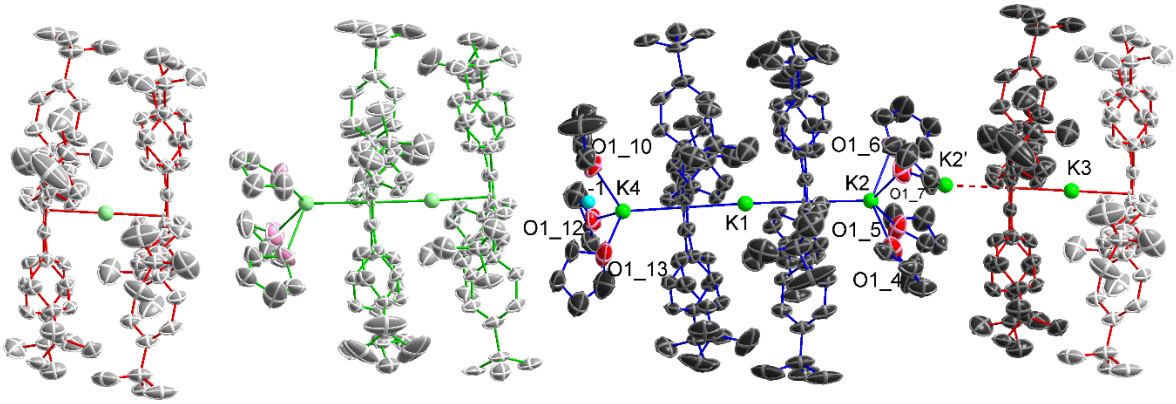

Figure 24: Solid-state structure of 21a; H atoms are omitted for clarity; thermal ellipsoids are shown at 50% probability levels. Pale colored atoms are generated by symmetry. Alternate positions of disordered solvent molecules and lattice solvent molecules are omitted for clarity.

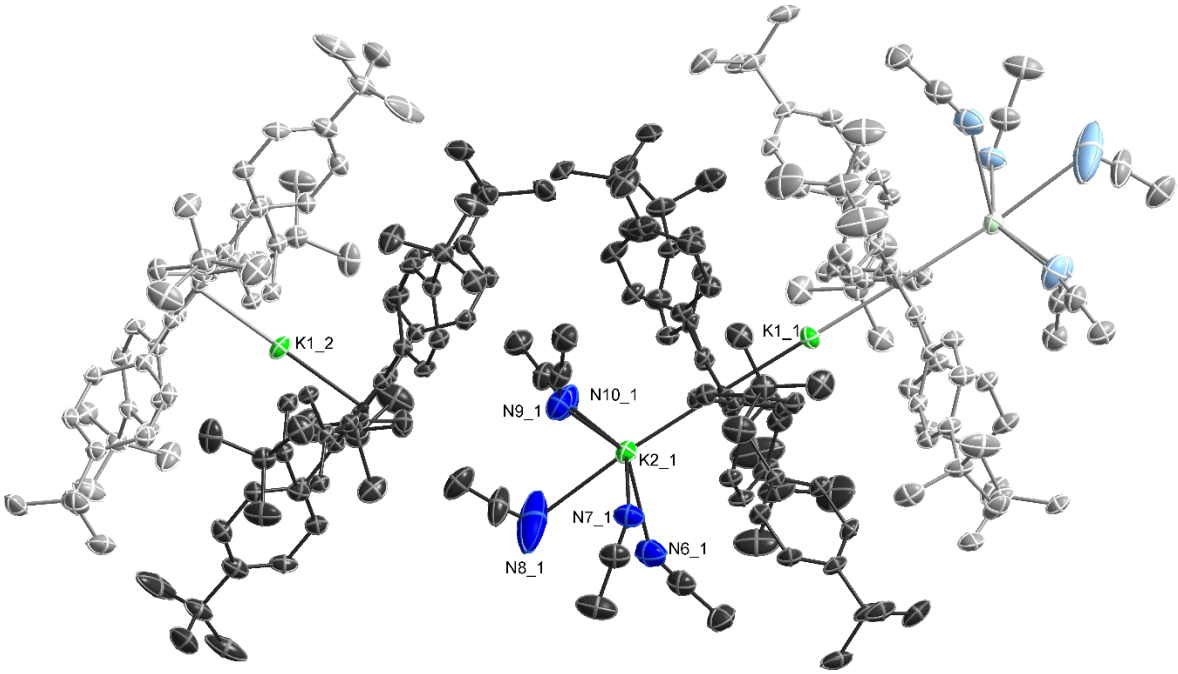

Figure 25: Solid-state structure of 21b; H atoms are omitted for clarity; thermal ellipsoids are shown at 50% probability levels. Pale colored atoms are generated by symmetry. Alternate positions of disordered solvent molecules and lattice solvent molecules are omitted for clarity.

4.2.2 Salt Methathesis Reactions with Divalent Germanium, Tin, and Lead Halides

Alkali metal pentaarylcyclopentadienyl complexes are of potential interest as Cp-transfer reagents in organometallic synthesis. Since the Cp$^{Big\textit{t}\text{-}Bu}$-substituent showed less disorder problems compared to the *n*-Bu and *i*-Pr substituted analogues, Cp$^{Big\textit{t}\text{-}Bu}$K **21** was used for salt metathesis reactions with $GeCl_2$·dioxane, SnI_2, and PbI_2 in THF. This resulted in all cases in the formation of the corresponding homoleptic complexes Cp$^{Big\textit{t}\text{-}Bu}{}_2$M **24** - **26**.[133]

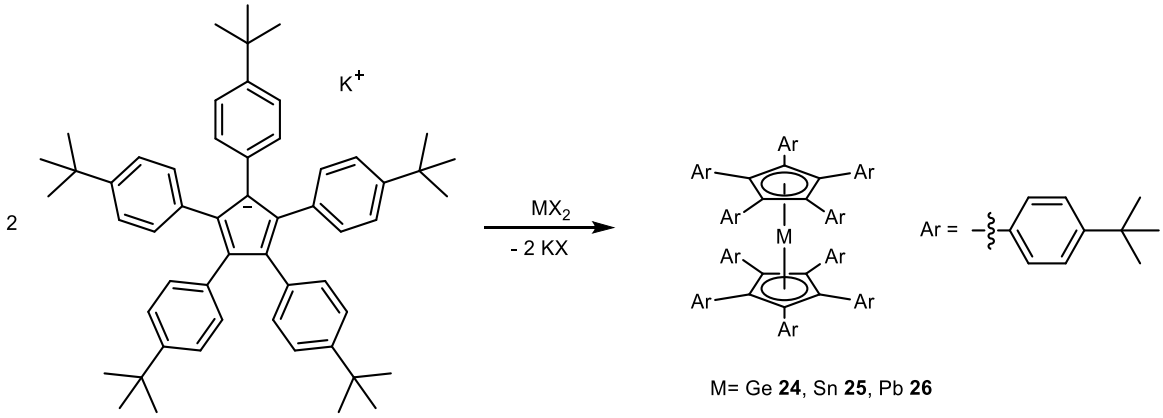

Scheme 22: Salt methathesis reactions between Cp$^{Big\ \textit{t}\text{-}Bu}$K and $GeCl_2$·dioxane, SnI_2, and PbI_2 in THF, resulting in the formation of the homoleptic metallocenes

The products could be crystallized from THF. The structures are discussed below together with other homoleptic complexes of divalent metals.

4.2.3 Salt Methathesis Reactions with Pnictogen Halides

Due to the labile $Cp^{Big\ t\text{-}Bu}$–E bond, it was hypothesized that compounds of the formula $Cp^{Big\ t\text{-}Bu}$–ECl_2 might be valuable synthetic aquivalents for the synthon ·ECl_2. Therefore salt metathesis reactions of $Cp^{Big\ t\text{-}Bu}K$ with pnictogen chlorides ECl_3 (E = P, As, Sb, Bi) were investigated.

Reactions of $Cp^{Big\ t\text{-}Bu}K$ **21** with ECl_3 (E = P, As, Sb, Bi) occurred with elimination of KCl and formation of $Cp^{Big\ t\text{-}Bu}ECl_2$ (E = P **27**, As **28**, Sb **29**, Bi **30**), which were isolated after re-crystallization from solutions in *n*-hexane as colorless crystalline solids in almost quantitative yields (Scheme 23). Unfortunately, single-crystals of X-ray quality were only obtained for **28**. ^{1}H and ^{13}C NMR spectra of **27 – 30** recorded in THF-d_8 solution show the expected resonances of the cyclopentadienyl substituents. The ^{13}C NMR resonances of the C_5 ring are clearly different from those of the ionic alkali metal compounds **9 – 23**, shifting from 132.8 ppm for the arsenic compound **28** to 126.4 ppm for the bismuth compound **30**. These results are consistent with the decreasing electronegativity of the pnictogen atom. The ^{13}C NMR resonance of the cyclopentadienyl atoms of the phosphorus compound **27** could not be determined due to rapid intramolecular conversion, resulting in a significant peak broadening. The [1,5]-sigmatropic rearrangement is also evident in the VT ^{1}H NMR spectra of **27** (Figure 26).

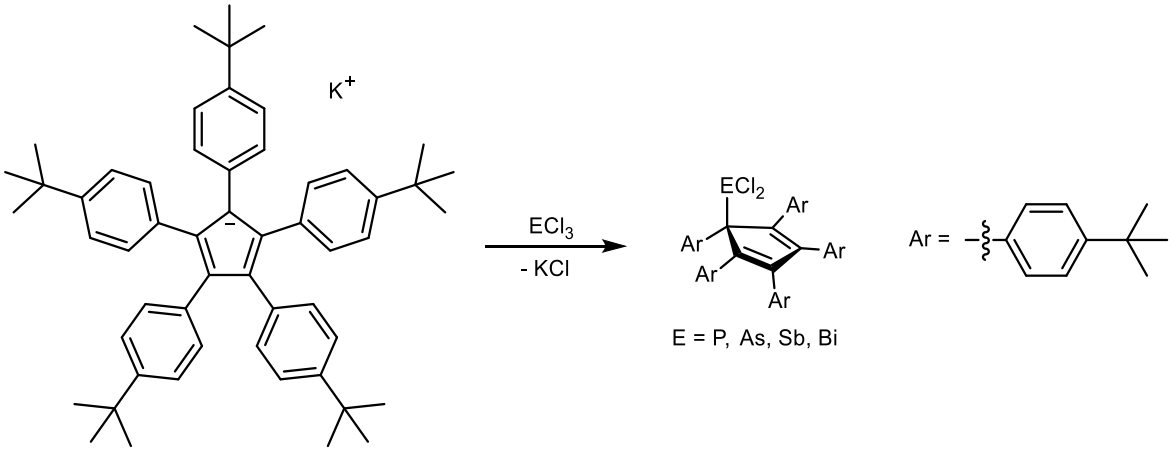

Scheme 23: Synthesis of $Cp^{Big\ t\text{-}Bu}ECl_2$ (E = P 27, As 28, Sb 29, Bi 30) by salt metathesis reactions between $Cp^{Big\ t\text{-}Bu}K$ 21 and ECl_3.

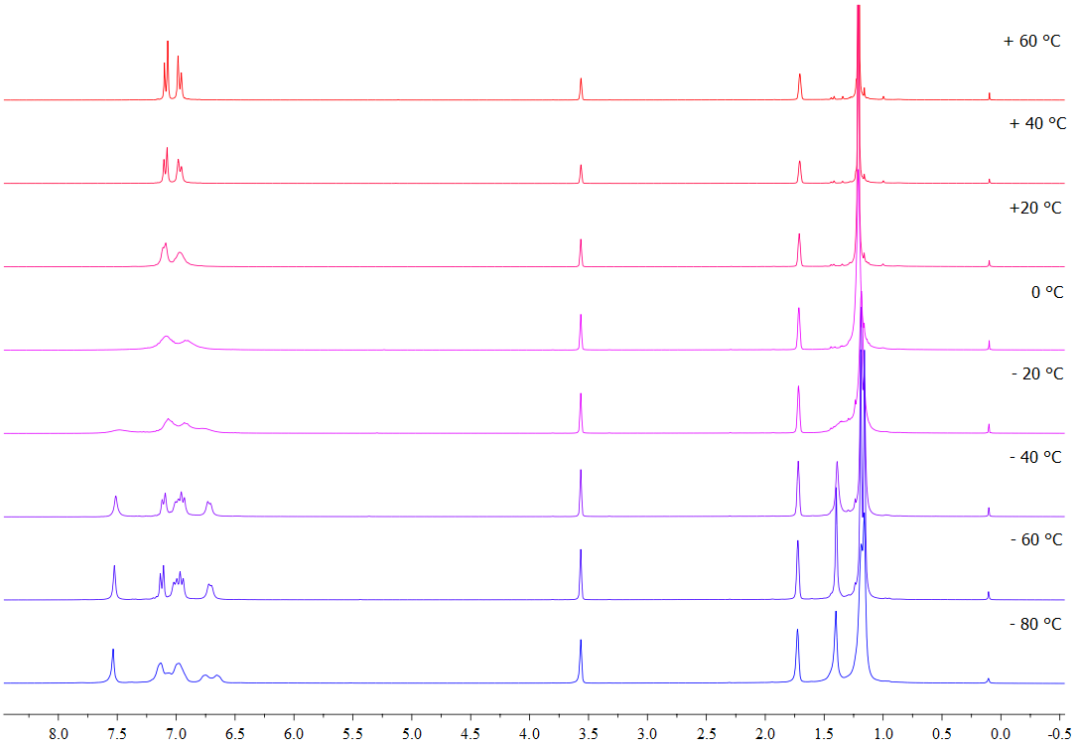

Figure 26: Variable-temperature ^{1}H NMR spectrum of of Cp(4-*t*-Bu-Ph)$_5$PCl$_2$ 27 in THF-*d*$_8$.

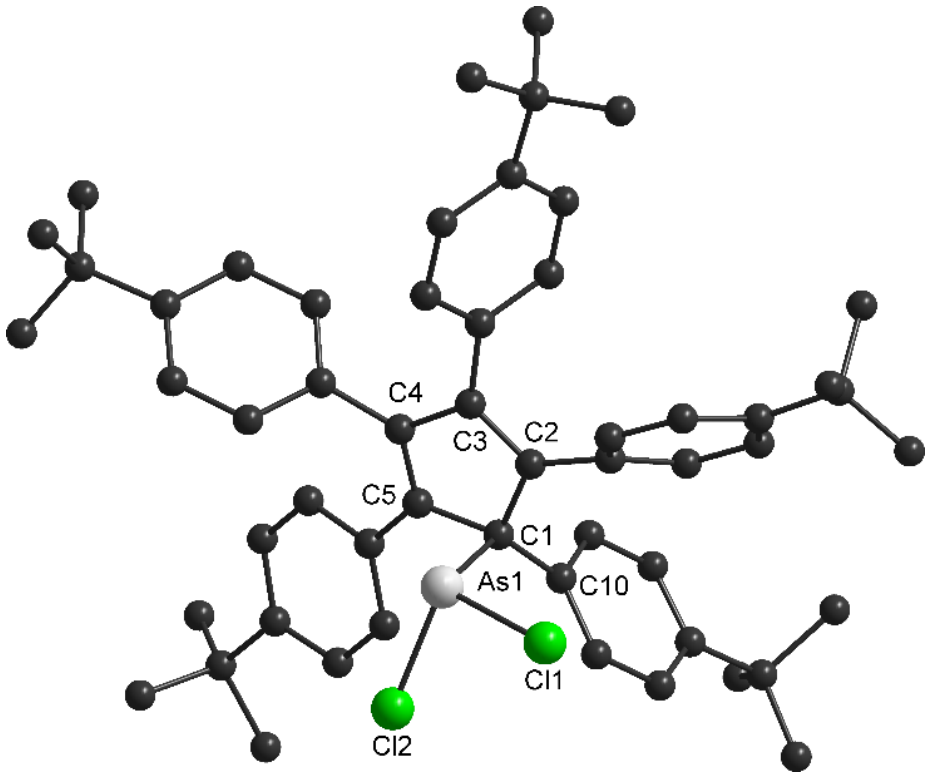

Figure 27: Solid-state structure of 28. H atoms and disordered parts are omitted for clarity; atoms displayed as spheres of arbitrary radii.

Crystals of **28** suitable for a single-crystal X-ray diffraction study were obtained by slow crystallization from *n*-hexane at 25 °C. **28** crystallizes in the monoclinc space goup $P2_1/n$ with one molecule in the asymmetric unit.

The arsenic atom in **28** adopts an almost perpendicular orientation to the central C_5 ring and the As1-C1 bond length of 2.0590(18) Å is typical for an As-C σ bond, whereas the As1-C1-C10 bond angle of 124.26(13)° is significantly larger than the expected value for a sp^3-hybridized carbon atom. The other As-C_{Cp} distances in **28** are substantially longer (As1-C2 2.5677(2) Å, As1-C5 2.6138(2) Å, As1-C3 3.0828(2) Å, As1-C4 3.0616(3) Å) and not indicative of a covalent interaction. Therefore, **28** should be regarded as a η^3 Cp complex. Almost identical As1-C1 bond lengths have been reported for Cp*AsX_2 complexes (X = F 2.026(10) Å, Cl 2.035(7) Å, Br 2.052(10) Å, I 2.066(10) Å),[52] Cp^*_2AsCl (2.038(3) Å, 2.045(3) Å)[53] as well as *i*-$Pr_4(H)C_5AsCl_2$ (2.056(6) Å),[54] whereas the As-C bond lengths in the sigma-bonded As_4 butterfly-type structure $(Cp^{Big\ n\text{-}Bu})_2As_4$ (2.1003(25) Å, 2.0941(23) Å) are slightly elongated.[58] The As1-C2 and As1-C5 bond distances in the Cp*AsX_2 complexes are slightly shorter compared to those in **28**, hence the bonding nature of the Cp* substituents was described as "pseudo η^3". Moreover, intermolecular Cp···As interactions as was observed in Cp*$AsCl_2$ were not observed in **28**, which can be attributed to the higher steric demand of the $Cp^{Big\ t\text{-}Bu}$ ligand.

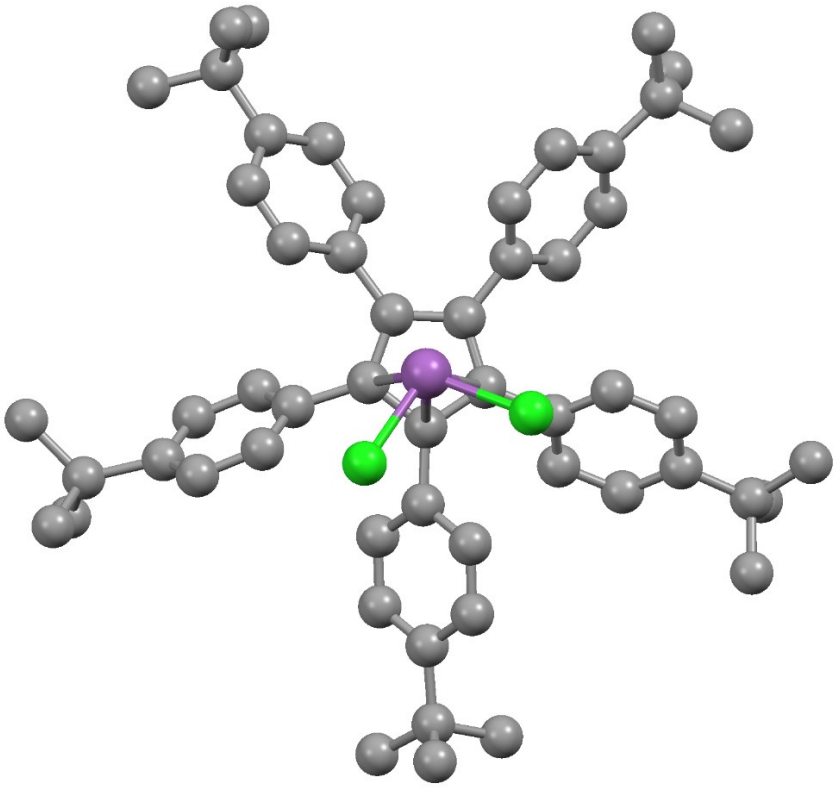

Figure 28: One of the disordered components of the crystal structure of $Cp^{Big\ t\text{-}Bu}SbCl_2$ 29 crystallized from *n*-hexane. Hydrogen atoms are omitted for clarity. Atoms are depicted as spheres of arbitrary radii.

29 crystallized in the monoclinic crystal system in the space group C_2 (Figure 28). Due to problems with refinement caused by a high degree of disorder, the bond angles and lengths obtained are not meaningful. The connectivity, however, can be considered secure.

The suitability of $Cp^{Big\ t\text{-}Bu}AsCl_2$ **28** to serve as a synthetic aquivalent of the synthon $\cdot AsCl_2$ has been demonstrated by Helling *et. al.*[134]

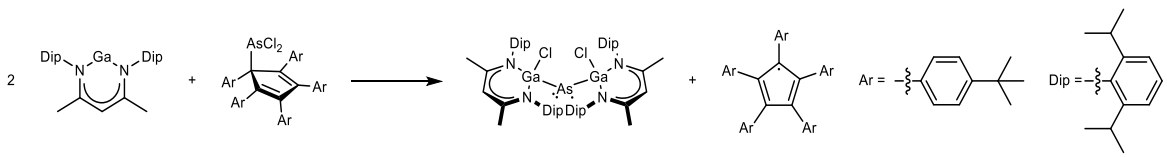

Scheme 24: Application of $Cp^{Big\ t\text{-}Bu}AsCl_2$ 28 in the preparation of an arsenic centered radical.[134]

4.3 Pentaarylcyclopentadienyl Radicals

It has long been hypothesised that cyclopentadienyl radicals should exist as two valence tautomers as a result of a Jahn-Teller distortion, but at the time this work was started this had not been clearly demonstrated by sc-XRD (*vide supra*). Therefore, an aim of this work was to provide clear experimental evidence supporting the existence of two valence tautomers in cyclopentadienyl radicals with symmetric substitutions. To achieve this, the bulky pentaarylcyclopentadienyl systems presented above were used. The additional substituents in either the *para*- (**31–33**) or *meta*-positions (**34**, **35**) (Scheme 26) prevent radical dimerization without introducing steric strain or compromising the symmetry of the central cyclopentadienyl ring. Additionally, the aryl substituents serve a secondary purpose: they facilitate the transmission of structural information from the cyclopentadienyl skeleton to the aryl groups through conjugation, and the resulting structure is effectively frozen through aromatic ring interactions in the crystal lattice. This strategy allowes the observation of the Jahn-Teller distortion phenomenon in the solid-state. The resulting Cp radicals were further analyzed by various techniques, including UV/Vis and EPR spectroscopy, as well as cyclovoltammetry (CV).

The oxidation of **31-K–35-K** (**32-K** equals **21** from above) was first studied by H. Micha Weinert *via* CV in THF and was found to be reversible, indicating the stability of the corresponding radicals. The observed oxidation potentials $E_{1/2}$ are in accordance with the electronic influences of the substituents (**31-K**/**31**: −1.06 V; **32-K**/**32**: −1.00 V; **33-K**/**33**: −0.48 V; **34-K**/**34**: −1.11 V; **35-K**/**35**: −0.68 V). Since **31-K – 35-K** were found to be rather strong reducing agents, the mild oxidant CuCl was employed for preparation of **31–35** to prevent overoxidation (Scheme 25).

In addition to CuCl, other oxidants such as silver or ferrocenium salts were tested and found to be effective. However, CuCl was found to be the most convenient choice due to its ease of use in terms of separating excess reagent and the by-

products Cu and KCl, all of which are insoluble in non-coordinating solvents.

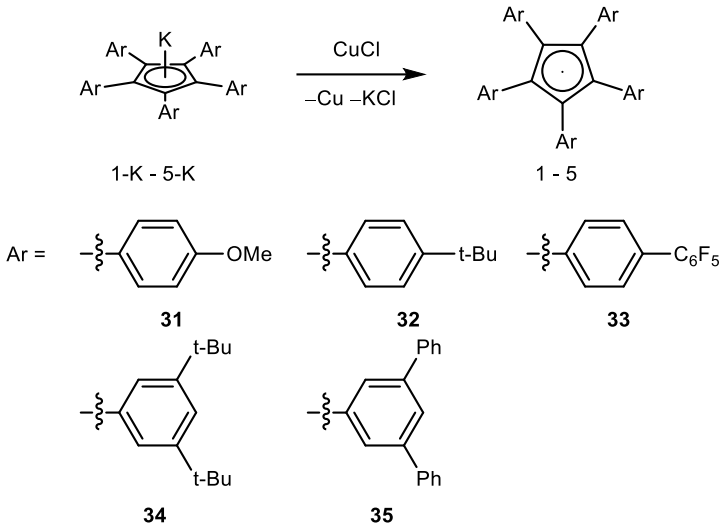

Scheme 25: Synthesis of cyclopentadienyl radicals 31–35 from the corresponding potassium salts 31-K–35-K by one-electron oxidation with CuCl.

The same synthetic protocol was also applied to $Cp^{Big\ CF3}K$, $Cp^{Big\ n\text{-}Bu}K$, and $Cp^{Big\ i\text{-}Pr}K$. The radical of $Cp^{Big\ CF3}$ was not formed under these conditions and the corresponding radicals of $Cp^{Big\ n\text{-}Bu}$, and $Cp^{Big\ i\text{-}Pr}$ could not be isolated due to their high solubility in all organic solvents tested.

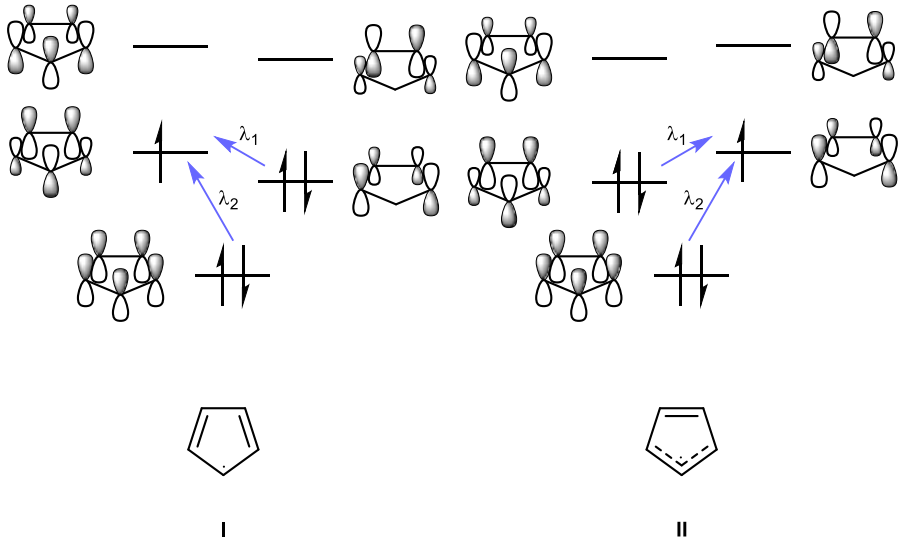

Figure 29: Possible valence tautomers of a cyclopentadienyl radical and selected electronic transitions (blue, see below).

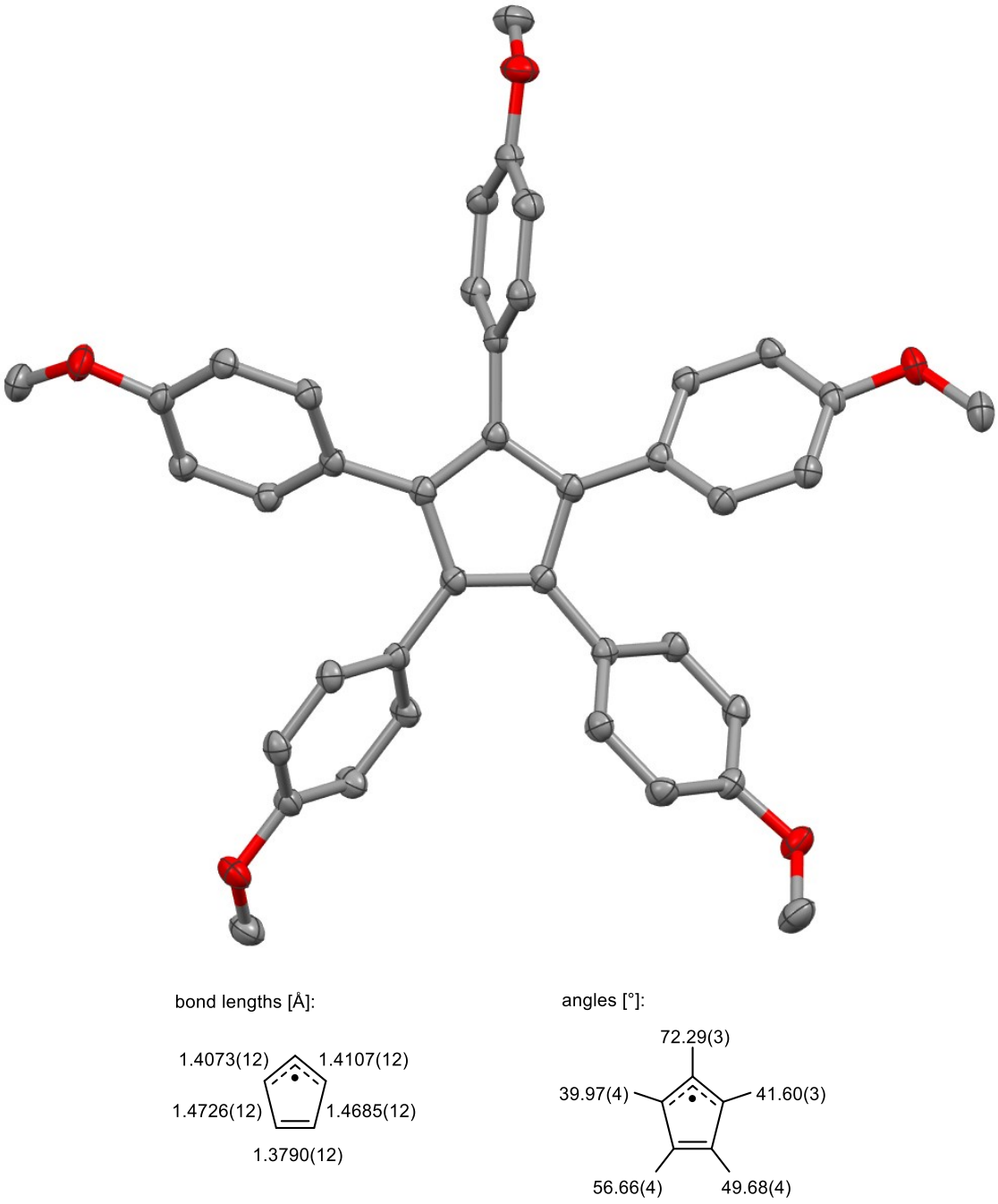

Figure 30: Solid-state structure of $Cp^{Big\ OMe}$. 31 with bond lengths in the cyclopentadienyl ring and dihedral angles between the aryl groups and the plane of the cyclopentadienyl ring. Hydrogen atoms are omitted for clarity.

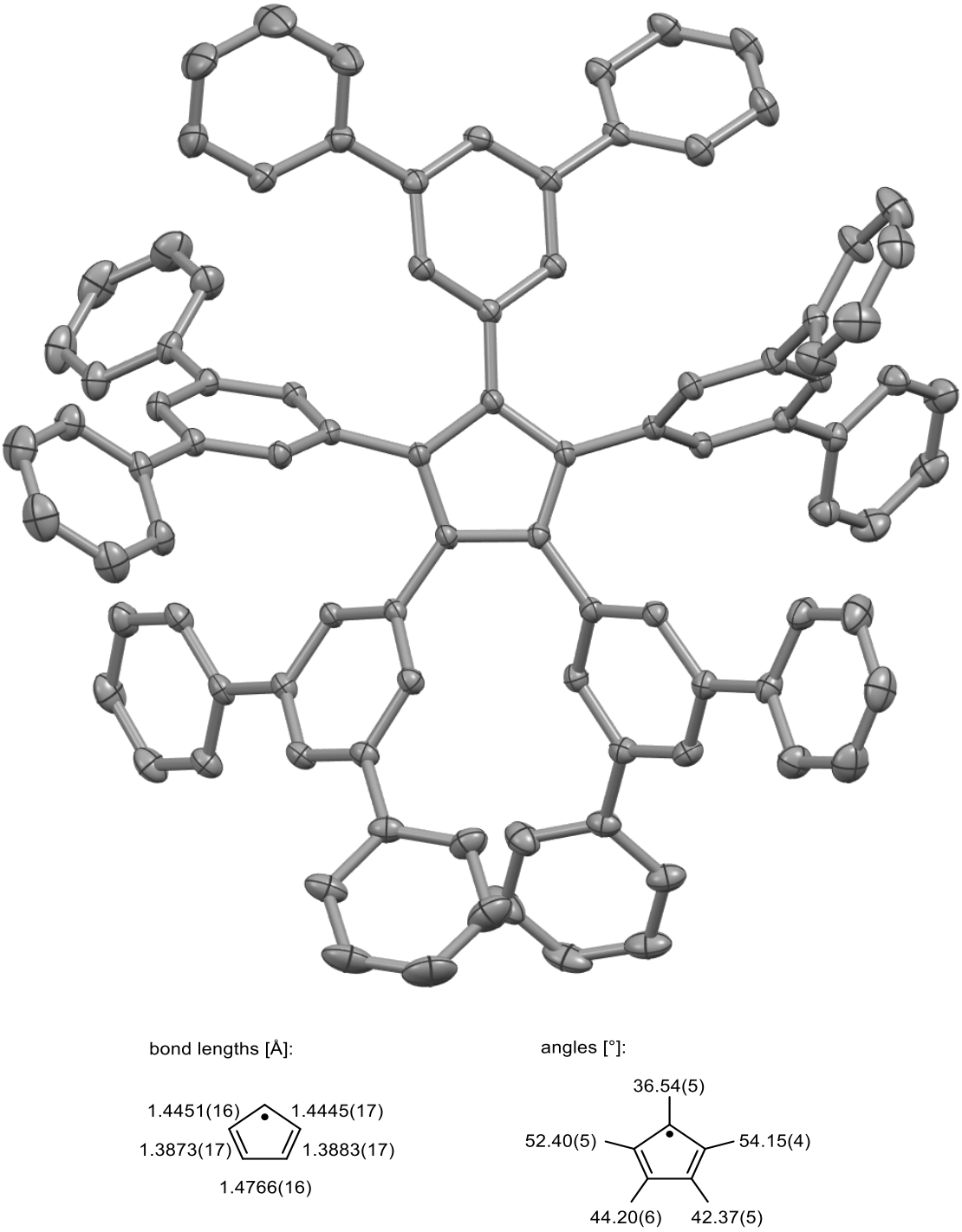

Figure 31: Solid-state structure of $Cp^{Big\ Ph2}$. 35 with bond lengths in the cyclopentadienyl ring and dihedral angles between the aryl groups and the plane of the cyclopentadienyl ring. Hydrogen atoms and minor components of disorder are omitted for clarity.

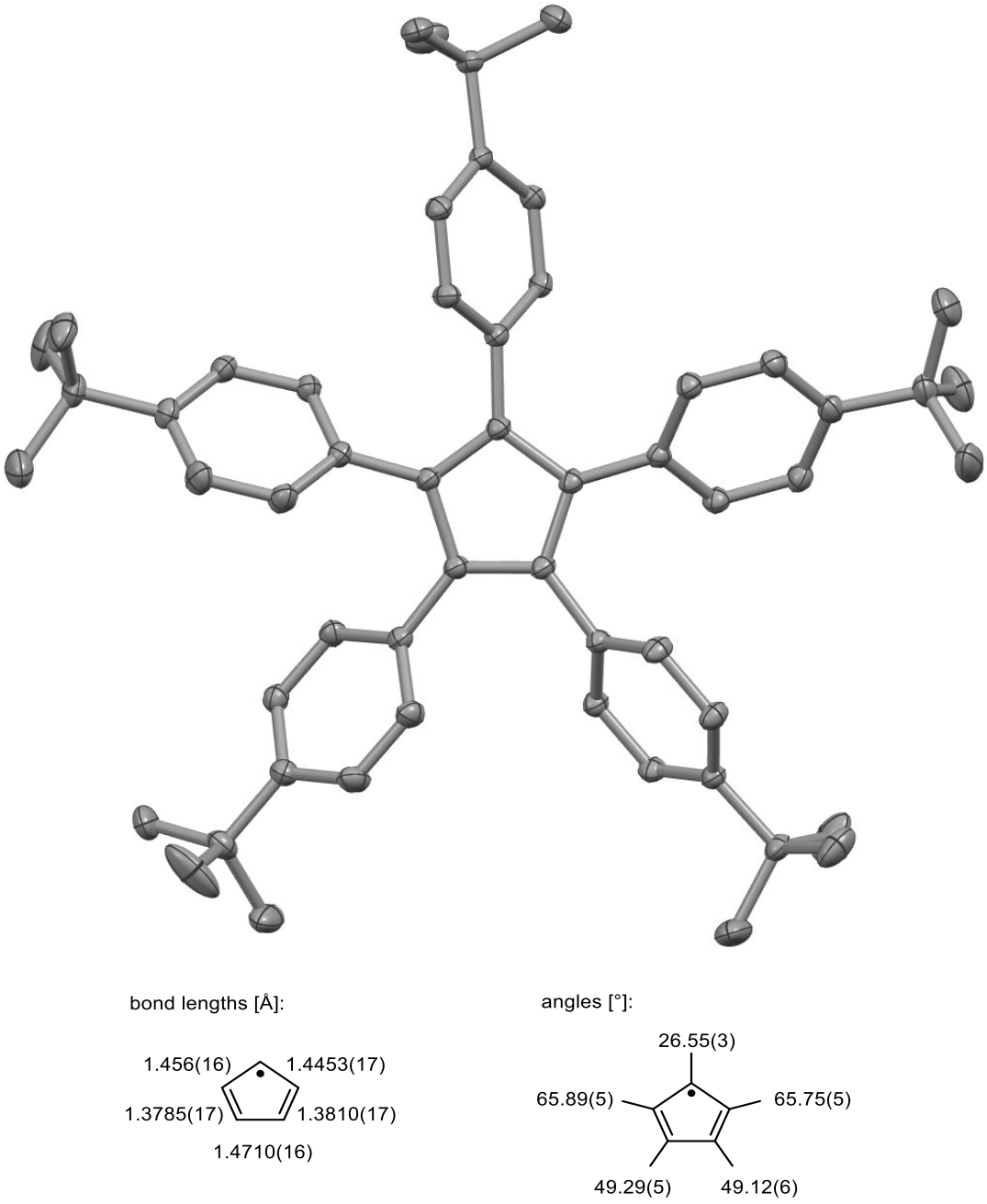

Figure 32: Solid-state structure of $Cp^{Big\ t\text{-}Bu}$. 32 with bond lengths in the cyclopentadienyl ring and dihedral angles between the aryl groups and the plane of the cyclopentadienyl ring. Hydrogen atoms and minor components of disorder are omitted for clarity.

The resulting radicals **31–35** have been successfully isolated in their pure form and exhibit excellent stability at ambient temperature under an argon atmosphere for several months without undergoing decomposition. These radicals are soluble in aromatic hydrocarbons and THF. Additionally, radicals **32** and **34** display solubility in hexane and pentane as well. By storing saturated solutions of **31**, **32**, and **35** in benzene, *n*-pentane, and benzene/*n*-hexane respectively at 25 °C, single-crystals

suitable for X-ray diffraction were obtained. Crystallization of **33** and **34** was achieved using benzene and *n*-hexane at 25 °C, although the resulting crystals were not suitable for sc-XRD.

The crystal structures showed distinct Jahn-Teller distortions. Notably, both valence tautomers were observed. Radicals **32** and **35** exhibited the type **I** geometry, while radical **31** exhibited the type **II** distortion of the Cp ring (Figure 29).

Compound **31** adopts the "allyl radical" type valence tautomer **II** (Figure 29). The C–C bond lengths within the allyl unit of compound **31** measure approximately 1.41 Å, which is consistent with the values observed in crystalline aryl-substituted allyl radicals (1.40 Å – 1.41 Å)[135] and the parent allyl radical in the gas phase (1.43 Å).[136] The remaining C–C bond lengths within the Cp ring of compound **31** are approximately 1.47 Å and 1.38 Å, which align closely with the expected values for C–C single and double bonds between sp^2-hybridized carbon atoms. This supports the depicted Lewis structure of compound **31**, which shows alternating single and double bonds.

Compounds **32** and **35** exhibit a molecular structure in the single-crystals that corresponds to the "localized radical" tautomers **I** (Figure 29). The C–C bond lengths adjacent to the radical center in compounds **32** and **35** are longer at 1.45 Å compared to compound **31**. However, the remaining C–C bond lengths closely resemble those observed in compound **31**, with values of approximately 1.47 Å and 1.38 Å. The alternating pattern of these bond lengths in compounds **32** and **35** resembles the depicted Lewis structure. Similar geometrical distortions have been observed in the gas-phase analysis of the parent Cp radical, although to a lesser extent.[137]

Quantum chemical computations performed by Prof. Dr. Gebhard Haberhauer support the sc-XRD measurements, accurately reproducing the measured bond lengths in the cyclopentadienyl core with a maximum deviation of 0.011 Å.[138] Valence tautomers **I** and **II** have distinct geometric structures but possess nearly identical energies (Table 4). The computations also reveal the distribution of spin densities in the tautomers, providing additional information not directly obtained from the Solid-state structures (Table 6). The computed results align with the

assigned Lewis structures (Figure 30 – Figure 32). Analysis of the aryl group torsion angles demonstrates that higher spin densities on carbon atoms correspond to a closer-to-planar conformation. This correlation is evident in both the computational results and the crystal structures (Figure 30 – Figure 32).

Thus, the arrangement of aryl groups influences the structure of the Cp core, creating an energy difference that prevents re-tautomerization in the crystalline environment, thereby enabling the observation of distinct tautomers.

UV/Vis spectroscopy was employed to assess the electronic properties of the radicals in solution. The UV/Vis spectra display a strong absorption band at 611-656 nm and a weaker band at 498-523 nm, with enhanced intensity in the para-substituted compounds (Figure 33).

Table 4: Absolute energies [au] of tautomers I and II of the pentaarylcyclopentadienyl radicals 31-35 calculated using (a) UB3LYP-D3BJ/6-31G*[139] and (b) UB3LYP-D3BJ/def2-TZVP//UB3LYP-D3BJ/6-31G*.[140]

	Tautomer	a	b
1	**I**	−1921.5679370	−1922.2780200
1	**II**	−1921.5679340	−1922.2780140
2	**I**	−2135.3221430	−2136.0726390
2	**II**	−2135.3221330	−2136.0726300
3	**I**	−4984.9993220	−4987.0740300
3	**II**	−4984.9993200	−4987.0740510
4	**I**	−3659.7972400	−3661.0678170
4	**II**	−3659.7972540	−3661.0678480
5	**I**	−2921.7598490	−2922.7787680
5	**II**	−2921.7598450	−2922.7787680

Table 5: Calculated bond distances [Å] of the tautomers I and II of the pentaarylcyclopentadienyl radicals 31-35.

	Tautomer	C1-C2	C2-C3	C3-C4	C4-C5	C5-C1
1	**I**	1.44753	1.38911	1.48461	1.38983	1.44616
2	**I**	1.45237	1.38543	1.48579	1.39142	1.44207
3	**I**	1.44745	1.38801	1.48568	1.38859	1.44647
4	**I**	1.45433	1.38503	1.48520	1.39344	1.44009
5	**I**	1.44675	1.38935	1.48450	1.38938	1.44670
1	**II**	1.41672	1.47278	1.37978	1.47585	1.41216
2	**II**	1.42621	1.46623	1.38000	1.48187	1.40277
3	**II**	1.41942	1.47088	1.37909	1.47820	1.40855
4	**II**	1.43336	1.46038	1.38248	1.48390	1.39799
5	**II**	1.41530	1.47332	1.38011	1.47451	1.41343

Table 6: Calculate spin densities of the tautomers I and II of the pentaarylcyclopentadienyl radicals 31-35.

	Tautomer	C1	C2	C3	C4	C5
1	**I**	+0.474	−0.110	+0.253	+0.262	−0.115
2	**I**	+0.493	−0.095	+0.234	+0.298	−0.136
3	**I**	+0.490	−0.114	+0.261	+0.267	−0.118
4	**I**	+0.482	−0.086	+0.219	+0.306	−0.143
5	**I**	+0.498	−0.118	+0.267	+0.267	−0.118
1	**II**	−0.177	+0.424	+0.041	+0.071	+0.406
2	**II**	−0.175	+0.470	−0.018	+0.136	+0.380
3	**II**	−0.180	+0.448	+0.021	+0.092	+0.406
4	**II**	−0.161	+0.474	−0.054	+0.177	+0.341
5	**II**	−0.185	+0.438	+0.049	+0.062	+0.431

Quantum chemical computations by Prof. Dr. Gebhard Haberhauer were employed to support the interpretation of the UV/Vis spectra.[138] The main absorption band in the visible region around 600 nm is attributed to the electron transition from the HOMO-2 to the SOMO (λ_2, Figure 29, Table 7). The forbidden transition between the HOMO-1 and the SOMO, expected in the near-infrared region at approximately 1700 nm (λ_1; Figure 29, Table 7), was outside the frequency range accessible to our equipment and was therefore not observed. Weaker absorption bands around 500 nm result from transitions between aryl-centered orbitals and the SOMO. A comparison of the UV/Vis spectra reveals that substituents with π-donating or -accepting properties (such as Ph, C_6F_5, OMe) induce a bathochromic shift and higher absorption coefficients. The influence of these substituents is more pronounced in the *para*-positions, where the orbital coefficients of the transition orbitals are larger.

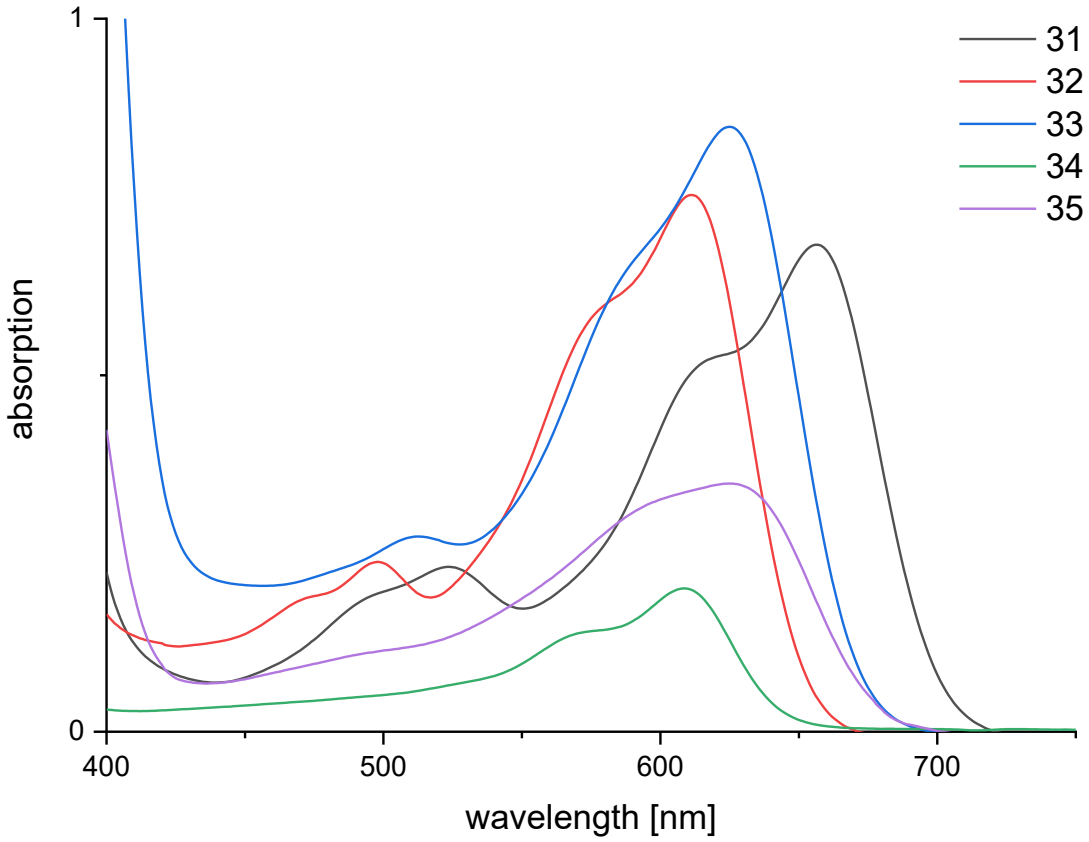

Figure 33: UV/Vis spectra of the cyclopentadienyl radicals 31-35 in toluene (50 µM).

Table 7: Vertical singlet excitations of the tautomers I and II of the pentaarylcyclopentadienyl radicals 31-35.

	Tautomer	$S_0 \rightarrow S_1$ λ_1 [nm]	$S_0 \rightarrow S_2$ λ_2 [nm]
31	**I**	1671.65	553.41
32	**I**	1668.78	520.44
33	**I**	1705.33	530.87
34	**I**	1663.63	528.91
35	**I**	1779.75	536.20
31	**II**	1667.04	553.02
32	**II**	1673.12	520.37
33	**II**	1714.38	530.87
34	**II**	1664.51	529.00
35	**II**	1791.93	536.29

The electronic properties of the cyclopentadienyl radicals have also been examined by EPR spectroscopy by Dr. Blaise L. Geoghegan and Dr. George E. Cutsail III.[138] Despite the unequal distribution of spin density observed in the solid-state structures, the EPR spectra exhibit equal spin populations for all cyclopentadienyl carbon atoms. Such observations can be either attributed to the rapid reorientation of the radicals at room temperature or an electronic valence equilibrium that occurs within the timescale of the EPR experiment (approximately 10^{-7} s). The spectra of compounds **34** and **35** can be accurately simulated by utilizing hyperfine couplings of 2.01 and 2.10 MHz for the *ortho*- and *para*- protons, respectively. This behavior is consistent with a Hückel-like spin density distribution.[141] The spectra, however, do not exhibit resolved signals for the weaker ^{1}H couplings of the meta substituents. This lack of resolution is expected, given the low spin density at the *meta*-position.[142]

The EPR spectrum of *para*-OMe substituted radical **31** does not exhibit resolved hyperfine splittings. It can be simulated as a broad $S = 1/2$ signal. On the contrary,

the spectrum of compound **32** is well reproduced by considering two groups of ten protons. These protons originate from the *ortho*- (1.97 MHz) and *meta*- (0.75 MHz) nuclei on the phenyl rings. Compound **33** shows an even more complex spectrum as additional hyperfine splittings arise from the ^{19}F nuclei on the *para*-C_6F_5 group. The EPR spectrum of compound **33** can be accurately reproduced by including two groups of 10 protons corresponding to the *ortho*- (1.95 MHz) and *meta*- (1.40 MHz) positions on the phenyl rings. Furthermore, the simulation incorporates 15 equivalent ^{19}F nuclei with 0.50 MHz hyperfine couplings originating from the *ortho*- and *para*-positions of the *para*-C_6F_5 group. These hyperfine couplings follow the same spin density distribution and Hückel pattern as the phenyl groups. The *para*-C_6F_5 substituent, being highly electron-withdrawing, facilitates spin delocalization through the fluorine p-orbitals. This leads to a significantly larger spin density observed at the *meta*-carbons of the phenyl ring.

Frozen solution spectra were also measured, but were much more broadened and their hyperfine contributions could not be resolved.[138] Additional ENDOR measurements and DFT computations can be found in the original publication.[138]

Table 8: Simulated EPR parameters for 31–35. (All *g* values and hyperfine couplings are isotropic. Gaussian line-widths measured peak-to-peak.)

Simulation	g_{iso}	$^{ortho}a_{iso}$ [MHz]	$^{meta}a_{iso}$ [MHz]	$^{para}a_{iso}$ [MHz]	Line-width [Gauss]
31	2.00253	-	-	-	2.650
32	2.00240	1.97	0.79	-	0.250
33(^1H)	2.00241	1.95	1.40	-	0.165
33(^{19}F)		0.50	-	0.50	
34	2.00239	2.01	-	2.01	0.180
55	2.00239	2.10	-	2.10	0.240

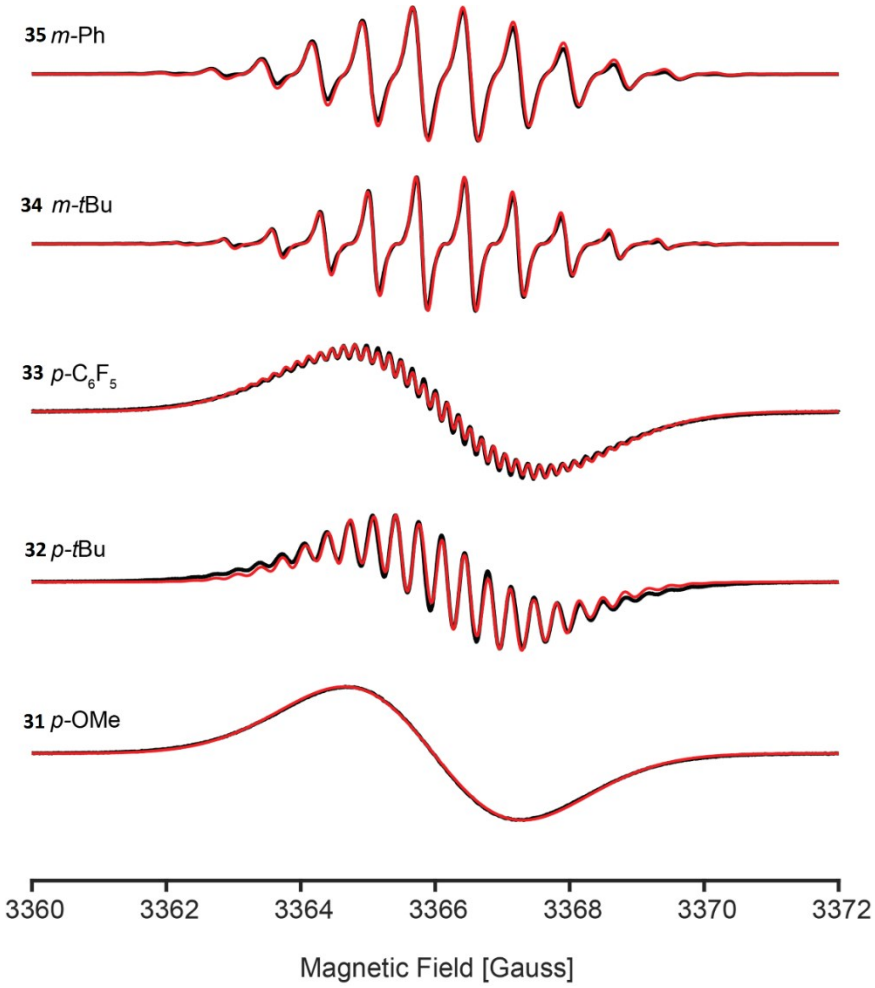

Figure 34: Experimental (black) and simulated (red) room-temperature CW X-band EPR spectra for 31–35.[138]

4.4 Reactions of Cyclopentadienyl Radicals with Activated Metals

The stable cyclopentadienyl radicals mentioned earlier have the potential to undergo direct reactions with elemental metals, leading to the formation of cyclopentadienyl metal compounds. The $Cp^{Big\ t\text{-}Bu}$ ligand was again selected for this study due to its high tendency for crystallization compared to other pentaarylcyclopentadienyl ligands.

The $Cp^{Big\ t\text{-}Bu}$ · radical **32** reacts with magnesium anthracene or metal amalgams of group 2 (Ca, Sr, Ba), group 13 (Ga, In, Tl), and group 14 (Sn, Pb). These metal amalgams are formed by mixing the respective metals with Hg. The reaction results in the formation of homoleptic metallocenes, $Cp^{Big\ t\text{-}Bu}{}_2M$ (M = Mg **36**, Ca **37**, Sr **38**, Ba **39**, Sn **25**, Pb **26**), as well as half metallocenes, $Cp^{Big\ t\text{-}Bu}M$ (M = Ga **40**, In **41**, Tl **42**), in almost quantitative yields (Scheme 27). Additionally, the reaction of radical **32** with mercury yields $Cp^{Big\ t\text{-}Bu}{}_2Hg$ **43**. The low oxidation potential of radical **34**

prevents the formation of the highest oxidation states of group 13 (+III) and group 14 metals (+IV).

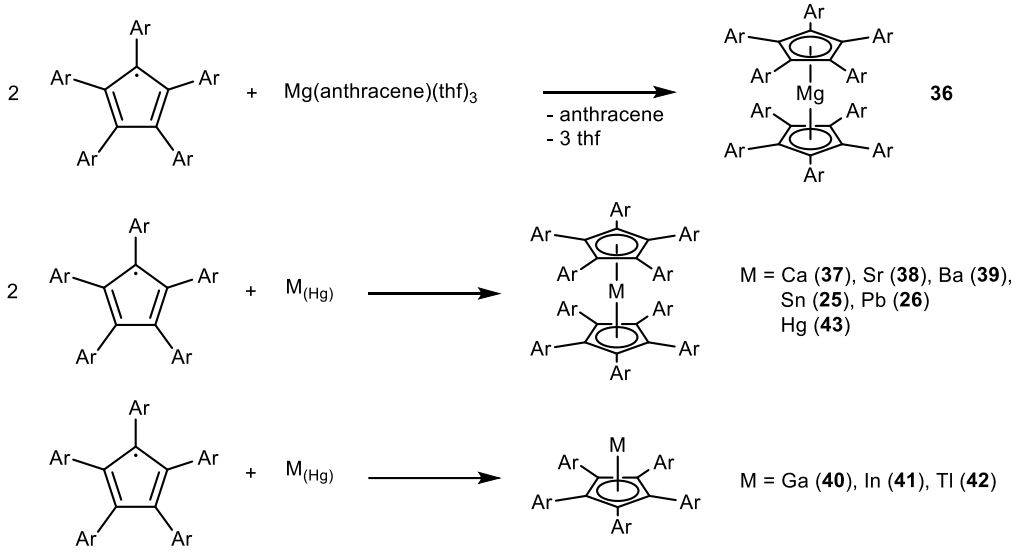

Scheme 27: Synthesis of main group cyclopentadienyl compounds from cyclopentadienyl radicals and amalgams.

Compounds **25**, **26**, and **37 – 43** exhibit solubility in toluene, benzene, and THF, with the exception of **41** and **42**, which are only slightly soluble in THF.

The structures of the group 2 and group 14 metallocenes, with the exception of compound **37**, were determined using single-crystal X-ray diffraction.

The crystals of the group 13 half-metallocenes diffracted poorly. Therefore, detailed structural information could not be obtained. In the case of compound **40**, the data set obtained suggested the formation of a disordered chain-like structure, but the disorder was too pronounced to be completely resolved during refinement. Compounds **36** and **24 – 26** exhibit centrosymmetric structures, where the metal atoms are located at the inversion centers. These compounds crystallize in different space groups: $P\bar{1}$ (**36**), $C2/c$ (**24**), $P2_1/n$ (**25**), and $P\bar{1}$ (**26**). Compounds **38** and **39** crystallize in the monoclinic space group $P2_1/n$, while compound **43** crystallizes in space group $P\bar{1}$ with the molecule placed on a general position.

In these compounds, the aryl groups adopt a propeller-like conformation, which is attributed to intramolecular CH$\cdots\pi$ interactions.

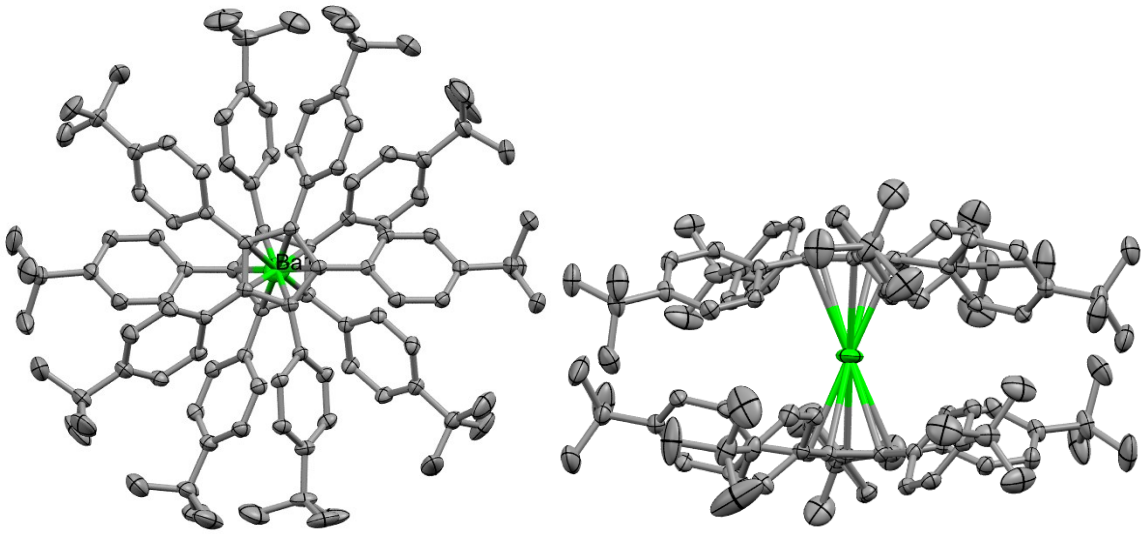

Figure 35: Front (left) and side (right) view of $Cp^{Big\ t\text{-}Bu}{}_2Ba$ 39 as a typical $Cp^{Big\ t\text{-}Bu}{}_2M$ metallocene. Hydrogen atoms and minor components of disorder are omitted for clarity. The other metallocene structures are depicted in the original publication.[133]

The metal atoms in compounds **36**, **38**, **39**, and **24 - 26** are linearly coordinated by two η^5-coordinated $Cp^{Big\ t\text{-}Bu}$ ligands. The metal atoms are positioned nearly above the center of the cyclopentadienyl rings.

In contrast, compound **43** exhibits η^1-coordination of $Cp^{Big\ t\text{-}Bu}$ ligands in the solid-state (Figure 36). However, the variable temperature ^1H NMR spectra of compound **43** in toluene-d_8, as shown in Figure 37, indicate that the aryl groups remain equivalent within the temperature range of −80 °C to 100 °C. This suggest a highly fluxional behavior in solution and indicates that the molecule undergoes sigmatropic shifts with a very low energy barrier, allowing for rapid interconversion of the aryl groups. At temperatures above 40 °C, increased dissociation into $Cp^{Big\ t\text{-}Bu}\cdot$ and mercury metal was observed both in ^1H NMR spectra and visually (mercury droplets and blue color of $Cp^{Big\ t\text{-}Bu}\cdot$).

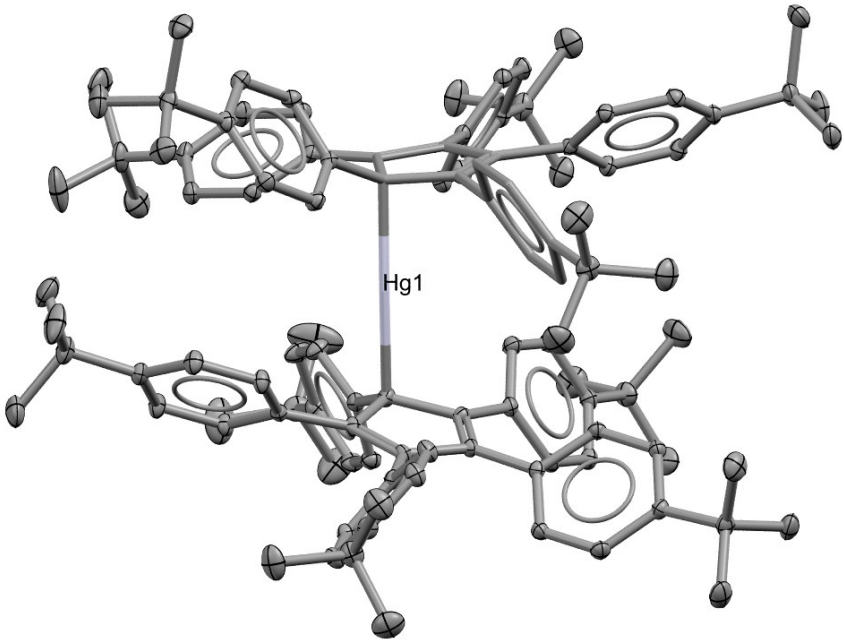

Figure 36. Solid-state structure of $Cp^{Big\ t\text{-}Bu}{}_2Hg$ 43. Hydrogen atoms and minor components of disorder are omitted for clarity.

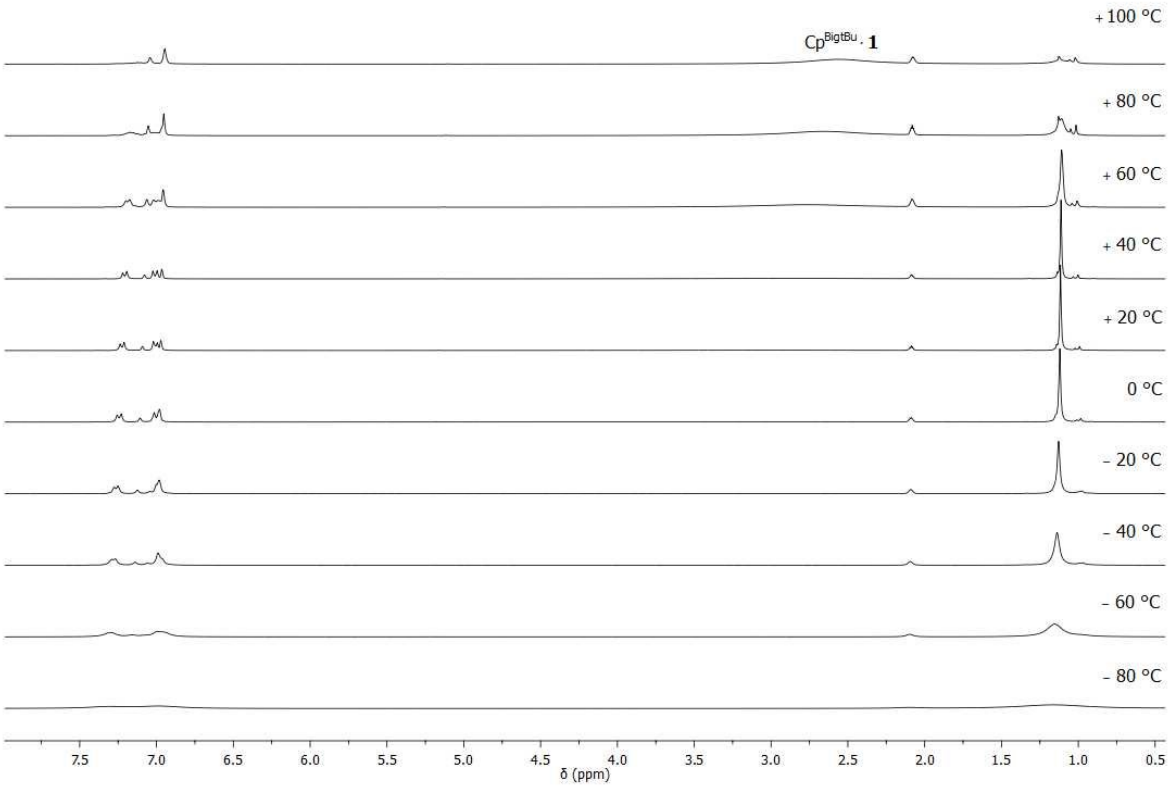

Figure 37: VT ^{1}H NMR spectra of $Cp^{Big\ t\text{-}Bu}{}_2Hg$ 43 in toluene-d_8.

Table 9: Selected bond lengths [Å] and angles [°] of 36, 38, 39, 24, 25, 26, 43, 44. C_r = best plane of C_1-C_5; C_c = centroid of Cp ring; [a] for non-parallel planes C_r-C_c. Any values related to centroids are not available with s.u.; [b] C_c–Ga–C_r; [c] C-Hg-C 174.69(5)°

	36	38	39	24	25	26	43	13
M-C_r	2.0624(6)	2.4923(10), 2.4935(10)	2.6413(7), 2.6411(7)	2.2417(5)	2.3995(8)	2.4587(8)	2.1989(13), 2.1370(14)	1.9351(8)
M-C_c	2.063	2.492, 2.495	2.642, 2.641	2.242	2.400	2.459	2.631, 2.734	1.936
Cr/Cr[a]	4.125	4.984, 4.986	5.282, 5.282	4.483	4.799	4.918	4.724, 4.307	–
C_c-M-C_c	180	177.8	178.3	180	180	180	147.7[c]	174.3[b]

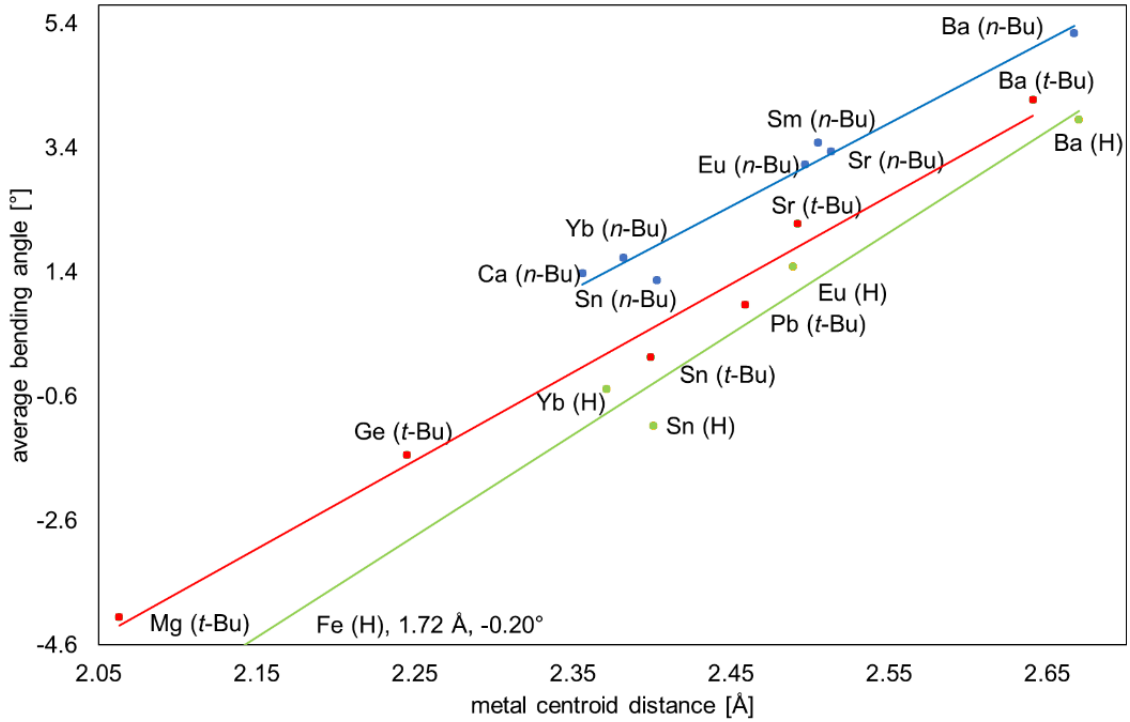

Figure 38: Average bending angles for decaarylmetallocenes with different *para*-substituents. The bending angle is defined as the angle between the Cp plane and the C_{Cp}-C_{ipso} bond. Positive angles indicate aryl groups bending towards each other. The data for *t*-Bu substituted complexes are derived from this work, while the remaining data are obtained from the literature.

The bending angles of the aryl groups in decaarylmetallocenes conform to the previously mentioned behavior (Figure 15). Specifically, for large metal ions, the aryl groups tend to bend towards each other, while for small metal ions, they bend away from each other. Including the identity of the *para*-substituent in the study revealed that the attractive forces between the aryl groups are stronger for *n*-butylphenyl groups compared to unsubstituted phenyl groups. This increased

attraction is likely due to enhanced dispersion interactions. In the case of *t*-butylphenyl groups, the effects lie somewhere in between, resulting from a combination of attractive forces and steric repulsion (Figure 38).

To verify the monovalent nature of the group 13 half-metallocenes **40 – 42**, for which suitable single-crystals were not obtained, **40 – 42** were reacted with (coe)$Cr(CO)_5$. This reagent has been previously utilized for synthesizing $CpGaCr(CO)_5$ and $Cp^*GaCr(CO)_5$ complexes.[143,144] It was found that only compound **40** reacted with (coe)$Cr(CO)_5$, resulting in the formation of the expected chromium pentacarbonyl complex $Cp^{Big\ t\text{-}Bu}GaCr(CO)_5$ **44** (Scheme 28). This reaction confirms the monovalent nature of compound **40**.

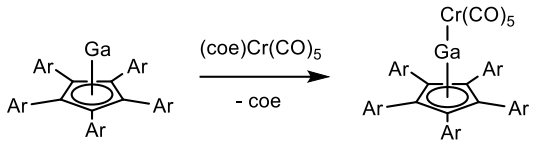

Scheme 28: Synthesis of $Cp^{Big\ t\text{-}Bu}GaCr(CO)_5$ 44 from $Cp^{Big\ t\text{-}Bu}Ga$ 40.

The ^1H and ^{13}C NMR spectra of compound **44** exhibit resonances corresponding to the $Cp^{Big\ t\text{-}Bu}$ ligand as expected. In the ^{13}C NMR spectrum, additional resonances originating from the carbonyl groups were observed, with chemical shifts of 223.39 ppm (CO axial) and 218.23 ppm (CO equatorial).

In the IR spectrum of compound **44**, two A_1 (2056 cm^{-1}, 1948 cm^{-1}) and one E (1928 cm^{-1}) vibrational modes were observed. These vibrations correspond to the symmetrical and asymmetrical stretching of the *transoid* and *cisoid* CO groups, which is in line with the expected C_{4v} symmetric $M(CO)_5$ fragment.

Furthermore, an IR forbidden B_1 fundamental stretching mode was detected at 1982 cm^{-1}. The presence of this band can be attributed to the perturbation of the ideal C_{4v} symmetry in the molecule.[145]

The shift of the *transoid* CO band to a lower wavenumber from the CO absorption band in $Cr(CO)_6$ (2000 cm^{-1}) suggests that the $Cp^{Big\ t\text{-}Bu}Ga$ ligand exhibits a weaker π-acceptor character in comparison to CO. Comparable finding were reported for the $Cp^*GaCr(CO)_5$ (A_1 2052, 1918 cm^{-1}; E: 1902 cm^{-1}; B_1: 1982 cm^{-1}),[143] whereas only two IR absorption bands were reported for $CpGaCr(CO)_5$ (2074, 1953 cm^{-1}).[144]

Single-crystals of **44** were obtained from a solution in benzene at 25 °C (Figure 39). **44** crystallizes in the monoclinic space group $P2_1/n$ with one molecule and two additional solvent molecules in the asymmetric unit. In compound **44**, the Ga atom exhibits an η^5-coordination mode to the cyclopentadienyl ring, similar to what is observed in metallocenes. The Ga–C distances in **44** range from 2.2683(17) to 2.3136(16) Å, with an average value of 2.2897 Å. This is consistent with the Ga–C distances reported for Cp*GaCr(CO)$_5$ (2.260(3) – 2.282(4) Å; average 2.260(3) Å), which also features an η^5-coordinated Cp substituent.[143] The C_c–Ga–Cr angles become more linear with increasing steric demand of the cyclopentadienyl substituent (**44** 174.3°, Cp*GaCr(CO)$_5$ 167.4°, CpGaCr(CO)$_5$ 164.2°).[143,144] The Ga–Cr distance of 2.3931(4) Å is similar to the distance reported for CpGaCr(CO)$_5$ (2.3955(3) Å)[144] and Cp*GaCr(CO)$_5$ (2.4046(7) Å).[143]

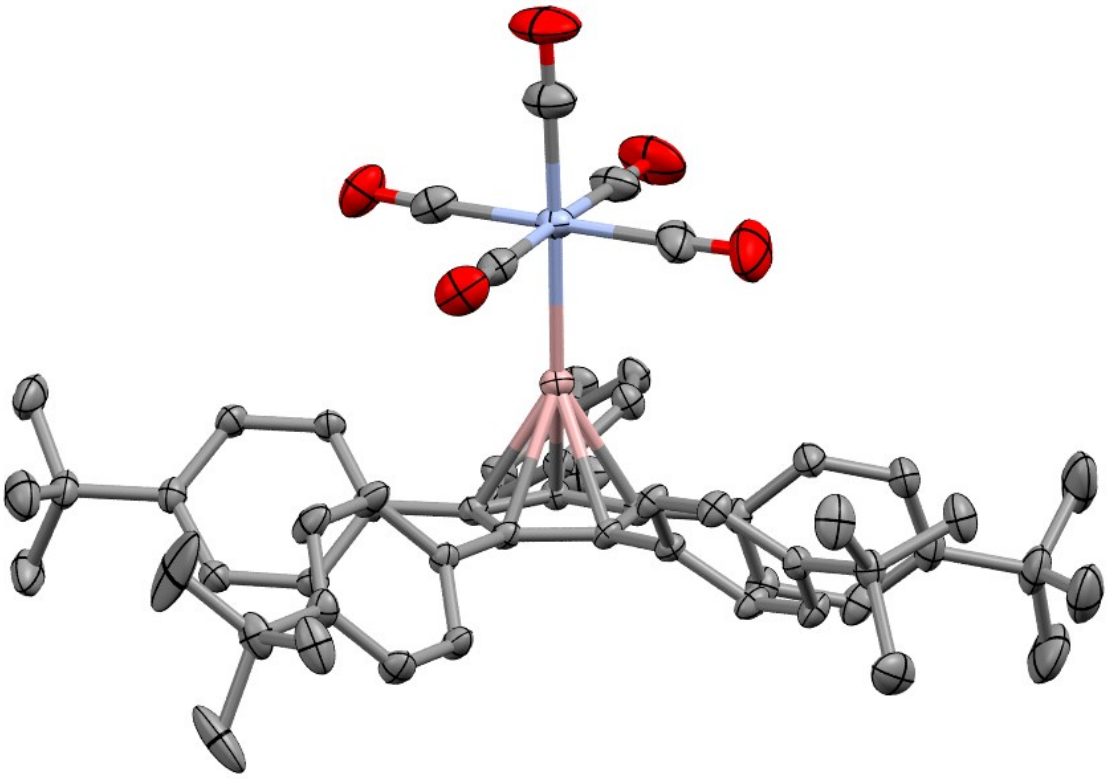

Figure 39: Solid-state structure of 44. H atoms of solvent molecules and disordered parts are omitted for clarity. Selected bond lengths [Å] and angles [°]: Ga1–Cr1 2.3931(4), Ga1–C1 2.2683(17), Ga1–C2 2.2965(16), Ga1–C3 2.3136(16), Ga1–C4 2.2996(16), Ga1–C5 2.2703(17), Cr1–C1_1 2.894(3), Cr1–C1_2 2.904(2), Cr1–C1_3 2.904(2), Cr1–C1_4 2.896(2), Cr1–C1_5 2.866(2); Ga1–Cr1–C1_5 177.30(8), Ga1–Cr1–C1_1 89.33(7), C1_1–Cr1–C1_3 178.50(10), Cr1–C12 2.894(3) .

A strong *trans* effect of the Cp$^{Big\,t\text{-}Bu}$Ga ligand in **44** is also observed in the crystal structure, resulting in a significant shortening of the *transoid* Cr–CO_{ax} bond length (1.866(2) Å) compared to the equatorial Cr–CO_{eq} bond lengths (av. 1.899 Å).

4.5 Attempts to Prepare Unfluorinated Cyclopentadienyl Cations

Several attempts have been made to prepare the cyclopentadienyl cations corresponding to the cyclopentadienyl radicals presented above, mainly by halide abstraction from cyclopentadienyl halides.

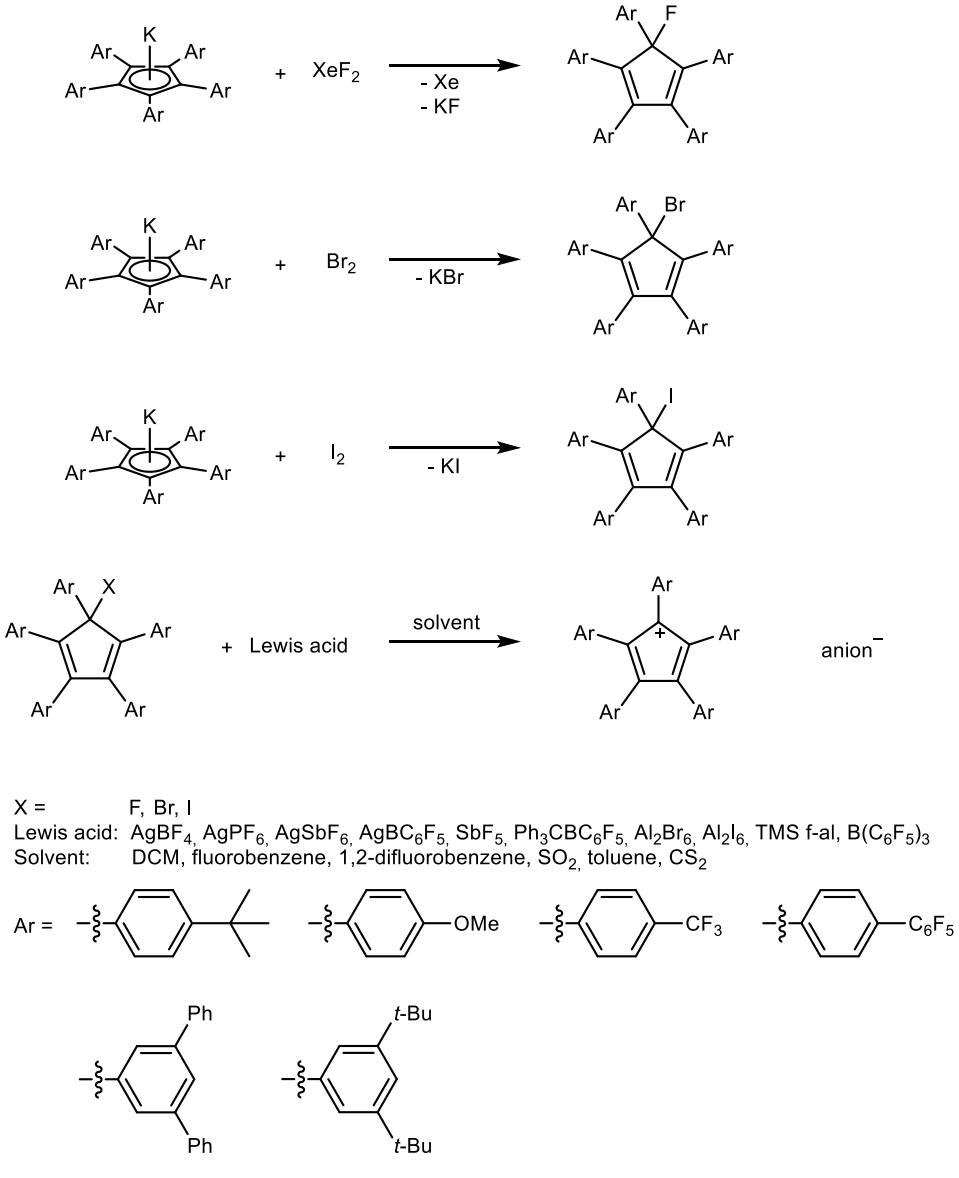

Scheme 29: Synthesis routes to cyclopentadienyl halides and attempts to prepare the corresponding cations.

The latter could be prepared by the reaction of cyclopentadienyl potassium salts with elemental halides (Br_2, I_2) in THF or with XeF_2 in acetonitrile. The preparation

of cyclopentadienyl chlorides was not attempted because of the inconvenience of handling gaseous chlorine and the lack of advantages over bromides or iodides.

Numerous attempts were made to abstract halide anions from cyclopentadienyl halides using various Lewis acids to generate different anions. This was done with the expectation of increasing the likelihood of crystallization. The reactions were typically performed at low temperatures (−78 °C). Unfortunately, none of these attempts were successful, frequently without clear reasons for the failures.

It has been previously reported that pentararylcyclopentadienyl cations can decompose via C–C bond formation between the *ortho*-positions of adjacent aryl groups.[39]

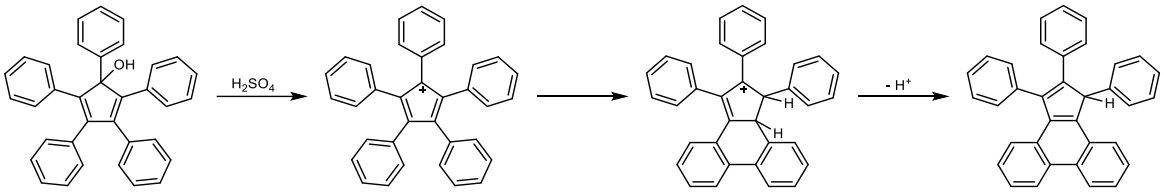

Scheme 30: Decomposition of the pentaphenylcyclopentadienyl cation in concentrated sulfuric acid.[39]

4.6 The Perfluoropentaphenylcyclopentadienyl System

The above mentioned investigations have shown that in order to prevent the decomposition of the pentaarylcyclopentadienyl cations, weak points such as C–H bonds should be avoided. In particular, the *ortho*-positions must be protected to prevent C–C bond formation. In addition, sterically demanding substituents are preferred to inhibit dimerization reactions. Pentafluorophenyl groups were considered a suitable choice due to their steric demand and chemical stability. However, the high electron deficiency of this compound would require synthesis under strongly oxidizing or strongly Lewis acidic conditions.

4.6.1 Synthesis

Attempts were made to synthesize perfluoropentaphenylcyclopentadienole using the palladium catalyzed route described above, but unfortunately, no defined product was obtained.

Consequently, an alternative approach was pursued (Scheme 31).

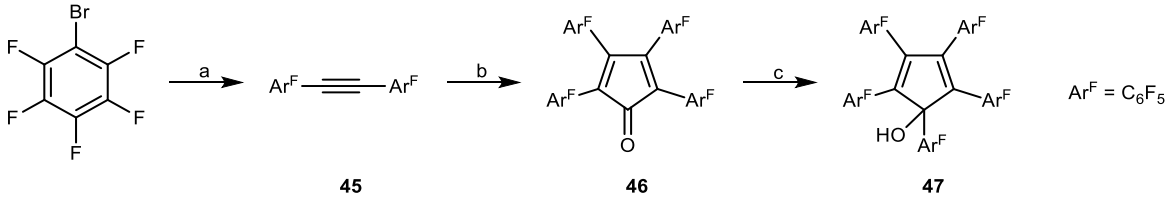

Scheme 31: Synthesis of pentakis(pentafluorophenyl)cyclopentadienole 47. a) EtMgBr in THF/Et_2O (*i*), diglyme, CuBr (*ii*), tribromoethylene, diglyme, 120 °C (*iii*); b) $Co_2(CO)_8$, decaline, 25 °C, then 190 °C (*i*), I_2 (ii); c) C_6F_5MgBr, THF, −78 °C to 25 °C.

In the first reaction (a, Scheme 31) bromopentafluorobenzene is first metallated using ethylmagnesium bromide in diethyl ether. This reaction has the advantage that the product, pentafluorophenylmagnesium bromide, is stable for weeks at 25 °C, in contrast to pentafluorophenyl lithium, which is typically handled at −78 °C and decomposes at higher temperatures. Pentafluorophenylmagnesium bromide can also be prepared directly from bromopentafluorobenzene, but the reaction is accompanied by the formation of black by-products. Pentafluorophenylmagnesium bromide is then converted into pentafluorophenylcopper which reacts with tribromoethene to form bis(pentafluorophenyl)ethyne **45**.[146]

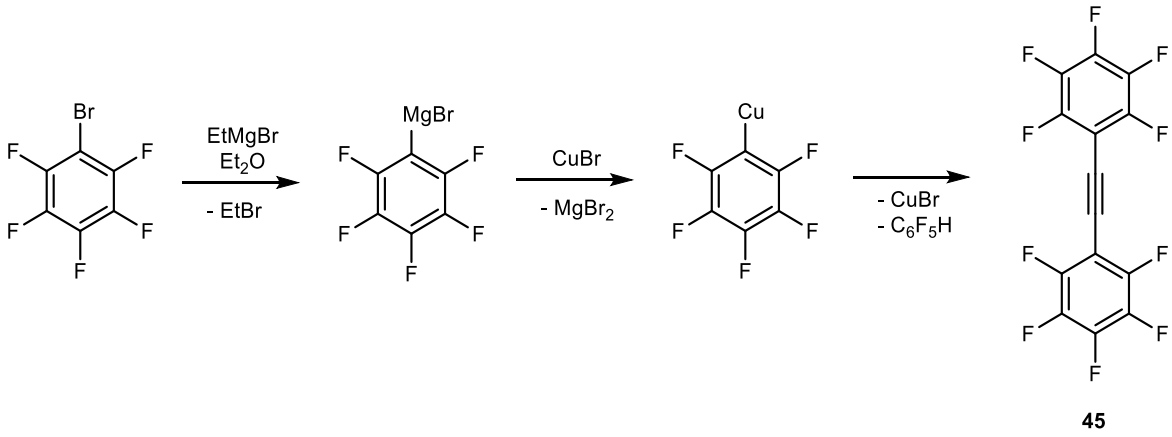

Scheme 32: Synthesis of perfluorotolane 45.

The next reaction (b, Scheme 31) is a modified Pauson-Khand-reaction,[147] which begins with the formation of a dicobalt hexacarbonyl acetylene complex,[148] which is thermally decomposed under incorporation of a CO molecule and then oxidized with iodine to the corresponding cyclopentadienone (Scheme 33). Omitting the oxidation step yields a cobalt-containing complex of unknown structure.

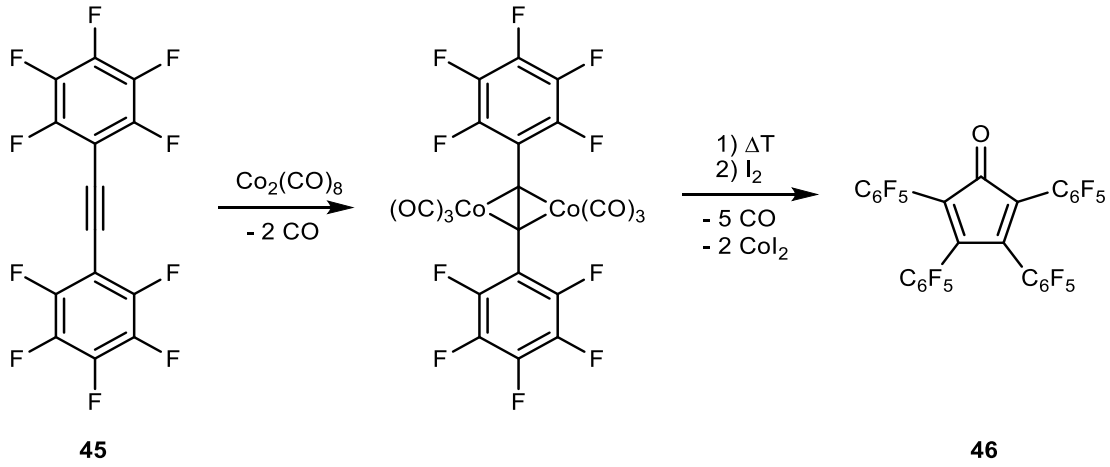

Scheme 33: Synthesis of perfluoropentaphenylcyclopentadienone 46.

46 is then reacted with pentafluorophenyl magnesium bromide to form pentakis(pentafluorophenyl)cyclopentadienole **47**. The reaction succeeds only when the Grignard reagent is added at −78 °C and the reaction mixture is the slowly warmed to 25 °C (Scheme 34). Otherwise, conjugate addition to the double bonds is the predominant reaction.

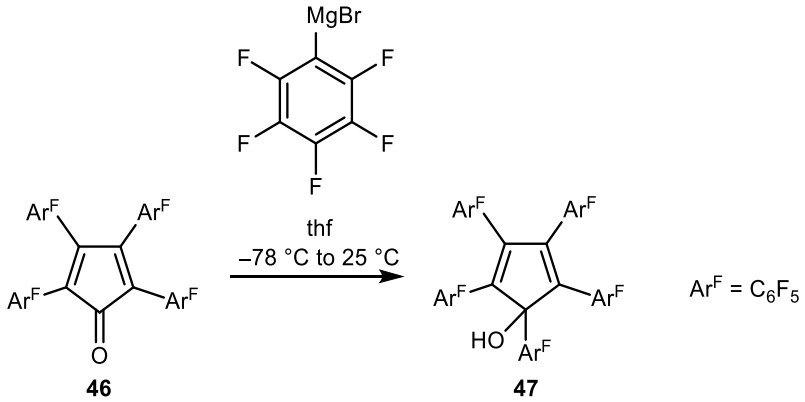

Scheme 34: Synthesis of perfluoropentaphenylcyclopentadienole 47.

The reactivity of compound **47** was found to be remarkably low, which can be attributed to two factors. Firstly, the formation of the energetically unfavorable Cp cation intermediate **48** hinders S_N1 reactions. Secondly, the bulky C_6F_5 substituents provide steric protection. For instance, **47** exhibits stability towards triflic anhydride with or without strong bases (such as pyridine or 4-dimethylaminopyridine), HBr in acetic acid, and PCl_5 at temperatures up to 110 °C in toluene.

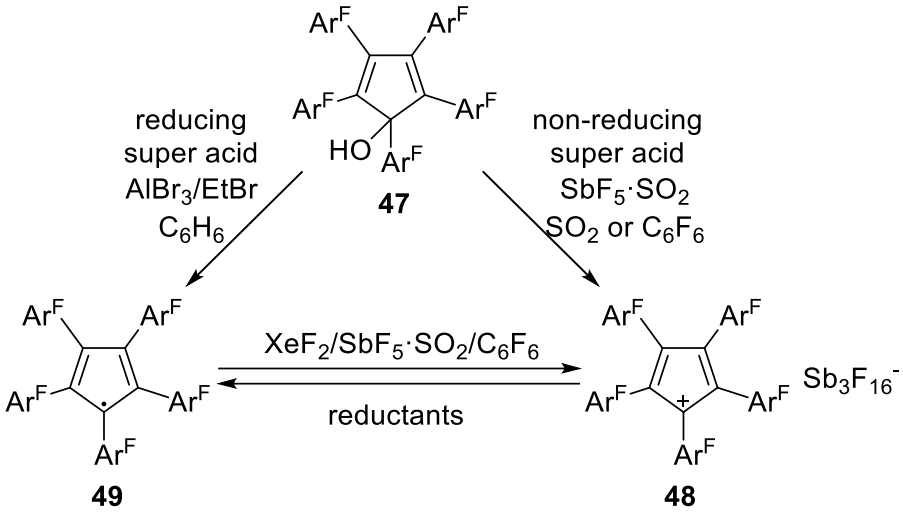

Scheme 35: Alcohol 47 can be reacted with reducing or non-reducing Lewis acids to prepare radical 49, and 48, respectively. These compounds can be interconverted through oxidation or reduction processes.

However, under superacidic conditions, **47** reacts with $SbF_5{\cdot}SO_2$ to form **48**, containing the desired Cp cation **48**$^+$. In contrast, when reacted with the Friedel-Crafts-type superacid system $AlBr_3$/EtBr/benzene (Scheme 35), it forms the corresponding cyclopentadienyl radical **49**. To handle the high oxidation potential of **48**, solvents resistant to these conditions (SO_2, hexafluorobenzene) are required. Furthermore, oxidation of radical **49** with an excess of XeF_2 and $SbF_5{\cdot}SO_2$ in C_6F_6 also yields **48**. Conversely, reactions of **48** with weak reducing agents such as alkanes, dichloromethane (DCM), difluorobenzene, and even polypropylene syringes yield radical **49**.

In situ NMR spectroscopy showed the complete conversion of **47** in the reaction with $SbF_5{\cdot}SO_2$ in SO_2. After the addition of $SbF_5{\cdot}SO_2$, the ^{19}F NMR spectrum (Figure 40, red) shows more signals than expected for the Cp cation salt **48** (three signals of *para*-fluorine atoms for a C_2 symmetric structure; one signal of *para*-fluorine atoms for a time-averaged C_5 symmetric structure). It is unclear whether this is due to impurities, equilibria between different species, formation of contact ion pairs, or other reasons.

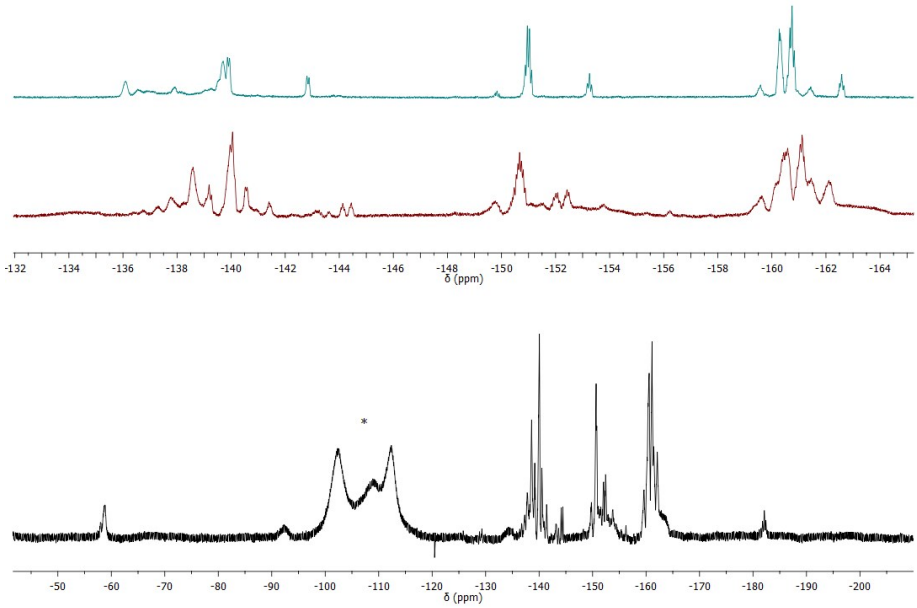

Figure 40: ^{19}F NMR spectra in liquid SO_2 at –30 °C of pentakis(pentafluorophenyl)cyclopentadienol 47 before (top, cyan) and after (middle, red and bottom, black) the addition of five equivalents of SbF_5·SO_2 using a glass capillary with acetone-d_6 as reference. The multiplet marked with an asterisk arises from $Sb_nF_mOH_o$ species.

The different species can be easily distinguished visually. While the alcohol **47** is pale yellow, the cation salt **48** is deep blue and the radical **49** is pink. This was also quantitatively analyzed by UV/Vis spectroscopy. **47** does not exhibit significant absorption in the visible region. **48** and **49** show absorption maxima at 678 nm and 546 nm, respectively (Figure 41). The UV/Vis spectra have also been predicted by quantum chemical methods by Prof. Dr. Gebhard Haberhauer. The measured spectra are well reproduced by the computations. When comparing the measured spectrum of **48** with the predicted spectra for the singlet Cp cation and the triplet Cp cation, it indicates that **48**$^+$ predominantly exists in the singlet state in the hexafluorobenzene solution.

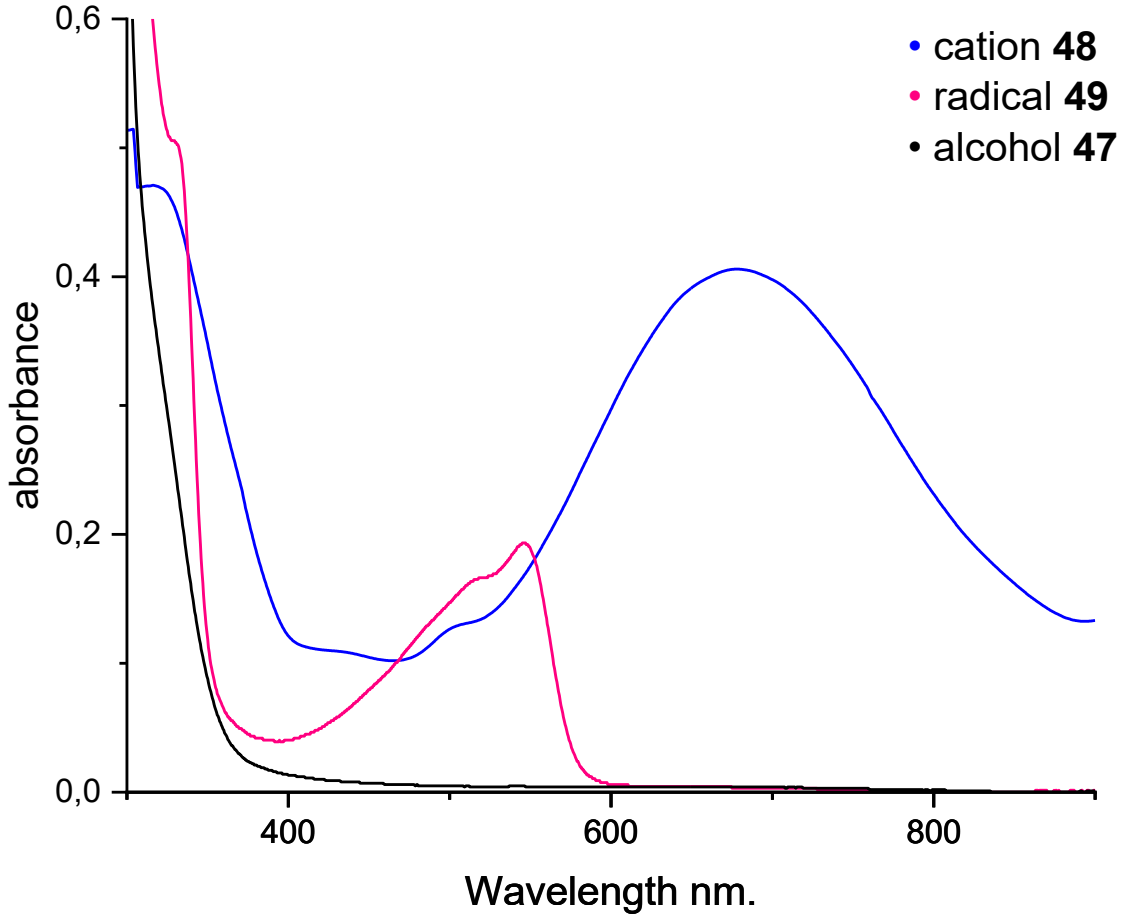

Figure 41: UV/Vis spectra of cation salt 48, radical 49, and alcohol 47 (50 µmol/L in hexafluorobenzene). The solution of 48 contained an excess (250 µmol/L) of $SbF_5 \cdot SO_2$ to scavenge traces of reducing agents or nucleophiles. Quantitative results for 48 may be imprecise because the concentration of 48 was not accurately known due to difficulties in the handling of its solution with a slightly leaking glass syringe.

Solutions of **48** in SO_2 and **49** in toluene were also examined by Blaise L. Geoghegan and Dr. George Cutsail III using EPR spectroscopy. The EPR spectrum of **49** showed a characteristic signal consistent with a Cp radical, with a g value of 2.0033 and a line width of 0.75 mT (Figure 43). No EPR signal was detected for **48** in solution at room temperature. It is important to note that the absence of a signal does not provide conclusive evidence for the complete absence of molecules in the triplet state.

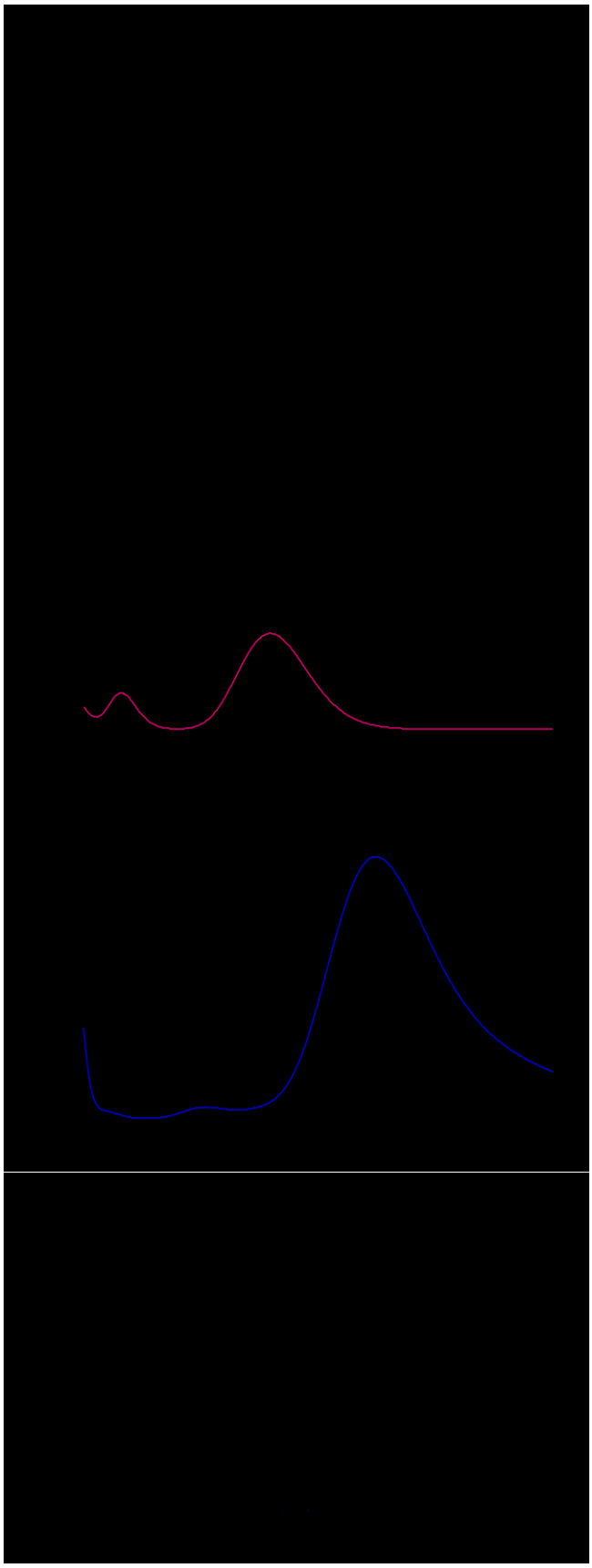

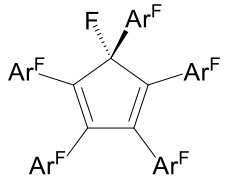

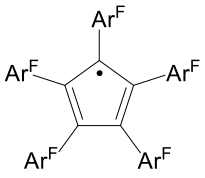

49

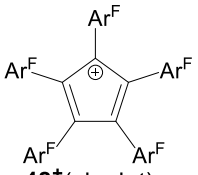

48⁺(singlet)

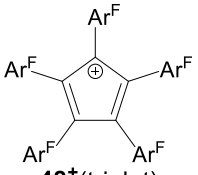

48⁺(triplet)

Figure 42: UV/Vis spectra of cyclopentadienyl fluoride (a), radical 49 (b) as well as of the singlet (c) and triplet (d) state of 48^+ calculated by Prof. Dr. Gebhard Haberhauer at TD-PBE0 (SMD, hexafluorobenzene)/def2-TZVP//B3LYP-D3BJ/TZP level of theory.

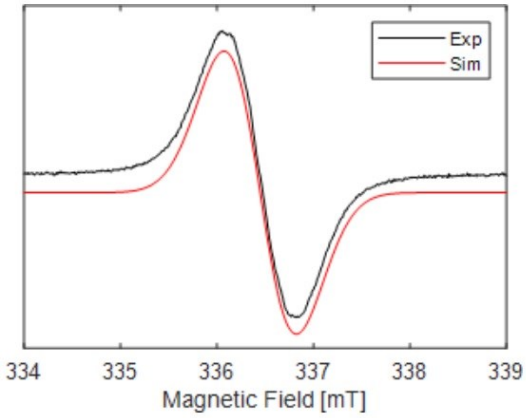

Figure 43: EPR spectrum of the pentakis(pentafluorophenyl)cyclopentadienyl radical 49. For the simulation, a g-value of 2.0033 and a linewidth (peak-to-peak) of 0.75 mT were used.

A magnetic susceptibility measurement conducted by Daniel J. SantaLucia on the crystalline solvate $Cp(C_6F_5)_5Sb_3F_{16} \cdot 1.5\ C_6F_5$ **48a** confirms that the ground state of the compound is diamagnetic. The observed temperature-independent paramagnetism is attributed to Van Vleck paramagnetism, which arises from the mixing of the low-lying excited aromatic triplet state with the ground state under the influence of an applied magnetic field, providing additional evidence that the triplet state must be close in energy but higher in energy than the singlet state (Figure 45).[149]

Because $\chi_P T$ = 0.019 $cm^3\ mol^{-1}$ K at 2 K (as opposed to the expected 0 $cm^3\ mol^{-1}$ K for the singlet system) (Figure 45), it was necessary to model a $\vec{S} = 1/2$ paramagnetic impurity in the sample of 4.6%. This impurity arose from a small portion of the sample being oxidized, which was observed as a thin layer of pink powder on the top of the susceptibility sample (Figure 44). The non-linearity in the susceptibility data is due to imperfect correction of diamagnetism for the sample holder, since it was observed that the uncorrected data is completely linear (Figure 45).

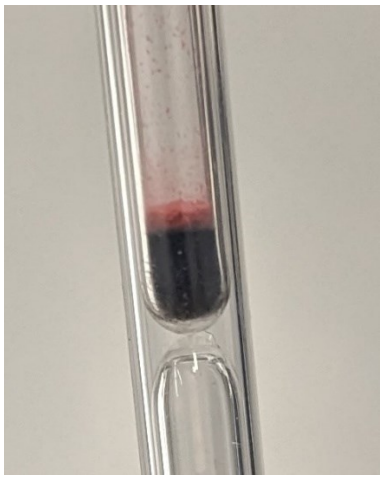

Figure 44: SQUID sample after measurement. A layer with the pink color of the radical 49 is clearly visible and probably results from traces of reducing agents.

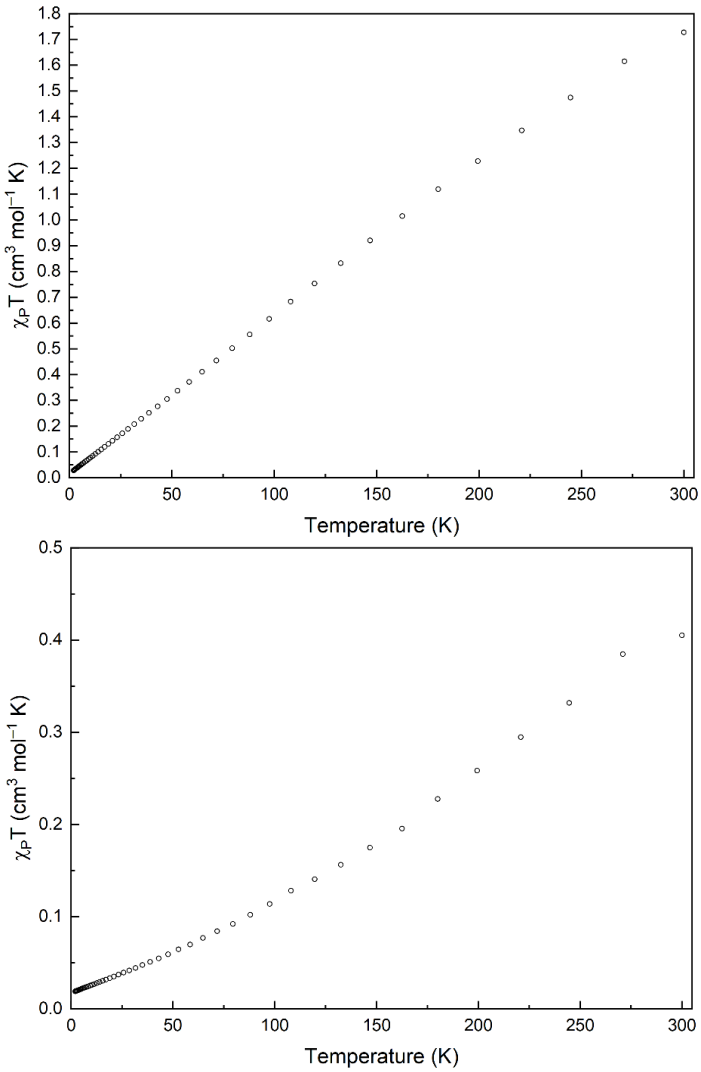

Figure 45: (Top) Uncorrected paramagnetic susceptibility data for 48a; (bottom) paramagnetic susceptibility data corrected for inherent diamagnetism of the sample holder.

Cyclic voltammetry (SO_2, NBu_4SbF_6) was conducted by Susanne Rupf on a solution of the radical **49** to determine the potential at which it is oxidized to the cation **48**$^+$. The measurement showed that the interconversion of **49** and **48**$^+$ occurs at an anodic peak potential of E_{pa} = +2.30 V vs. ferrocene (Figure 46 and Figure 47). Despite the larger π-system, this value is significantly higher than the anodic peak potential for the oxidation of the perfluorinated trityl radical to its cation $C(C_6F_5)_3^+$ (+1.11 V vs. Cp_2Fe in 1,2-difluorobenzene),[150] possibly indicating antiaromatic destabilization of the cation.

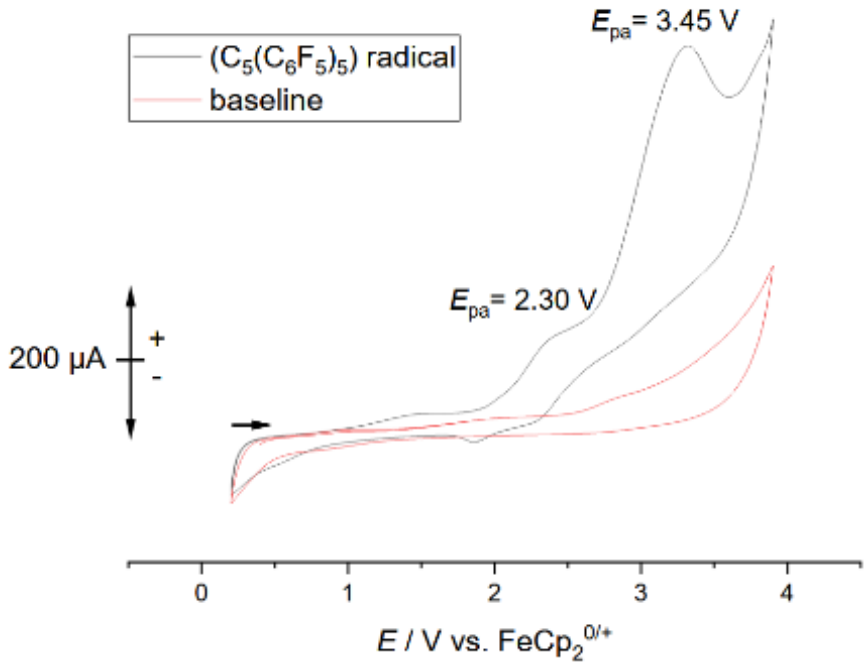

Figure 46: Cyclic voltammogram of the pentakis(pentafluorophenyl)cyclopentadienyl radical 49 at −20 °C in SO_2 with NBu_4SbF_6. The first redox event at E_{pa} = 2.30 V is assigned to the oxidation of radical 49 to cation 48$^+$. The cause of the second redox event at E_{pa} = 3.45 V is unclear, but it is only observable in the presence of the sample and is possibly attributable to the subsequent oxidation of the aryl groups.

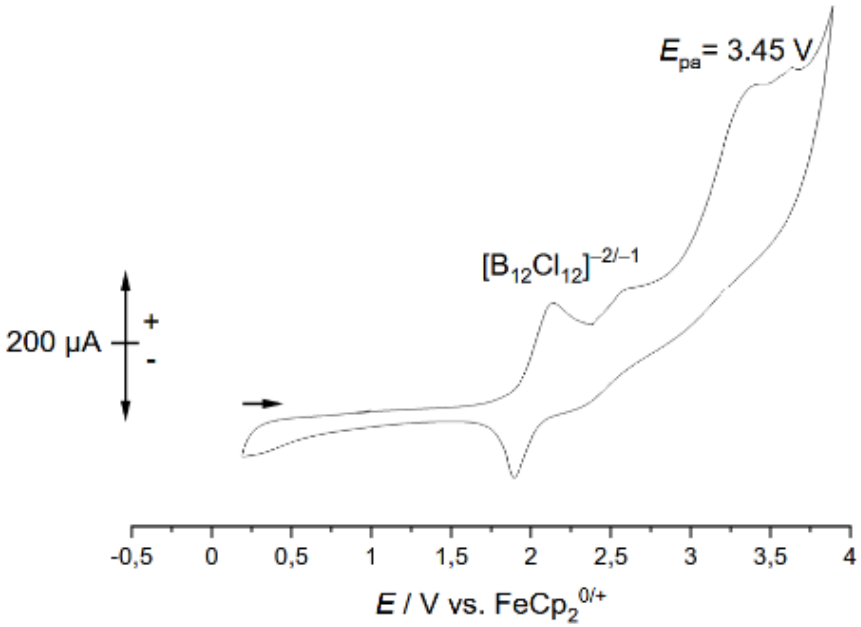

Figure 47: Cyclic voltammogram of the pentakis(pentafluorophenyl)cyclopentadienyl radical 49 with $Li_2B_{12}Cl_{12}$ as reference at −20 °C in SO_2 with NBu_4SbF_6.

The CV experiments were performed with the Cp radical **49** starting from 0 V and going to higher potentials. Two oxidation processes were observed above 2 V which were referenced with $Li_2B_{12}Cl_{12}$ whose oxidation potential vs. ferrocene is known (oxidation from the dianion to a monoanion at 2.11 V and from the monoanion to a neutral species at 2.67 V).[151] It should be noted that due to the high reactivity of the generated species an unspecified decomposition of the mixture was observed during the second oxidation and reduction cycle in the referencing experiment. A possible oxidation of the conducting salt was ruled out by measuring the conducting salt alone (see baseline in Figure 46).

The results of the CV measurements were confirmed by calculating the reaction enthalpy of the isodesmic reaction shown in Scheme 36.

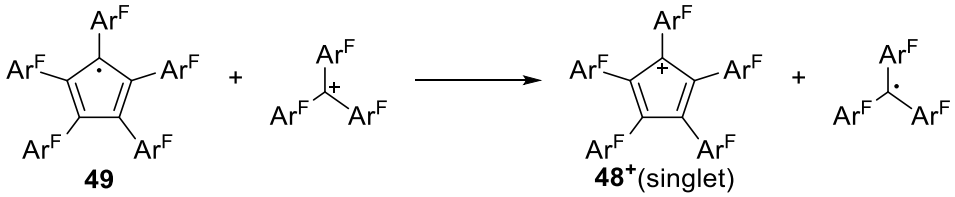

Scheme 36: Isodemic reaction between the perfluorinated cyclopentadienyl radical 49 and the perfluorinated trityl cation to the perfluorinated cyclopentadienyl cation 48^+ and the perfluorinated trityl radical.

The quantum chemical computations were performed by Prof. Dr. Gebhard Haberhauer at the DLPNO-CCSD(T)/cc-pVTZ level of theory. The calculated oxidation potential for **49** is 0.94 V (21.7 kcal/mol) higher than that for the perfluorotrityl radical (observed difference: 1.19 V).

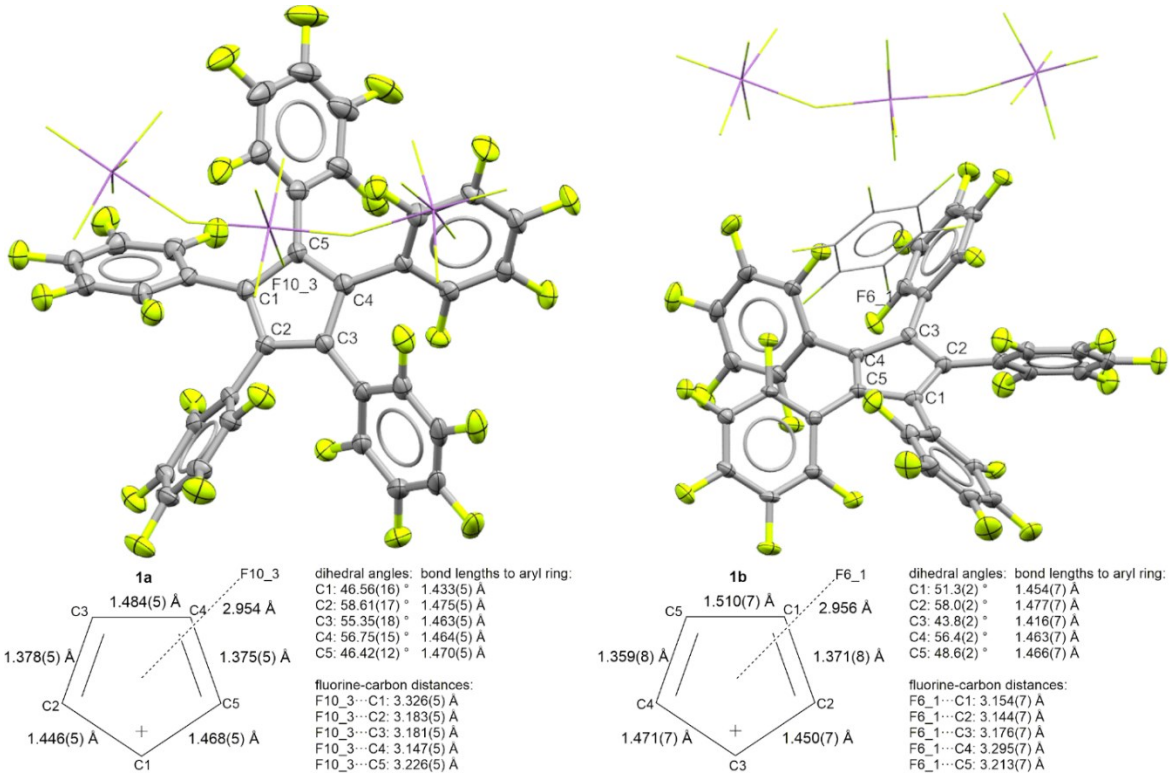

Figure 48: Solid-state structures of 48a (left) and 48b (right), including selected bond lengths and dihedral angles between the Cp plane and the aryl groups (defined as best fit planes of the five Cp carbon atoms and six aryl carbon atoms). Anions and solvent molecules are depicted as wireframe models. Ellipsoids are drawn at a probability level of 50%. Non-participating solvent molecules are omitted for clarity.

It was possible to crystallize **48** from a solution in hexafluorobenzene at 6 °C. Different crystallization experiments yielded two distinct solvates, $Cp(C_6F_5)_5Sb_3F_{16}\cdot 1.5C_6F_6$ (**48a**) and $Cp(C_6F_5)_5Sb_3F_{16}\cdot 2C_6F_6$ (**48b**, Figure 48).

Despite intentionally choosing a solvent (C_6F_6) and a counteranion ($Sb_3F_{16}^-$) with a low nucleophilicity, the Cp cations in both structures exhibit a weak interaction with a negatively polarized fluorine atom from either the counter anion ($Cp(C_6F_5)_5Sb_3F_{16}$ **48a** in $Cp(C_6F_5)_5Sb_3F_{16}\cdot 1.5\ C_6F_6$) or the solvent ($Cp(C_6F_5)_5C_6F_6$ **48b** in $Cp(C_6F_5)_5Sb_3F_{16}\cdot 2\ C_6F_6$). The distances between the carbon atoms of the Cp ring and these fluorine atoms (Figure 48) fall within the range of the sum of van der Waals radii of carbon and fluorine (3.17 Å).[152] These distances do not indicate a covalent interaction. Furthermore, the sums of bond angles of all carbon atoms in

the Cp ring are all above 359.0°, ruling out the presence of a tetrahedrally coordinated carbon atom. As a comparison, the corresponding cyclopentadiene **53** (discussed below) with a hydrogen atom instead of fluorine has a sum of bond angles of 334.5(5)° or 332.6(4)° (two independent molecules) between the carbon atoms at the tetracoordinate carbon atom.

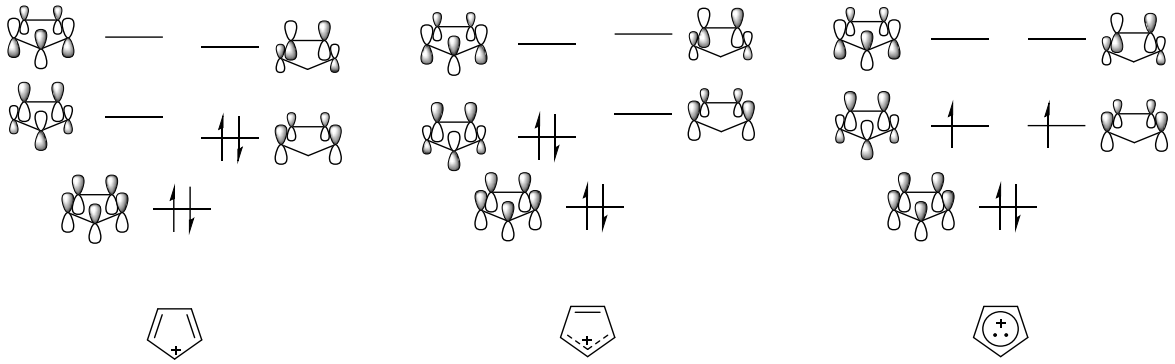

Figure 49: Triplet cyclopentadienyl cation (right) and two possible valence tautomers of a singlet cyclopentadienyl cation (left and middle).

Further quantum mechanical computations were performed by Prof. Dr. Gebhard Haberhauer to gain a deeper understanding of the electronic structures. Key structures were optimized, and energies of the singlet and triplet states of the cyclopentadienyl cation **48⁺** (Figure 49 left and right) were calculated using DFT approaches. Geometry optimizations were carried out using (U)B3LYP and (U)CAM-B3LYP[153] computations and atom-pairwise dispersion correction with Becke-Johnson damping (D3BJ). Open-shell singlet states were calculated with the "guess = mix" keyword, and restricted open-shell computations yielded the same energy values as closed-shell computations. Single-point computations were performed using the double-hybrid method B2PLYP-D3BJ/TZ2P[154] and DLPNO-CCSD(T) with various basis sets (from def2-SVP to def2-QZVPP).

The singlet-triplet gaps calculated with various methods can be found in Table 10 and Table 11. These results suggest that the triplet state is energetically favored over the singlet state in the gas phase. When the proximity of the anion is taken into account, the singlet state gets less unfavorable and was even preferred in one case (B2PLYP-D3BJ/TZ2P//B3LYP-D3BJ/TZP). When the computations are performed with the geometrical data from sc-XRD measurements, the singlet state is clearly preferred (Table 12).

Table 10: Energy (Δ*E*) and Gibbs energy (Δ*G*) of the triplet state of 48^+ and 48^+ SbF_6^- relative to the singlet state in kcal/mol. [a] The zeroth order regular approximation (ZORA)[155] to the Dirac equation was used.

method	molecule	Δ*E*	Δ*G*
cam-B3LYP-D3BJ/6-31G(d)	**48^+**	-6.20	-5.43
cam-B3LYP-D3BJ/6-311++G(d,p)	**48^+**	-5.55	-4.58
B3LYP-D3BJ/6-31G*	**48^+**	-5.62	-5.39
B3LYP-D3BJ/TZP[a]	**48^+**	-4.96	-5.45
B3LYP-D3BJ/TZP[a]	**48^+ SbF_6^-**	-3.65	-2.54
B2PLYP-D3BJ/TZ2P//B3LYP-D3BJ/TZP[a]	**48^+**	-2.27	-2.77
B2PLYP-D3BJ/TZ2P//B3LYP-D3BJ/TZP[a]	**48^+ SbF_6^-**	-0.75	+0.36

These computations show that the preference of the singlet state is a result of the proximity of a negatively polarized fluorine atom, leading to the localization of the positive charge on one specific carbon atom. Consequently, the interaction between the anion and the differently polarized carbon centers becomes stronger, as compared to the interaction with five equally polarized carbon atoms. This increased interaction arises from the shorter distance between the anion and the localized carbon atom.

The calculated APT (atomic polar tensor) and NBO (natural bond orbitals) charges provide further insights. In the singlet cation, a pronounced localization of the positive charge at C1 is observed, whereas in the triplet cation, the positive charge is delocalized over all five carbon atoms. These findings are illustrated in Figure 50.

Table 11: Energy (Δ*E*) of the triplet state of 48^+ relative to the singlet state. The geometrical data for these single point computations stem from the B3LYP-D3BJ/TZP computations. The values are given in kcal/mol.

method	Δ*E*
DLPNO-CCSD(T)/def2-SVP	-5.8
DLPNO-CCSD(T)/cc-pVDZ	-5.9
DLPNO-CCSD(T)/def2-TZVPP	-6.4
DLPNO-CCSD(T)/cc-pVTZ	-5.8
DLPNO-CCSD(T)/def2-QZVPP	-5.6

Table 12: Energy (Δ*E*) of the triplet state relative to the singlet state in kcal/mol. The geometrical data for these single point computations stem from the X-ray structure analyses.

method	molecule	Δ*E*
B3LYP-D3BJ/TZP	**48a**	+0.6
	48b	+5.0
B2PLYP-D3BJ/TZ2P	**48a**	+4.2
	48b	+8.1
DLPNO-CCSD(T)/def2-SVP	**48a**	+3.0
	48b	+6.7
DLPNO-CCSD(T)/def2-TZVPP	**48a**	+2.4
	48b	+6.5

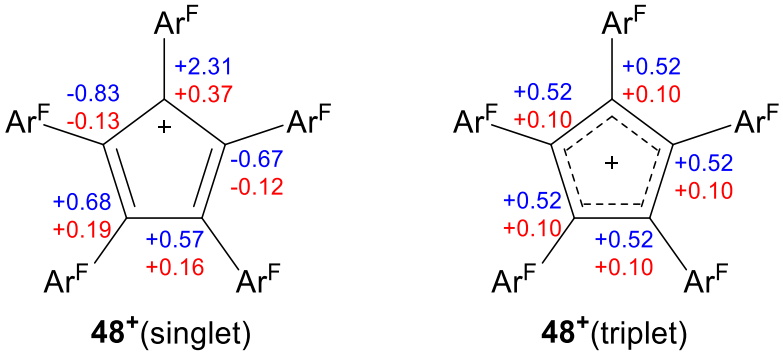

Figure 50: APT (atomic polar tensor) charges (blue; CAM-B3LYP-D3BJ/6-311++G(d,p)) and NBO (natural bond orbitals) charges (red; CAM-B3LYP/def2-TZVP//CAM-B3LYP-D3BJ/6-311++G(d,p)) of 48⁺ in the singlet and triplet.

Upon comparing the calculated C−C bond lengths in the triplet state of the cyclopentadienyl cation **48⁺**, it is observed that nearly identical bond lengths are obtained (1.431−1.434 Å for B3LYP-D3BJ/TZP). This observation supports the aromatic nature of the triplet system. In contrast to the triplet state, the singlet state of cation **48⁺** exhibits a pronounced C−C bond length alternation, as observed in both computational computations (1.366−1.539 Å for B3LYP-D3BJ/TZP) and measured solid-state structures of the cyclopentadienyl cations **48a** (1.375−1.484 Å) and **48b** (1.359−1.510 Å). This further supports that the cyclopentadienyl cation salts (**48a** and **48b**) adopt singlet states in the solid-state.

The HOMA values of the calculated (B3LYP-D3BJ/TZP) and experimentally determined geometries for **48⁺**(S) and **48⁺**(T) have been calculated: HOMA(**48⁺**(S)(calculated)) = −0.69, HOMA(**48⁺**(T) (calculated)) = +0.49, HOMA(**48a**(measured)) = +0.01 and HOMA(**48b**(measured)) = −0.39.

That is, while the triplet state of **48⁺** should be aromatic, the calculated singlet state of **48⁺** and the cyclopentadienyl cation **48b** found in the solid-state are antiaromatic while **48a** can rather be considered as non-aromatic by this criterion.

NICS (Nucleus Independent Chemical Shift) values were calculated using CAM-B3LYP along a line perpendicular to the center of the ring plane, spanning a distance of 5 Å, with a step size of 0.1 Å. This analysis was performed for both the singlet and triplet states of the cyclopentadienyl cation **48⁺** (Figure 51). Consistent with the other results, this indicates that the triplet state of the cyclopentadienyl cation **48⁺**

exhibits aromatic behavior, while the singlet state displays anti-aromatic characteristics.

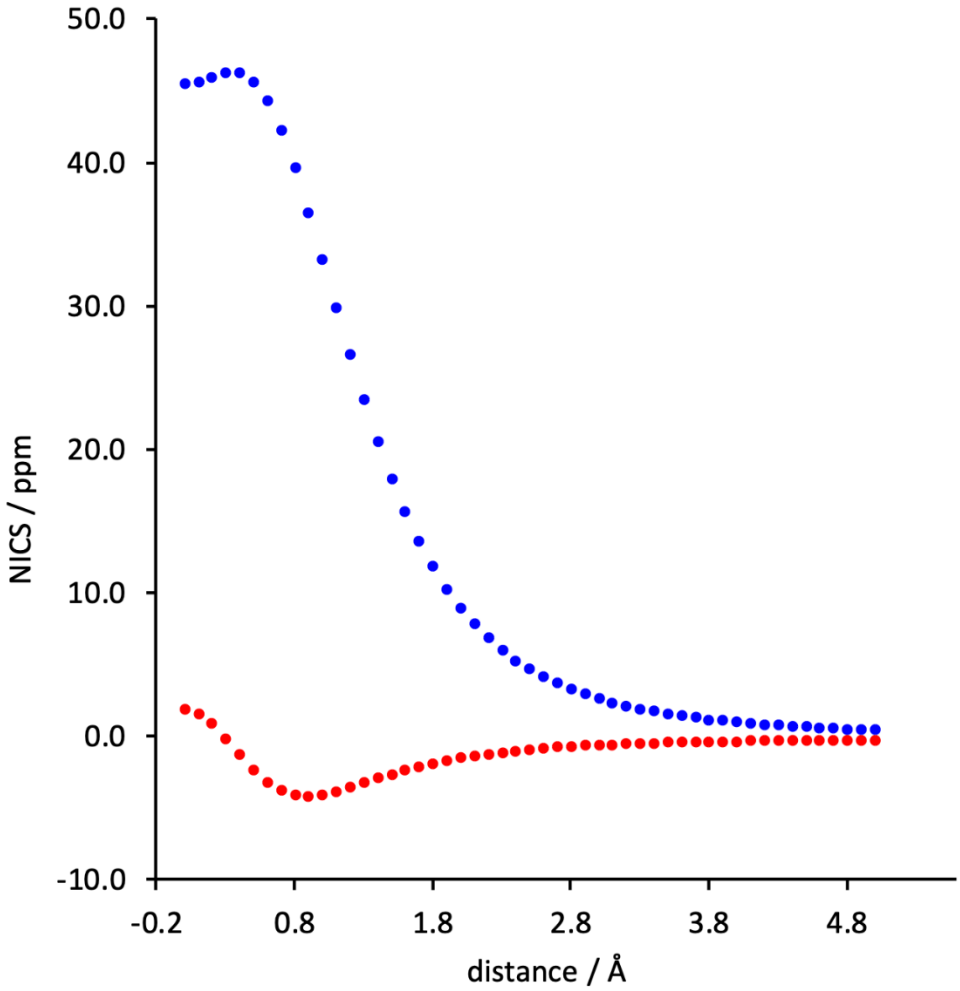

Figure 51: NICS scans of 48^+ calculated using CAM-B3LYP/def2-TZVP//CAM-B3LYP-D3BJ/6-311++G(d,p). Blue-colored curve refers to singlet state and red-colored curve refers to triplet state.

The Lewis acidity of $Cp(C_6F_5)_5^+$ was quantified by Moritz Malischewski by calculating its hydride (HIA) and fluoride ion affinities (FIA). The calculated values for HIA and FIA were found to be high, with HIA at 1014 kJ/mol and FIA at 774 kJ/mol. These values even exceed those of the highly reactive perfluorotritylium cation $C(C_6F_5)_3^+$ (HIA: 955 kJ/mol; FIA: 697 kJ/mol), which was already used for comparison above.[150]

When considering solvation effects, the calculated HIA and FIA are significantly lower, with values of 448 kJ/mol (HIA in CH_2Cl_2) and 246 kJ/mol (FIA in CH_2Cl_2). Similarly, accounting for solvation in other solvents, such as SO_2, results in lower values of 455 kJ/mol (HIA in SO_2) and 223 kJ/mol (FIA in SO_2). Nevertheless, to

stabilize $Cp(C_6F_5)_5^+$ as a room temperature stable salt, an excess of the powerful Lewis acid SbF_5 (FIA: 496 kJ/mol) was necessary.

4.6.2 Reactivity

48 was found to readily react with the weak Lewis base carbon monoxide in C_6F_6 or SO_2, but unfortunately no crystalline product was isolated. It is proposed that a carbonyl complex **51** is formed, similar to the previously reported synthesis of an isoelectronic borole carbonyl complex obtained from the reaction of CO with the highly Lewis acidic perfluoropentaphenylborole.[156] The formation of **51** was indirectly confirmed by hydrolysis leading to the corresponding carboxylic acid **52**, which was identified by ^{19}F NMR spectroscopy and sc-XRD. **52** underwent decarboxylation under the hydrolysis conditions (H_2O, 25 °C), resulting in the formation of the novel pentakis(pentafluorophenyl)cyclopentadiene **53**.

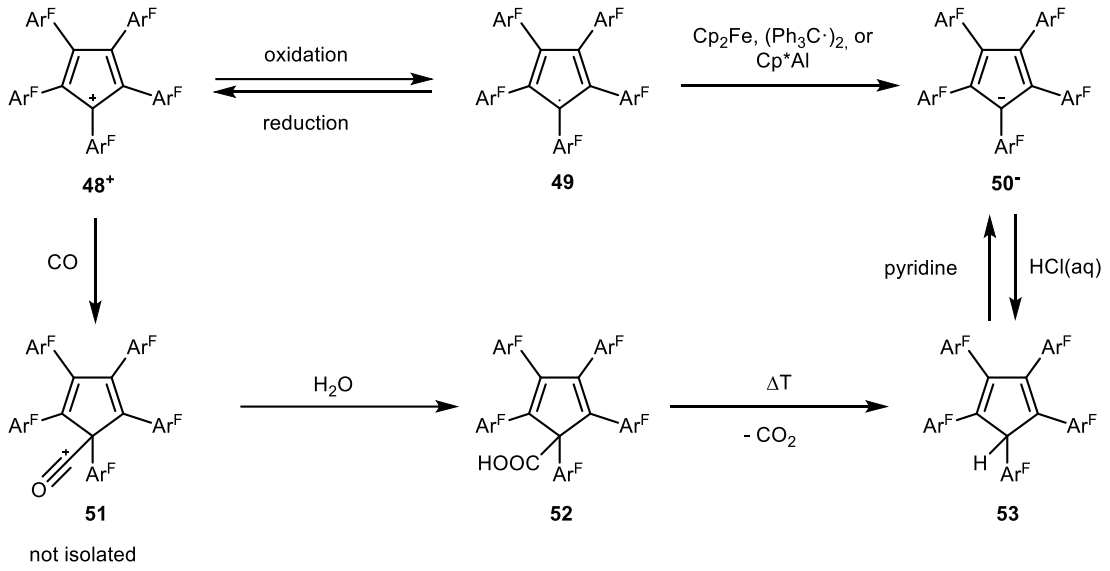

Scheme 37: Reactions of 48 – 53.

Reed and Richardson proposed pentakis(pentafluorophenyl)cyclopentadienide **50**$^-$, the conjugated base of **53** as a "carbon-based weakly coordinating anion", but did not prepare it.[157] Compared to the known pentacyanocyclopentadiene[157] and pentakis(trifluoromethyl)cyclopentadiene,[158] compound **53** is anticipated to be less acidic. However, its larger size and the presence of non-basic C_6F_5 side arms, as well as its stability to polymerization and HF formation, render it an interesting candidate as a strong carbon acid that forms a weakly coordinating anion. The pK_a

value of **53** was estimated by chemical means to be between -1 and 4.76, because **50**$^-$ is protonated by hydrochloric acid, but not by acetic acid, while **53** can be deprotonated with pyridine to give the pyridinium salt pyrH-**50**.[159]

An alternative method for obtaining salts of anion **50**$^-$ is through the direct reaction of radical **49** with reducing agents. Cyclic voltammetry studies by H. Micha Weinert using **49** (1,2-difluorobenzene, $NBu_4B(Ph\text{-}3,5(CF_3)_2)_4$) demonstrated a reversible reduction to form **50**$^-$ at a half-wave potential of 0.48 V vs. ferrocene.

50$^-$ may prove useful as an "innocent" oxidant, which avoids the production of undesirable byproducts typically associated with traditional one-electron oxidants like NO^+ or Ag^+, thereby circumventing separation challenges or adverse reactivity. Furthermore, reactions involving **49** can be visually monitored due to its intense pink color. Compound **49** can be purified by sublimation and stored for several months, even in the presence of air and moisture. It can also be washed with water without significant decomposition. To evaluate its practical applicability, compound **49** was reacted with ferrocene, Gomberg's dimer $(Ph_3C\cdot)_2$, and Cp*Al (Scheme 37), in all cases yielding the respective salts of anion **3** ($FeCp_2^+$ **50**$^-$ (**50a**), Ph_3C^+ **50**$^-$ (**50b**), $(Cp^*)_2Al^+$ **50**$^-$ (**50c**)) in single-crystalline and pure form. The Solid-state structures of **50a-c** have been determined by sc-XRD. These structures exhibit nearly symmetrical Cp rings with C−C bond lengths ranging from 1.405 Å to 1.415 Å (Table S1). The cations are positioned in close proximity to the negatively charged Cp ring, with the shortest distances between the Cp centroid and the hydrogen atoms measuring 2.546 Å – 3.131 Å (Table 13, Figure 56– Figure 60).

The crystal structures of **45**, hexakis(pentafluorophenyl)benzene, **49** (crystallized from benzene and SO_2), **52**, and **53** were also measured (Figure 52 – Figure 55, Figure 59, Figure 60).

Table 13: Bond lengths in the Cp ring and shortest distance of the Cp centroid to an adjacent hydrogen atom for 50a-c.

	50a	**50b**	**50c**
bond length (Å) of C1-C2	1.405(5)	1.406(3)	1.409(3)
bond length (Å) of C2-C3	1.408(5)	1.409(3)	1.420(3)
bond length (Å) of C3-C4	1.415(6)	1.412(3)	1.401(3)
bond length (Å) of C4-C5	1.411(5)	1.409(3)	1.414(3)
bond length (Å) of C5-C1	1.405(5)	1.411(3)	1.411(3)
distance (Å) between centroid(Cp) and next H	2.546	2.683	3.131

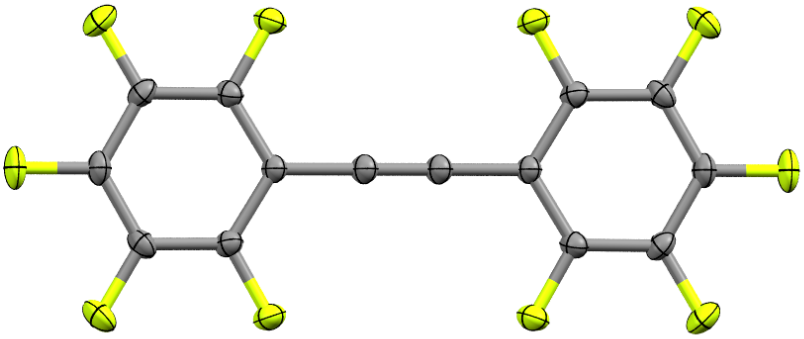

Figure 52 Solid-state structure of bis(pentafluorophenyl)ethyne 45, crystallized from benzene. Ellipsoids are drawn at a probability level of 50%.

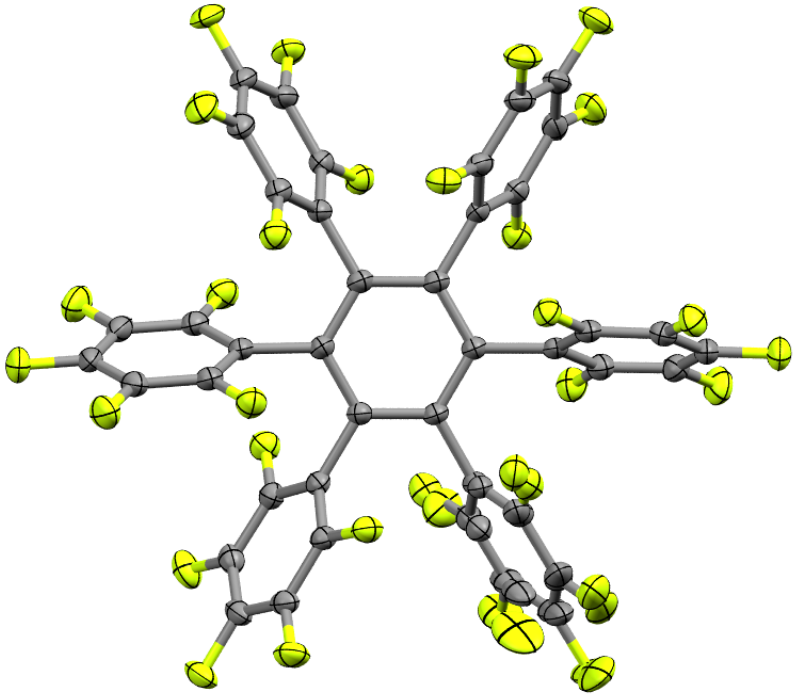

Figure 53 Solid-state structure of hexakis(pentafluorophenyl)benzene. Ellipsoids are drawn at a probability level of 50%. Hexakis(pentafluorophenyl)benzene was obtained as a by-product in the synthesis of C and crystallized from toluene/DCM.

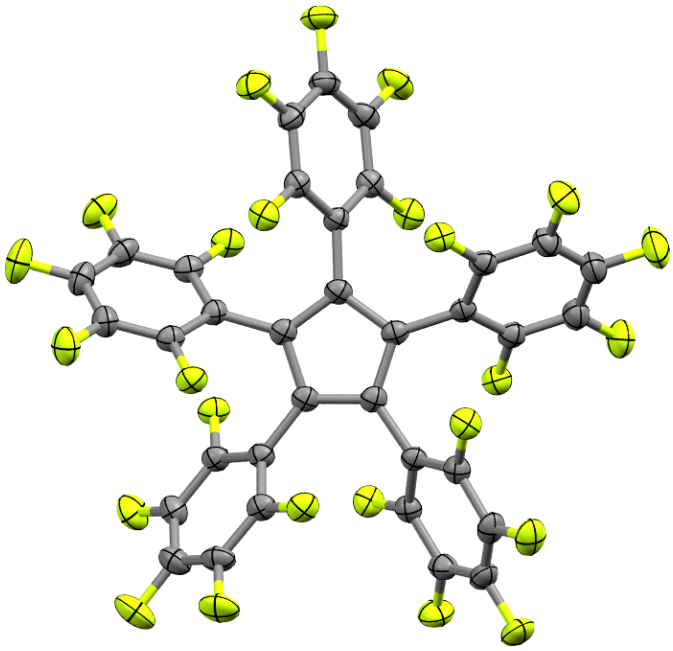

Figure 54: Solid-state structure of pentakis(pentafluorophenyl)cyclopentadienyl radical 49, crystallized from benzene. Ellipsoids are drawn at a probability level of 50%.

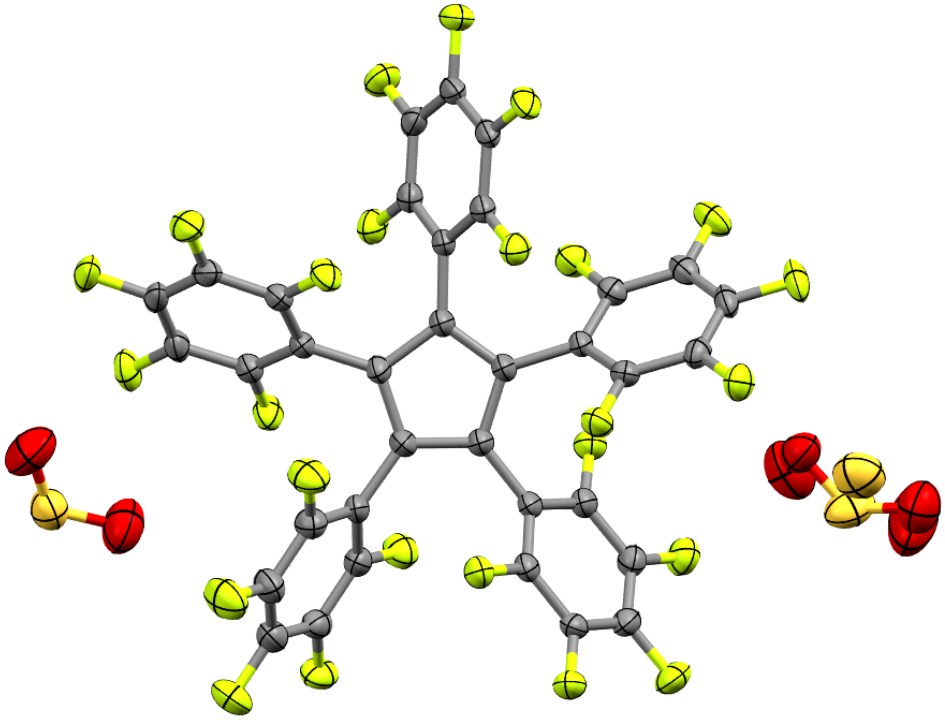

Figure 55: Solid-state structure of pentakis(pentafluorophenyl)cyclopentadienyl radical 49, crystallized from SO_2. Ellipsoids are drawn at a probability level of 50%.

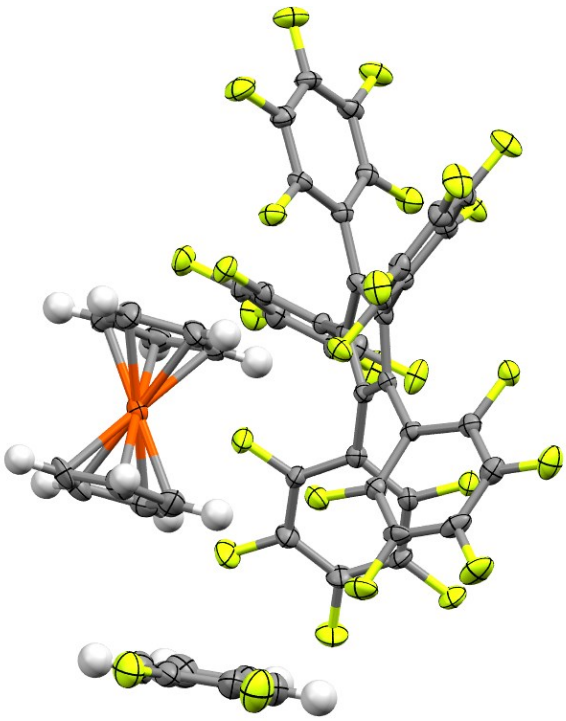

Figure 56: Solid-state structure of ferrocenium pentakis(pentafluorophenyl)-cyclopentadienide 50a, crystallized from 1,2-difluorobenzene/hexane. Ellipsoids are drawn at a probability level of 50%.

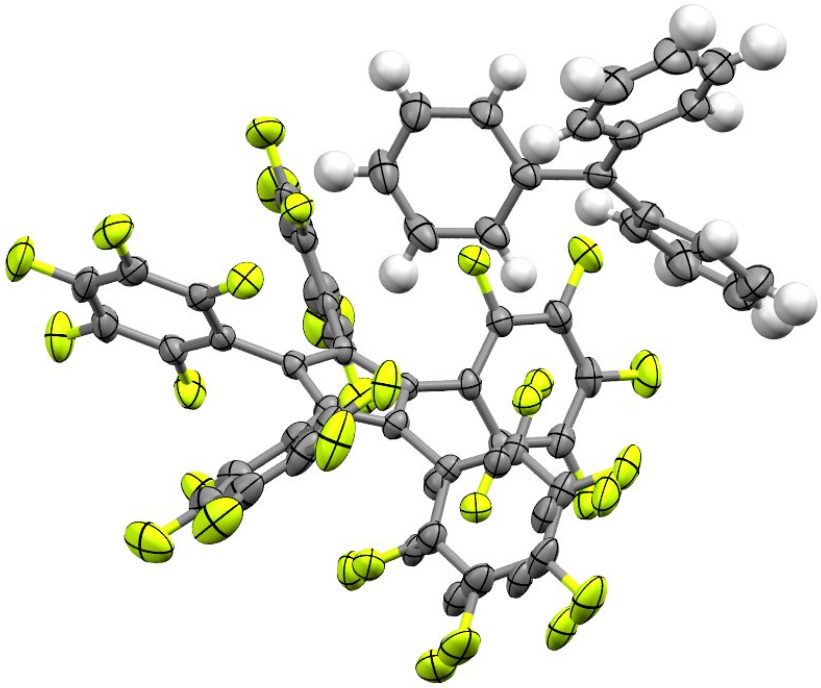

Figure 57: Solid-state structure of tritylium pentakis(pentafluorophenyl)-cyclopentadienide 50b, crystallized from toluene. Ellipsoids are drawn at a probability level of 50%.

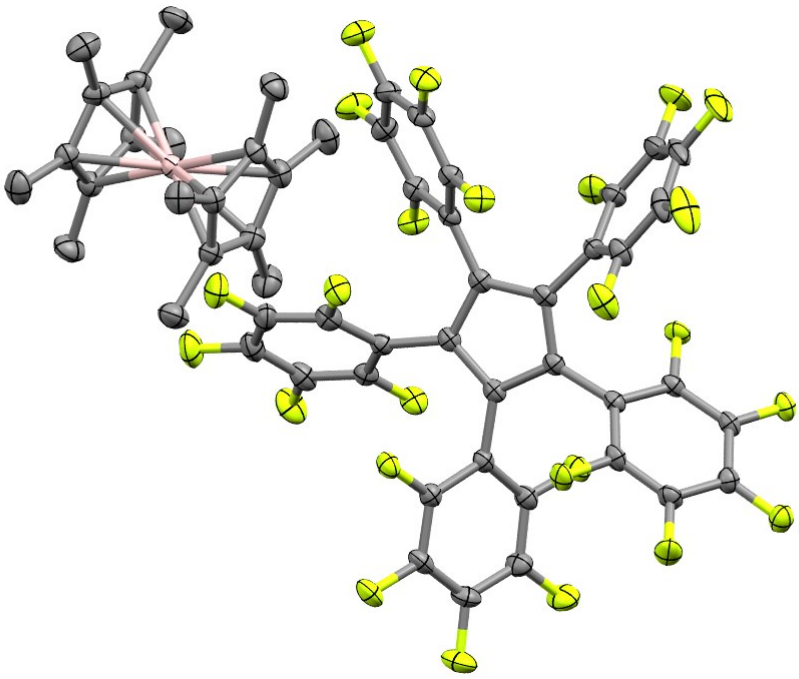

Figure 58: Solid-state structure of decamethylaluminocenium pentakis(pentafluoro-phenyl)cyclopentadienide 50c, crystallized from benzene. Ellipsoids are drawn at a probability level of 50%. Hydrogen atoms are omitted for clarity.

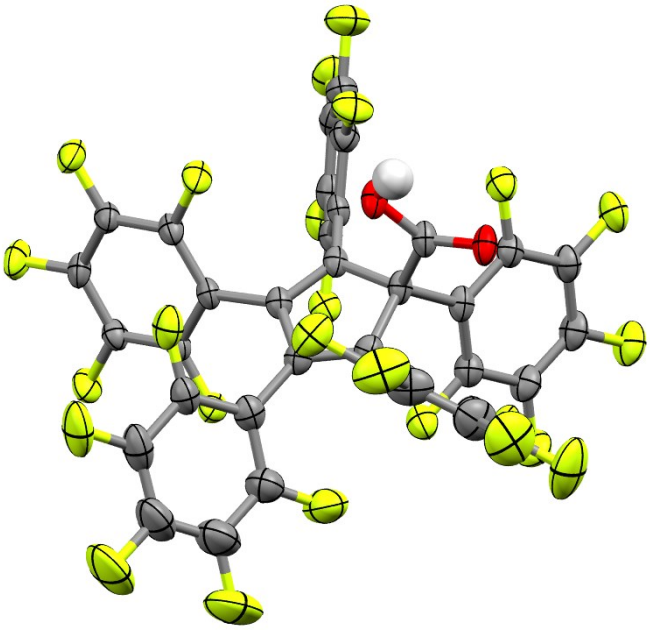

Figure 59: Solid-state structure of pentakis(pentafluorophenyl)-cyclopentadienylcarboxylic acid 52, crystallized from hexafluorobenzene/hexane. Ellipsoids are drawn at a probability level of 50%.

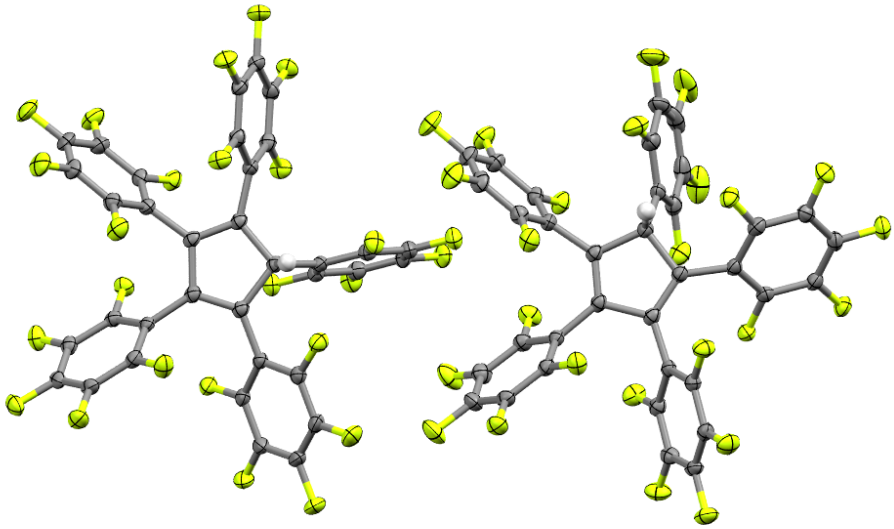

Figure 60: Asymmetric unit of pentakis(pentafluorophenyl)cyclopentadiene 53, featuring two independent molecules, crystallized from acetonitrile/hexane. Ellipsoids are drawn at a probability level of 50%.

More information on the crystal structures can be found in a separate publication.[160]

5 Conclusion and Outlook

The goal of this work was the study of the chemical behavior and properties of pentaaryl cyclopentadienyl anions, radicals, and cations.

The cyclopentadienes **1 – 8** which were required as precursors could be prepared by a fivefold palladium catalyzed Heck reaction in a one pot protocol. This enabled the manipulation of the solubility, crystallization behaviour, and the steric and electronic properties of the resulting cyclopentadienes and their follow-up products.

Deprotonation of these cyclopentadienes with alkali metal bis(trimethylsilyl)amides resulted in all cases in the formation of alkali metal salts **9–23** comprising the corresponding cyclopentadienyl anions. Their behavior in solution and in the solid-state was investigated by multinuclear NMR spectroscopy and sc-XRD. These alkali salts could be used in salt metathesis reactions resulting in other metal compounds.

Oxidation of the cyclopentadienyl anions resulted in the formation of stable, isolable cyclopentadienyl radicals **31–35**. Sc-XRD of these radicals provided experimental evidence for their Jahn Teller distortion in the solid-state. In solution, a permanent distortion could not be observed by EPR spectroscopy, potentially due to fast tautomerization.

The resulting radicals could also be used to prepare cyclopentadienyl metal compounds **36–43** by their reaction with activated elemental metals. Activation was mainly achieved by dissolving the metals in mercury.

The preparation of the corresponding cyclopentadienyl cations was also attempted, but no defined product could be isolated due to the high reactivity and fast decomposition of these systems.

In order to eliminate all possibly weak points (such as C-H bonds) that could lead to decomposition, the perfluorination of the pentaarylcyclopentadienyl scaffold was considered. Unfortunately, the preparation of perfluoropentaphenylcyclopentadiene **53** was not possible by the usual Heck protocol mentioned above, but a different route via perfluorotolane **45** and perfluorotetraphenylcyclopentadienone **46** was successful and yielded

perfluoropentaphenylcyclopentadienol **47**. This could be dehydroxylated to the corresponding cyclopentadienyl radical **49** which was found to be a useful oxidant. It was used as a precursor to different salts **50a–d** of the corresponding cyclopentadienyl anion and to the cyclopentadiene **53**.

The synthesis of cyclopentadienyl cation **48**$^+$ was finally achieved under highly oxidizing and Lewis acidic conditions. Either, radical **49** was oxidized by $XeF_2/SbF_5 \cdot SO_2$ or a hydroxide ion was abstracted from **47** by an excess of $SbF_5 \cdot SO_2$. As **48**$^+$ reacts even with weak reductants like DCM and weak Lewis bases like CO, this necessitated the use of solvents which are inert to these conditions (C_6F_6 or SO_2). **48**$^+$ could be crystallized in form of a room-temperature stable salt with the $[Sb_3F_{16}]^-$ anion.

Cyclopentadienyl cations can be present in the triplet or singlet state. In the singlet state, two different valence tautomers can further be distinguished. All these forms have a similar anticipated energy. In the solid-state, **48**$^+$ was found to be present in the singlet state, comprising the valence tautomer with the positive charge mainly localized on one carbon atom. This could be confirmed by the characteristic bond lenghts alternation which was observed by sc-XRD and predicted by quantum mechanical computations. Temperature dependent magnetic susceptibility measurements also provided evidence for a singlet ground state in the solid-state and indicate the presence of an energetically low lying triplet state. UV/Vis spectroscopy combined with quantum mechanical computations also implies that **48**$^+$ is predominantly present in the singlet state in solution. Both in the solid-state and in solution, the singlet state, exhibiting a higher charge localization than the triplet state, is probably favored due to its more effective interaction with a negatively polarized atom of either the solvent or the counteranion. As a planar singlet system with four cyclic conjugated π electrons, **48**$^+$ represents one of the few examples for an isolable antiaromatic molecule.

Being a strong Lewis acid, **48**$^+$ reacts with the weak Lewis base CO. The product could be hydrolyzed to the cyclopentadienyl carboxylic acid **52**, which decarboxylates to cyclopentadiene **53**.

The use of the perfluoropentaphenylcyclopentadienyl system as a ligand in coordination chemistry is still completely unexplored and might result in new insights and applications due to its weakly electron donating character combined with a high stability. The perfluoropentaphenylcyclopentadienyl radical might also become a useful innocent oxidant in synthetic applications due to its convenient oxidation potential (0.48 V vs. ferrocene) and inertness towards air and moisture in the solid-state.

6 Experimental Part

6.1.1 Synthesis of $Cp^{Big\ n\text{-}Bu}H$ 1

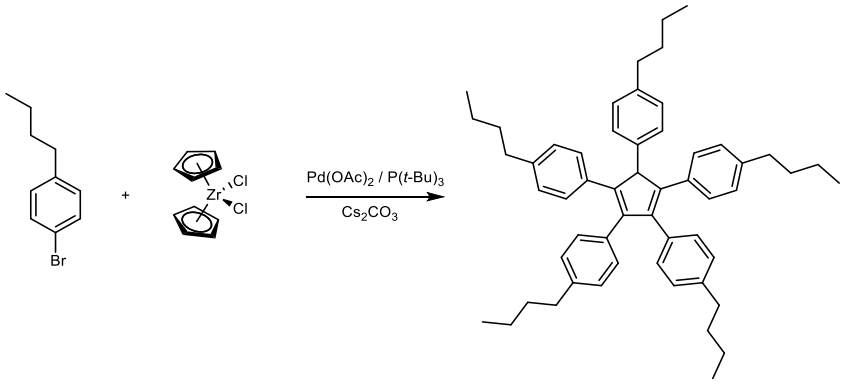

Pentakis-(4-*n*-butylphenyl)cyclopentadiene was synthesized according to an adapted literature procedure.[12–14]

96 mmol (31.2 g) of cesium carbonate, 160 mL of dry DMF, 102 mmol (17 mL, 21.7 g) of 1-bromo-4-*n*-butylbenzene, 2 mmol (0.802 g) of tri-*t*-butylphosphine, 8 mmol (2.34 g) of zirconocene dichloride, and 2 mmol (0.46 g) of palladium(II) acetate were sequentially added to a 250 mL Schlenk flask. The mixture was heated to 140 °C in a sealed flask for five days. During this time, the reaction mixture changed color from green and red to brown. After this period, 20 mL HCl_{aq} (37%) was added and the reaction mixture was diluted with 300 mL of dichloromethane. The organic phase was separated, dried with $MgSO_4$, and concentrated on a rotary evaporator followed by vacuum distillation at 80 °C to remove residual solvent. The resulting brown oil was purified by column chromatography (silica, *n*-hexane:DCM 4:1) and crystallized from a mixture of 10 mL *n*-hexane and 100 mL isopropanol at −30 °C.

Yield: 4.7 g (3.24 mmol, 81%) ^{1}H-NMR (300 MHz, $CDCl_3$, 25 °C) δ 7.16 – 6.73 (m, 20H, C_{Ar}), 4.99 (s, 1H, Cp*H*), 2.66 – 2.32 (m, 10H, ArCH_2), 1.51 (m, 10H, $ArCH_2CH_2$), 1.41 – 1.15 (m, 10H, $ArCH_2CH_2CH_2$), 1.01 – 0.75 (m, 15H, $ArCH_2CH_2CH_2CH_3$). Other analytical data match those reported in the literature.[93]

6.1.2 Synthesis of $Cp^{Big\ i\text{-}Pr}H$ 2

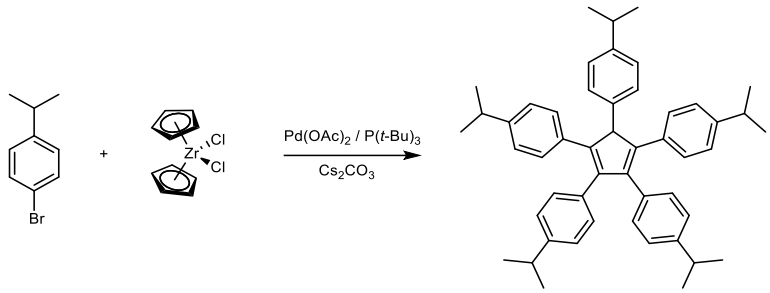

Pentakis-(4-isopropylphenyl)cyclopentadiene was synthesized according to an adapted literature procedure.[12–14]

96 mmol (31.2 g) of cesium carbonate, 160 mL of dry DMF, 102 mmol (20.3 g, 15 mL) of 1-bromo-4-isopropylbenzene, 2 mmol (0.802 g) of tri-*t*-butylphosphine, 8 mmol (2.34 g) of zirconocene dichloride, and 2 mmol (0.46 g) of palladium(II) acetate were sequentially added to a 250 mL Schlenk flask. The mixture was heated to 140 °C in a sealed flask for five days. During this time, the reaction mixture changed color from green and red to brown. After this period, 20 mL HCl_{aq} (37%) was added and the reaction mixture was diluted with 300 mL of dichloromethane. The organic phase was separated, dried with magnesium sulfate, concentrated on a rotary evaporator and subjected to vacuum distillation at 80 °C to remove residual solvent. The resulting brown oil was purified by column chromatography (silica, hexane:DCM 4:1) and crystallized from 50 mL of acetone at –30 °C.

Yield: 3.3 g (5.0 mmol, 62%) ^{1}H NMR (300 MHz, $CDCl_3$, 25 °C) δ 7.32 – 6.87 (m, 20H, C_{Ar}), 5.13 (s, 1H, Cp*H*), 2.89 (m, 5H, ArC*H*), 1.47 – 1.14 (m, 30H, ArCH(CH_3)$_2$). Other analytical data match those reported in the literature.[107]

6.1.3 Synthesis of $Cp^{Big\ t\text{-}Bu}H$ 3

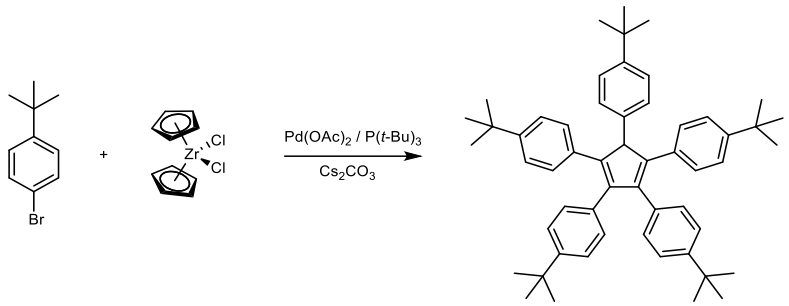

Pentakis-(4-*t*-butylphenyl)cyclopentadiene ($Cp^{Big\ t\text{-}Bu}H$) was synthesized according to an adapted literature procedure.[86–88]

336 mmol (71.6 g, 58.3 mL) of 1-bromo-4-*t*-butylbenzene, 336 mmol (109 g) of cesium carbonate, 28 mmol (8.81 g) of zirconocene dichloride, 2 mmol (0.450 g) of palladium(II) acetate, and 4 mmol (0.810 g) of tri-*t*-butylphosphine were suspended in 560 mL of dry DMF. The mixture was heated to 140 °C in a closed 1 L nitrogen flask for twenty hours. The resulting brown suspension was cooled to room temperature, treated with 100 mL HCl_{aq} (37%), and diluted with distilled water to a final volume of 1 L. The precipitated brown solid was filtered and washed three times with 100 mL of distilled water. The filter cake was dissolved in a mixture of 400 mL of methanol and 400 mL of cyclohexane, then filtered and transferred to a separatory funnel. The methanol phase was discarded, and the extraction with methanol was repeated. The cyclohexane phase was then concentrated on a rotary evaporator and subjected to vacuum distillation at 80 °C to remove volatile components. The crude product obtained in this manner was dissolved in 100 mL of dichloromethane and filtered through 50 mL silica. The product was eluted with an additional 200 mL of dichloromethane, and the combined filtrates were evaporated using a rotary evaporator. The pre-purified crude product was dissolved in 100 mL of hot toluene, mixed with 100 mL of methanol, and left to crystallize overnight at −30 °C. The crystallized colorless product was isolated by filtration, washed with 100 mL cold methanol (−30 °C), and dried *in vacuo*.

Yield: 22.0 g (53%) Mp: 240 °C Anal. calcd. for $C_{55}H_{66}$: C 90.85, H 9.15%, Found: C 91.3, H 9.24%.^{1}H-NMR: (300 MHz, $CDCl_3$) δ = 7.21 – 7.14 (m, 4H, H_{Ar}), 7.10 (d, $^3J_{HH}$ = 8.3 Hz, 4H, H_{Ar}), 7.04 – 6.94 (m, 8H, H_{Ar}), 6.90 (d, $^3J_{HH}$ = 8.3 Hz, 4H, H_{Ar}), 5.04 (s,

1H, Cp*H*), 1.25 (s, 18H, $H_{t\text{-Bu}}$), 1.23 (s, 9H, $H_{t\text{-Bu}}$), 1.19 (s, 18H, $H_{t\text{-Bu}}$). ^{13}C-NMR: (75 MHz, $CDCl_3$) δ = 149.26 (C_{Ar}), 148.72 (C_{Ar}), 145.24 (C_{Ar}), 137.99 (C_{Ar}), 136.26 (C_{Ar}), 134.08 (C_{Ar}), 133.34 (C_{Ar}), 132.93 (C_{Ar}), 132.88 (C_{Ar}), 129.78 (C_{Ar}), 129.00 (C_{Ar}), 128.40 (C_{Ar}), 125.45 (C_{Ar}), 124.63 (C_{Ar}), 124.57 (C_{Ar}), 34.59 (C^6), 34.54 (C^6), 34.46 (C^6), 31.48 (C^7), 31.42 (C^7), 31.36 (C^7). IR: 2959, 2903, 2866, 1516, 1503, 1475, 1461, 1393, 1362, 1268, 1113, 1018, 855, 833, 589, 566, 546 cm^{-1}.

6.1.4 Synthesis of $Cp^{Big\ Ph2}H$ 4

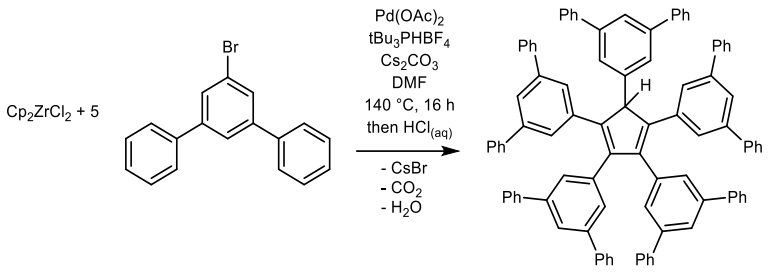

80,9 mmol (25.0 g) of 5'-bromo-*m*-terphenyl, 6.26 mmol (1.83 g) of zirconocene dichloride, 80.9 mmol (26.4 g) of cesium carbonate, 1.26 mmol (365 mg) of tri-*t*-butylphosphonium tetrafluoroborate and 0.623 mmol (140 mg) of palladium(II) acetate were dissolved in 250 mL of dimethylformamide and stirred for 16 h at 140 °C. The dark brown reaction mixture was cooled to room temperature and 200 mL $HCl_{(aq)}$ (37%) and 200 mL of toluene were added. The two phases were separated and the (upper) organic phase was washed two more times with 200 mL $HCl_{(aq)}$ (37%). The aqueous phases were discarded, and the organic phase was dried with $MgSO_4$. The dried organic phase was filtered through a pad of silica (100 mL silica), which was washed with 100 mL toluene. The light brown combined filtrates were concentrated on a rotary evaporator and freed of any left volatiles at 1 µbar/100 °C. The raw product obtained in this way was combined with 12.5 mmol (2.5 g) of $KN(TMS)_2$ and dissolved in 50 mL of THF. All volatiles were removed *in vacuo* and the product was re-crystallized thrice from toluene/*n*-hexane (50 mL/100 mL) at −30 °C. The obtained crystals (7.96 mmol, 10.5 g, 64%) were dried *in vacuo*. The product obtained in this way contains one equivalent of THF, which cannot be removed *in vacuo*.

7.96 mmol (10.5 g) $Cp^{Big\ Ph2}K{\cdot}THF$ was suspended in 200 mL toluene and 50 mL of $HCl_{(aq)}$ (10%, 153 mmol) was added. The upper (organic) phase was separated, dried with $MgSO_4$, concentrated on a rotary evaporator, and freed of any left volatiles at 1 µbar/100 °C. The product was then dissolved in 80 mL benzene, diluted with 500 mL *n*-hexane and crystallized at −30 °C. $Cp^{Big\ Ph2}H$ is obtained as a white, free flowing powder.

Yield 5.9 g, (4.89 mmol, 39% with respect to zirconocene dichloride). Mp. 278 °C Anal. calcd. for $C_{95}H_{66}$: C, 94.5; H, 5.51%. Found: C, 94.3; H, 5.49%. ^1H NMR (400

MHz, C_6D_6) δ 8.02 (d, $^4J_{HH}$ = 1.6 Hz, 4H, H_{ortho}, β to CpH), 7.93 (d, $^4J_{HH}$ = 1.7 Hz, 2H, H_{ortho}, bonded to CpH), 7.85 (d, $^4J_{HH}$ = 1.7 Hz, 4H, H_{ortho}, α to CpH), 7.73 (t, $^4J_{HH}$ = 1.7 Hz, 2H, H_{para}, α to CpH), 7.52 (t, $^4J_{HH}$ = 1.6 Hz, 2H, H_{para}, β to CpH), 7.49 (t, $^4J_{HH}$ = 1.7 Hz, 1H, H_{para}, bonded to CpH), 7.44 – 7.38 (m, 4H, Ph), 7.38 – 7.32 (m, 16H, Ph), 7.15 – 7.02 (m, 30H, Ph), 5.75 (s, 1H, CpH). ^{13}C NMR (101 MHz, C_6D_6) δ 147.2 (C_{Cp}, β to CpH), 145.9 (C_{Cp}, α to CpH), 143.2, 143.0, 142.1, 141.6, 141.5, 140.8, 138.4, 136.4, 129.0, (at least three signals including C_{ortho}, α to CpH), 127.7 - 127.5 (several overlapping signals including C_{ortho}, bound to CpH and C_{ortho}, β to CpH), 125.9 (C_{para}, bound to CpH), 125.7 (C_{para}, α to CpH), 125.2 (C_{para}, β to CpH) 62.6 (C_{Cp}-H). IR ν = 3034, 1587, 1494, 1412, 1076, 1027, 881, 757, 695, 612 cm^{-1}.

Comments: $Cp^{Big\ Ph2}H$ is purified in the form of its potassium salt, which can be hydrolyzed to obtain pure $Cp^{Big\ Ph2}H$. This indirect route is advantageous, as $Cp^{Big\ Ph2}K$·THF is purified more easily than $Cp^{Big\ Ph2}H$.

6.1.5 Synthesis of $Cp^{Big\ t\text{-}Bu2}H$ 5

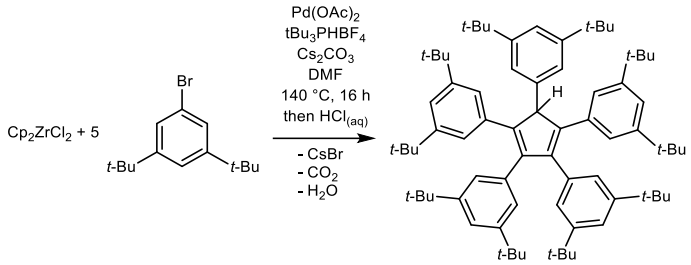

Pentakis-4-methoxycyclopentadiene ($Cp^{Big\ OMe}H$) was synthesized according to an adapted literature procedure.[90]

2.00 mmol (584 mg) Cp_2ZrCl_2, 24.0 mmol (4.44 g) 3,5-dimethyl-1-bromobenzene, 24.0 mmol (7.82 g) cesium carbonate, 0.500 mmol (112 mg) palladium(II) acetate, 2.00 mmol (404 mg) tri-*t*-butylphosphine, and 50 mL DMF were combined in a Schlenk tube. The mixture was heated to 130 °C for 24 hours, resulting in the formation of a creamy brown slurry. After cooling the Schlenk tube and its contents to room temperature and exposing them to air, 150 mL of DCM was added, followed by *p*-toluenesulfonic acid (9.12 g, 48.0 mmol). The mixture was stirred at room temperature for 15 minutes and then passed through 50 mL silica gel to obtain a brown solution. All volatiles were removed *in vacuo*.

The crude product was directly used in the synthesis of $Cp^{Big\ t\text{-}Bu2}K$ **34-K**. Pure **5** can be obtained by the hydrolysis of this product as described for **4**.

Analytical data match those reported in the literature.[90]

6.1.6 Synthesis of $Cp^{Big\ OMe}H$ 6

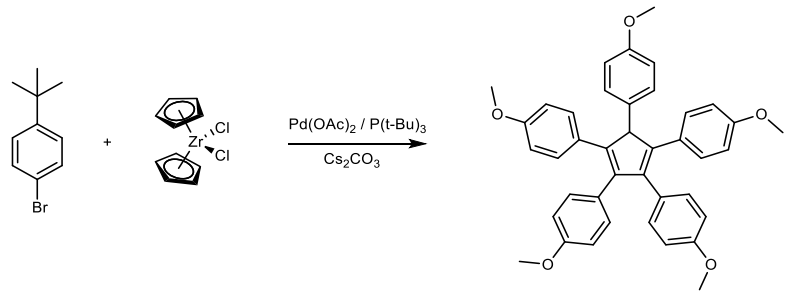

Pentakis-4-methoxycyclopentadiene ($Cp^{Big\ OMe}H$) was synthesized according to an adapted literature procedure.[88]

18 mmol (3.37 g, 2.26 mL) of 1-bromo-4-methoxybenzene, 18 mmol (5.9 g) of cesium carbonate, 1.5 mmol (0.44 g) of zirconocene dichloride, 0.15 mmol (34 mg) of palladium(II) acetate, and 0.3 mmol (87 mg) of tri-*t*-butylphosphonium tetrafluoroborate were sequentially suspended in 60 mL of dry NMP. The mixture was heated to 140 °C for 24 h. The resulting brown suspension was cooled to room temperature and diluted with 50 mL toluene and 50 mL $HCl_{(aq)}$ (37%). The aqueous phase was discarded and the organic phase was dried with $MgSO_4$ and filtered through 50 mL silica gel. All volatiles were removed at the rotary evaporator and the product was crystallized from 2 mL toluene. Yield 750 mg (1.03 mmol, 69%)
Analytical data match those reported in the literature.[88]

6.1.7 Synthesis of 4-(Pentafluorophenyl)bromobenzene

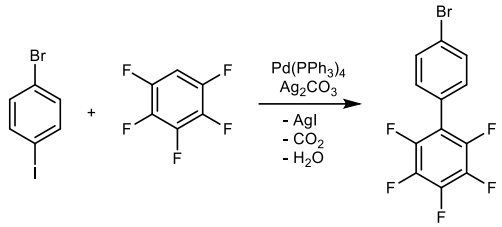

4-(Pentafluorophenyl)bromobenzene was prepared according to an adapted literature procedure.[161]

50 mmol (14.1 g) 4-bromoiodobenzene, 55 mmol (9.24 g, 6.1 mL) pentafluorobenzene, 25 mmol (6.9 g) Ag_2CO_3 and 86 µmol (100 mg) $Pd(PPh_3)_4$ were dissolved in 50 mL DMF and stirred for 24 h at 80 °C. The resulting dark suspension was filtered and the solid washed with 100 mL of DCM. 100 mL $HCl_{(aq)}$ (37%) was added to the combined filtrates in a separatory funnel. The organic phase was separated, dried with $MgSO_4$, filtered and the solvent was evaporated by use of a rotary evaporator. The resulting light-yellow foam was dissolved in 80 mL of boiling hexane, hot filtered and stored for 24 h at −30 °C, yielding 7.8 g of white crystals of 4-(pentafluorophenyl)bromobenzene, which were separated by filtration and dried *in vacuo*. A second crop of 3.65 g was obtained from the reduced mother liquor (combined yield 71%). Analytical data are identical to those reported in the literature.[161]

6.1.8 Synthesis of $Cp^{Big\ C6F5}H$ 7

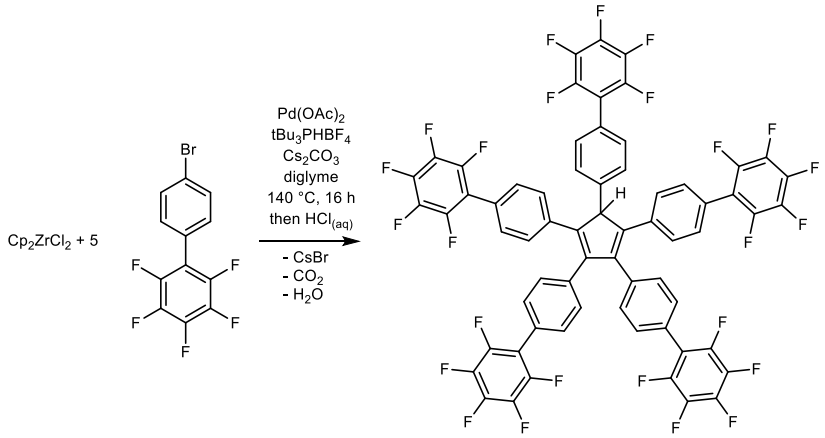

26.4 mmol (8.53 g) of 4-(pentafluorophenyl)bromobenzene, 2.2 mmol (643 mg) of zirconocene dichloride, 26.4 mmol (8.60 g) of Cs_2CO_3, 1.32 mmol (383 mg) of tri-*t*-butylphosphonium tetrafluoroborate and 0.44 mmol (99 mg) of palladium(II) acetate were dissolved in 20 mL diglyme and stirred for 16 h at 140 °C. The reddish-brown reaction mixture was cooled to room temperature and 100 mL of $HCl_{(aq)}$ (37%) and 100 mL of toluene were added. The two phases were separated, and the organic phase was washed five times with 100 mL of $HCl_{(aq)}$ (37%). The aqueous phases were discarded, and the organic phase was dried with $MgSO_4$. The dried organic phase was filtered through a pad of silica (50 mL of silica), which was washed with 100 mL of toluene. The light brown combined filtrates were concentrated on a rotary evaporator and freed of any remaining volatiles at 1 µbar/100 °C. The raw product was then purified by column chromatography (*n*-hexane/DCM 4:1) The product is in the second band with a blue fluorescence. The product was freed of any remaining volatiles at 1 µbar/100 °C, leaving behind yellow crystalline $Cp^{Big\ C6F5}H$.

Yield: 2.00 g, (1.57 mmol, 36%). Anal calcd. for $C_{65}H_{21}F_{25}$: C, 61.1; H, 1.66%. Found: C, 61.1; H, 1.77%. Mp. 242 °C. ^{1}H NMR (400 MHz, C_6D_6) δ 7.41 (d, $^3J_{HH}$ = 8.4 Hz, 2H, Cp-Ar-CH_{ortho}, bound to CpH), 7.31 (d, $^3J_{HH}$ = 8.5 Hz, 4H, Cp-Ar-CH_{ortho}, *α* to CpH), 7.30 (d, $^3J_{HH}$ = 8.4 Hz, 4H, Ar-CH_{ortho}, *β* to CpH), 7.26 (d, $^3J_{HH}$ = 8.4 Hz, 2 H, Cp-Ar-CH_{meta}, bound to CpH), 7.14 (d, $^3J_{HH}$ = 8.2 Hz, 4 H, Ar-CH_{meta}, *β* to CpH), 7.03 (d, $^3J_{HH}$ = 8.2 Hz, 4 H, Ar-CH_{meta}, α to CpH), 5.14 (s, 1 H, Cp-C*H*). ^{13}C NMR (101 MHz, C_6D_6) δ 147.4 (Cp-*C*, *α* to CpH), 144.7 (Cp-*C*; *β* to CpH), 144.2 (dm, $^1J_{CF}$ = 239 Hz, 3 C_6F_{5ortho}),

139.3 (Cp-Ar-*C*H$_{ipso}$, bound to CpH), 140.6 (dm, $^{1}J_{CF}$ = 257 Hz, 3 C$_6$F$_{5para}$), 136.8 (Cp-Ar-*C*H$_{ipso}$; β to CpH), 138.0 (dm, $^{1}J_{CF}$ = 249 Hz, 3 C$_6$F$_{5meta}$), 136.4 (Cp-Ar-*C*H$_{ipso}$, α to CpH), 131.2 (Cp-Ar-*C*H$_{meta}$, bound to CpH), 130.7 (Cp-Ar-*C*H$_{ortho}$; α to CpH), 130.6 (Cp-Ar-*C*H$_{meta}$; α to CpH), 130.4 (Cp-Ar-*C*H$_{meta}$; β to CpH), 129.6 (Cp-Ar-*C*H$_{ortho}$; β to CpH), 129.0 (Cp-Ar-*C*H$_{ortho}$, bound to CpH), 126.2 (Cp-Ar-*C*H$_{para}$; β to CpH), 125.9 (Cp-Ar-*C*H$_{para}$, bound to CpH), 125.8 (Cp-Ar-*C*H$_{para}$; α to CpH), 115.2 (m, 3 C$_6$F$_{5ipso}$), 63.2 (Cp-*C*H). ^{19}F NMR (376 MHz, C$_6$D$_6$) δ -143.95 – -144.19 (m, 10F, C$_6$F$_{5ortho}$), -155.33 (t, 2F, $^{3}J_{FF}$ = 21.6 Hz, C$_6$F$_{5para}$), -155.55 – -155.72 (m, 3F, C$_6$F$_{5para}$), -162.15 – -162.56 (m, 10 F, C$_6$F$_{5meta}$). IR ν = 1487, 1403, 1322, 1062, 981, 850, 748 cm^{-1}.

6.1.9 Synthesis of $Cp^{Big\ CF3}H$ 8

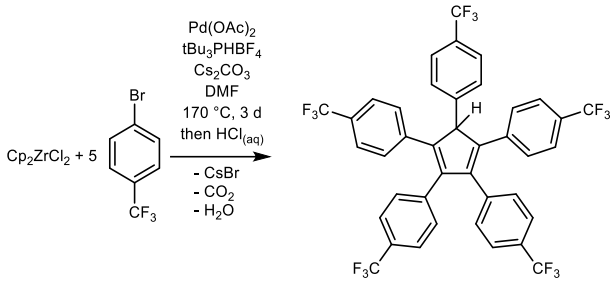

$Cp^{Big\ CF3}H$ was prepared according to an adapted literature procedure.[131]

In an inert atmosphere, 1.20 mmol (0.36 g) tri-*t*-butylphosphonium tetrafluoroborate, 0.50 mmol (0.11 g) palladium(II) acetate, and 61.2 mmol (19.9 g) cesium carbonate were combined in a sealed tube. 5.0 mmol (1.46 g) zirconocene dichloride and 60.0 mmol (13.5 g) 4-bromobenzotrifluoride, dissolved in 20 mL of dry DMF, were added to the tube. The resulting mixture was heated to 140 °C for 16 h. The reaction mixture was then transferred to a beaker and 250 mL of CH_2Cl_2 were added, followed by the addition of 10.0 mmol (1.90 g) *p*-toluenesulfonic acid monohydrate. Filtration through a pad of silica, followed by concentration under reduced pressure, yielded a brown oil. Further purification by column chromatography (using a solvent gradient from pentane/ CH_2Cl_2 98:2, to pentane/ CH_2Cl_2 90:10) resulted in the desired product as a yellow solid (1.46 g, 19%).

Analytical data match those reported in the literature.[131]

6.1.10 Synthesis of $Cp^{Big\ i\text{-}Pr}Li$ 9

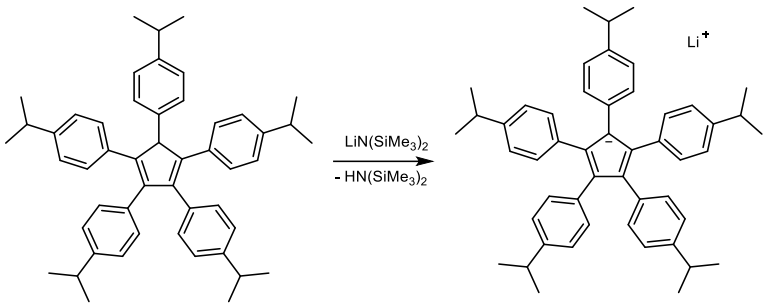

0.2 mmol (131 mg) of $Cp^{Big\ i\text{-}Pr}H$ and 0.2 mmol (33 mg) of $LiN(SiMe_3)_2$ were dissolved in acetonitrile (3 mL) and the resulting light-yellow solution was stirred for 1 h at ambient temperature. All volatiles were removed under reduced pressure at 100 °C, yielding $Cp^{Big\ i\text{-}Pr}Li$ as a colorless crystalline solid.

Yield: 118 mg (0.178 mmol, 89%). Mp. 189 °C (dec.). Anal. calcd. for $C_{50}H_{55}Li$: C, 90.59; H, 8.36%. Found: C, 90.56; H, 8.31%. ^{1}H NMR (300 MHz, CD_3CN, 25 °C): δ 1.17 (d, $^3J_{HH}$ = 6.9 Hz, 30 H, C*H*$_3$), 2.69-2.83 (m, 5 H, C*H*), 6.70 (d, $^3J_{HH}$ = 8.3 Hz, 10 H, Ar-*H*), 6.77 (d, $^3J_{HH}$ = 8.1 Hz, 10 H, Ar-*H*). ^{13}C NMR (75.5 MHz, CD_3CN, 25 °C): δ 24.52 (*C*H$_3$), 34.19 (*C*H), 121.13 (Cp-*C*), 125.17 (Ar-*C*H), 132.50 (Ar-*C*H), 141.96 (Ar-*C*), 142.43 (Ar-*C*). ^{7}Li NMR (117 MHz, CD_3CN, 25 °C): δ –2.26. IR: ν = 3022, 2958, 2928, 2868, 1504, 1460, 1410, 1382, 1362, 1053, 1018, 833, 787, 600, 566, 442 cm^{-1}.

6.1.11 Synthesis of $Cp^{Big\ i\text{-}Pr}Na$ 10

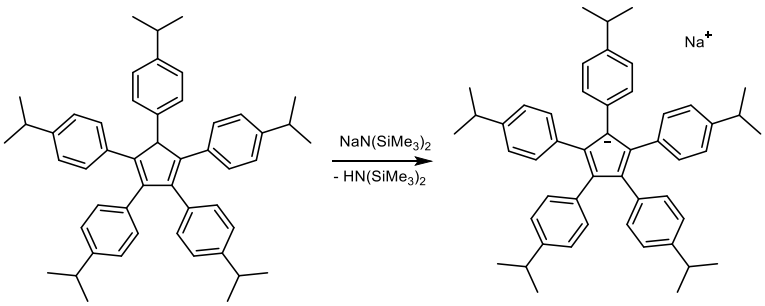

0.2 mmol (131 mg) $Cp^{Big\ i\text{-}Pr}H$ and 0.2 mmol (37 mg) $NaN(SiMe_3)_2$ were dissolved in 3 mL of acetonitrile and the resulting light-yellow solution was stirred for 1 h at ambient temperature. All volatiles were removed under reduced pressure at 100 °C, yielding $Cp^{Big\ i\text{-}Pr}Na$ as a colorless crystalline solid.

Yield: 132 mg (0.194 mmol, 97%). Mp. 202 °C (dec.). Anal. calcd. for $C_{50}H_{55}Na$: C, 88.45; H, 8.17%. Found: C, 87.25; H, 8.07%. ^1H NMR (300 MHz, CD_3CN, 25 °C): δ 1.19 (d, $^3J_{HH}$ = 6.9 Hz, 30 H, C*H*$_3$), 2.73-2.82 (m, 5 H, C*H*), 6.72 (d, $^3J_{HH}$ = 7.7 Hz, 10 H, Ar-*H*), 6.79 (d, $^3J_{HH}$ = 7.9 Hz, 10 H, Ar-*H*). ^{13}C NMR (75.5 MHz, CD_3CN, 25 °C): δ 24.55 (*C*H$_3$), 34.21 (*C*H), 121.13 (Cp-*C*), 125.17 (Ar-*C*H), 132.53 (Ar-*C*H), 141.93 (Ar-*C*), 142.45 (Ar-*C*). ^{23}Na NMR (79 MHz, CD_3CN, 25 °C): δ –7.82. IR: ν = 3024, 2958, 2931, 2870, 1514, 1459, 1148, 1051, 1014, 851, 836, 773, 692, 567 cm^{-1}.

6.1.12 Synthesis of $Cp^{Big\ i\text{-}Pr}K$ 11

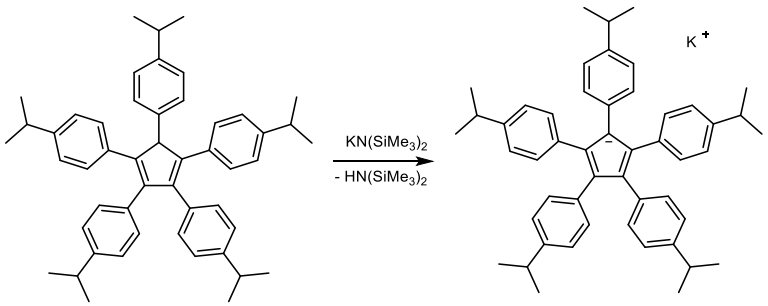

$Cp^{Big\ i\text{-}Pr}H$ (131 mg, 0.2 mmol) and $KN(SiMe_3)_2$ (40 mg, 0.2 mmol) were dissolved in acetonitrile (3 mL) and the resulting light-yellow solution was stirred for 1 h at ambient temperature. All volatiles were removed under reduced pressure at 100 °C, yielding $Cp^{Big\ i\text{-}Pr}K$ as a colorless crystalline solid.

Yield: 130 mg (0.188 mmol, 94%). Mp. 267 °C (dec.). Anal. calcd. for $C_{50}H_{55}K$: C, 86.40; H, 7.98%. Found: C, 84.95; H, 7.97%. ^{1}H NMR (300 MHz, CD_3CN, 60 °C): δ 1.21 (d, $^3J_{HH}$ = 6.9 Hz, 30 H, C*H*$_3$), 2.72-2.86 (m, 5 H, C*H*), 6.69 (d, $^3J_{HH}$ = 8.1 Hz, 10 H, Ar-*H*), 6.77 (d, $^3J_{HH}$ = 8.2 Hz, 10 H, Ar-*H*). ^{13}C NMR (75.5 MHz, CD_3CN, 60 °C): δ 24.70 (*C*H$_3$), 34.45 (*C*H), 121.37 (Cp-*C*), 125.51 (Ar-*C*H), 132.71 (Ar-*C*H), 141.49 (Ar-*C*), 143.12 (Ar-*C*). IR: ν = 3013, 2959, 2931, 2869, 1515, 1459, 1361, 1149, 1051, 1013, 851, 833, 773, 689, 567 cm^{-1}.

6.1.13 Synthesis of $Cp^{Big\ i\text{-}Pr}Rb$ 12

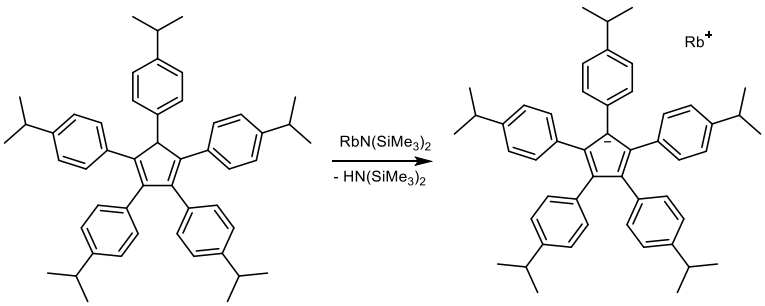

$Cp^{Big\ i\text{-}Pr}H$ (131 mg, 0.2 mmol) and $RbN(SiMe_3)_2$ (50 mg, 0.2 mmol) were dissolved in acetonitrile (3 mL) and the resulting light-yellow solution was stirred for 1 h at ambient temperature. All volatiles were removed under reduced pressure at 100 °C, yielding $Cp^{Big\ i\text{-}Pr}Rb$ as a colorless crystalline solid.

Yield: 134 mg (0.176 mmol, 90%). Mp. 381 °C (dec.). Anal. calcd. for $C_{50}H_{55}Rb$: C, 81.00; H, 7.48%. Found: C, 80.85; H, 7.37%. ^{1}H NMR (300 MHz, THF-d_8, 25 °C): δ 1.16 (d, $^3J_{HH}$ = 6.9 Hz, 30 H, CH_3), 2.65-2.79 (m, 5 H, C*H*), 6.66 (d, $^3J_{HH}$ = 8.4 Hz, 10 H, Ar-*H*), 6.72 (d, $^3J_{HH}$ = 8.3 Hz, 10 H, Ar-*H*). ^{13}C NMR (75.5 MHz, THF-d_8, 25 °C): δ 24.61 (*C*H$_3$), 34.48 (*C*H), 120.89 (Cp-*C*), 125.07 (Ar-*C*H), 132.27 (Ar-*C*H), 140.34 (Ar-*C*), 142.42 (Ar-*C*). ^{87}Rb NMR (98 MHz, CD_3CN, 25 °C): δ –14.77. IR: ν = 3013, 2958, 2931, 2869, 1514, 1460, 1149, 1052, 1013, 850, 833, 773, 689, 566 cm^{-1}.

6.1.14 Synthesis of $Cp^{Big\ i\text{-}Pr}Cs$ 13

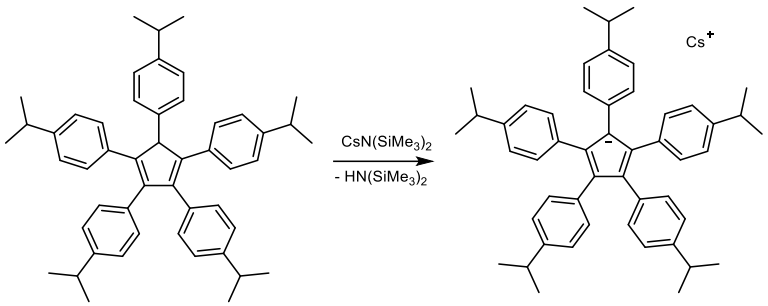

0.2 mmol (131 mg) $Cp^{Big\ i\text{-}Pr}H$ and 0.2 mmol (58 mg) $CsN(SiMe_3)_2$ were dissolved in 3 mL acetonitrile and the resulting light-yellow solution was stirred for 1 h at ambient temperature. All volatiles were removed under reduced pressure at 100 °C, yielding $Cp^{Big\ i\text{-}Pr}Cs$ as a colorless crystalline solid.

The product can be crystallized from THF or acetonitrile at –30 °C, yielding colorless crystals.

Yield: 147 mg (0.187 mmol, 93% (before re-crystallization)). Mp. >400 °C. Anal. calcd. for $C_{50}H_{55}Cs$: C, 76.13; H, 7.03%. Found: C, 76.15; H, 6.95%. ^{1}H NMR (300 MHz, Tol-d_8, 25 °C): δ 1.17 (d, $^3J_{HH}$ = 6.8 Hz, 30 H, CH_3), 2.65-2.74 (m, 5 H, C*H*), 6.59 (s, br., 20 H, Ar-*H*). ^{13}C NMR (75.5 MHz, Tol-d_8, 25 °C): δ 24.25 (*C*H$_3$), 33.94 (*C*H), 121.90 (Cp-*C*), 126.54 (Ar-*C*H), 131.07 (Ar-*C*H), 136.75 (Ar-*C*), 143.95 (Ar-*C*). ^{133}Cs NMR (39.4 MHz, Tol-d_8, 25 °C): δ –226.30. IR: ν = 3015, 2956, 2929, 2866, 1607, 1512, 1456, 1362, 1148, 1051, 851, 830, 808, 771, 688, 567 cm^{-1}.

6.1.15 Synthesis of $Cp^{Big\ n\text{-}Bu}Li$ 14

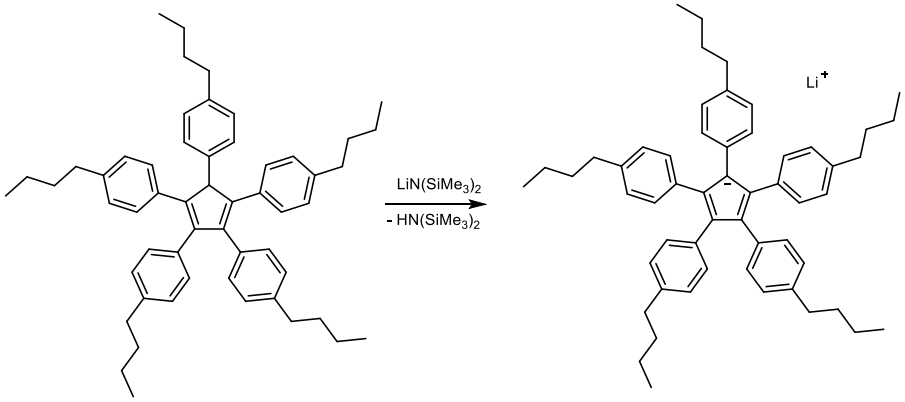

A light-yellow solution of 0.1 mmol (73 mg) $Cp^{Big\ n\text{-}Bu}H$ and 0.1 mmol (17 mg) $LiN(SiMe_3)_2$ in 1mL benzene was stirred for 1 h at ambient temperature. All volatiles were removed under reduced pressure at 100 °C, yielding a colorless crystalline solid.

Yield: 65 mg (0.090 mmol, 90%). Mp. 154 °C (dec.). Anal. calcd. for $C_{55}H_{65}Li$: C, 90.12; H, 8.94%. Found: C, 90.10; H, 8.89%. ^{1}H NMR (300 MHz, CD_3CN, 25 °C): δ 0.92 (t, $^3J_{HH}$ = 7.3 Hz, 15 H, CH_3), 1.25-1.38 (m, 10 H, CH_2), 1.47-1.57 (m, 10 H, CH_2), 2.46 (t, $^3J_{HH}$ = 7.7 Hz, 10 H, CH_2), 6.64 (d, $^3J_{HH}$ = 8.1 Hz, 10 H, Ar-*H*), 6.70 (d, $^3J_{HH}$ = 8.2 Hz, 10 H, Ar-*H*). ^{13}C NMR (75.5 MHz, CD_3CN, 25 °C): δ 14.31 (*C*H_3), 23.12 (*C*H_2), 34.61 (*C*H_2), 35.79 (*C*H_2), 120.96 (Cp-*C*), 127.27 (Ar-*C*H), 132.42 (Ar-*C*H), 136.32 (Ar-*C*), 141.75 (Ar-*C*). ^{7}Li NMR (117 MHz, CD_3CN, 25 °C): δ –2.73. IR: ν = 2955, 2926, 2870, 2857, 1504, 1458, 1412, 1018, 830, 750, 569 cm^{-1}.

6.1.16 Synthesis of $Cp^{Big\ n\text{-}Bu}Na$ 15

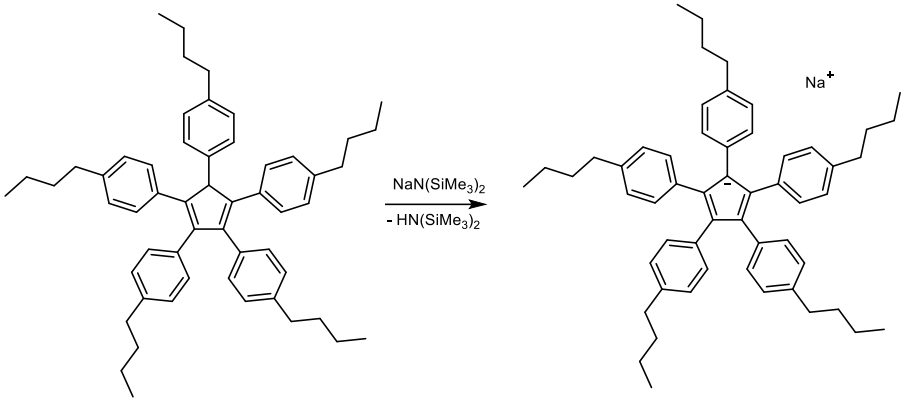

0.2 mmol (145 mg) $Cp^{Big\ n\text{-}Bu}H$ and 0.2 mmol (37 mg) $NaN(SiMe_3)_2$ were suspended in 3 mL benzene and stirred for 3 h at 60 °C. All volatiles were removed under reduced pressure at 100 °C, yielding a colorless solid.

Yield: 139 mg (0.186 mmol, 93%). Mp. 162 °C (dec.). Anal. calcd. for $C_{55}H_{65}Na$: C, 88.18; H, 8.75%. Found: C, 87.90; H, 8.70%. ^{1}H NMR (300 MHz, CD_3CN, 25 °C): δ 0.93 (t, $^3J_{HH}$ = 7.3 Hz, 15 H, C*H*$_3$), 1.27-1.39 (m, 10 H, C*H*$_2$), 1.49-1.59 (m, 10 H, C*H*$_2$), 2.48 (t, $^3J_{HH}$ = 7.6 Hz, 10 H, C*H*$_2$), 6.66 (d, $^3J_{HH}$ = 8.1 Hz, 10 H, Ar-*H*), 6.72 (d, $^3J_{HH}$ = 8.0 Hz, 10 H, Ar-*H*). ^{13}C NMR (75.5 MHz, CD_3CN, 25 °C): δ 14.35 (*C*H$_3$), 23.13 (*C*H$_2$), 34.63 (*C*H$_2$), 35.82 (*C*H$_2$), 120.95 (Cp-*C*), 127.29 (Ar-*C*H), 132.45 (Ar-*C*H), 136.36 (Ar-*C*), 141.72 (Ar-*C*). ^{23}Na NMR (79 MHz, CD_3CN, 25 °C): δ –7.80. IR: ν = 3023, 2955, 2925, 2854, 1513, 1463, 1438, 1116, 1015, 847, 833, 763, 686 cm^{-1}.

6.1.17 Synthesis of $Cp^{Big\ n\text{-}Bu}K$ 16

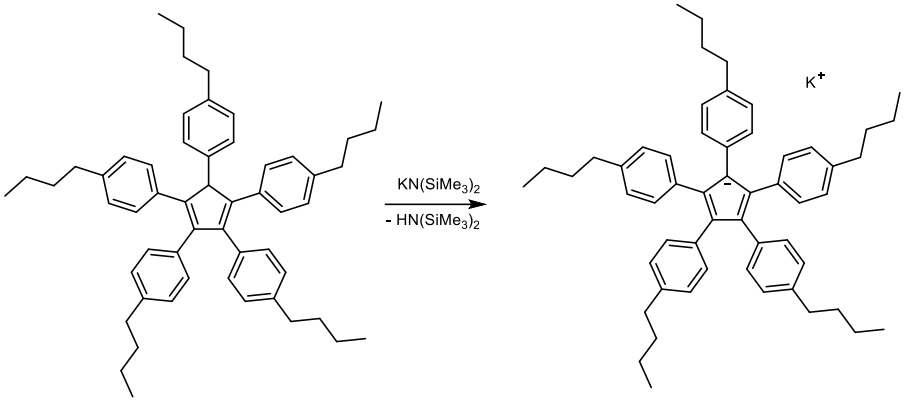

A solution of 0.1 mmol (73 mg) $Cp^{Big\ n\text{-}Bu}H$ and 0.1 mmol (20 mg) $KN(SiMe_3)_2$ in 2 mL acetonitrile was stirred for 1 h at ambient temperature. All volatiles were removed under reduced pressure at 100 °C, yielding a colorless solid.

Yield: 70 mg (0.091 mmol, 91%). The product was identified by ^1H NMR spectroscopy. Analytical data were identical to those published in the literature.[91]

6.1.18 Synthesis of $Cp^{Big\ n\text{-}Bu}Rb$ 17

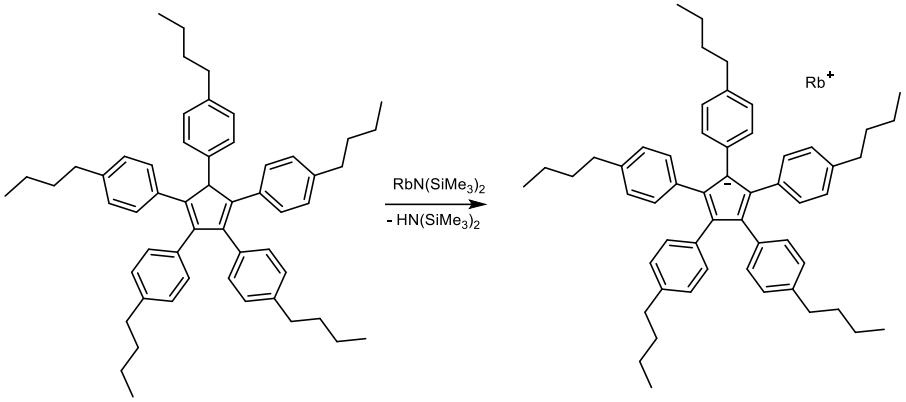

0.1 mmol (73 mg) $Cp^{Big\ n\text{-}Bu}H$ and 0.1 mmol (25 mg) $RbN(SiMe_3)_2$ were suspended in 3mL acetonitrile and stirred for 4 h at 60 °C. All volatiles were removed under reduced pressure at 100 °C, yielding a colorless solid.

Yield: 76 mg (0.094 mmol, 94%). Mp. 217 °C (dec.). Anal. calcd. for $C_{55}H_{65}Rb$: C, 81.40; H, 8.07%. Found: C, 81.33; H, 7.97%. ^{1}H NMR (300 MHz, THF-d_8, 25 °C): δ 0.92 (t, $^3J_{HH}$ = 7.3 Hz, 15 H, CH_3), 1.27-1.39 (m, 10 H, CH_2), 1.52 (s, br., 10 H, CH_2), 2.44 (s, br., 10 H, CH_2), 6.62 (s, br., 20 H, Ar-*H*). ^{13}C NMR (75.5 MHz, THF-d_8, 25 °C): δ 14.39 (*C*H$_3$), 23.20 (*C*H$_2$), 34.79 (*C*H$_2$), 36.14 (*C*H$_2$), 120.83 (Cp-*C*), 127.30 (Ar-*C*H), 132.23 (Ar-*C*H), 136.29 (Ar-*C*), 140.18 (Ar-*C*). ^{87}Rb NMR (98 MHz, CD_3CN, 25 °C): δ –9.22. IR: ν = 3014, 2957, 2923, 2854, 1608, 1514, 1457, 1378, 1140, 1115, 1016, 847, 831, 760, 683, 564, 548 cm^{-1}.

6.1.19 Synthesis of $Cp^{Big\ n\text{-}Bu}Cs$ 18

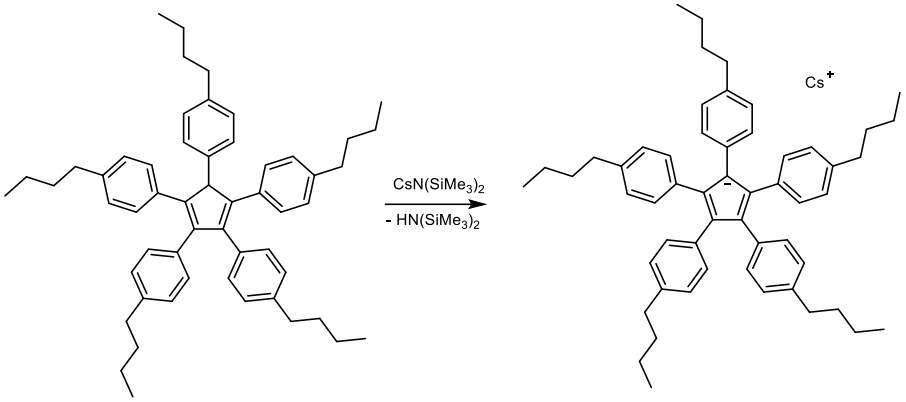

A solution of 0.4 mmol (291 mg) $Cp^{Big\ n\text{-}Bu}H$ and 0.4 mmol (117 mg) $CsN(SiMe_3)_2$ in 5 mL toluene was stirred for 3 h at ambient temperature. All volatiles were removed under reduced pressure at 100 °C, yielding a colorless solid, which was re-crystallized from acetonitrile at –30 °C.

Yield: 312 mg (0.363 mmol, 91%). Mp. 253 °C (dec.). Anal. calcd. for $C_{55}H_{65}Cs$: C, 76.90; H, 7.63%. Found: C, 76.40; H, 7.63%. ^1H NMR (300 MHz, Tol-d_8, 25 °C): δ 0.92 (t, $^3J_{HH}$ = 7.2 Hz, 15 H, CH_3), 1.25-1.36 (m, 10 H, CH_2), 1.45-1.55 (m, 10 H, CH_2), 2.41 (s, br., 10 H, CH_2), 6.61 (s, br., 20 H, Ar-*H*). ^{13}C NMR (75.5 MHz, Tol-d_8, 25 °C): δ 14.29 (*C*H_3), 23.10 (*C*H_2), 34.11 (*C*H_2), 35.81 (*C*H_2), 121.84 (Cp-*C*), 128.56 (Ar-*C*H), 130.94 (Ar-*C*H), 136.72 (Ar-*C*), 138.11 (Ar-*C*). ^{133}Cs NMR (39.4 MHz, Tol-d_8, 25 °C): δ –225.65. IR: ν = 3016, 2955, 2925, 2855, 1607, 1514, 1456, 1377, 1140, 1115, 1016, 847, 831, 761, 684, 547 cm^{-1}.

6.1.20 Synthesis of $Cp^{Big\ t\text{-}Bu}Li$ 19

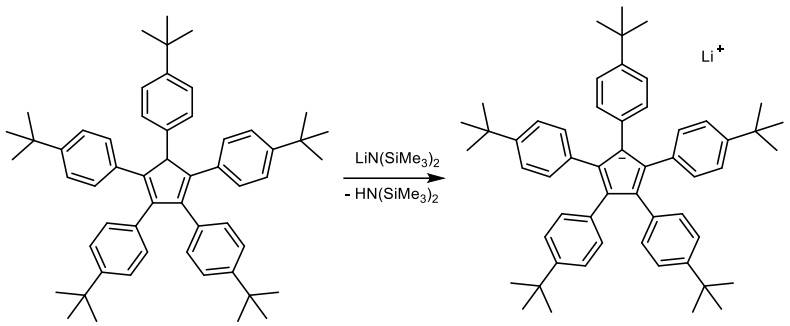

0.3 mmol (218 mg) $Cp^{Big\ t\text{-}Bu}H$ and 0.3 mmol (50 mg) $LiN(SiMe_3)_2$ were dissolved in 3 mL acetonitrile and stirred for 1 h at ambient temperature. All volatiles were removed under reduced pressure at 100 °C, yielding a colorless solid. Single-crystals of this product were obtained by layering a concentrated solution in THF with hexane. This procedure is not suitable for preparative purposes, since **19** partially decomposes in the presence of THF even under vigorously dry conditions, yielding varying amounts of $Cp^{Big\ t\text{-}Bu}H$.

Yield: 208 mg (0.284 mmol, 95%). Mp. >400 °C (dec.). Anal. calcd. for $C_{55}H_{65}Li$: C, 90.12; H, 8.94%. Found: C, 90.78; H, 9.19%. The broad ^{1}H and ^{13}C NMR signals of **19** do not allow a reliable assignment and integration. ^{1}H NMR (300 MHz, CD_3CN, 25 °C): δ 1.24, 5.78-8.15. ^{13}C NMR (151 MHz, CD_3CN, 25 °C): δ 20.16-49.98, 107.31-160.36. ^{7}Li NMR (112 MHz, CD_3CN, 25 °C): δ -2.52. IR: ν = 3032, 2955, 2901, 2866, 1513, 1361, 1286, 1149, 1039, 852, 834, 693, 569, 558 cm^{-1}.

6.1.21 Synthesis of $Cp^{Big\ t\text{-}Bu}Na$ 20

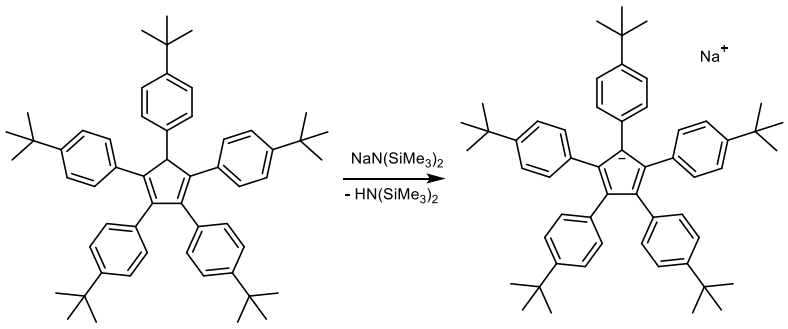

A light-yellow solution of 0.3 mmol (218 mg) $Cp^{Big\ t\text{-}Bu}H$ and 0.3 mmol (55 mg) $NaN(SiMe_3)_2$ in 3 mL THF was stirred for 1 h at ambient temperature. The solvent was partly removed under reduced pressure until a crystalline solid began to precipitate. Gentle heating to 60 °C yielded a clear solution, which was cooled to 0 °C. Colorless crystals formed within 16 h, which were isolated from the mother liquor by decantation. Removing all volatiles from the mother liquor under reduced pressure at 100 °C gave a second fraction. The yield is given for the isolated crystals.

Yield: 158 mg (0.212 mmol, 71%). Mp. >400 °C (dec.). Anal. calcd. for $C_{55}H_{65}Na$: C, 88.19; H, 8.75%. Found: C, 87.82; H, 8.39%. The broad ^1H NMR signals of **20** do not allow a reliable assignment and integration. ^1H NMR (600 MHz, THF-d_8, 25 °C): δ 0.62-1.75, 6.15-7.36. ^{13}C NMR (126 MHz, THF-d_8, 25 °C): δ 32.27 (CH_3), 34.67 ($C(CH_3)_3$), 119.41 (Cp-*C*), 123.56 (Ar-*C*H), 132.59 (Ar-*C*H), 138.39 (Ar-*C*), 144.41 (Ar-*C*). ^{23}Na NMR (79 MHz, THF-d_8, 25 °C): δ − 13.67. IR: ν = 3032, 2958, 2903, 2866, 1513, 1460, 1361, 1270, 1151, 1015, 852, 834, 776, 694, 569 cm^{-1}.

6.1.22 Synthesis of $Cp^{Big\ t\text{-}Bu}K$ 21

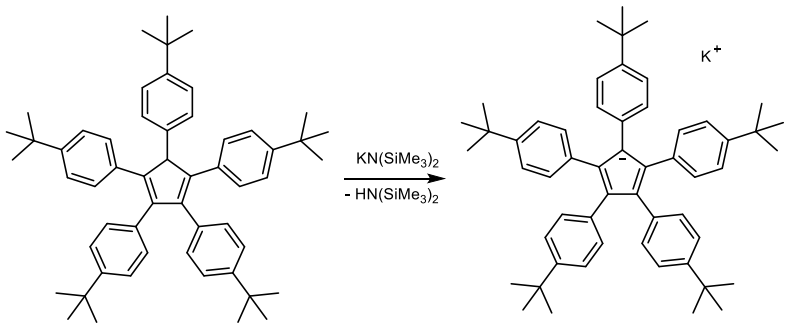

A light-yellow solution of 0.3 mmol (218 mg) $Cp^{Big\ t\text{-}Bu}H$ and 0.3 mmol (60 mg) $KN(SiMe_3)_2$ in 3 mL THF was stirred for 1 h at ambient temperature. The solvent was partly removed under reduced pressure until a crystalline solid began to precipitate. Gentle heating to 60 °C yielded a clear solution, which was layered with 3 mL n-hexane and cooled to 0 °C Colorless crystals formed within 16 h, which were isolated from the mother liquor by decantation. Removing all volatiles from the mother liquor under reduced pressure at 100 °C gave a second fraction. The yield is given for the isolated crystals.

Yield: 217 mg (282 mmol, 94%). Mp. >400 °C. Anal. calcd. for $C_{55}H_{65}K$: C, 86.33; H, 8.56%. Found: C, 86.5; H, 8.57%. ^{1}H NMR (500 MHz, THF-d_8, 25 °C): δ 1.23 (s, 45 H, CH_3), 6.58 (d, $^3J_{HH}$ = 7.6 Hz, 10 H, Ar-*H*), 6.78 (d, $^3J_{HH}$ = 7.6 Hz, 10 H, Ar-*H*). ^{13}C NMR (126 MHz, THF-d_8, 25 °C): δ 32.09 (*C*H_3), 34.65 (*C*$(CH_3)_3$), 120.63 (Cp-*C*), 123.90 (Ar-*C*H), 131.91 (Ar-*C*H), 139.37 (Ar-*C*), 144.71 (Ar-*C*). IR: ν = 3018, 2961, 2930, 2866, 1516, 1461, 1361, 1270, 1152, 1119, 1012, 851, 833, 774, 690, 571 cm^{-1}.

6.1.23 Synthesis of $Cp^{Big\ t\text{-}Bu}Rb$ 22

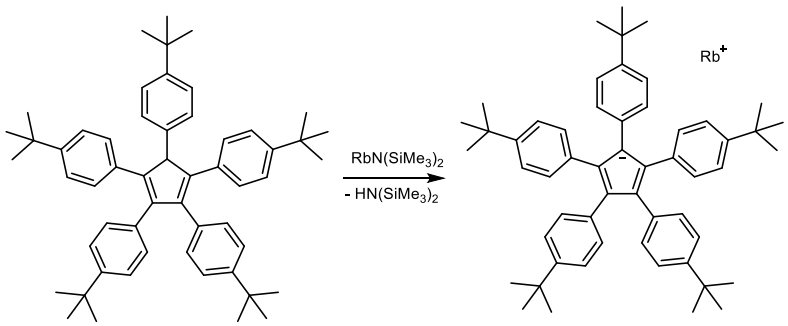

A light-yellow solution of 0.3 mmol (218 mg) $Cp^{Big\ t\text{-}Bu}H$ and 0.3 mmol (74 mg) $RbN(SiMe_3)_2$ in 3 mL THF was stirred for 1 h at ambient temperature. The solvent was partly removed under reduced pressure until a crystalline solid began to precipitate. Gentle heating to 60 °C yielded a clear solution, which was layered with 3 mL n-hexane and cooled to 0 °C Colorless crystals formed within 16 h, which were isolated from the mother liquor by decantation. Removing all volatiles from the mother liquor under reduced pressure at 100 °C gave a second fraction. The yield is given for the isolated crystals.

Yield: 197 mg (244 mmol, 81%). Mp. >400 °C. Anal. calcd. for $C_{55}H_{65}Rb$: C, 81.40; H, 8.07%. Found: C, 81.08; H, 8.12%. ^1H NMR (300 MHz, THF-d_8, 25 °C): δ 1.24 (s, 45 H, CH_3), 6.62 (d, $^3J_{HH}$ = 7.0 Hz, 10 H, Ar-*H*), 6.84 (d, $^3J_{HH}$ = 7.0 Hz, 10 H, Ar-*H*). ^{13}C NMR (75 MHz, THF-d_8, 25 °C): δ 32.09 (*C*H_3), 34.88 (*C*(CH_3)$_3$), 121.01 (Cp-*C*), 124.02 (Ar-*C*H), 131.94 (Ar-*C*H), 139.64 (Ar-*C*), 144.82 (Ar-*C*). ^{78}Rb NMR (98 MHz, CD_3CN, 25 °C): δ 1.66. IR: ν = 3016, 2958, 2903, 2865, 1515, 1361, 1268, 1151, 1012, 851, 832, 690, 871 cm^{-1}.

6.1.24 Synthesis of $Cp^{Big\ t\text{-}Bu}Cs$ 23

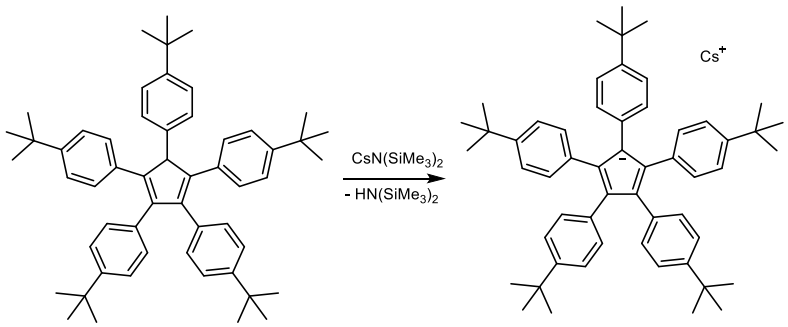

0.3 mmol (218 mg) $Cp^{Big\ t\text{-}Bu}H$ and 0.3 mmol (74 mg) $CsN(SiMe_3)_2$ were dissolved in 3 mL THF and the resulting light-yellow solution was stirred for 1 h at ambient temperature. All volatiles were removed under reduced pressure at 100 °C, yielding a colorless solid. The product was re-crystallized from pyridine at ambient temperature.

Yield: 242 mg (282 mmol, 94%). Mp. >400 °C. Anal. calcd. for $C_{55}H_{65}Cs$: C, 76.90; H, 7.63%. Found: C, 76.96; H, 7.11%. ^1H NMR (600 MHz, THF-d_8, 25 °C): δ 1.22 (s, 45 H, CH_3), 6.57 – 6.77 (m, 10 H, Ar-*H*), 6.77 – 6.98 (m, 10 H, Ar-*H*). ^{13}C NMR (126 MHz, THF-d_8, 25 °C): δ 31.53 (*C*H_3), 34.18 (*C*$(CH_3)_3$), 120.91 (Cp-*C*), 123.43 (Ar-*C*H), 131.47 (Ar-*C*H), 139.45 (Ar-*C*), 144.15 (Ar-*C*). ^{133}Cs NMR (39 MHz, THF-d_8, 25 °C): δ − 143.71. IR: ν = 3020, 2959, 2904, 2866, 1515, 1361, 1268, 1151, 1013, 851, 832, 690, 572 cm^{-1}.

6.1.25 Synthesis of $Cp^{Big}t\text{-}Bu_2Ge$ 24

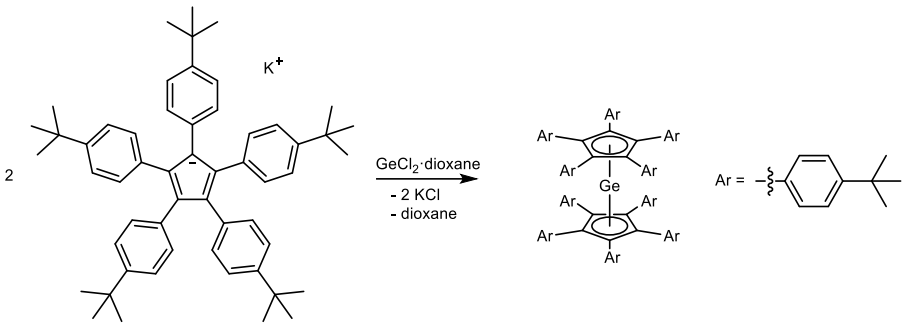

0.2 mmol (153 mg) $Cp^{Big\ t\text{-}Bu}K$ and 0.1 mmol (23 mg) $GeCl_2$·dioxane were dissolved in 2 mL THF and stirred for 1 h at ambient temperature. The resulting yellow suspension was filtered and the filtrate was stored at −30 °C for 12 h, yielding yellow block-type crystals, which were isolated by decantation from the mother liquor and dried *in vacuo*.

Yield: 124 mg (0.081 mmol, 81%). Mp. 317 °C (dec.). Anal. calcd. for $C_{110}H_{130}Ge$: C, 86.65; H, 8.59%. Found: C, 85.70; H, 8.41%. ^{1}H NMR (300 MHz, THF-d_8, 25 °C): δ 6.73 (br s, 10 H, C_{meta}), 6.66 (d, $^3J_{HH}$ = 8.6 Hz, 10 H, C_{ortho}), 1.24 (s, 45 H, CH_3). ^{13}C NMR (75.5 MHz, THF-d_8, 25 °C): δ 149.38 (C_{para}), 133.39 (C_{ortho}), 131.85 (C_{ipso}), 127.39 (C_{Cp}), 124.36 (C_{meta}), 35.05 ($C(CH_3)_3$), 31.92 (CH_3). IR: ν = 2961, 2903, 2866, 1516, 1475, 1461, 1392, 1362, 1270, 1152, 1120, 1100, 1016, 852, 835, 776, 694, 572, 473, 447 cm^{-1}.

6.1.26 Synthesis of $Cp^{Big\ t\text{-}Bu}{}_2Sn$ 25

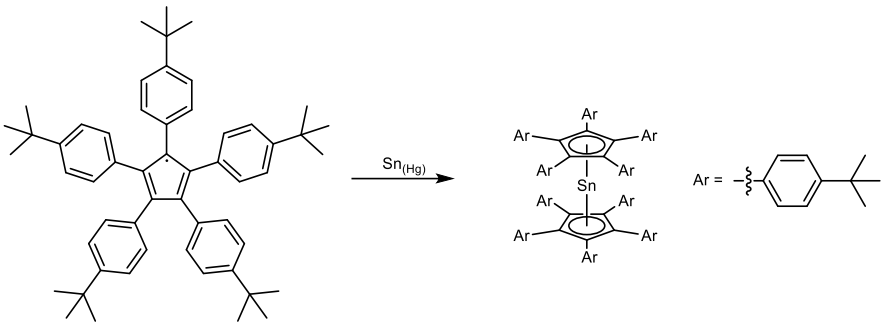

A solution of 0.2 mmol (145 mg) $Cp^{Big\ t\text{-}Bu}$· in 10 mL of THF was added to a solution of 0.6 mmol (71 mg) Sn in 1 mL of mercury, yielding a deep blue/metallic biphasic solution that was stirred for 12 h at ambient temperature. The resulting yellow solution was decanted from the metallic phase and all volatiles were removed under reduced pressure, yielding the product as a colorless solid. The product was re-crystallized from THF at −30 °C.

Yield: 132 mg (0.084 mmol, 84%). Mp. 327 °C (dec.). Anal. calcd. for $C_{110}H_{130}Sn$: C, 84.10; H, 8.34%. Found: C, 84.50; H, 8.18%. ^{1}H NMR (300 MHz, THF-d_8, 25 °C): δ 6.76 (d, $^3J_{HH}$ = 8.2 Hz, 10 H, C_{meta}), 6.66 (d, $^3J_{HH}$ = 8.2 Hz, 10 H, C_{ortho}), 1.22 (s, 45 H, CH_3). ^{13}C NMR (75.5 MHz, THF-d_8, 25 °C): δ 149.14 (C_{para}), 133.14 (C_{ortho}), 132.32 (C_{ipso}), 126.42 (C_{Cp}), 123.86 (C_{meta}), 34.99 ($C(CH_3)_3$), 31.86 (CH_3). IR: ν = 2961, 2903, 2867, 1517, 1461, 1392, 1362, 1261, 1151, 1119, 1099, 1049, 1016, 850, 833, 797, 776, 691, 570, 474, 447, 384 cm^{-1}.

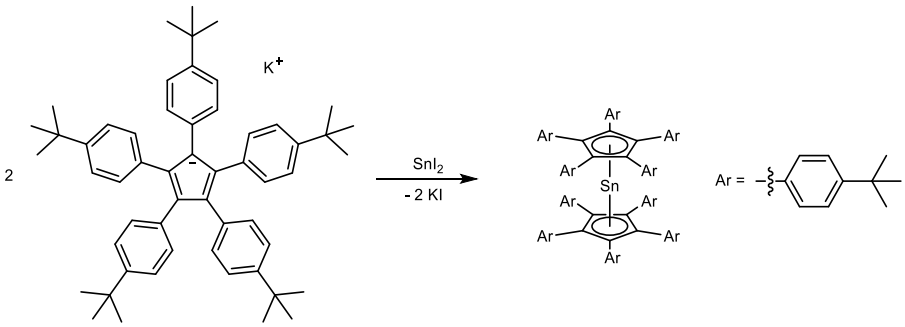

Alternative synthesis: 0.2 mmol (153 mg) $Cp^{Big\ t\text{-}Bu}K$ and 0.1 mmol (37 mg) SnI_2 were dissolved in 2 mL THF and stirred for 1 h at ambient temperature. The resulting yellow suspension was filtered and the filtrate was stored at −30 °C for 12 h, yielding yellow block-type crystals, which were isolated by decantation from the mother liquor and dried *in vacuo*. Yield: 126 mg (0.080 mmol, 80%).

6.1.27 Synthesis of $Cp^{Big\ t\text{-}Bu}{}_2Pb$ 26

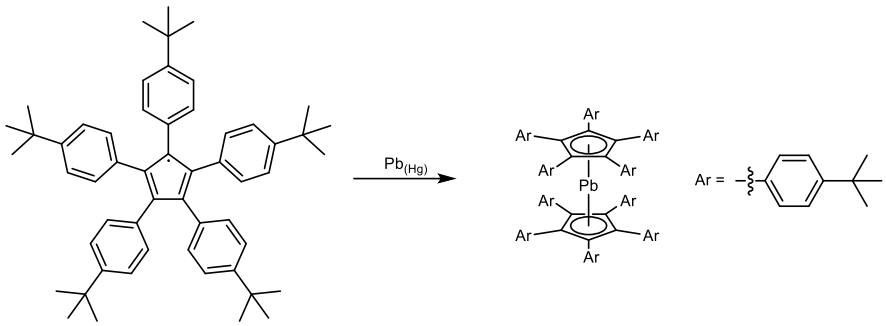

A solution of 0.2 mmol (145 mg) $Cp^{Big\ t\text{-}Bu}$ · in 10 mL of THF was added to a solution of 0.6 mmol (124 mg) Pb in 1 mL of mercury, yielding a deep blue/metallic biphasic solution that was stirred for 12 h at ambient temperature. The resulting red solution was decanted from the metallic phase and all volatiles were removed under reduced pressure, yielding the product as a red solid. The product was re-crystallized from THF at −30 °C.

Yield: 132 mg (0.079 mmol, 79%). Mp. 280 °C (dec.). Anal. calcd. for $C_{110}H_{130}Pb$: C, 79.62; H, 7.90%. Found: C, 79.87; H, 7.70%. ^{1}H NMR (300 MHz, THF-d_8, 25 °C): δ 6.80 (d, $^3J_{HH}$ = 8.2 Hz, 10 H, C_{meta}), 6.63 (d, $^3J_{HH}$ = 8.2 Hz, 10 H, C_{ortho}), 1.24 (s, 45 H, CH_3). ^{13}C NMR (75.5 MHz, THF-d_8, 25 °C): δ 149.02 (C_{para}), 133.24 (C_{ortho}), 132.06 (C_{ipso}), 127.46 (C_{Cp}), 124.53 (C_{meta}), 34.95 ($C(CH_3)_3$), 31.88 (CH_3). IR: ν = 2961, 2903, 2866, 1513, 1475, 1460, 1392, 1362, 1270, 1199, 1151, 1120, 1100, 1049, 1014, 852, 836, 776, 692, 635, 572, 544, 471, 445 cm^{-1}.

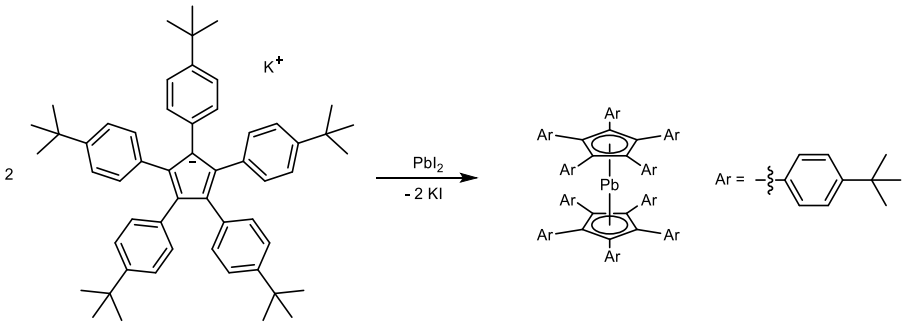

Alternative synthesis: 0.2 mmol (153 mg) $Cp^{Big\ t\text{-}Bu}K$ and 0.1 mmol (46 mg) PbI_2 were dissolved in 2 mL of THF and stirred for 1 h at ambient temperature. The red suspension was filtered and the filtrate was stored at −30 °C for 12 h, yielding yellow red block-type crystals, which were isolated by decantation from the mother liquor and dried *in vacuo*. Yield: 141 mg (0.085 mmol, 85%).

6.1.28 Synthesis of $Cp^{Big\ t\text{-}Bu}PCl_2$ 27

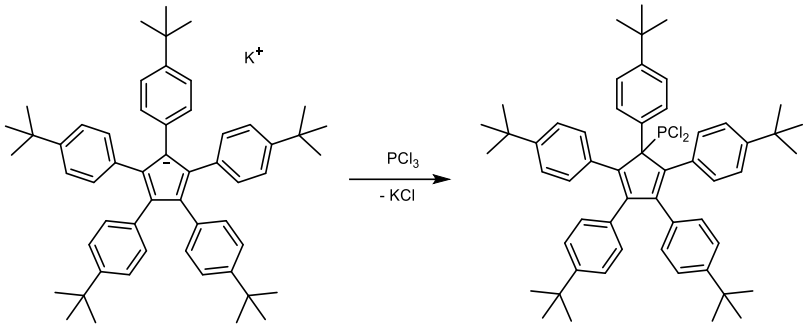

A solution of 0.05 mmol (38 mg) $Cp^{Big\ t\text{-}Bu}K$ in 0.25 mL THF was added to a solution of 0.05 mmol (6.9 mg, 4.4 µL) PCl_3 in 0.25 mL THF and stirred for 1 h. The resulting greenish solution was centrifuged and the clear, greenish supernatant solution was decanted. All volatiles were removed under reduced pressure at ambient temperature, yielding a yellow powder, which was dissolved in 1 mL of *n*-hexane and again centrifuged to remove possible traces of KCl. The supernatant solution was decanted, and all volatiles were removed under reduced pressure at ambient temperature, yielding a yellow crystalline solid.

Yield: 37.6 mg (45.4 mmol, 91%). Mp. 181 °C (dec.). Anal. calcd. for $C_{55}H_{65}PCl_2$: C, 79.78; H, 7.91%. Found: C, 78.95; H, 7.57%. ^{1}H NMR (300 MHz, THF-d_8, 60 °C): δ 1.21 (s, 45 H, CH_3), 6.97 (d, $^3J_{HH}$ = 8.4 Hz, 10 H, Ar-*H*), 7.09 (d, $^3J_{HH}$ = 8.4 Hz, 10 H, Ar-*H*). ^{13}C NMR (151 MHz, THF-d_8, 25 °C): δ 31.56 (*C*H_3), 35.03 (*C*$(CH_3)_3$), 125.20 (Ar-*C*H), 130.62 (Ar-*C*H), 133.53 (Ar-*C*), 150.52 (Ar-*C*). The signal of the Cp-*C* atom could not be observed. ^{31}P NMR (122 MHz, THF-d_8, 25 °C): δ 46.47. IR: ν = 3033, 2958, 2903, 2867, 1503, 1461, 1393, 1363, 1268, 1120, 1018, 830, 567, 487 cm^{-1}.

6.1.29 Synthesis of $Cp^{Big\ t\text{-}Bu}AsCl_2$ 28

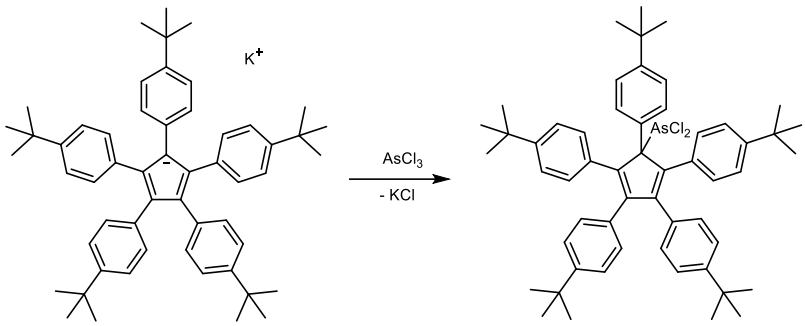

A solution of 0.05 mmol (38 mg) $Cp^{Big\ t\text{-}Bu}K$ in 0.25 mL THF was added to a solution of 0.05 mmol (9.1 mg, 4.2 µL) $AsCl_3$ in 0.25 mL THF and stirred for 1 h. The resulting greenish solution was centrifuged and the clear, greenish supernatant solution was decanted. All volatiles were removed under reduced pressure at ambient temperature, yielding a yellow powder, which was dissolved in 1 mL of *n*-hexane and again centrifuged to remove possible traces of KCl. The supernatant solution was decanted, and all volatiles were removed under reduced pressure at ambient temperature, yielding a yellow crystalline solid. The product was crystallized from *n*-hexane at −30 °C.

Yield: 41.8 mg (47.9 mmol, 96%). Mp. 154 °C (dec.). Anal. calcd. for $C_{55}H_{65}AsCl_2$: C, 75.76; H, 7.51%. Found: C, 76.14; H, 7.66%. ^{1}H NMR (600 MHz, THF-d_8, 25 °C): δ 1.26 (s, 45 H, CH_3), 7.00 (d, $^3J_{HH}$ = 8.7 Hz, 10 H, Ar-*H*), 7.14 (d, $^3J_{HH}$ = 8.7 Hz, 10 H, Ar-*H*). ^{13}C NMR (151 MHz, THF-d_8, 25 °C): δ 31.54 (*C*H_3), 35.08 (*C*(CH_3)$_3$), 125.21 (Ar-*C*H), 131.22 (Ar-*C*H), 132.29 (Ar-*C*), 133.80 (Cp-*C*), 150.95 (Ar-*C*). IR: ν = 3031, 2961, 2903, 2868, 1495, 1462, 1363, 1268, 1118, 1016, 852, 833, 686, 567 cm^{-1}.

6.1.30 Synthesis of $Cp^{Big\ t\text{-}Bu}SbCl_2$ 29

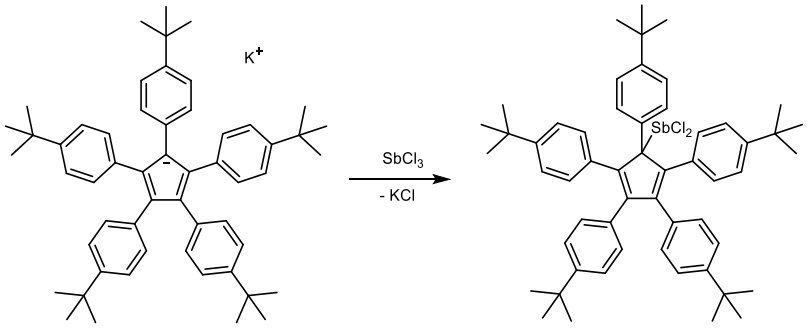

A solution of 0.05 mmol (38 mg) $Cp^{Big\ t\text{-}Bu}K$ in 0.25 mL THF was added to a solution of 0.05 mmol (11.4 mg) $SbCl_3$ in 0.25 mL THF and stirred for 1 h. The resulting greenish solution was centrifuged and the clear, greenish supernatant solution was decanted. All volatiles were removed under reduced pressure at ambient temperature, yielding a yellow powder, which was dissolved in 1 mL of *n*-hexane and again centrifuged to remove possible traces of KCl. The supernatant solution was decanted, and all volatiles were removed under reduced pressure at ambient temperature, yielding a yellow crystalline solid. The product was crystallized from *n*-hexane at −30 °C.

Yield: 40.0 mg (43.5 mmol, 87%). Mp. 134 °C (dec.). Anal. calcd. for $C_{55}H_{65}SbCl_2$: C, 71.9; H, 7.13%. Found: C, 74.3; H, 7.46%. ^{1}H NMR (600 MHz, THF-d_8, 25 °C): δ 1.24 (s, 45 H, CH_3), 6.93 (d, $^3J_{HH}$ = 8.4 Hz, 10 H, Ar-*H*), 7.09 (d, $^3J_{HH}$ = 8.4 Hz, 10 H, Ar-*H*). ^{13}C NMR (151 MHz, THF-d_8, 25 °C): δ 31.60 (*C*H_3), 35.05 (*C*$(CH_3)_3$), 124.97 (Ar-*C*H), 131.02 (Cp-*C*), 131.43 (Ar-*C*), 132.12 (Ar-*C*H), 150.50 (Ar-*C*). IR: ν = 3034, 2962, 2904, 2867, 1462, 1362, 1269, 1016, 851, 833, 691, 569 cm^{-1}.

6.1.31 Synthesis of $Cp^{Big\ t\text{-}Bu}BiCl_2$ 30

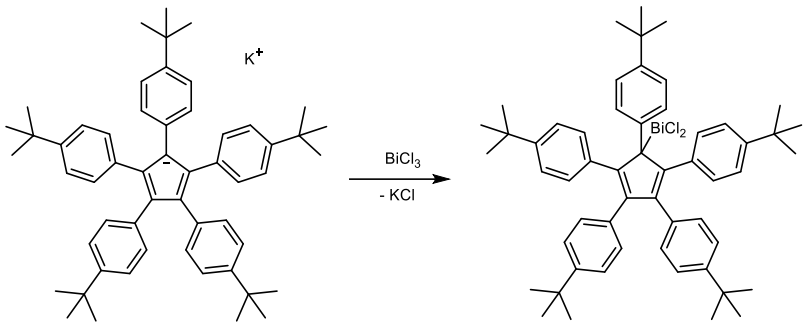

A solution of 0.05 mmol (38 mg) $Cp^{Big\ t\text{-}Bu}K$ in 0.25 mL THF was added to a solution of 0.05 mmol (11.4 mg) $SbCl_3$ in 0.25 mL THF and stirred for 1 h. The resulting greenish solution was centrifuged and the clear, greenish supernatant solution was decanted. All volatiles were removed under reduced pressure at ambient temperature, yielding a yellow powder, which was dissolved in 1 mL of *n*-hexane and again centrifuged to remove possible traces of KCl. The supernatant solution was decanted, and all volatiles were removed under reduced pressure at ambient temperature, yielding a brown crystalline solid.

Yield: 46.2 mg (45.9 mmol, 92%). Mp. 179 °C (dec.). Anal. calcd. for $C_{55}H_{65}BiCl_2$: C, 65.67; H, 6.51%. Found: C, 67.0; H, 6.62%. ^{1}H NMR (600 MHz, THF-d_8, 25 °C): δ 1.23 (s, 45 H, CH_3), 6.90 (d, $^3J_{HH}$ = 8.3 Hz, 10 H, Ar-*H*), 7.04 (d, $^3J_{HH}$ = 8.3 Hz, 10 H, Ar-*H*). ^{13}C NMR (151 MHz, THF-d_8, 25 °C): δ 31.78 (*C*H$_3$), 34.96 (*C*(CH$_3$)$_3$), 124.68 (Ar-*C*H), 127.40 (Cp-*C*), 132.57 (Ar-*C*), 132.70 (Ar-*C*H), 149.26 (Ar-*C*). IR: ν = 3031, 2958, 2904, 2868, 1362, 1268, 1016, 851, 834, 570 cm^{-1}.

6.1.32 Synthesis of $Cp^{Big\ OMe}K$ 31-K

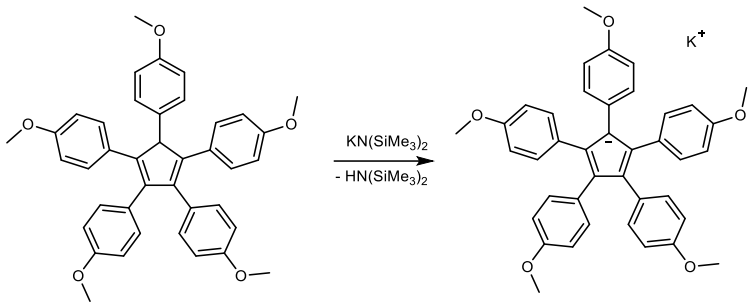

1 mmol (634 mg) of $Cp^{Big\ OMe}H$ and 1 mmol (199 mg) of $KN(TMS)_2$ were dissolved in 10 mL of THF and stirred for 30 minutes. All volatiles were removed *in vacuo*. The remaining white solid was washed with 5 mL of toluene and 10 mL of *n*-hexane. Removal of all volatiles *in vacuo* yielded $Cp^{Big\ OMe}K$ in the form of a colorless powder.

Yield: 480 mg, 0.756 mmol, 76%. M.p >400 °C. Elemental analysis for $C_{40}H_{35}O_5K$: calcd.: C, 75.7; H, 5.56, O, 12.6%. Found: C, 75.7; H, 5.65; O, 12.9%. ^{1}H NMR (400 MHz, C_6D_6) δ 7.30 – 6.00 (br m, 20H, Ar-C*H*), 3.68 (s, 15H, OCH_3). ^{13}C NMR (101 MHz, C_6D_6) δ 112.9 (Ar-CH), 55.6 (Cp-Ar-C_{meta}), 141.9 (OCH_3). Some signals are not observed due to line broadening. IR ν = 3020, 2941, 2833, 1609, 1523, 1458, 1240, 1174, 1106, 1031, 822, 757, 685, 536 cm^{-1}.

6.1.33 Synthesis of $Cp^{Big\ C6F5}K$ 33-K

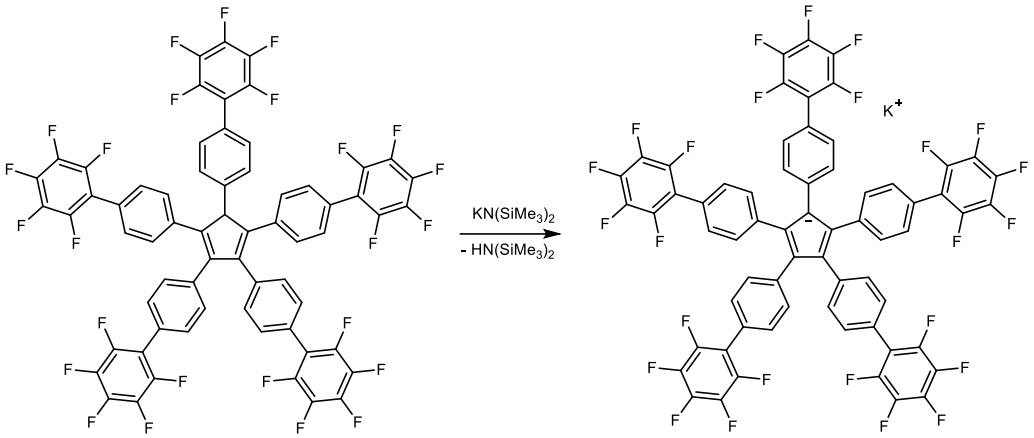

117 µmol (150 mg) of $Cp^{Big\ C6F5}H$ and 117 µmol (23 mg) $KN(TMS)_2$ were dissolved in 1 mL of benzene and stirred for 30 minutes. The product precipitates as a yellow powder. The mother liquor was removed by filtration and the remaining yellow solid washed with 3 mL of *n*-hexane and dried *in vacuo*.

Yield: 100 mg, 76 mmol, 65%. M.p >400 °C. Elemental analysis for $C_{65}H_{20}F_{25}K$: C, 59.4; H, 1.53%. Found: C, 59.8; H, 1.70%. ^{1}H NMR (400 MHz, THF) δ 7.03 (s , Ar-C*H*). ^{13}C NMR (101 MHz, THF) δ 145.2 (d, $^1J_{CF}$ = 247 Hz, C_6F_{5ortho}), 144.8 (Cp-Ar-*C*H_{para}), 140.2 (d, $^1J_{CF}$ = 264 Hz, C_6F_{5para}), 138.8 (d, $^1J_{CF}$ = 247 Hz, C_6F_{5meta}), 132.9 (Cp-Ar-*C*H), 129.0 (Cp-Ar-*C*H), 122.6 (Cp-Ar-*C*H_{ipso}), 119.6 (Cp-*C*), 118.5 (t, $^2J_{CF}$ = 17 Hz, C_6F_{5ipso}). ^{19}F NMR (376 MHz, THF) δ -144.67 (dd, $^3J_{FF}$ = 23.3, 7.7 Hz, 10F, C_6F_{5ortho}), -161.01 (t, $^3J_{FF}$ = 20.7 Hz, 5F, C_6F_{5para}), -165.64 (m, 10F, C_6F_{5meta}). IR ν = 1491, 1063, 981, 850, 753 cm^{-1}.

6.1.34 Synthesis of $Cp^{Big\ t\text{-}Bu2}K$ 34-K

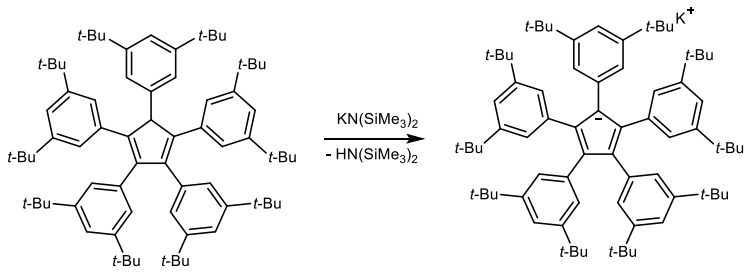

1 mmol (1008 mg) of $Cp^{Big\ t\text{-}Bu2}H$ and 1 mmol (199 mg) of $KN(TMS)_2$ were suspended in 10 mL of THF and stirred for 30 minutes. All volatiles were removed *in vacuo*, yielding a white solid that was dissolved in 10 mL of hot THF and stored at −30 °C for 24 h. The product was isolated by filtration and dried *in vacuo*. It contains 1.5 equivalents of THF, which cannot be removed.

Yield: (948 mg, 0.822 mmol, 82%. Elemental Anal. calcd. for $C_{75}H_{105}K \cdot 1.5$ THF: C, 84.3; H, 10.22%. Found: C, 84.2; H, 10.17%. M.p. >400 °C (reversible color change at approx. 300 °C from white to yellow. ^{1}H NMR (400 MHz, C_6D_6) δ 6.85 (br m, 5H, Cp-Ar-CH_{para}), 6.71 (br m, 10H, Cp-Ar-CH_{ortho}), 3.61 (m, THF), 1.77 (m, THF), 1.03 (s, 90 H, C(CH_3)$_3$). ^{13}C NMR (101 MHz, C_6D_6) δ 148.7, 142.4, 126.8 (Cp-Ar-C_{ortho}), 116.1, 68.2 (THF), 35.0 (*C*(CH$_3$)$_3$), 32.0 (C(*C*H$_3$)$_3$), 26.4 (THF). Some signals are not assigned because of the lack of signals in the ^{1}H-^{13}C HMBC spectrum. IR ν = 2955, 2903, 2872, 1586, 1470, 1360, 1247, 1047, 899, 875, 713 cm^{-1}.

6.1.35 Synthesis of $Cp^{Big\ Ph2}K$ 35-K

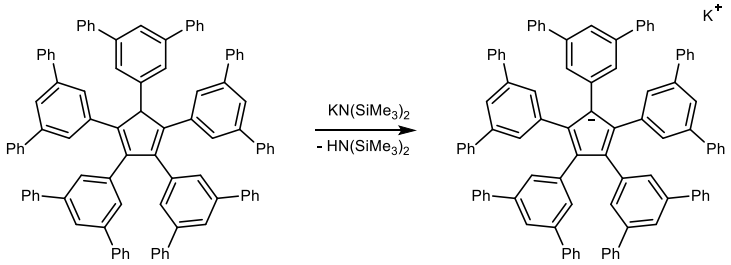

0.2 mmol (242 mg) of $Cp^{Big\ Ph2}H$ and 0.2 mmol (40 mg) of $KN(TMS)_2$ were dissolved in 2 mL of benzene and stirred for 30 minutes. All volatiles were removed *in vacuo*. The resulting yellow solid was dissolved in 2 mL of benzene. Addition of 10 mL of *n*-hexane resulted in precipitation of the product, which was isolated by filtration and washed with 5 mL of *n*-hexane. All volatiles were removed *in vacuo*.

Yield: 220 mg, 177 mmol, 89%). Elemental anal. for $C_{95}H_{65}K$: C, 91.6; H, 5.26%. Found: C, 91.3; H, 5.29%. M.p: 200 °C (dec.). ^{1}H NMR (400 MHz, C_6D_6) δ 7.77 (t, $^4J_{HH}$ = 1.6 Hz, 5H, Cp-Ar-CH_{para}), 7.74 (d, $^4J_{HH}$ = 1.7 Hz, 10H, Cp-Ar-CH_{ortho}), 7.54 – 7.48 (m, 20H, Ph-CH_{ortho}), 7.18 – 7.12 (m, 20 H, Ph-CH_{meta}), 7.04 (tt, $^3J_{HH}$ = 7.7 Hz, $^4J_{HH}$ =1.2 Hz, 10 H Ph-CH_{para}). ^{13}C NMR (101 MHz, C_6D_6) δ 142.5 (Ph-C_{ipso}), 142.0 (Cp-Ar-C_{meta}), 141.9 (Cp-Ar-C_{ipso}), 130.6 (Cp-Ar-CH_{ortho}), 129.0 (Ph-CH_{meta}), 127.6 (Ph-CH_{ortho}), 127.3 (Ph-CH_{para}), 122.1 (Cp-*C*), 121.8 (Cp-Ar-C_{para}). IR ν = 3035, 1582, 1490, 1075, 1027, 879, 757, 695, 613 cm^{-1}.

6.1.36 Synthesis of $Cp^{Big\ OMe}$· 31

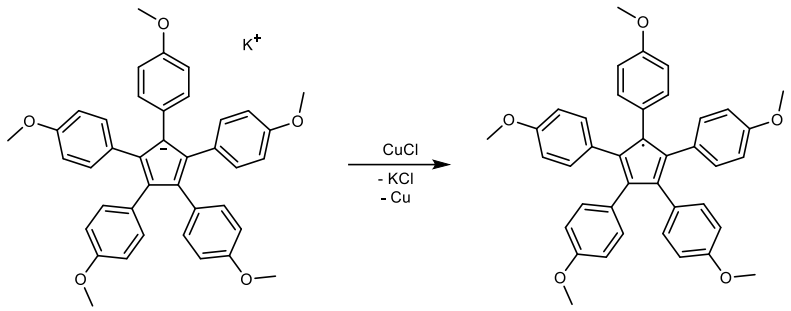

0.2 mmol (127 mg) of $Cp^{Big\ OMe}K$ were combined with 0.6 mmol (59 mg) of CuCl, suspended in 2 mL of THF and stirred for 16 h. All volatiles were then removed *in vacuo*, and the resulting residue was extracted with 10 mL of benzene. The extract was concentrated *in vacuo* until it became slightly viscous and stored for 24 h at 25 °C, yielding $Cp^{Big\ OMe}$· in form of blue needles, which were separated by filtration and dried *in vacuo*.

Yield: 70 mg, (0.117 mmol, 60%). M.p. 240 °C. Elemental analysis: A reliable elemental analysis was not obtained due to the fast decomposition of **31** in the presence of oxygen. IR ν = 2955, 2837, 1590, 1505, 1457, 1349, 1283, 1241, 1171, 1098, 1021, 800, 687, 540 cm^{-1}. UV/Vis (toluene): λ_{max} (log ε) = 373 (4.41), 523 (3.67), 656 nm (4.14).

6.1.37 Synthesis of $Cp^{Big\ t\text{-}Bu}$ · 32

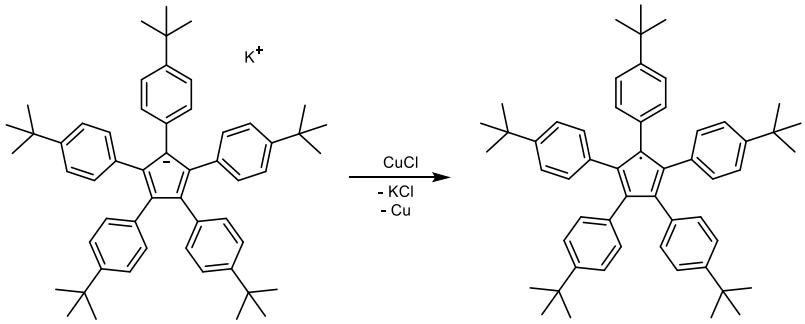

1 mmol (765 mg) $Cp^{Big\ t\text{-}Bu}K$ and 3 mmol (297 mg) CuCl were stirred for 12 h at ambient temperature in 10 mL THF. The resulting blue suspension was evaporated *in vacuo*, the remaining solid residue re-suspended in 30 mL of *n*-hexane and filtered. The filtrate was dried *in vacuo*, yielding $Cp^{Big\ t\text{-}Bu}$ · as blue crystalline solid. $Cp^{Big\ t\text{-}Bu}$ ·can be crystallized by slow evaporation of a solution in *n*-pentane at 25 °C.

Yield: 689 mg (0.949 mmol, 95%). Mp. 305 °C Elemental analysis: A reliable elemental analysis was not obtained due to the fast decomposition of **32** in the presence of oxygen. ^{1}H NMR (300 MHz, C_6D_6, 25 °C): δ 3.00 (br s). IR: ν = 2961, 2903, 2866, 1475, 1461, 1392, 1362, 1268, 1120, 1100, 1016, 850, 835, 777, 694, 632, 570, 553 cm^{-1} UV/Vis (toluene): λ_{max} (log ε) = 363 (4.62), 498 (3.68), 611 nm (4.18).

6.1.38 Synthesis of $Cp^{Big\ C6F5}$· 33

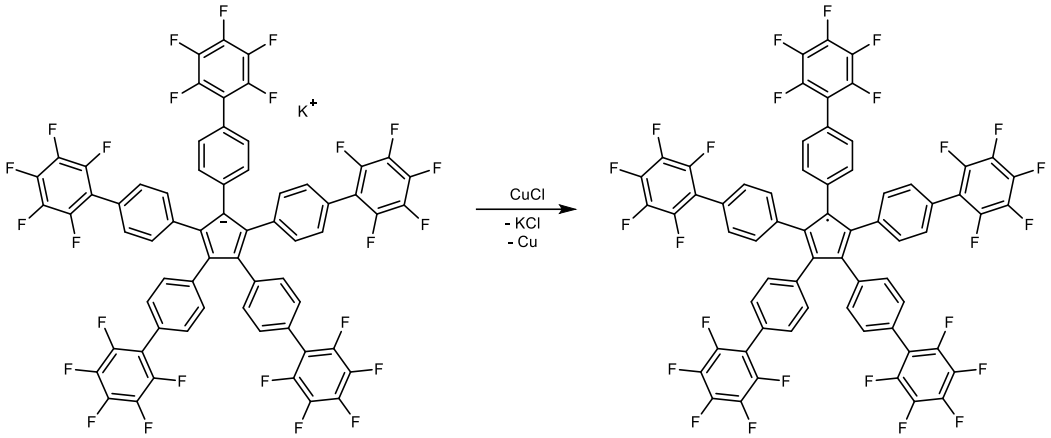

65.7 mg (50 µmol) of $Cp^{Big\ C6F5}K$ were combined with 14.8 mg (150 µmol) of CuCl, suspended in 0.5 mL of THF and stirred for 16 h. All volatiles were then removed *in vacuo*, and the residue was extracted with 2 mL of toluene. Removal of the solvent *in vacuo* gave a blue solid, which was dissolved in 0.5 mL of benzene and stored for 24 h at 25 °C. $Cp^{Big\ C6F5}$· crystallized as thin blue needles, which were separated by filtration, washed with 1 mL of *n*-hexane and dried *in vacuo*.

Yield: 15 mg (11.8 µmol, 24%). Mp. 90 °C (dec. without melting). A reliable elemental analysis was not obtained due to the fast decomposition of **33** in the presence of oxygen. IR ν = 1490, 1402, 1324, 1261, 1063, 983, 853, 757 cm^{-1}. UV/Vis (toluene): λ_{max} (log ε) = 382 (4.72), 513 (3.74), 625 nm (4.23).

6.1.39 Synthesis of $Cp^{Big\ t\text{-}Bu2\cdot}$ 34

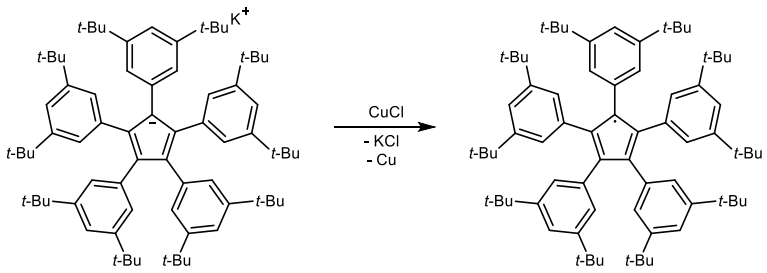

0.2 mmol (231 mg) of $Cp^{Big\ t\text{-}Bu2}K \cdot 2$ THF were combined with 0.6 mmol (59 mg) of CuCl, suspended in 2 mL of THF and stirred for 16 h. All volatiles were removed *in vacuo*, and the residue was extracted with 10 mL of *n*-hexane. The extract was concentrated *in vacuo* until incipient crystallization. The crystals were redissolved by warming and the solution was stored for 24 h at 25 °C, yielding $Cp^{Big\ t\text{-}Bu2\cdot}$ in form of blue needles, which were separated by filtration and dried *in vacuo*. The product contains one equivalent of *n*-hexane.

Yield: 134 mg (0.133 mmol, 67%). Mp. 320 °C (the crystals gradually lose their luster before melting, probably due to the evaporation of solvent). Anal. calcd. for $C_{75}H_{105}$: C, 89.5; H, 10.5%. Found: C, 89.2; H, 10.7%. IR ν = 2955, 2867, 1589, 1465, 1363, 1251, 912, 878, 710, 496 cm^{-1}. UV/Vis (toluene): λ_{max} (log ε) = 356 (4.04), 609 nm (3.60).

6.1.40 Synthesis of $Cp^{Big\ Ph2}$. 35

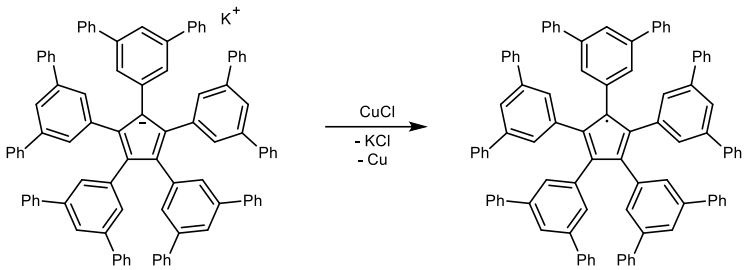

1 mmol (1245 mg) of $Cp^{Big\ Ph2}K$ (1 mmol (1390 mg) of $Cp^{Big\ Ph2}K$ ·THF can also be used) were combined with 3 mmol (297 mg) of CuCl, suspended in 10 mL of THF and stirred for 16 h. All volatiles were removed *in vacuo*, and the residue was extracted with 20 mL of benzene. The extract was concentrated *in vacuo* to 10 mL, and 30 mL of *n*-hexane were added upon stirring. The stirring was stopped immediately after the addition and within 1 h the product crystallized in form of shiny blue needles, which were separated by filtration and dried *in vacuo*.

Yield: 788 mg (0.654 mmol, 65%). Mp. 267 °C. Anal. calcd. for $C_{95}H_{65}$: C, 94.6; H, 5.43%. Found: C, 94.7; H, 5.51%. IR ν = 3032, 1580, 1487, 1360, 1070, 1024, 885, 754, 684, 613 cm^{-1}. UV/Vis (toluene): λ_{max} (log ε) = 338 (4.31), 623 nm (3.84).

6.1.41 Synthesis of $Cp^{Big\ t\text{-}Bu}{}_2Mg$ 36

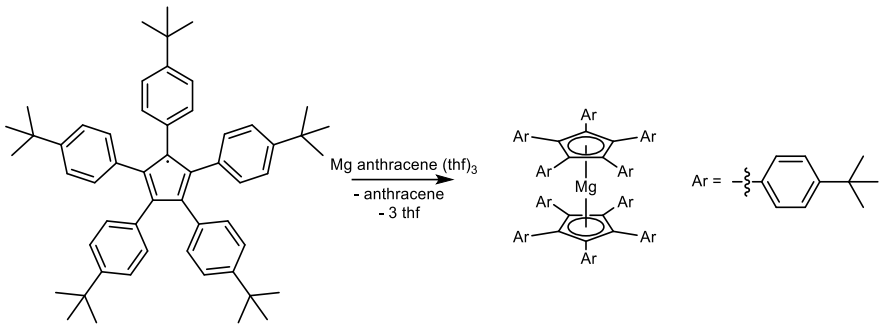

0.2 mmol (145 mg) $Cp^{Big\ t\text{-}Bu}$ · and 0.1 mmol (42 mg) magnesium anthracene·3 THF were suspended in 10 mL of toluene and stirred for 1 h at ambient temperature. The resulting brownish suspension was filtered and the filtrate concentrated until incipient crystallization. The crystals were dissolved by warming, and colorless crystals formed upon storage at ambient temperature within 12 h, which were isolated by decantation, again re-crystallized from 2 mL of toluene at –30 °C and dried *in vacuo*.

Yield: 132 mg (0.045 mmol, 45%). Mp. >400 °C. Anal. calcd. for $C_{110}H_{130}Mg$: C, 89.48; H, 8.87%. Found: C, 90.45; H, 9.02%. ^{1}H NMR (300 MHz, C_6D_6, 25 °C): δ 7.21 (d, $^3J_{HH}$ = 8.5 Hz, 10 H, C_{ortho}), 6.96 (d, $^3J_{HH}$ = 8.5 Hz, 10 H, C_{meta}), 1.29 (s, 45 H, CH_3). ^{13}C NMR (75.5 MHz, C_6D_6, 25 °C): δ 148.68 (C_{para}), 133.07 (C_{ortho}), 132.54 (C_{ipso}), 124.47 (C_{meta}), 121.29 (C_{Cp}), 34.53 ($C(CH_3)_3$), 31.60 (CH_3). IR: ν = 2959, 2903, 2866, 1513, 1475, 1461, 1393, 1360, 1271, 1201, 1149, 1122, 1100, 1014, 852, 836, 776, 694, 572, 494, 407 cm^{-1}.

6.1.42 Synthesis of $Cp^{Big\ t\text{-}Bu}{}_2Ca$ 37

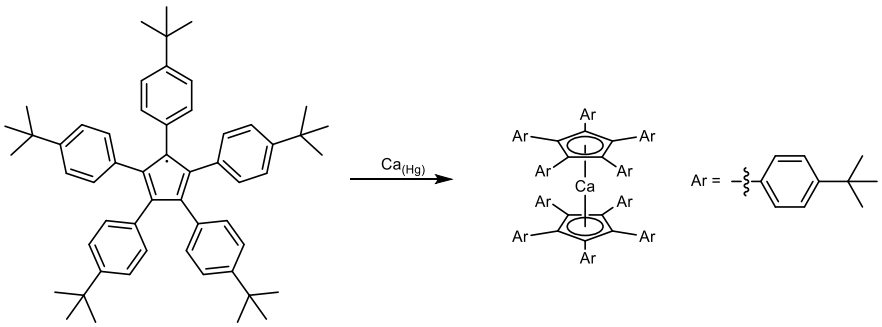

A solution of 0.2 mmol (145 mg) $Cp^{Big\ t\text{-}Bu}$ in 10 mL of THF was added to a solution of 0.6 mmol (24 mg) Ca in 1 mL of mercury, yielding a deep blue/metallic biphasic solution that was stirred for 12 h at ambient temperature. The resulting yellow solution was decanted from the metallic phase and all volatiles were removed under reduced pressure, yielding the product as a colorless solid. The product was re-crystallized from benzene at ambient temperature.

Yield: 118 mg (0.079 mmol, 79%) Mp. >400 °C. Anal. calcd. for $C_{110}H_{130}Ca$: C, 88.53; H, 8.78%. Found: C, 88.01; H, 9.05%. ^{1}H NMR (300 MHz, C_6D_6, 25 °C): δ 7.08 (d, $^3J_{HH}$ = 8.4 Hz, 10 H, C_{ortho}), 6.96 (d, $^3J_{HH}$ = 8.4 Hz, 10 H, C_{meta}), 1.30 (s, 45 H, CH_3). ^{13}C NMR (75.5 MHz, C_6D_6, 25 °C): δ 148.33 (C_{para}), 133.77 (C_{ipso}), 131.98 (C_{ortho}), 125.08 (C_{meta}), 124.13 (C_{Cp}), 34.54 ($C(CH_3)_3$), 31.69 (CH_3). IR: ν = 2959, 2903, 2867, 1513, 1475, 1461, 1392, 1368, 1016, 850, 833, 776, 692, 570 cm^{-1}.

6.1.43 Synthesis of $Cp^{Big\ t\text{-}Bu}{}_2Sr$ 38

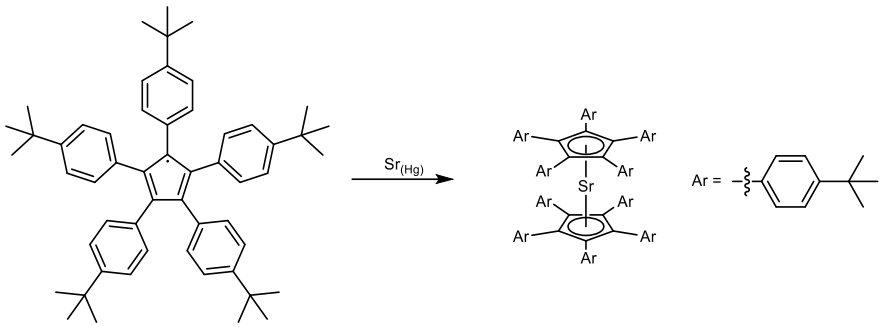

A solution of 0.2 mmol (145 mg) $Cp^{Big\ t\text{-}Bu}$ in 10 mL of THF was added to a solution of 0.6 mmol (53 mg) Sr in 1 mL of mercury, yielding a deep blue/metallic biphasic solution that was stirred for 12 h at ambient temperature. The resulting yellow solution was decanted from the metallic phase and all volatiles were removed under reduced pressure, yielding the product as a colorless solid. The product was re-crystallized from benzene at ambient temperature.

Yield: 114 mg (0.074 mmol, 74%) Mp. >400 °C. Anal. calcd. for $C_{110}H_{130}Sr$: C, 88.80; H, 8.51%. Found: C, 88.75; H, 8.23%. ^{1}H NMR (300 MHz, C_6D_6, 25 °C): δ 6.97 (m, 20 H, C_{ortho}, C_{meta}), 1.29 (s, 45 H, CH_3). ^{13}C NMR (75.5 MHz, C_6D_6, 25 °C): δ 148.09 (C_{para}), 134.48 (C_{ipso}), 131.36 (C_{ortho}), 125.41 (C_{meta}), 123.60 (C_{Cp}), 34.54 ($C(CH_3)_3$), 31.72 (CH_3). IR: ν = 2961, 2903, 2866, 1514, 1475, 1460, 1360, 1270, 1198, 1154, 1120, 1100, 1013, 853, 837, 829,803, 777, 694, 572, 559 cm^{-1}.

6.1.44 Synthesis of $Cp^{Big\ t\text{-}Bu}{}_2Ba$ 39

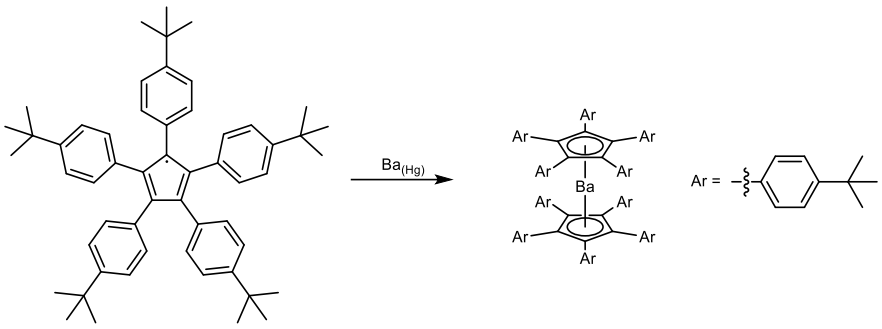

A solution of 0.2 mmol (145 mg) $Cp^{Big\ t\text{-}Bu}$ in 10 mL of THF was added to a solution of 0.6 mmol (82 mg) Ba in 1 mL of mercury, yielding a deep blue/metallic biphasic solution that was stirred for 12 h at ambient temperature. The resulting yellow solution was decanted from the metallic phase and all volatiles were removed under reduced pressure, yielding the product as a colorless solid. The product was re-crystallized from benzene at ambient temperature.

Yield: 136 mg (0.085 mmol, 85%) Mp. >400 °C. Anal. calcd. for $C_{110}H_{130}Ba$: C, 83.12; H, 8.24%. Found: C, 84.12; H, 8.35%. ^{1}H NMR (300 MHz, C_6D_6, 25 °C): δ 6.98 (d, $^3J_{HH}$ = 8.4 Hz, 10 H, C_{meta}), 6.88 (d, $^3J_{HH}$ = 8.4 Hz, 10 H, C_{ortho}), 1.29 (s, 45 H, CH_3). ^{13}C NMR (75.5 MHz, C_6D_6, 25 °C): δ 147.94 (C_{para}), 134.99 (C_{ipso}), 130.68 (C_{ortho}), 125.65 (C_{meta}), 124.40 (C_{Cp}), 34.54 ($C(CH_3)_3$), 31.74 (CH_3). IR: ν = 2961, 2905, 2866, 1516, 1475, 1461, 1393, 1362, 1270, 1199, 1154, 1100, 1120, 1013, 852, 836, 776, 692, 635, 572, 557, 473 cm^{-1}.

6.1.45 Synthesis of $Cp^{Big\ t\text{-}Bu}$ Ga 40

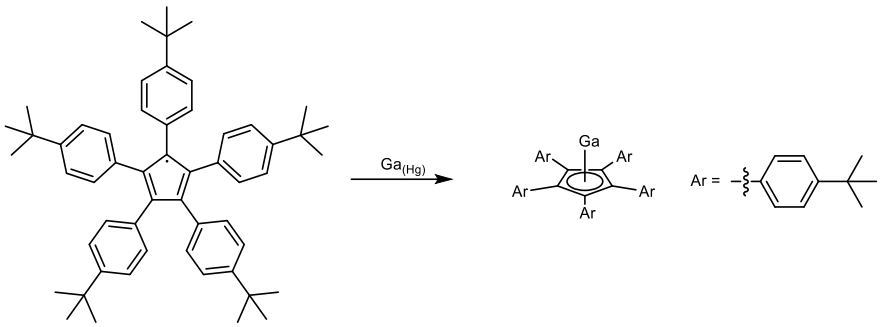

A solution of 0.2 mmol (145 mg) $Cp^{Big\ t\text{-}Bu}$ in 10 mL of THF was added to a solution of 0.6 mmol (42 mg) Ga in 1 mL of mercury, yielding a deep blue/metallic biphasic solution that was stirred for 12 h at ambient temperature. The resulting yellow solution was decanted from the metallic phase and all volatiles were removed under reduced pressure, yielding the product as a colorless solid.

Yield: 144 mg (0.181 mmol, 90%). Mp. >400 °C. Anal. calcd. for $C_{55}H_{65}Ga$: C, 83.01; H, 8.23%. Found: C, 81.97; H, 8.11%. ^{1}H NMR (300 MHz, THF-d_8, 25 °C): δ 6.98 (d, $^{3}J_{HH}$ = 8.3 Hz, 10 H, C_{meta}), 6.81 (d, $^{3}J_{HH}$ = 8.3 Hz, 10 H, C_{ortho}), 1.22 (s, 45 H, CH_3). ^{13}C NMR (75.5 MHz, THF-d_8, 25 °C): δ 149.23 (C_{para}), 132.96 (C_{ipso}), 132.41 (C_{ortho}), 124.70 (C_{meta}), 123.70 (C_{Cp}), 34.94 ($C(CH_3)_3$), 31.71 (CH_3). IR: ν = 2958, 2905, 2869, 1516, 1465, 1362, 1270, 1152, 1120, 1014, 833, 776, 691, 570, 474 cm^{-1}.

6.1.46 Synthesis of $Cp^{Big\ t\text{-}Bu}In$ 41

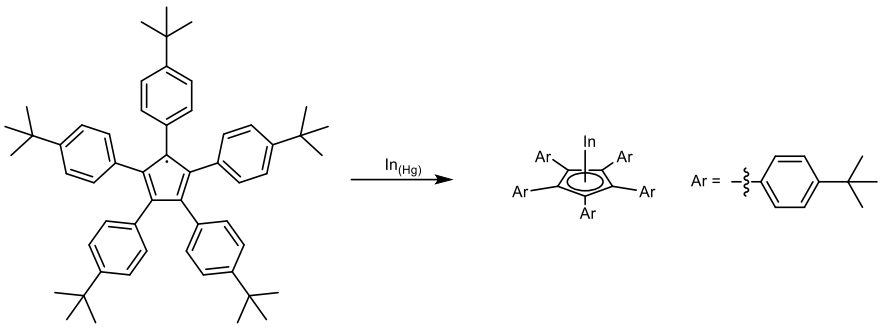

A solution of 0.2 mmol (145 mg) $Cp^{Big\ t\text{-}Bu}$· in 10 mL of THF was added to a solution of 0.6 mmol (69 mg) In in 1 mL of mercury, yielding a deep blue/metallic biphasic solution that was stirred for 12 h at ambient temperature. The resulting yellow solution was decanted from the metallic phase and all volatiles were removed under reduced pressure, yielding the product as a colorless solid. The product was re-crystallized from THF at –30 °C.

Yield: 90 mg (0.108 mmol, 54%). Mp. >400 °C. Anal. calcd. for $C_{55}H_{65}In$: C, 78.56; H, 7.79%. Found: C, 77.50; H, 7.69%. ^{1}H NMR (300 MHz, THF-d_8, 25 °C): δ 6.97 (d, $^3J_{HH}$ = 8.4 Hz, 10 H, C_{meta}), 6.84 (d, $^3J_{HH}$ = 8.4 Hz, 10 H, C_{ortho}), 1.22 (s, 45 H, CH_3). ^{13}C NMR (75.5 MHz, THF-d_8, 25 °C): δ 148.24 (C_{para}), 134.69 (C_{ipso}), 132.62 (C_{ortho}), 124.50 (C_{meta}), 123.86 (C_{Cp}), 34.87 ($C(CH_3)_3$), 31.74 (CH_3). IR: ν = 2959, 2903, 2866, 1516, 1475, 1461, 1392, 1360, 1270, 1198, 1152, 1120, 1100, 1013, 850, 833, 774, 690, 572, 554, 471, 445, 382 cm^{-1}.

6.1.47 Synthesis of $Cp^{Big\ t\text{-}Bu}Tl$ 42

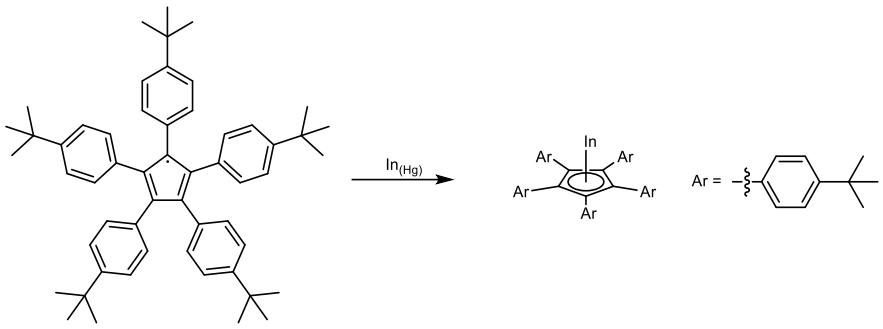

A solution of 0.2 mmol (145 mg) $Cp^{Big\ t\text{-}Bu}$· in 10 mL of THF was added to a solution of 0.6 mmol (123 mg) Tl in 1 mL of mercury, yielding a deep blue/metallic biphasic solution that was stirred for 12 h at ambient temperature. The resulting yellow suspension was decanted from the metallic phase and all volatiles were removed under reduced pressure, yielding the product as a yellow solid.

Yield: 178 mg (0.192 mmol, 96%). Mp. 122 °C (dec.). Anal. calcd. for $C_{55}H_{65}Tl$: C, 70.99; H, 7.04%. Found: C, 70.63; H, 7.24%. ^1H NMR (300 MHz, THF-d_8, 25 °C): δ 6.91 (br s, 45 H), 6.82 (br s, 45 H), 1.22 (br s, 45 H). IR: ν = 2959, 2903, 2866, 1516, 1475, 1461, 1392, 1360, 1270, 1198, 1152, 1120, 1100, 1013, 850, 832, 774, 690, 636, 570, 554, 472, 444 cm^{-1}.

Alternative synthesis: Solutions of 0.2 mmol (145 mg) $Cp^{Big\ t\text{-}Bu}H$ and 0.2 mmol (50 mg, 14.2 µL) TlOEt in 2 mL of *n*-hexane were combined, instantaneously yielding a yellow powder that was isolated by filtration, washed with 2 mL of *n*-hexane and dried *in vacuo*.

Yield: 182 mg (0.196 mmol, 98%)

6.1.49 Synthesis of $Cp^{Big\ t\text{-}Bu}{}_2Hg$ 43

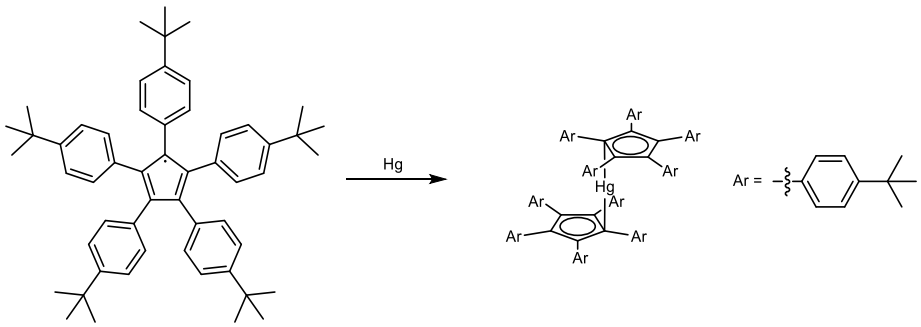

0.2 mmol (145 mg) $Cp^{Big\ t\text{-}Bu}$· and 6.8 mmol (0.1 ml, 1.355 g) mercury were suspended in 10 mL of toluene and stirred for 12 h at ambient temperature. The resulting greenish blue solution was decanted from the metallic phase and the filtrate concentrated until incipient crystallization. The crystals were dissolved by slight warming, and yellow crystals formed upon storage at ambient temperature within 12 h, which were isolated by decantation and dried *in vacuo*. **43** always contains a small amount of **32** adhering to the surface of the crystals, which cannot be completely removed because **43** partly decomposes to **32** upon contact to solvents.

Yield: 99 mg (0.060 mmol, 60%). ^{1}H NMR (300 MHz, C_6D_6, 25 °C): δ 7.32 (d, $^{3}J_{HH}$ = 8.1 Hz, 10 H, C_{ortho}), 7.04 (d, $^{3}J_{HH}$ = 8.1 Hz, 10 H, C_{meta}), 1.12 (s, 45 H, CH_3). ^{13}C NMR (75.5 MHz, C_6D_6, 25 °C): δ 148.82 (C_{para}), 133.80 (C_{ipso}), 131.67 (C_{Cp}), 131.53 (C_{ortho}), 125.22 (C_{meta}), 34.41 ($C(CH_3)_3$), 31.40 (CH_3). IR: ν = 2959, 2903, 2866, 1513, 1475, 1461, 1393, 1360, 1271, 1201, 1149, 1122, 1100, 1014, 852, 836, 776, 694, 572, 494, 407 cm^{-1}. The melting point and elemental composition of the product were not determined due to its assumed toxicity. In addition, **43** was always obtained together with small amounts of **32** as stated before.

6.1.50 Synthesis of $Cp^{Big\ t\text{-}Bu}GaCr(CO)_5$ 44

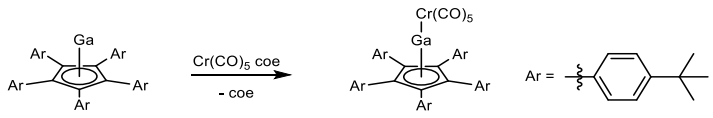

0.025 mmol (20 mg) $Cp^{Big\ t\text{-}Bu}Ga$ and 0.025 mmol (8 mg) $Cr(CO)_5$·cyclooctadiene were dissolved in benzene (0.5 mL) and stirred for 1 h at ambient temperature. Upon concentration of the resulting solution *in vacuo*, the product crystallized in form of large yellow blocks, which were isolated by decantation and dried *in vacuo*.

Yield: 17 mg (0.017 mmol, 70%). Mp. 250 °C (dec.). Anal. calcd. for $C_{60}H_{65}CrGaO_5$: C, 72.95; H, 6.63%. Found: C, 72.24; H, 6.36%. ^{1}H NMR (300 MHz, C_6D_6, 25 °C): δ 7.25 (d, $^3J_{HH}$ = 8.5 Hz, 10 H, C_{ortho}), 7.03 (d, $^3J_{HH}$ = 8.5 Hz, 10 H, C_{meta}), 1.05 (s, 45 H, CH_3). ^{13}C NMR (75.5 MHz, C_6D_6, 25 °C): δ 223.39 (CO_{axial}), 218.23 ($CO_{equatorial}$), 150.74 (C_{para}), 131.65 (C_{ortho}), 129.48 (C_{ipso}), 125.64 (C_{meta}), 123.86 (C_{Cp}), 34.51 ($C(CH_3)_3$), 31.20 (CH_3). IR: ν = 2964, 2096, 2870, 2056, 1982, 1946, 1928, 19091518, 1462, 1401, 1393, 1363, 1260, 1146, 1089, 1016, 865, 852, 835, 796, 702, 690, 671, 654, 646, 572, 494, 465, 391 cm^{-1}.

6.1.51 Synthesis of Bis(pentafluorophenyl)ethyne 45

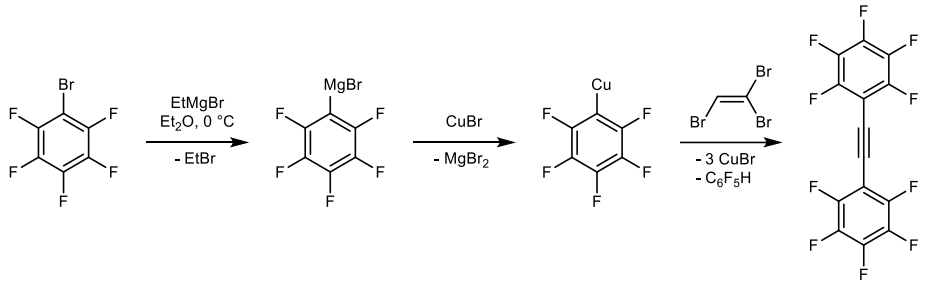

Caution!: Pentafluorophenyl copper and the complex of pentafluorophenylmagnesium bromide with diethyl ether have not, to the best of my knowledge, been reported to be explosive. However, a variation of the preparation described here, in which the complex of pentafluorophenylmagnesium bromide with diglyme was dried *in vacuo*, resulted in a vigorous decomposition under build-up of pressure which destroyed the apparatus. This happened only once although the preparation was carried out several times. Caution should be exercised because the exact cause of the decomposition is unknown. The following procedure avoids isolation of this complex.

400 mmol (9.72 g) of magnesium turnings were suspended in diethyl ether (133 mL). At 0 °C 400 mmol (43.59 g, 29.9 mL) bromoethane was slowly added to this suspension. The resulting mixture was warmed to room temperature and stirred overnight. The light gray solution was cooled to 0 °C and 400 mmol (98.78 g, 50.65 mL) of bromopentafluorobenzene, 500 mmol (67.1 g, 71.4 mL) of diglyme (diethylene glycol dimethyl ether), and 400 mmol (57 g) of CuBr were slowly added in sequence. The resulting white semi-solid mass was dried *in vacuo* for 1 h and then re-suspended in 400 mL diglyme. 100 mmol (9.76 mL, 26.47 g) of tribromoethylene were added slowly at 0 °C. The suspension slowly turned brown upon stirring at 120 °C for 24 h. It was then diluted on air with 500 mL ethyl acetate, 100 mL saturated $NH_4Cl_{(aq)}$ solution, 40 mL acetic acid, and 200 mL H_2O. The aqueous phase was discarded, and the organic phase was washed five times with H_2O. It was then dried with $MgSO_4$, concentrated on a rotary evaporator, and stripped of any remaining volatiles at 10^{-3} mbar. A by-product (probably decafluorobiphenyl) was

removed by sublimation at 60 °C/10^{-3} mbar. The remaining crude product was crystallized from methanol at –30 °C.

Yield: 14.4 g (40.1 mmol, 40%). ^{19}F NMR (376 MHz, C_6D_6) δ -135.61 – -135.75 (m, 4F, *ortho*), -150.34 (t, 2F, $^3J_{FF}$ = 22.0 Hz, *para*), -161.29 – -161.47 (m, 4F, *meta*), ppm. Other analytical data match those reported in the literature.[162]

Comments: The protocol was adapted from a literature procedure.[146] In contrast to Webb and Gilman, we found a higher reaction temperature and the use of diglyme instead of THF more convenient due to the shorter reaction time. The aqueous workup prevents the formation of finely divided Cu_2O, which is otherwise difficult to remove by filtration.

6.1.52 Synthesis of Tetrakis(pentafluorophenyl)cyclopentadienone 46

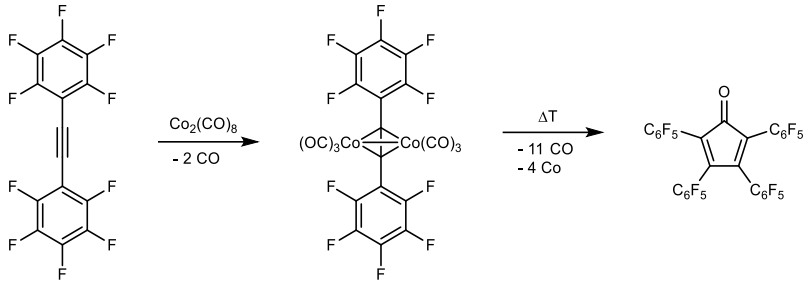

40.1 mmol (14.4 g) of bis(pentafluorophenyl)ethyne and 42.1 mmol (14.4 g) of $Co_2(CO)_8$ were suspended in decaline (100 mL) and stirred until gas evolution has stopped (4 h). The solution was then stirred at 190 °C for 24 hours. A metal mirror was formed. The flask was cooled to room temperature, the solution was diluted with 100 mL of ethyl acetate and 86.3 mmol (21.9 g) of I_2 was added. The suspension was stirred until dissolution of the metal mirror and complete cessation of gas evolution (15 min). The solution was diluted with ethyl acetate (500 mL) and washed with aqueous $NaHSO_3$ solution (200 mL, 30%). The aqueous phase was discarded. The organic phase was dried with $MgSO_4$ and filtered over about 50 mL of active Al_2O_3. All volatiles were removed first on a rotary evaporator and then by distillation at up to 160 °C/10^{-3} mbar. The product was then washed with 100 mL of *n*-hexane at −78 °C and recrystallized from $CHCl_3$ at −30 °C.

Yield: 12.0 g (16.1 mmol, 80%). ^{19}F NMR (376 MHz, C_6D_6) δ -137.57 – -137.82 (m, 8F, *ortho*), -145.76 (t, 2F, $^3J_{FF}$ = 21.6 Hz, *para*), 147.97 (t, 2F, $^3J_{FF}$ = 21.6 Hz, *para*), -157.96 – -158.17 (m, 4F, *meta*), -159.25 – -159.44 (m, 4F, *meta*) ppm. Other analytical data match those reported in the literature.[5]

Comments: Variations of this procedure omitting the oxidation step have been known for a long time,[6] but in my hands, the main product of these reactions was a cobalt-containing complex of unknown structure. Oxidation of this complex with iodine yields the desired product.

6.1.53 Synthesis of Pentakis(pentafluorophenyl)cyclopentadienol 47

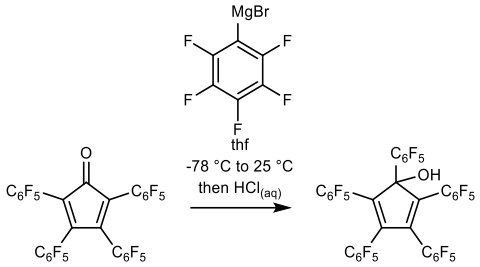

19.3 mmol (4.77 g, 2.41 mL) of bromopentafluorobenzene were slowly added at 0 °C to a solution of 19.3 mmol (6.44 mL) EtMgBr in diethyl ether (3 mol/L). All volatiles were removed *in vacuo* and the resulting colorless solid was redissolved in THF (10 mL). This solution was slowly added at −78 °C to a suspension of tetrakis(pentafluorophenyl)cyclopentadienone (16.1 mmol, 12.0 g) in THF (100 mL). The resulting mixture was gradually warmed to 25 °C within 4 h. Then 3 mL HCl_{aq} (37%), 100 mL diethyl ether and 100 mL of water were added. The aqueous phase was discarded and the organic phase was washed with 100 mL of water. The solution was dried with $MgSO_4$ and all volatiles were removed under reduced pressure using a rotary evaporator. The product was purified by column chromatography (*n*-hexane/diethyl ether 20:1; R_f = 0.30; colorless band with a blue fluorescence).

Yield: 10.3 g (11.3 mmol, 58%). Mp. 216 °C. ^{19}F NMR (565 MHz, CD_2Cl_2) δ -134.96 (br s, 1F, $HOCC_6F_5$, *ortho*), -137.97 (br s, not integratable, $HOCCCC_6F_5$, *ortho*) -138.92 (m, 2F, $HOCCC_6F_5$, *ortho*), -139.53 (d, 2F, $^3J_{FF}$ = 21.7 Hz, $HOCCC_6F_5$, *ortho*), -144.02 (d, 2F, $^3J_{FF}$ = 21.3 Hz, $HOCC_6F_5$, *ortho*), -150.01(t, 2F, $^3J_{FF}$ = 20.8 Hz, $HOCCC_6F_5$ or $HOCCCC_6F_5$, *para*), -150.10 (t, 2F, $^3J_{FF}$ = 21.0 Hz, $HOCCC_6F_5$ or $HOCCCC_6F_5$, *para*), -152.60 (t, 1F, $^3J_{FF}$ = 21.2 Hz, $HOCC_6F_5$, *para*), -159.73 (td, 2F, $^3J_{FF}$ = 21.7 Hz, 7.7 Hz, $HOCCC_6F_5$, *meta*), -159.85 (td, 2F, $^3J_{FF}$ = 21.8 Hz, 7.7 Hz, $HOCCC_6F_5$, *meta*), -160.08 (td, 2F, $^3J_{FF}$ = 21.7 Hz, 7.7 Hz, $HOCCCC_6F_5$, *meta*), -160.45 (br t, 2F, $^3J_{FF}$ = 21.4 Hz, $HOCC_6F_5$, *meta*), -162.30 (br t, 2F, $^3J_{FF}$ = 20.9 Hz, $HOCC_6F_5$, *meta*). ^{1}H NMR (400 MHz, C_6D_6) δ 3.40 (s, CpOH). ^{13}C{^{19}F} NMR (151 MHz, CD_2Cl_2) δ 148.04 ($HOCC_6F_5$, *ortho*), 145.24 ($HOCCCC_6F_5$, *ortho*), 144.86 ($HOCC_6F_5$, *ortho*), 144.48 ($HOCCC_6F_5$, *ortho*), 144.35 ($HOCCC_6F_5$, *ortho*), 142.72 ($HOCCC_6F_5$ or $HOCCCC_6F_5$, *para*), 142.65

($HOCCC_6F_5$ or $HOCCCC_6F_5$, *para*), 141.84, 141.83, 141.76 ($HOCC_6F_5$, *para*), 138.77 ($HOCC_6F_5$, *meta*), 138.26 ($HOCCCC_6F_5$, *meta*), 138.20 ($HOCCC_6F_5$, *meta*), 138.09 ($HOCC_6F_5$, *meta*), 137.86 ($HOCC_6F_5$, *meta*), 135.85 (HOCCC), 109.43 (HOCC), 106.76 ($HOCC_6F_5$ or $HOCCC_6F_5$, *ipso*), 106.36 ($HOCC_6F_5$ or $HOCCC_6F_5$, *ipso*), 90.36 (HOC). IR ν = 3601, 1646, 1514, 1484, 1341, 1305, 1118, 1088, 982, 912, 803, 731 cm^{-1}.

6.1.54 Synthesis of Pentakis(pentafluorophenyl)cyclopentadienyl hexadecafluorotriantimonate 48

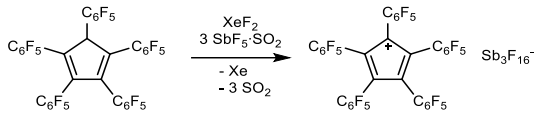

10 µmol (8.6 mg) of the pentakis(pentafluorophenyl)cyclopentadienyl radical and 40 µmol (11.2 mg) of $SbF_5{\cdot}SO_2$ were suspended in 0.5 mL of hexafluorobenzene. 200 µmol (33.9 mg) of XeF_2 were added and the mixture was stirred for 30 min at 25 °C, resulting in the formation of a colorless gas, a deep blue solution, and a blue precipitate. The solution was decanted from the solid by using a glass syringe, sealed in a glass ampoule, and stored at 6 °C for three days.

The first run of this reaction gave the solvate $Cp(C_6F_5)_5Sb_3F_{16}{\cdot}2\ C_6F_5$, all subsequent runs gave $Cp(C_6F_5)_5Sb_3F_{16}{\cdot}1.5\ C_6F_5$. The yield varied from 8.6 mg to 15.1 mg (47–81%) for solvate $Cp(C_6F_5)_5Sb_3F_{16}{\cdot}2\ C_6F_5$ and was not determined for $Cp(C_6F_5)_5Sb_3F_{16}{\cdot}1.5\ C_6F_5$.

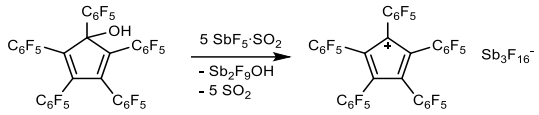

Alternative preparation: 10 µmol (9.1 mg) pentakis(pentafluorophenyl)cyclopentadienol and 40 µmol (11.2 mg) $SbF_5{\cdot}SO_2$ were suspended in 0.5 mL hexafluorobenzene and stirred for 30 min at 25 °C, resulting in the formation of a deep blue solution and a blue precipitate. The solution was decanted from the solid using a glass syringe, and further treated as above, yielding crystals with identical cell parameters and color.

In situ NMR spectroscopy: 10 µmol (9.1 mg) Pentakis(pentafluorophenyl)cyclopentadienol were dissolved in 0.5 mL of SO_2 at −78 °C in a PTFE-capped NMR tube, which also contained a capillary with acetone-d_6 and the first NMR spectrum was measured at −30 °C. The solution was again cooled to −78 °C, 50 µmol (14.0 mg) $SbF_5{\cdot}SO_2$ were sublimed into the NMR tube, and the second NMR spectrum was measured at −30 °C.

Comments: The use of a glass syringe is necessary, because Pentakis(pentafluorophenyl)cyclopentadienyl hexadecafluorotriantimonate reacts

immediately with polypropylene syringes. An excess of XeF_2 is also necessary because $SbF_5 \cdot SO_2$ catalyzes the reaction of XeF_2 with hexafluorobenzene. For the second preparation the formation of hydroxide-containing counteranions $Sb_3(OH)_nF_{(16-n)}$ cannot be completely excluded. Crystals for sc-XRD were therefore obtained from the first reaction.

UV/Vis (hexafluorobenzene): λ_{max} (log ε) = 678 nm (4.68).

Caution!: When XeF_2 and $SbF_5 \cdot SO_2$ are premixed and the solvent is added subsequently, a vigorous reaction with flame formation may occur even in the absence of air.

6.1.55 Synthesis of the Pentakis(pentafluorophenyl)cyclopentadienyl Radical 49

1 mmol (912 mg) pentakis(pentafluorophenyl)cyclopentadienol and 20 mmol (5.33 g) $AlBr_3$ were suspended in 3 mL of benzene and 10 mmol (1.09 g, 746 µL) of bromoethane were slowly added at 0 °C. The red suspension was warmed to 25 °C, stirred for 30 min, and subsequently cooled to 0 °C. The suspension was filtered, and the filtrate was discarded. The solid was quenched with 200 mmol (3.6 g) ice and the mixture was kept at 25 °C until completely thawed. The solution was then removed by filtration and the solid was washed rapidly three times with 10 mL of water at 0 °C. All volatiles were removed under reduced pressure and the solid was sublimed at 150 °C/10^{-3} mbar over 2 days. The sublimate was crystallized three times from 1 mL of toluene and again all volatiles were removed *in vacuo*.

Yield: 484 mg (541 µmol, 54%). Mp. 236 °C, evaporates undecomposed at approx. 300 °C. IR ν = 1647, 1517, 1487, 1383, 1344, 1312, 1138, 1104, 1079, 983, 919, 911, 836, 730, 654, 542 cm^{-1}. UV/Vis (hexafluorobenzene): λ_{max} (log ε) = 546 nm (3.41).
Comments: The washing steps can be performed in a Büchner funnel without the need for an inert gas atmosphere, since crystalline **49** is stable under these conditions. The mother liquors and the liquid portion of the reaction mixture contain mainly pentakis(pentafluorophenyl)cyclopentadiene and can be used for the preparation of pyridinium pentakis(pentafluorophenyl)cyclopentadienide **50d**.

6.1.56 Synthesis of Ferrocenium Pentakis(pentafluorophenyl)cyclopentadienide 50a

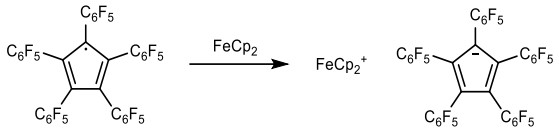

5 µmol (4.5 mg) pentakis(pentafluorophenyl)cyclopentadienyl radical and 6 µmol (1.1 mg) ferrocene were dissolved in 0.3 mL 1,2-difluorobenzene. The product was crystallized by vapor phase diffusion with 3 mL *n*-hexane.

Yield: 3.5 mg (3.2 µmol, 65%). Mp. 232 °C. ^{19}F NMR (565 MHz, THF-d_8) δ -142.96 (dd, 10F, $^{3}J_{FF}$ = 25.2 Hz, $^{4}J_{FF}$ = 8.3 Hz, *ortho*), -163.13 (t, 5F, $^{3}J_{FF}$ = 21.5 Hz, *para*), -166.38 – -166.51 (m, 10F, *meta*). ^{13}C NMR (151 MHz, CD_2Cl_2) δ 145.1 (d, $^{1}J_{FC}$ = 243 Hz, *meta*), 139.2 (d, $^{1}J_{FC}$ = 243 Hz, *para*), 138.3zz (dt, $^{1}J_{FC}$ = 246 Hz, *ortho*, $^{2}J_{FC}$ = 14.5 Hz), 116.7 (t, $^{2}J_{FC}$ = 19.3 Hz, *ipso*), 108.5 ($C_5(C_6F_5)_5$). IR ν = 3111, 3075, 1514, 1471, 1418, 1282, 1267, 1098, 976, 915, 849, 759, 540 cm^{-1}.

6.1.57 Synthesis of Tritylium Pentakis(pentafluorophenyl)cyclopentadienide 50b

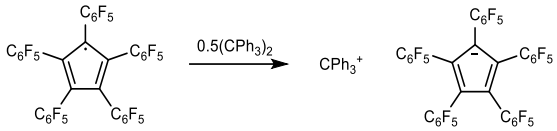

5 µmol (4.5 mg) of pentakis(pentafluorophenyl)cyclopentadienyl radical and 3 µmol (1.7 mg) of trityl$_2$·toluene were heated to 110 °C in 0.5 mL of toluene until all solids were dissolved (about 10 min). The solution was then slowly cooled to 25 °C and left undisturbed for 24 h, resulting in the formation of large yellow-green needles.

Yield: 4.9 mg (4.4 µmol, 87%). Mp. 227 °C. ^{19}F NMR (565 MHz, CD_2Cl_2) δ -142.71 (dd, 10F, $^3J_{FF}$ = 25.6 Hz, $^4J_{FF}$ = 7.4 Hz, *ortho*), -161.53 (t, 5F, $^3J_{FF}$ = 21.5 Hz, *para*), -164.97 – -165.16 (m, 10F, *meta*). ^{1}H NMR (400 MHz, CD_2Cl_2) δ 7.91 (br s). The signals in the ^{13}C NMR spectrum were too broad to be well resolved. IR ν = 2945, 1574, 1516, 1479, 1350, 1290, 1181, 1099, 982, 916, 839, 764, 701, cm^{-1}.

6.1.58 Synthesis of Decamethylaluminocenium Pentakis(pentafluorophenyl)-cyclopentadienide 50c

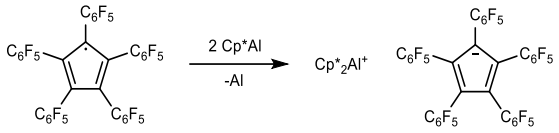

5 µmol (4.5 mg) of pentakis(pentafluorophenyl)cyclopentadienyl radical and 10 µmol (1.6 mg) of Cp*Al were heated to 110 °C in 0.5 mL of toluene until all reagents dissolved (about 10 min). This process was accompanied by the formation of a gray, finely dispersed solid (probably aluminum metal). The solution was then cooled to 25 °C. The grayish solid formed was isolated by centrifugation and extracted with 0.5 mL CH_2Cl_2. The extract was evaporated to dryness at 25 °C/10^{-3} mbar.
The formation of single-crystals was achieved by immersing the product in a small glass tube (5 mm diameter) containing 1 mL of benzene and heating the lower end of the solution to 80 °C, while keeping the upper end at 25 °C.

Yield: 5.3 mg (4.9 µmol, 89%, before crystallization). Mp. 230 °C. ^{19}F NMR (565 MHz, CD_2Cl_2) δ -142.74 (dd, 10F, $^3J_{FF}$ = 25.5 Hz, $^4J_{FF}$ = 7.0 Hz, *ortho*), -161.57 (t, 5F, $^3J_{FF}$ = 21.0 Hz, *para*), -165.04 – -165.17 (m, 10F, *meta*). ^{1}H NMR (600 MHz, CD_2Cl_2) δ 2.16. ^{13}C NMR (151 MHz, CD_2Cl_2) δ 144.4 (d, $^1J_{FC}$ = 241 Hz, *meta*), 138.9 (d, $^1J_{FC}$ = 248 Hz, *para*), 137.8 (dt, $^1J_{FC}$ = 248 Hz, *ortho*, $^2J_{FC}$ = 14.0f Hz), 119.3 (C_5Me_5), 115.5 (t, $^2J_{FC}$ = 19.3 Hz, *ipso*), 107.9 ($C_5(C_6F_5)_5$) 10.4 (C_5Me_5). IR ν = 2952, 2914, 2867, 1514, 1481, 1098, 982, 916, 653, 623, 574, 538 cm^{-1}.
Comments: The unusual shape of the ^{1}H NMR signal has been reported previously.[163]

6.1.59 Synthesis of Pyridinium Pentakis(pentafluorophenyl)cyclopentadienide 50d

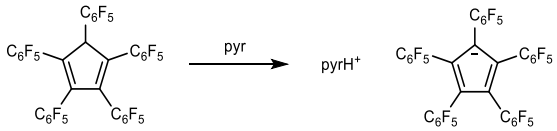

The combined mother liquors of **49**, including the soluble fraction of the reaction mixture, were washed with dilute hydrochloric acid (1 mol/L), dried with $MgSO_4$, and degassed by three freeze-thaw-pump cycles. 1 mmol (79.1 mg; 80.7 µL) of pyridine was added, initiating the formation of a colorless precipitate, which was removed by filtration, washed three times with 3 mL of benzene, and dried under reduced pressure.

Yield 302 mg (314 µmol, 31 %, with respect to reagent **46**). Mp. 218 °C. ^{19}F NMR (565 MHz, THF-d_8) δ -143.02 (dd, 10F, $^3J_{FF}$ = 24.6 Hz, $^4J_{FF}$ = 7.7 Hz, *ortho*), -162.62 (t, 5F, $^3J_{FF}$ = 21.3 Hz, *para*), -166.03 – -166.22 (m, 10F, *meta*). ^{1}H NMR (400 MHz, THF-d_8) δ 8.56 – 8.53 (m, 2H, *ortho*), 7.56 (tt, 1H, $^3J_{HH}$ = 7.6 Hz, $^4J_{HH}$ = 1.l9 Hz, *para*) 7.27 – 7.23 (m, 2H, *meta*). The signals in the ^{13}C NMR spectrum were too broad to be well resolved. IR ν = 1516, 1474, 1099, 978, 915, 750, 691, 620, 538 cm^{-1}.

6.1.60 Synthesis of Pentakis(pentafluorophenyl)cyclopentadienylcarboxylic Acid 52

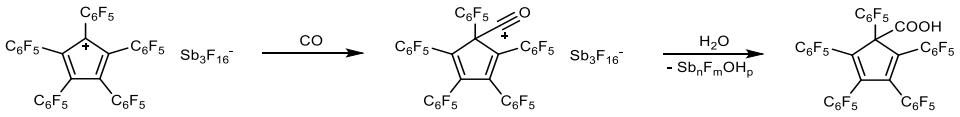

10 µmol (15.6 mg) of **48** was suspended in 0.5 mL of C_6F_6. The solution was degassed and 89 µmol (2 mL; 1.1 bar; 25 °C) of CO was added. The solution was stirred for 24 h, resulting in a color change from deep blue to pale yellow and the formation of brown solids. All volatiles were removed under vacuum. 1 mL of water and 1 mL of benzene were added to the solid residue. The phases were separated, the aqueous phase was discarded, and the organic phase was dried with $MgSO_4$. All volatiles were removed again under vacuum.

The product is a mixture of **52** and **53**, since **52** decomposes slowly to **53** under the conditions of the work-up and NMR measurement. Single-crystals of **52** were obtained by vapor phase diffusion of *n*-hexane into a concentrated solution of **52** in hexafluorobenzene at 6 °C.

Yield: 7 mg. ^{19}F NMR (565 MHz, C_6D_6) δ -132.34 (br s, 1F, *ortho*), -135.05 (br s, 1F, *ortho*), -138.42 (d, 2F, $^3J_{FF}$ = 21.6 Hz, *ortho*), -139.28 – -139.48 (m, not integratable due to overlap and uneven baseline, *ortho*), -145.35 (t, 2F, $^3J_{FF}$ = 21.7 Hz, *para*), -146.33 (d, 2F, $^3J_{FF}$ = 21.7 Hz, *para*), -148.23 (d, 2F, $^3J_{FF}$ = 21.7 Hz, *para*), 158.0 – 158.41 (m, 9F, *meta*) 160.05 (td, 1H, $^3J_{FF}$ = 21.7 Hz, $^4J_{FF}$ = 6.1 Hz, *meta*).

Comment: Because **5** decomposes during column chromatography and on prolonged standing, only the ^{19}F NMR spectrum and sc-XRD data are reported.

6.1.61 Synthesis of Pentakis(pentafluorophenyl)cyclopentadiene 53

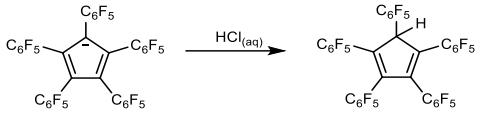

5 µmol of a salt of the pentakis(pentafluorophenyl)cyclopentadienide anion (**50a-d**) are suspended in 1 mL of hydrochloric acid (1 mol/L). The suspension is extracted three times with 1 mL of dichloromethane (DCM). The combined extracts are dried with $MgSO_4$ and all volatiles are removed under reduced pressure (3 h to ensure the removal of ferrocene, Cp*H, and pyridine). The yield is almost quantitative.

If larger amounts of **53** are desired, the following procedure is advantageous: 0.5 mmol (456 mg) pentakis(pentafluorophenyl)cyclopentadienol and 10 mmol (2.67 g) $AlBr_3$ were suspended in 1.5 mL benzene and 5 mmol (0.55 g, 373 µL) bromoethane were slowly added at 0 °C. The red suspension was warmed to 25 °C and stirred for 30 min. The suspension was quenched with 100 mmol (1.8 g) ice and the mixture was kept at 25 °C until completely thawed. 0.5 mmol (93 mg) ferrocene and 1.5 mL hydrochloric acid (1 mol/L) were added and the suspension was stirred for 30 min. It was then diluted with 10 mL DCM and the phases were separated. The aqueous phase was discarded and the organic phase was dried with $MgSO_4$. All volatiles were removed under vacuum. The crude product was dissolved in 5 mL hot toluene and filtered while hot. 0.5 mmol (39.6 mg; 40.6 µL) pyridine was added to the filtrate and the solution was stored at 25 °C for 24 h. The separated solids were isolated by filtration and dissolved in a mixture of 1.5 mL hydrochloric acid (1 mol /L) and 10 mL DCM. The aqueous phase was discarded and the organic phase was dried with $MgSO_4$. All volatiles were removed under vacuum.

Yield: 309 mg (345 mmol, 69%). Mp. 188 °C (dec.). ^{19}F NMR (565 MHz, C_6D_6) δ -139.13 (d, 2F, $^3J_{FF}$ = 21.0 Hz, $HCCC_6F_5$, *ortho*), -140.00 (d, 4F, $^3J_{FF}$ = 21.2 Hz, $HCCCC_6F_5$, *ortho*) -140.62 (d, 2F, $^3J_{FF}$ = 23.0 Hz, $HCCC_6F_5$, *ortho*), -141.18 (d, 1F, $^3J_{FF}$ = 18.2 Hz, HCC_6F_5, *ortho*), -143.18 (d, 2F, $^3J_{FF}$ = 21.6 Hz, HCC_6F_5, *ortho*), -147.69 (t, 2F, $^3J_{FF}$ = 21.7 Hz, $HCCC_6F_5$ or $HCCCC_6F_5$, *para*), -148.14 (t, 2F, $^3J_{FF}$ = 21.3 Hz, $HCCC_6F_5$ or $HCCCC_6F_5$, *para*), -149.62 (t, 1F, $^3J_{FF}$ = 21.5 Hz, HCC_6F_5, *para*), -158.72 – 158.93 (m, 6F, *meta*), -159.18 – 159.42 (m, 3F, *meta*), -159.67 (td, 1F, $^3J_{FF}$ = 21.6 Hz, $^4J_{FF}$ = 8 Hz,

HCC_6F_5, *meta*). ^1H NMR (400 MHz, C_6D_6) δ 5.91 (s, CpH). $^{13}C\{^{19}F\}$ DEPT-135 NMR (151 MHz, C_6D_6) δ 146.41 (d, $^3J_{HC}$ = 7.1 Hz HCC_6F_5, *ortho*), 145.94 (d, $^3J_{HC}$ = 5.7 Hz HCC_6F_5, *ortho*), 144.86 (s, $HCCC_6F_5$, *ortho*), 144.67 (s, $HCCCC_6F_5$, *ortho*), 144.31 (s, $HCCC_6F_5$, *ortho*), 142.47 (s, $HCCC_6F_5$ or $HCCCC_6F_5$, *para*), 142.31 (s, $HCCCC_6F_5$ or $HCCC_6F_5$, *para*), 142.08 (s, HCC_6F_5, *para*), 138.24 (s, $HCCC_6F_5$, *meta*), 138.21 (s, HCC_6F_5, *meta*), 138.18 (s, $HCCCC_6F_5$, *meta*), 138.17 (s, $HCCC_6F_5$, *meta*), 138.04 (s, $HCCCC_6F_5$, *meta*), 137.06 (s, HCC_6F_5, *meta*). $^{13}C\{^1H\}$ NMR (151 MHz, C_6D_6) δ 146 – 136 (several multiplets) 107.84 – 106.83 (m, *ipso*), 53.56 (s, HC). IR ν = 1656, 1522, 1491, 1445, 1315, 1105, 1080, 982, 935, 916, 841, 735, 652, cm^{-1}.

7 References

[1] T. J. Kealy, P. L. Pauson, *Nature* **1951**, *168*, 1039.

[2] S. A. Miller, J. A. Tebboth, J. F. Tremaine, *J. Chem. Soc.* **1952**, 632.

[3] E. Hückel, *Z. Physik* **1931**, *70*, 204.

[4] G. Wilkinson, M. Rosenblum, M. C. Whiting, R. B. Woodward, *J. Am. Chem. Soc.* **1952**, *74*, 2125.

[5] R. B. Woodward, M. Rosenblum, M. C. Whiting, *J. Am. Chem. Soc.* **1952**, *74*, 3458.

[6] R.D. Adams, *J. Organomet. Chem.* **2001**, *637-639*, 1.

[7] P. Jutzi, N. Burford, *Chem. Rev.* **1999**, *99*, 969.

[8] K. D. Glusac, R. N. Saicic, *Nat. Chem.* **2023**, *15*, 439.

[9] E. O. Fischer, R. Jira, *J. Organomet. Chem.* **2001**, *637-639*, 7.

[10] a) W. Kaminsky in *Ullmann's encyclopedia of industrial chemistry* (Hrsg.: F. Ullmann), John Wiley & Sons, [Hoboken, N.J.], **2005-**; b) W. Kaminsky, *Macromol. Chem. Phys.* **1996**, *197*, 3907; c) W. Kaminsky, *Macromolecules* **2012**, *45*, 3289.

[11] a) W. J. Evans, I. Bloom, W. E. Hunter, J. L. Atwood, *J. Am. Chem. Soc.* **1981**, *103*, 6507; b) W. J. Evans, L. A. Hughes, T. P. Hanusa, *J. Am. Chem. Soc.* **1984**, *106*, 4270.

[12] E. O. Fischer, R. Jira, *Z. Naturforsch. B* **1953**, *8*, 327.

[13] a) M. Faraday, *Phil. Trans. R. Soc.* **1825**, *115*, 440; b) R. Kaiser, *Angew. Chem. Int. Ed. Engl.* **1968**, *7*, 345; *Angew. Chem.* **1968**, *80*, 337.

[14] E.F.G. von Besánez, *Lehrbuch der Chemie: für den Unterricht auf Universitäten, technischen Lehranstalten und für das Selbststudium ; in drei Bänden. Lehrbuch der Organischen Chemie*, Vieweg, **1868**.

[15] a) A. Kekulé, *Ann. Chem. Pharm.* **1857**, *104*, 129; b) A. Kekulé, *Ann. Chem. Pharm.* **1858**, *106*, 129; c) G. Schultz, *Ber. Dtsch. Chem. Ges.* **1890**, *23*, 1265.

[16] R. Gleiter, G. Haberhauer, *Aromacity and other conjugation effects*, Wiley-VCH Verlag GmbH & Co. KGaA, Weinheim, **2012**.

[17] T. Arabatzis, *Representing electrons. A biographical approach to theoretical entities*, University of Chicago press, Chicago, London, **2006**.

[18] R. Willstätter, E. Waser, *Ber. Dtsch. Chem. Ges.* **1911**, *44*, 3423.

[19] A. T. Balaban, P. v. R. Schleyer, H. S. Rzepa, *Chem. Rev.* **2005**, *105*, 3436.

[20] a) R. Breslow, J. T. Groves, G. Ryan, *J. Am. Chem. Soc.* **1967**, *89*, 5048; b) R. Breslow, C. Yuan, *J. Am. Chem. Soc.* **1958**, *80*, 5991; c) T. J. Katz, *J. Am. Chem. Soc.* **1960**, *82*, 3784.

[21] R. Breslow, *Chem. Rec.* **2014**, *14*, 1174.

[22] a) M. R. Wasielewski, R. Breslow, *J. Am. Chem. Soc.* **1976**, *98*, 4222; b) R. Breslow, J. Brown, J. J. Gajewski, *J. Am. Chem. Soc.* **1967**, *89*, 4383; c) R. Breslow, M. Douek, *J. Am. Chem. Soc.* **1968**, *90*, 2698.

[23] L. Bosse, B. P. Mant, D. Schleier, M. Gerlach, I. Fischer, A. Krueger, P. Hemberger, G. Worth, *J. Phys. Chem. Lett.* **2021**, *12*, 6901.

[24] G. Maier, *Angew. Chem. Int. Ed. Engl.* **1974**, *13*, 425; *Angew. Chem*. **1974**, *86*, 491.

[25] a) H. Irngartinger, M. Nixdorf, N. H. Riegler, A. Krebs, H. Kimling, J. Pocklington, G. Maier, K.-D. Malsch, K.-A. Schneider, *Chem. Ber.* **1988**, *121*, 673; b) G. Maier, *Angew. Chem. Int. Ed. Engl.* **1988**, *27*, 309; *Angew. Chem*. **1988**, *100*, 317; c) G. Maier, R. Wolf, H.-O. Kalinowski, *Angew. Chem. Int. Ed. Engl.* **1992**, *31*, 738; *Angew. Chem*. **1992**, *104*, 764.

[26] S. R. Kass, *J. Org. Chem.* **2013**, *78*, 7370.

[27] J. I.-C. Wu, Y. Mo, F. A. Evangelista, P. von Ragué Schleyer, *Chem. Commun.* **2012**, *48*, 8437.

[28] R. Breslow, J. M. Hoffman, *J. Am. Chem. Soc.* **1972**, *94*, 2110.

[29] M. Saunders, R. Berger, A. Jaffe, J. M. McBride, J. O'Neill, R. Breslow, J. M. Hoffmann, C. Perchonock, E. Wasserman, et al., *J. Am. Chem. Soc.* **1973**, *95*, 3017.

[30] R. Breslow, R. Hill, E. Wasserman, *J. Am. Chem. Soc.* **1964**, *86*, 5349.

[31] N. C. Baird, *J. Am. Chem. Soc.* **1972**, *94*, 4941.

[32] V. Gogonea, P. v. R. Schleyer, P. R. Schreiner, *Angew. Chem. Int. Ed. Engl.* **1998**, *37*, 1945; *Angew. Chem*. **1998**, *110*, 2045.

[33] W. A. Yager, *J. Am. Chem. Soc.* **1963**, *85*, 2033.

[34] R. Breslow, H. W. Chang, R. Hill, E. Wasserman, *J. Am. Chem. Soc.* **1967**, *89*, 1112.

[35] W. Broser, H. Kurreck, P. Siegle, *Chem. Ber.* **1967**, *100*, 788.

[36] W. Broser, P. Siegle, H. Kurreck, *Chem. Ber.* **1968**, *101*, 69.

[37] R. Gompper, H. Glöckner, *Angew. Chem. Int. Ed. Engl.* **1984**, *23*, 53; *Angew. Chem*. **1984**, *96*, 48.

[38] J. B. Lambert, L. Lin, V. Rassolov, *Angew. Chem. Int. Ed.* **2002**, *41*, 1429; *Angew. Chem*. **2002**, *114*, 1487.

[39] R. Breslow, H. W. Chang, *J. Am. Chem. Soc.* **1961**, *83*, 3727.

[40] S. M. Rupf, P. Pröhm, M. Malischewski, *Chem. Commun.* **2020**, *56*, 9834.

[41] a) M. Otto, D. Scheschkewitz, T. Kato, M. M. Midland, J. B. Lambert, G. Bertrand, *Angew. Chem. Int. Ed. Engl.* **2002**, *41*, 2275; *Angew. Chem*. **2002**, *114*, 2379; b) J. N. Jones, A. H. Cowley, C. L. B. Macdonald, *Chem. Commun.* **2002**, 1520; c) T. Müller, *Angew. Chem. Int. Ed. Engl.* **2002**, *41*, 2276; *Angew. Chem*. **2002**, *114*, 2380; d) J. B. Lambert, *Angew. Chem. Int. Ed. Engl.* **2002**, *41*, 2278; *Angew. Chem*. **2002**, *114*, 2382.

[42] P. Costa, I. Trosien, J. Mieres-Perez, W. Sander, *J. Am. Chem. Soc.* **2017**, *139*, 13024.

[43] Z. Chen, C. S. Wannere, C. Corminboeuf, R. Puchta, P. v. R. Schleyer, *Chem. Rev.* **2005**, *105*, 3842.

[44] P. R. von Schleyer, H. Jiao, *Pure Appl. Chem.* **1996**, *68*, 209.

[45] A. Julg, P. Franois, *Theoret. Chim. Acta* **1967**, *8*, 249.

[46] T. M. Krygowski, M. Cyrański, *Tetrahedron* **1996**, *52*, 1713.

[47] J. A. Pople, K. G. Untch, *J. Am. Chem. Soc.* **1966**, *88*, 4811.

[48] P. v. R. Schleyer, C. Maerker, A. Dransfeld, H. Jiao, N. J. R. van Eikema Hommes, *J. Am. Chem. Soc.* **1996**, *118*, 6317.

[49] H. A. Jahn, E. Teller, *Proc. R. Soc. Lond. A* **1937**, *161*, 220.

[50] V. Gold, *The IUPAC Compendium of Chemical Terminology*, International Union of Pure and Applied Chemistry (IUPAC), Research Triangle Park, NC, **2019**.

[51] a) Bock, Gharagozloo-Hubmann, Sievert, Prisner, Havlas, *Nature* **2000**, *404*, 267; b) H. Bock, C. Arad, C. Näther, Z. Havlas, *J. Chem. Soc., Chem. Commun.*

1995, *0*, 2393; c) H. Bock, Z. Havlas, K. Gharagozloo-Hubmann, M. Sievert, *Angew. Chem. Int. Ed.* **1999**, *38*, 2240; *Angew. Chem*. **1999**, *111*, 2379; d) C. J. Adams, R. C. da Costa, R. Edge, D. H. Evans, M. F. Hood, *J. Org. Chem.* **2010**, *75*, 1168; e) H. Bock, C. Näther, Z. Havlas, A. John, C. Arad, *Angew. Chem. Int. Ed.* **1994**, *33*, 875; *Angew. Chem*. **1994**, *106*, 931; f) H. Bock, M. Sievert, C. L. Bogdan, B. O. Kolbesen, A. Wittershagen, *Organometallics* **1999**, *18*, 2387; g) J. Bordner, R. G. Parker, R. H. Stanford, *Acta Crystallogr B Struct Sci* **1972**, *28*, 1069; h) R. Breslow, J. T. Groves, *J. Am. Chem. Soc.* **1970**, *92*, 984; i) J. J. Brooks, W. Rhine, G. D. Stucky, *J. Am. Chem. Soc.* **1972**, *94*, 7346; j) S. Brydges, J. F. Britten, L. C. F. Chao, H. K. Gupta, M. J. McGlinchey, D. L. Pole, *Chem. Eur. J.* **1998**, *4*, 1201; k) X. Chen, X. Wang, Y. Sui, Y. Li, J. Ma, J. Zuo, X. Wang, *Angew. Chem. Int. Ed.* **2012**, *51*, 11878; *Angew. Chem*. **2012**, *124*, 12048; l) E. G. Cox, D. W. J. Cruickshank, J. A. S. Smith, *Proc. R. Soc. Lond. A* **1958**, *247*, 1; m) D. J. Cram, M. E. Tanner, R. Thomas, *Angew. Chem. Int. Ed. Engl.* **1991**, *30*, 1024; *Angew. Chem*. **1991**, *103*, 1048; n) K. Ebata, W. Setaka, T. Inoue, C. Kabuto, M. Kira, H. Sakurai, *J. Am. Chem. Soc.* **1998**, *120*, 1335; o) S. Z. Goldberg, K. N. Raymond, C. A. Harmon, D. H. Templeton, *J. Am. Chem. Soc.* **1974**, *96*, 1348; p) S. Harder, *Chem. Eur. J.* **1999**, *5*, 1852; q) H. Irngartinger, N. Riegler, K.-D. Malsch, K.-A. Schneider, G. Maier, *Angew. Chem. Int. Ed. Engl.* **1980**, *19*, 211; *Angew. Chem*. **1980**, *92*, 214; r) C. Janiak, R. Weimann, F. Görlitz, *Organometallics* **1997**, *16*, 4933; s) H. S. Kaufman, I. Fankuchen, H. Mark, *J. Chem. Phys.* **1947**, *15*, 414; t) T. Kitagawa, K. Ogawa, K. Komatsu, *J. Am. Chem. Soc.* **2004**, *126*, 9930; u) Kochi, Rathore, Magueres, *J. Org. Chem.* **2000**, *65*, 6826; v) K. Komatsu, T. Nishinaga, S. Aonuma, C. Hirosawa, K.'i. Takeuchi, H. J. Lindner, J. Richter, *Tetrahedron Lett.* **1991**, *32*, 6767; w) C. Kröhnke, V. Enkelmann, G. Wegner, *Angew. Chem. Int. Ed.* **1980**, *19*, 912; *Angew. Chem*. **1980**, *92*, 941; x) B. B. Laird, R. E. Davis, *Acta Crystallogr B Struct Sci* **1982**, *38*, 678; y) P. Le Maguères, S. V. Lindeman, J. K. Kochi, *J. Chem. Soc., Perkin Trans. 2* **2001**, 1180; z) G. Maier, J. Neudert, O. Wolf, *Angew. Chem. Int. Ed.* **2001**, *40*, 1674; *Angew. Chem*. **2001**, *113*, 1719; aa) O. Mallow, M. A. Khanfar, M. Malischewski, P. Finke, M. Hesse, E. Lork, T. Augenstein, F. Breher, J. R.

Harmer, N. V. Vasilieva et al., *Chem. Sci.* **2015**, *6*, 497; ab) A. Matsuura, K. Komatsu, *J. Am. Chem. Soc.* **2001**, *123*, 1768; ac) A. Matsuura, T. Nishinaga, K. Komatsu, *J. Am. Chem. Soc.* **2000**, *122*, 10007; ad) T. S. Navale, M. R. Talipov, R. Shukla, R. Rathore, *J. Phys. Chem. C* **2016**, *120*, 19558; ae) T. Nishinaga, K. Komatsu, N. Sugita, *J. Chem. Soc., Chem. Commun.* **1994**, 2319; af) T. Nishinaga, K. Komatsu, N. Sugita, H. J. Lindner, J. Richter, *J. Am. Chem. Soc.* **1993**, *115*, 11642; ag) J. H. Noordik, P. T. Beurskens, T. E. M. van den Hark, J. M. M. Smits, *Acta Crystallogr B Struct Sci* **1979**, *35*, 621; ah) J. H. Noordik, H. M. L. Degens, J. J. Mooij, *Acta Crystallogr B Struct Sci* **1975**, *31*, 2144; ai) J. H. Noordik, T. E. M. van den Hark, J. J. Mooij, A. A. K. Klaassen, *Acta Crystallogr B Struct Sci* **1974**, *30*, 833; aj) K. Ogawa, K. Komatsu, T. Kitagawa, *J. Org. Chem.* **2011**, *76*, 6095; ak) R. Rathore, A. S. Kumar, S. V. Lindeman, J. K. Kochi, *J. Org. Chem.* **1998**, *63*, 5847; al) R. Rathore, J. K. Kochi, *J. Org. Chem.* **1995**, *60*, 4399; am) W. E. Rhine, J. Davis, G. Stucky, *J. Am. Chem. Soc.* **1975**, *97*, 2079; an) S. V. Rosokha, J. K. Kochi, *J. Am. Chem. Soc.* **2001**, *123*, 8985; ao) A. Sekiguchi, K. Ebata, C. Kabuto, H. Sakurai, *J. Am. Chem. Soc.* **1991**, *113*, 7081; ap) A. Sekiguchi, K. Ebata, C. Kabuto, H. Sakurai, *J. Am. Chem. Soc.* **1991**, *113*, 1464; aq) A. Sekiguchi, T. Matsuo, M. Tanaka, *Organometallics* **2002**, *21*, 1072; ar) H. Sitzmann, H. Bock, R. Boese, T. Dezember, Z. Havlas, W. Kaim, M. Moscherosch, L. Zanathy, *J. Am. Chem. Soc.* **1993**, *115*, 12003; as) D. Sun, S. V. Lindeman, R. Rathore, J. K. Kochi, *J. Chem. Soc., Perkin Trans. 2* **2001**, 1585; at) D. Sun, S. V. Rosokha, J. K. Kochi, *J. Phys. Chem. B* **2007**, *111*, 6655; au) Tamm, Dressel, Frohlich, *J. Org. Chem.* **2000**, *65*, 6795; av) P. J. Wheatley, *J. Chem. Soc.* **1965**, 3136.

[52] M. J. Molski, M. A. Khanfar, H. Shorafa, K. Seppelt, *Eur. J. Org. Chem.* **2013**, *2013*, 3131.

[53] M. J. Molski, D. Mollenhauer, S. Gohr, B. Paulus, M. A. Khanfar, H. Shorafa, S. H. Strauss, K. Seppelt, *Chem. Eur. J.* **2012**, *18*, 6644.

[54] H. Shorafa, D. Mollenhauer, B. Paulus, K. Seppelt, *Angew. Chem. Int. Ed.* **2009**, *48*, 5845; *Angew. Chem.* **2009**, *121*, 5959.

[55] G. N. Lewis, *Valence and the Structure of Atoms and Molecules*, Chemical Catalog Company, Incorporated, **1923**.

[56] a) J. N. Brönsted, *Recl. Trav. Chim. Pays-Bas* **1923**, *42*, 718; b) T. M. Lowry, *J. Chem. Technol. Biotechnol.* **1923**, *42*, 43.

[57] J. Bjerrum, *Naturwissenschaften* **1951**, *38*, 461.

[58] R. P. Bell, *The proton in chemistry,* 2. Aufl., Cornell Univ. Pr, Ithaca, **1973**.

[59] G. A. Olah, G. K. Surya Prakash, r. Molnr, J. Sommer, *Superacid chemistry,* 2. Aufl., Wiley, Hoboken, N.J, **2009**.

[60] L. P. Hammett, A. J. Deyrup, *J. Am. Chem. Soc.* **1932**, *54*, 2721.

[61] P. L. Fabre, J. Devynck, B. Tremillon, *Chem. Rev.* **1982**, *82*, 591.

[62] H. Strehlow, H. Schneider, *Pure Appl. Chem.* **1971**, *25*, 327.

[63] P. Erdmann, J. Leitner, J. Schwarz, L. Greb, *Chemphyschem* **2020**, *21*, 987.

[64] I. Krossing, I. Raabe, *Angew. Chem. Int. Ed.* **2004**, *43*, 2066; *Angew. Chem*. **2004**, *116*, 2116.

[65] E. Martin, D. L. Hughes, S. J. Lancaster, *Inorg. Chim. Acta* **2010**, *363*, 275.

[66] a) I. Krossing, *Chem. Eur. J.* **2001**, *7*, 490; b) T. J. Barbarich, S. T. Handy, S. M. Miller, O. P. Anderson, P. A. Grieco, S. H. Strauss, *Organometallics* **1996**, *15*, 3776.

[67] C. A. Reed, *Acc. Chem. Res.* **1998**, *31*, 133.

[68] I. M. Riddlestone, A. Kraft, J. Schaefer, I. Krossing, *Angew. Chem. Int. Ed.* **2018**, *57*, 13982; *Angew. Chem*. **2018**, *130*, 14178.

[69] I. Krossing, I. Raabe, *Chem. Eur. J.* **2004**, *10*, 5017.

[70] a) B. Fiedler, D. Himmel, I. Krossing, J. Friedrich, *J. Chem. Theory Comput.* **2018**, *14*, 557; b) A. Budanow, M. Bolte, M. Wagner, H.-W. Lerner, *Eur. J. Inorg. Chem.* **2015**, *2015*, 2524.

[71] G. A. Olah, *Angew. Chem. Int. Ed. Engl.* **1995**, *34*, 1393; *Angew. Chem*. **1995**, *107*, 1519.

[72] a) J. F. Norris, *Am. Chem. J.* **1901**, 117; b) F. Kehrmann, F. Wentzel, *Ber. Dtsch. Chem. Ges.* **1901**, *34*, 3815.

[73] a) A. Baeyer, V. Villiger, *Ber. Dtsch. Chem. Ges.* **1902**, *35*, 1189; b) A. Baeyer, V. Villiger, *Ber. Dtsch. Chem. Ges.* **1902**, *35*, 3013.

[74] M. Gomberg, *Ber. Dtsch. Chem. Ges.* **1902**, *35*, 2397.

[75] H. Meerwein, K. van Emster, *Ber. dtsch. Chem. Ges. A/B* **1922**, *55*, 2500.

[76] a) F. Seel, *Z. Anorg. Allg. Chem.* **1943**, *250*, 331; b) H. Meerwein, P. Borner, O. Fuchs, H. J. Sasse, H. Schrodt, J. Spille, *Chem. Ber.* **1956**, *89*, 2060.

[77] D. E. Pearson, *J. Am. Chem. Soc.* **1950**, *72*, 4169.

[78] R. A. Moss, *J. Phys. Org. Chem.* **2014**, *27*, 374.

[79] S. Winstein, D. S. Trifan, *J. Am. Chem. Soc.* **1949**, *71*, 2953.

[80] F. Scholz, D. Himmel, F. W. Heinemann, P. v. R. Schleyer, K. Meyer, I. Krossing, *Science (New York, N.Y.)* **2013**, *341*, 62.

[81] M. Malischewski, K. Seppelt, *Angew. Chem. Int. Ed.* **2017**, *56*, 368; *Angew. Chem*. **2017**, *129*, 374.

[82] a) H. Hogeveen, P. W. Kwant, *Tetrahedron Lett.* **1973**, *14*, 1665; b) H. Hogeveen, P. W. Kwant, *J. Am. Chem. Soc.* **1974**, *96*, 2208; c) H. Hogeveen, P. W. Kwant, J. Postma, P.T. van Duynen, *Tetrahedron Lett.* **1974**, *15*, 4351; d) H. Hogeveen, E. M. G. A. van Kruchten, *J. Org. Chem.* **1981**, *46*, 1350; e) H. Hogeveen, P. W. Kwant, *Acc. Chem. Res.* **1975**, *8*, 413.

[83] C. R. Bailey, C. K. Ingold, H. G. Poole, C. L. Wilson, *J. Chem. Soc.* **1946**, 222.

[84] M. Schorpp, S. Rein, S. Weber, H. Scherer, I. Krossing, *Chem. Commun.* **2018**, *54*, 10036.

[85] a) L. deVries, *J. Org. Chem.* **1960**, *25*, 1838-1838; b) R. Threlkel, J. Bercaw, P. Seidler, J. Stryker, R. Bergman, *Org. Synth.* **1987**, *65*, 42; c) H. Sitzmann, *Z. Naturforsch. B* **1989**, *44*, 1293.

[86] G. Dyker, J. Heiermann, M. Miura, *Adv. Synth. Catal.* **2003**, *345*, 1127.

[87] G. Dyker, J. Heiermann, M. Miura, J.-I. Inoh, S. Pivsa-Art, T. Satoh, M. Nomura, *Chem. Eur. J.* **2000**, *6*, 3426.

[88] M. Miura, S. Pivsa-Art, T. Satoh, M. Nomura, G. Dyker, J. Heiermann, *Chem. Commun.* **1998**, 1889.

[89] R. Zhang, M. Tsutsui, D. E. Bergbreiter, *J. Organomet. Chem.* **1982**, *229*, 109.

[90] G. R. Giesbrecht, J. C. Gordon, D. L. Clark, B. L. Scott, *Dalton Trans.* **2003**, 2658.

[91] S. Harder, C. Ruspic, *J. Organomet. Chem.* **2009**, *694*, 1180.

[92] R. E. Dinnebier, U. Behrens, F. Olbrich, *Organometallics* **1997**, *16*, 3855.

[93] H. Schumann, A. Lentz, *Z. Naturforsch. B* **1994**, *49*, 1717.

[94] C. Janiak, H. Schumann, C. Stader, B. Wrackmeyer, J. J. Zuckerman, *Chem. Ber.* **1988**, *121*, 1745.

[95] G. B. Deacon, C. M. Forsyth, F. Jaroschik, P. C. Junk, D. L. Kay, T. Maschmeyer, A. F. Masters, J. Wang, L. D. Field, *Organometallics* **2008**, *27*, 4772.

[96] R. P. Kelly, T. D. M. Bell, R. P. Cox, D. P. Daniels, G. B. Deacon, F. Jaroschik, P. C. Junk, X. F. Le Goff, G. Lemercier, A. Martinez et al., *Organometallics* **2015**, *34*, 5624.

[97] S. Harder, D. Naglav, P. Schwerdtfeger, I. Nowik, R. H. Herber, *Inorg. Chem.* **2014**, *53*, 2188.

[98] C. Ruspic, J. R. Moss, M. Schürmann, S. Harder, *Angew. Chem. Int. Ed.* **2008**, *47*, 2121; *Angew. Chem*. **2008**, *120*, 2151.

[99] L. Orzechowski, D. F.-J. Piesik, C. Ruspic, S. Harder, *Dalton Trans*. **2008**, 4742.

[100] P. Köpf-Maier, C. Janiak, H. Schumann, *Inorg. Chim. Acta* **1988**, *152*, 75.

[101] P. Köpf-Maier, C. Janiak, H. Schumann, *J. Cancer Res. Clin. Oncol. (Journal of Cancer Research and Clinical Oncology)* **1988**, *114*, 502.

[102] R. D. Shannon, *Acta Cryst. A (Acta Crystallographica Section A)* **1976**, *32*, 751.

[103] L. D. Field, T. W. Hambley, P. A. Humphrey, A. F. Masters, P. Turner, *Inorg. Chem.* **2002**, *41*, 4618.

[104] L. R. Morss, *Chem. Rev.* **1976**, *76*, 827.

[105] a) V. Nair, A. Deepthi, *Chem. Rev.* **2007**, *107*, 1862; b) H. B. Kagan, J. Collin, J. L. Namy, C. Bied, F. Dallemer, A. Lebrun, *J. Alloys Compd.* **1993**, *192*, 191.

[106] W. J. Evans, T. A. Ulibarri, J. W. Ziller, *J. Am. Chem. Soc.* **1988**, *110*, 6877.

[107] N. J. C. van Velzen, S. Harder, *Organometallics* **2018**, *37*, 2263.

[108] W. J. Evans, K. J. Forrestal, J. W. Ziller, *J. Am. Chem. Soc.* **1998**, *120*, 9273.

[109] W. J. Evans, J. M. Perotti, S. A. Kozimor, T. M. Champagne, B. L. Davis, G. W. Nyce, C. H. Fujimoto, R. D. Clark, M. A. Johnston, J. W. Ziller, *Organometallics* **2005**, *24*, 3916.

[110] U. Chakraborty, M. Modl, B. Mühldorf, M. Bodensteiner, S. Demeshko, N. J. C. van Velzen, M. Scheer, S. Harder, R. Wolf, *Inorg. Chem.* **2016**, *55*, 3065.

[111] a) C. Janiak, H. Schumann in *Adv. Organomet. Chem.* (Hrsg.: F. G. A. Stone, R. West), Elsevier textbooks, s.l., **1991**, S. 291–393; b) R. Poli, *Chem. Rev.* **1991**, *91*, 509.

[112] a) M. Wallasch, G. Wolmershäuser, H. Sitzmann, *Angew. Chem. Int. Ed.* **2005**, *44*, 2597; *Angew. Chem*. **2005**, *117*, 2653; b) H. Sitzmann, T. Dezember, W. Kaim, F. Baumann, D. Stalke, J. Kärcher, E. Dormann, H. Winter, C. Wachter, M. Kelemen, *Angew. Chem. Int. Ed. Engl.* **1996**, *35*, 2872; *Angew. Chem*. **1996**, *108*, 3013; c) H. Sitzmann, D. Saurenz, G. Wolmershäuser, A. Klein, R. Boese, *Organometallics* **2001**, *20*, 700; d) M. D. Walter, P. S. White, *New J. Chem.* **2011**, *35*, 1842; e) H. Bauer, D. Weismann, G. Wolmershäuser, Y. Sun, H. Sitzmann, *Eur. J. Inorg. Chem.* **2014**, *2014*, 3072.

[113] H. Mahomed, A. Bollmann, J. Dixon, V. Gokul, L. Griesel, C. Grove, F. Hess, H. Maumela, L. Pepler, *Appl. Cat. A: General* **2003**, *255*, 355.

[114] J. C. Ruble, H. A. Latham, G. C. Fu, *J. Am. Chem. Soc.* **1997**, *119*, 1492.

[115] D. L. Greene, A. Chau, M. Monreal, C. Mendez, I. Cruz, T. Wenj, W. Tikkanen, B. Schick, K. Kantardjieff, *J. Organomet. Chem.* **2003**, *682*, 8.

[116] K. Ziegler, B. Schnell, *Liebigs Ann. Chem.* **1925**, *445*, 266.

[117] S. Heinl, G. Balázs, A. Stauber, M. Scheer, *Angew. Chem. Int. Ed.* **2016**, *55*, 15524; *Angew. Chem*. **2016**, *128*, 15751.

[118] D. C. Reitz, *J. Chem. Phys.* **1961**, *34*, 701.

[119] S. Heinl, S. Reisinger, C. Schwarzmaier, M. Bodensteiner, M. Scheer, *Angew. Chem. Int. Ed.* **2014**, *53*, 7639; *Angew. Chem*. **2014**, *126*, 7769.

[120] H. Sitzmann, R. Boese, *Angew. Chem. Int. Ed. Engl.* **1991**, *30*, 971; *Angew. Chem*. **1991**, *103*, 1027.

[121] H. Sitzmann, H. Bock, R. Boese, T. Dezember, Z. Havlas, W. Kaim, M. Moscherosch, L. Zanathy, *J. Am. Chem. Soc.* **1993**, *115*, 12003.

[122] H. Sitzmann, T. Dezember, O. Schmitt, F. Weber, G. Wolmershäuser, M. Ruck, *Z. Anorg. Allg. Chem.* **2000**, *626*, 2241.

[123] H. Sitzmann, T. Dezember, M. Ruck, *Angew. Chem. Int. Ed.* **1998**, *37*, 3113; *Angew. Chem*. **1998**, *110*, 3293.

[124] L. J. Karas, J. I. Wu, *Nat. Chem.* **2022**, *14*, 723.

[125] H. Vančik, I. Novak, D. Kidemet, *J. Phys. Chem. A* **1997**, *101*, 1523.

[126] R. Sievers, J. Parche, N. G. Kub, M. Malischewski, *Synlett* **2023**, *34*, 1079.

[127] G. Paprott, S. Lehmann, K. Seppelt, *Chem. Ber.* **1988**, *121*, 727.

[128] G. Paprott, D. Lentz, K. Seppelt, *Chem. Ber.* **1984**, *117*, 1153.

[129] G. Paprott, K. Seppelt, *J. Am. Chem. Soc.* **1984**, *106*, 4060.

[130] J. A. La Molina de Torre, P. Espinet, A. C. Albéniz, *Organometallics* **2013**, *32*, 5428.

[131] O. Verho, E. V. Johnston, E. Karlsson, J.-E. Bäckvall, *Chem. Eur. J.* **2011**, *17*, 11216.

[132] Y. Schulte, C. Stienen, C. Wölper, S. Schulz, *Organometallics* **2019**, *38*, 2381.

[133] Y. Schulte, H. Weinert, C. Wölper, S. Schulz, *Organometallics* **2020**, *39*, 206.

[134] C. Helling, C. Wölper, Y. Schulte, G. E. Cutsail, S. Schulz, *Inorg. Chem.* **2019**, *58*, 10323.

[135] a) N. Azuma, T. Ozawa, J. Yamauchi, *J. Chem. Soc., Perkin Trans. 2* **1994**, 203; b) N. Azuma, T. Ozawa, J. Yamauchi, *BCSJ* **1994**, *67*, 31.

[136] E. Vajda, J. Tremmel, B. Rozsondai, I. Hargittai, A. K. Maltsev, N. D. Kagramanov, O. M. Nefedov, *J. Am. Chem. Soc.* **1986**, *108*, 4352.

[137] B. E. Applegate, A. J. Bezant, T. A. Miller, *J. Chem. Phys.* **2001**, *114*, 4869.

[138] Y. Schulte, B. L. Geoghegan, C. Helling, C. Wölper, G. Haberhauer, G. E. Cutsail, S. Schulz, *J. Am. Chem. Soc.* **2021**, *143*, 12658.

[139] a) B. Miehlich, A. Savin, H. Stoll, H. Preuss, *Chem. Phys. Lett.* **1989**, *157*, 200; b) S. Grimme, S. Ehrlich, L. Goerigk, *J. Comp. Chem.* **2011**, *32*, 1456; c) C. Lee, W. Yang, R. G. Parr, *Phys. rev. B* **1988**, *37*, 785; d) A. D. Becke, *Phys. Rev. A* **1988**, *38*, 3098.

[140] a) K. Eichkorn, F. Weigend, O. Treutler, R. Ahlrichs, *Theor Chem Acta* **1997**, *97*, 119; b) F. Weigend, R. Ahlrichs, *Phys. Chem. Chem. Phys.* **2005**, *7*, 3297.

[141] a) A. Carrington, I.C.P. Smith, *Mol. Phys.* **1965**, *9*, 137; b) K. Möbius, H. van Willigen, A. H. Maki, *Mol. Phys.* **1971**, *20*, 289; c) W. T. Borden, E. R. Davidson, *J. Am. Chem. Soc.* **1979**, *101*, 3771.

[142] P. Neta, R. H. Schuler, *J. Phys. Chem.* **1973**, *77*, 1368.

[143] P. Jutzi, B. Neumann, G. Reumann, H.-G. Stammler, *Organometallics* **1998**, *17*, 1305.

[144] D. Naglav, B. Tobey, A. Schnepf, *Eur. J. Inorg. Chem.* **2013**, *2013*, 4146.

[145] a) E. O. Fischer, W. Bathelt, J. Müller, *Chem. Ber.* **1971**, *104*, 986; b) M. S. Davies, G. W. Allen, M. J. Aroney, T. W. Hambley, R. K. Pierens, *J. Mol. Struct.* **1994**, *326*, 81; c) F. T. Delbeke, G. P. van der Kelen, *J. Organomet. Chem.* **1974**, *64*, 239; d) M. J. Aroney, R. M. Clarkson, T. W. Hambley, R. K. Pierens, *J. Organomet. Chem.* **1992**, *426*, 331; e) M. S. Davies, R. K. Pierens, M. J. Aroney, *J. Organomet. Chem.* **1993**, *458*, 141.

[146] A. F. Webb, H. Gilman, *J. Organomet. Chem.* **1969**, *20*, 281.

[147] I. U. Khand, G. R. Knox, P. L. Pauson, W. E. Watts, *J. Chem. Soc. D* **1971**, 36a.

[148] H. Greenfield, H. W. Sternberg, R. A. Friedel, J. H. Wotiz, R. Markby, I. Wender, *J. Am. Chem. Soc.* **1956**, *78*, 120.

[149] E. C. S., *Nature* **1932**, *130*, 490.

[150] K. F. Hoffmann, D. Battke, P. Golz, S. M. Rupf, M. Malischewski, S. Riedel, *Angew. Chem. Int. Ed.* **2022**, *61*, e202203777; *Angew. Chem.* **2022**, *134*.

[151] R. T. Boeré, S. Kacprzak, M. Kessler, C. Knapp, R. Riebau, S. Riedel, T. L. Roemmele, M. Rühle, H. Scherer, S. Weber, *Angew. Chem. Int. Ed.* **2011**, *50*, 549; *Angew. Chem.* **2011**, *123*, 572.

[152] A. Bondi, *J. Phys. Chem.* **1964**, *68*, 441.

[153] T. Yanai, D. P. Tew, N. C. Handy, *Chem. Phys. Lett.* **2004**, *393*, 51.

[154] S. Grimme, *J. Chem. Phys* **2006**, *124*, 34108.

[155] E. van Lenthe, A. Ehlers, E.-J. Baerends, *J. Chem. Phys* **1999**, *110*, 8943.

[156] A. Fukazawa, J. L. Dutton, C. Fan, L. G. Mercier, A. Y. Houghton, Q. Wu, W. E. Piers, M. Parvez, *Chem. Sci.* **2012**, *3*, 1814.

[157] C. Richardson, C. A. Reed, *Chem. Commun.* **2004**, 706.

[158] a) R. Sievers, M. Sellin, S. M. Rupf, J. Parche, M. Malischewski, *Angew. Chem. Int. Ed.* **2022**, *61*, e202211147; *Angew. Chem*. **2022**, *134*, e202211147; b) E. D. Laganis, D. M. Lemal, *J. Am. Chem. Soc.* **1980**, *102*, 6633.

[159] R. N. Goldberg, N. Kishore, R. M. Lennen, *J. Phys. Chem. Ref. Data* **2002**, *31*, 231.

[160] Y. Schulte, C. Wölper, S. M. Rupf, M. Malischewski, G. Haberhauer, S. Schulz, *Structural Characterization and Reactivity of a Room Temperature-Stable, Antiaromatic Cyclopentadienyl Cation Salt*, **2023**.

[161] C.-Y. He, Q.-Q. Min, X. Zhang, *Organometallics* **2012**, *31*, 1335.

[162] B. Inés, S. Holle, D. Bock, M. Alcarazo, *Synlett* **2014**, *25*, 1539.

[163] C. T. Burns, P. J. Shapiro, P. H. M. Budzelaar, R. Willett, A. Vij, *Organometallics* **2000**, *19*, 3361.*llic Chemistry* **1969**, *20*, 281.

8 Appendix

8.1 List of Figures

8.2 List of Schemes

8.3 List of Tables

8.4 List of Compounds

1 $Cp^{Big\ n\text{-}Bu}H$

2 $Cp^{Big\ i\text{-}Pr}H$

3 $Cp^{Big\ t\text{-}Bu}H$

4 $Cp^{Big\ Ph2}H$

5 $Cp^{Big\ t\text{-}Bu2}H$

6 $Cp^{Big\ OMe}H$

7 $Cp^{Big\ C6F5}H$

8 $Cp^{Big\ CF3}H$

Numbering scheme of pentaarylcyclopentadienyl alkaline metal compounds.

metal	R = 4-*i*-Pr-Ph	R = 4-*n*-Bu-Ph	R = 4-*t*-Bu-Ph
Li	**9**	**14**	**19**
Na	**10**	**15**	**20**
K	**11**	**16**	**21**
Rb	**12**	**17**	**22**
Cs	**13**	**18**	**23**

24 $Cp^{Big\ t\text{-}Bu}{}_2Ge$

25 $Cp^{Big\ t\text{-}Bu}{}_2Sn$

26 $Cp^{Big\ t\text{-}Bu}{}_2Pb$

27 $Cp^{Big\ t\text{-}Bu}PCl_2$

28 $Cp^{Big\ t\text{-}Bu}AsCl_2$

29 $Cp^{Big\ t\text{-}Bu}SbCl_2$

30 $Cp^{Big\ t\text{-}Bu}BiCl_2$

31 $Cp^{Big\ OMe}$.

32 $Cp^{Big\ t\text{-}Bu}$.

33 $Cp^{Big\ C6F5}$.

34 $Cp^{Big\ t\text{-}Bu2}$.

35 $Cp^{Big\ Ph2}$.

36 $Cp^{Big\ t\text{-}Bu}{}_2Mg$

37 $Cp^{Big\ t\text{-}Bu}{}_2Ca$

38 $Cp^{Big\ t\text{-}Bu}{}_2Sr$

39 $Cp^{Big\ t\text{-}Bu}{}_2Ba$

40 $Cp^{Big\ t\text{-}Bu}Ga$

41 $Cp^{Big\ t\text{-}Bu}In$

42 $Cp^{Big\ t\text{-}Bu}Tl$

43 $Cp^{Big\ t\text{-}Bu}{}_2Hg$

44 $Cp^{Big\ t\text{-}Bu}GaCr(CO)_5$

45 Bis(pentafluorophenyl)ethyne

46 Perfluorotetraphenylcyclopentadienone

47 Pentakis(pentafluorophenyl)cyclopentadienole

48 Pentakis(pentafluorophenyl)cyclopentadienyl hexadecafluorotriantimonate

48a Pentakis(pentafluorophenyl)cyclopentadienyl hexadecafluorotriantimonate with 1.5 C_6F_6

48b Pentakis(pentafluorophenyl)cyclopentadienyl hexadecafluorotriantimonate with 2 C_6F_6

48$^+$ Pentakis(pentafluorophenyl)cyclopentadienyl cation

49 Pentakis(pentafluorophenyl)cyclopentadienyl radical

50$^-$ Pentakis(pentafluorophenyl)cyclopentadienide anion

50a Ferrocenium pentakis(pentafluorophenyl)cyclopentadienide

50b Tritylium pentakis(pentafluorophenyl)cyclopentadienide

50c Decamethylaluminocenium pentakis(pentafluorophenyl)cyclopentadienide

50d Pyridinium pentakis(pentafluorophenyl)cyclopentadienide

51 Pentakis(pentafluorophenyl)cyclopentadienyl carbonyl cation

52 Pentakis(pentafluorophenyl)cyclopentadienyl carboxylic acid

53 Pentakis(pentafluorophenyl)cyclopentadiene

8.5 List of Abbreviations

Ar	aryl
coe	*cis*-cyclooctene
Cp	cyclopentadienyl
CV	cyclic voltammetry
DCM	dichloromethane
dec.	decomposition
DFT	density functional theory
DMF	*N,N*-dimethylformamide
ENDOR	electron nuclear double resonance
EPR	electron paramagnetic resonance
HClaq	aqueous hydrochloric acid
IR	infrared
NICS	nucleus independent chemical shift
NMP	*N*-methylpyrrolidone

NMR	nuclear magnetic resonance
ppm	parts per million
PTFE	polytetrafluoroethylene
sc-XRD	single-crystal X-ray diffraction
SN1	nucleophilic substitution reaction with unimolecular rate determining step
THF	tetrahydrofuran
TMS	trimethylsilyl
UV/vis	ultraviolet and visible spectroscopy
VT	variable temperature
WCA	weakly coordinating anion

8.6 List of Publications

Structural Characterization and Reactivity of a Room Temperature-Stable, Antiaromatic Cyclopentadienyl Cation Salt

Y. Schulte, C. Wölper, S. M. Rupf, M. Malischewski, Daniel J. SantaLucia, Frank Neese, G. Haberhauer, S. Schulz, *Nature Chemistry.* Accepted in Principle, **2023**.

Metal-coordinated distibene and dibismuthene dications - isoelectronic analogues of butadiene

H. M. Weinert, Y. Schulte, A. Gehlhaar, C. Wölper, G. Haberhauer, S. Schulz, *Chem. Commun.* **2023**, *59*, 7755.

Comparing London dispersion pnictogen-π interactions in naphthyl-substituted dipnictanes

A. Gehlhaar, E. Schiavo, C. Wölper, Y. Schulte, A. A. Auer, S. Schulz, *Dalton Trans.* **2022**, *51*, 5016.

Cooperative Effect in Binuclear Zinc Catalysts in the ROP of Lactide

S. Ghosh, Y. Schulte, C. Wölper, A. Tjaberings, A. H. Gröschel, G. Haberhauer, S. Schulz, *Organometallics* **2022**, *41*, 2698.

Observation of Discrete Valence Tautomers in Crystalline Cyclopentadienyl Radicals

Y. Schulte, B. L. Geoghegan, C. Helling, C. Wölper, G. Haberhauer, G. E. Cutsail, S. Schulz, *J. Am. Chem. Soc.* **2021**, *143*, 12658.

Direct Synthesis of Pentaarylcyclopentadienyl Sandwich and Half-Sandwich Complexes of s-, p-, and d-Block Metals

Y. Schulte, H. Weinert, C. Wölper, S. Schulz, *Organometallics* **2020**, *39*, 206.

Synthesis of a Ga-Stabilized As-Centered Radical and a Gallastibene by Tailoring Group 15 Element-Carbon Bond Strengths

C. Helling, C. Wölper, Y. Schulte, G. E. Cutsail, S. Schulz, *Inorg. Chem.* **2019**, *58*, 10323.

Synthesis and Structures of s- and p-Block Metal Complexes Containing Sterically Demanding Pentaarylcyclopentadienyl Substituents

Y. Schulte, C. Stienen, C. Wölper, S. Schulz, *Organometallics* **2019**, *38*, 2381.

Conference Contributions:

Stable Cyclopentadienyl Cations, Radicals, and Anions (Poster)

Y. Schulte, S. Schulz, *21st Conference on Inorganic Chemistry*, **2022**, Marburg, Germany.

Observation of Distinct Valence Tautomers in Crystalline Cyclopentadienyl Radicals (Talk)

Y. Schulte, S. Schulz, *GDCh-Wissenschaftsforum Chemie* **2021**, online.

Observation of Distinct Valence Tautomers in Crystalline Cyclopentadienyl Radicals (Poster)

Y. Schulte, S. Schulz, *GDCh-Wissenschaftsforum Chemie* **2021**, online.

From Stable Cyclopentadienyl Radicals to Bulky Main Group Metallocenes (Poster)

Y. Schulte, S. Schulz, *GDCh-Wissenschaftsforum Chemie* **2019**, Aachen, Germany.

8.7 Curriculum Vitae

Der Lebenslauf ist in der Online-Version aus Gründen des Datenschutzes nicht enthalten.

8.8 Copyright Permissions

The permission to use the content of Figure 1, 2, 11, 12, and 13 was granted from the copyright holders.

8.9 Eidesstattliche Erklärung

Hiermit erkläre ich an Eides statt, dass ich die vorliegende Dissertation mit dem Titel

Pentaarylcyclopentadienylsystems

Anions, Radicals and Cations

eigenständig angefertigt habe. Alle wörtlich oder inhaltlich übernommenen Textstellen wurden als solche kenntlich gemacht und die verwendeten Quellen entsprechend zitiert. Diese Dissertation hat in dieser oder ähnlichen Form noch keiner Prüfungsbehörde vorgelegen und kein vorheriges Promotionsvorhaben ist endgültig gescheitert.

Essen, den 18.09.2023

_____

Yannick Schulte